Microbial stabilization and protein functionality of plant-based liquids using pulsed electric fields

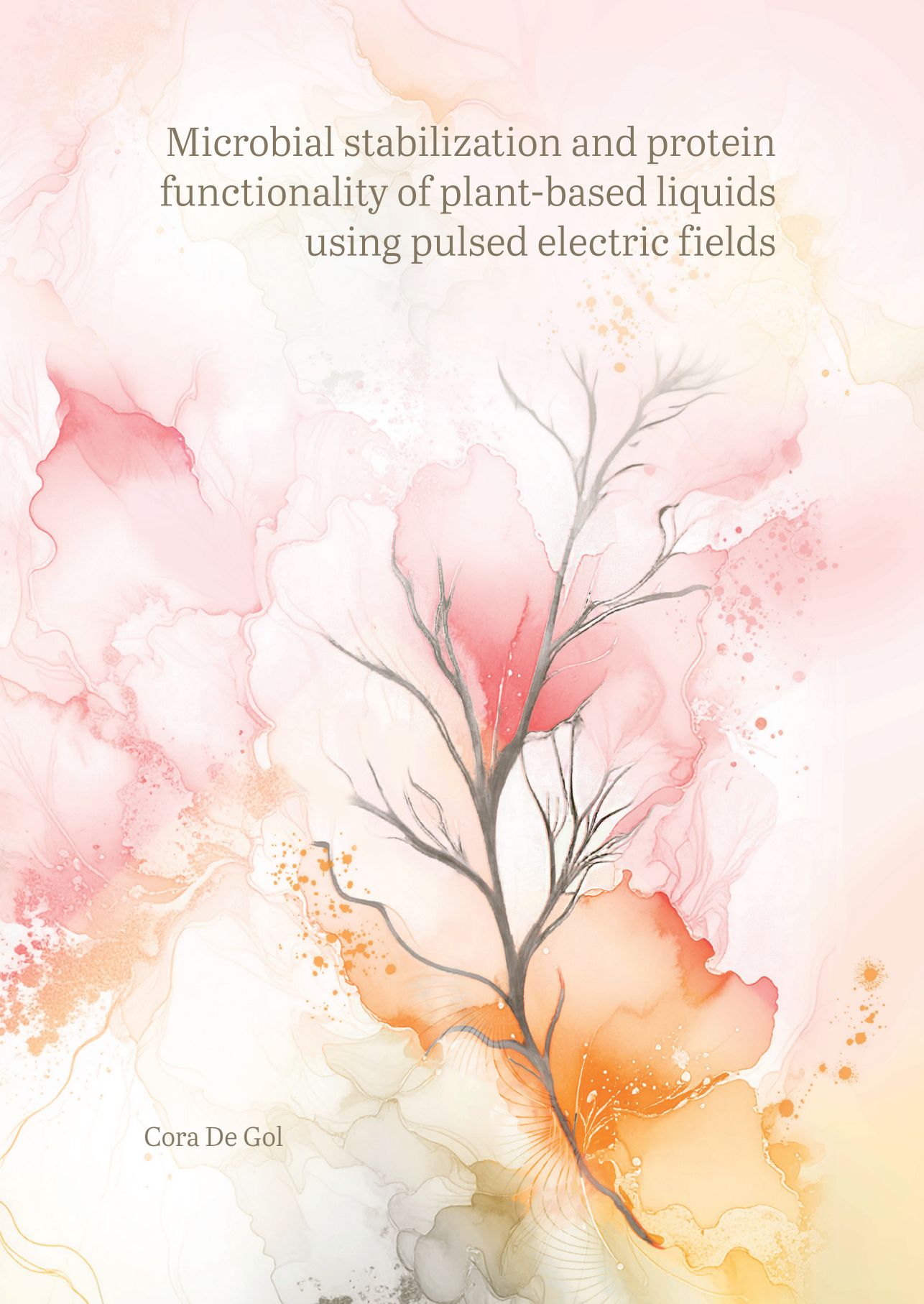

Cora De Gol

Propositions

1. The electrical conductivity of the food matrix determines the efficiency of PEF treatments.

   (this thesis)

2. At comparable time-temperature treatments, ohmic heating is advantageous over conventional heating for functionality and structure modifications of plant-based proteins.

   (this thesis)

3. Understanding processes at the molecular scale unlocks large-scale transformation in food systems.

4. Food sciences rely heavily on model systems, ignoring the complexity of real foods.

5. The role consumers play in shaping the food system through their food choices is underestimated.

6. We learn to parent like we learn to dance – by trusting each other, step by step.

Propositions belonging to the thesis, entitled

Microbial stabilization and protein functionality of plant-based liquids using pulsed electric fields

Cora De Gol
Wageningen, 17 June 2026

Microbial stabilization and protein functionality of plant-based liquids using pulsed electric fields

Cora De Gol

Thesis committee

Promotors

Prof. Dr *ir* M. H. Zwietering
Professor of Food Microbiology
Wageningen University & Research

Prof. Dr *ir* H. M. W. den Besten
Professor in Food Microbiology
Wageningen University & Research

Co-promotor

Prof. Dr *ir* M. Beyrer
Professor in Food Processing
HES-SO Valais/Wallis – School of Engineering, Sion, Switzerland

Other members

Prof. Dr *ir* A. J. van der Goot, Wageningen University & Research
Dr C. Siemer, Elea Technology GmbH, Quakenbrück, Germany
Prof. Dr E. Scholten, Wageningen University & Research
Dr *ir* M. N. Nierop Groot, Wageningen University & Research

This research was conducted under the auspices of the VLAG Graduate School (Biobased, Biomolecular, Chemical, Food and Nutrition Sciences).

Microbial stabilization and protein functionality of plant-based liquids using pulsed electric fields

Cora De Gol

Thesis

submitted in fulfilment of the requirements for the degree of doctor
at Wageningen University
by the authority of the Rector Magnificus,
Prof. Dr C. Kroeze,
in the presence of the
Thesis Committee appointed by the Academic Board
to be defended in public
on Wednesday 17 June 2026
at 3:30 p.m. in the Omnia Auditorium.

Cora De Gol

Microbial stabilization and protein functionality of plant-based liquids using pulsed electric fields,

201 pages

PhD thesis, Wageningen University, Wageningen, the Netherlands (2026)
With references, with summary in English
https://doi.org/10.18174/681940

Table of contents

Chapter 1	General introduction	7
Chapter 2	Gelling capacity of cell-disrupted *Chlorella vulgaris* and its texture effect in extruded meat substitutes	27
Chapter 3	Pulsed electric field treatment for preservation of *Chlorella* suspensions and retention of gelling capacity	51
Chapter 4	Pulsed electric field combined with preheating to preserve mildly extracted pea protein	77
Chapter 5	Effects of pulsed electric field and thermal treatment on the structural and techno-functional properties of mildly extracted pea proteins	97
Chapter 6	General discussion	121
	References	149
	Summary	179
	List of symbols	183
	List of abbreviations	185
	Acknowledgements	189
	About the author	193
	List of publications	195
	Overview of training activities	197
	Authorship statement	199

1



General introduction

1.1 Food system's sustainability and challenges

Our current food system is responsible for up to 30% of global greenhouse gas (GHG) emissions, leading to ocean acidification and biodiversity loss, and 70% of freshwater use, among other environmental issues (Willett et al., 2019). As a comparison, such emissions – estimated at 16 – 18 Gt CO_2-eq per year – are nearly twice as high as the combined annual emissions of the United States (USA) and the European Union (EU) (EC 2024; Tubiello et al., 2022). In parallel, significant challenges, driven by global population growth, climate change, and the intensification of natural resource use, further amplify the urgency to rethink the system.

According to the intergovernmental panel on climate change (IPCC), demand-side strategies such as shifting to sustainable, healthy diets and reducing food waste could potentially reduce the GHG emissions in the food sector by 44%, down to 10 Gt CO_2-eq per year, by 2050 (IPCC, 2023). These actions could also substantially reduce energy, water and land use, while enhancing biodiversity and ecosystem restoration (Agyemang et al., 2022; Smetana et al., 2023). A widely recognized mitigation option is the **shift from animal protein to plant-based alternatives**. This transition not only reduces environmental impacts but also promotes human health, protects animal welfare, and supports social and economic viability, aligning with 12 of the 17 sustainable development goals (SDGs) set for 2030 (Figure 1.1) (Chen et al., 2022a).

Achieving a successful transition requires coordinated efforts from industry, policymakers and consumer stakeholders (Agyemang et al., 2022). On the food production side, this involves improving agricultural practice, reevaluating food processing and preservation methods, and developing alternative food products and technologies. Moreover, governmental interventions such as regulatory measures, taxes and subsidies, and education initiatives are necessary to inform and guide the consumers towards sustainable and healthy food selection. Additionally, financial support for the development of innovative technologies is also required. For consumers, sustainable food options must be accessible, affordable, healthy, nutritious and sensory appealing, meeting expectations of taste, texture and appearance.

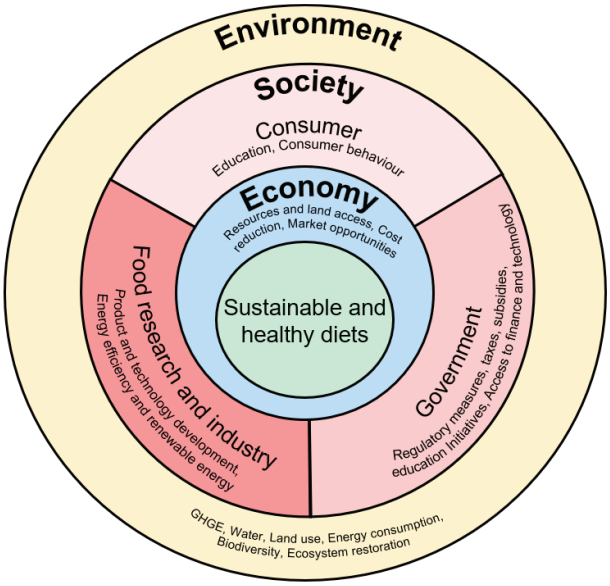

Figure 1.1: Stakeholders and pillars for sustainable development involved in the transition toward a more sustainable and healthy diet pattern. GHGE: greenhouse gas emission.

1.2 Plant-based foods to substitute animal proteins

1.2.1 Daily protein recommendation and consumption

Adopting a plant-based protein diet and reducing animal protein consumption, especially meat, is key to shifting toward a more sustainable and healthy diet. Indeed, the production of animal foods (meat, aquaculture, eggs and dairy) uses the majority of the world's farmland (~ 83%), contribute to excessive GHG emissions (~ 57%), despite providing only ~ 40% of our protein and ~ 18% of our calories (Poore & Nemecek, 2018). Moreover, most of the cultivated protein-rich cereals (~ 70% in Europe) are currently used to feed animals, competing with human nutrition (EC, 2019). The shift toward a plant-based diet would not only reduce tremendously food-related emissions and land use, but it would also benefit the population's health. The Swiss federal office of food safety and veterinary affairs (OSAV) recommends a daily protein consumption per capita (18 – 65 years) of 0.83 g/kg body weight (bw), from varied and mixed animal and plant protein sources, with a maximum of three portions of meat per week (~ 280 g meat per week). This corresponds to a daily consumption of ~ 0.57 g meat/kg bw for an average bw of 70 kg (or ~ 0.09 – 0.14 g protein/kg bw, considering the different protein contents (15 – 25 g/100 g) of meat products). Indeed, despite the high-quality of animal protein (digestibility, essential amino acid (EAA) content, and amino acid (AA) quantity) and the source of iron and vitamin B12, consuming only

animal-based foods to meet daily protein needs is not recommended due to health concerns (obesity, type two diabetes and cardiovascular diseases) and sustainability issues (Willett et al., 2019). Table 1.1 displays the daily consumption of meat, animal- and plant-based proteins worldwide and in different regions.

Table 1.1: Daily consumption of meat, protein, from animal (meat vs other animal-based) and plant sources, in g per capita and in g per kg body weight (bw), assuming an average bw of 70 kg

Country or region	Meat[a]		Protein[b]		Animal-based protein[b]				Plant-based protein[b]	
					Total protein		From meat			
	g	g/kg bw	g	g/kg bw	g	g/kg bw	g	g/kg bw	g	g/kg bw
World	120.9	1.73	90.5	1.29	37.7	0.54	18.7	0.27	52.8	0.75
China	193.3	2.76	128.0	1.83	52.1	0.74	28.9	0.41	75.9	1.08
USA	333.5	4.76	115.9	1.66	82.7	1.18	50.1	0.72	33.2	0.47
Europe	213.0	3.04	112.3	1.60	68.1	0.97	32.6	0.47	44.2	0.63
Africa	48.5	0.69	57.5	0.82	15.5	0.22	7.8	0.11	42.0	0.60

[a] FAO, 2024a; [b] FAO, 2024b

The current world consumption deviates significantly from the nutritional recommendations, with a daily protein consumption of 1.29 g/kg bw and a daily meat consumption of 1.73 g/kg bw. China is the largest protein consumer, with a daily consumption of 1.83 g/kg bw, primarily from plant-based proteins. In contrast, in the USA, animal-based proteins consumption is roughly three times higher than plant-based protein intake. While China, the USA and Europe all overconsume proteins, Africa struggles to meet the basic requirements, with a daily protein consumption of 0.82 g/kg bw. Therefore, mitigation strategies should target major consumers by reducing overall protein consumption, particularly by encouraging USA consumers to drastically cut meat consumption and shift to plant-based proteins, whereas for Africa, such strategy is not applicable due to existing nutritional deficiencies.

1.2.2 Proteins for plant-based foods

To help with the transition from animal- toward plant-based protein, **plant-based meat and dairy substitutes** have emerged on the market (Michel et al., 2021). They offer consumers a protein-rich alternative to dairy and meat products while showing similar texture, flavor, and ease of use. The manufacturing process typically includes protein extraction, drying and texturization. The protein content, quality and functionality of the protein ingredient are key to obtaining the desired final product – especially for meat substitutes, which contain 10 – 20% protein content and show fibrous texture (Siegrist et al., 2024). More precisely, protein should show high gelling capacity, without being denatured when extracted from the raw material and dried (He et al., 2020). The texturization is typically achieved through extrusion,

a thermomechanical process involving hydration (50 – 70% moisture), denaturation and intermolecular binding of biopolymers (proteins and potentially polysaccharides) at high temperatures combined with high shear stress and pressure. Even if the manufacturing process of meat or dairy substitutes increases environmental impacts compared to unprocessed grains or pulses, substitutes are more convenient and still more sustainable than animal-based options. For example, Tang et al. (2024) compared the environmental impact of plant-based meat substitutes with beef burgers through a cradle-to-fork system boundary life cycle assessment (LCA). They reported a 65% reduction in GHG emissions and a 45% reduction in water consumption (Table 1.2).

Table 1.2: Comparative analysis of environmental impact of protein-rich products for three impact categories (GHG emission, land and water use) per kg product and per kg protein. BB: beef burger, MS: meat substitute, SPI: soy protein isolate, PPI: pea protein isolate, PPC: pea protein concentrate, PPE: pea protein extract, MA: microalgae, GHG: greenhouse gas

Protein ingredient	System boundaries	Protein content (g/100 g)	Impact Category					
			GHG emission (kg CO_2-eq/kg)		Land use (m^2year/kg)		Water use (L/kg)	
			Product	Protein	Product	Protein	Product	Protein
BB[a]	Cradle to fork	30	66.7	222.3	40.2	134.0	500	1667
MS[a]		10 – 20[b]	23.3	~ 93.2	7.1	~ 28.4	300	~ 1200
Soybeans[c]	Product manufacturing	40	0.6	1.5	n.a.	n.a.	n.a.	n.a.
SPI[c]		90	20.2	22.4	n.a.	n.a.	n.a.	n.a.
PPI[d]	Cradle to processing	79	4.2	5.3	6.5	8.2	79.3	100.6
PPC[d]		43	0.7	1.6	3.5	8.2	19.8	46.2
PPE[d]		62	1.7	2.7	3.6	5.8	42.5	68.3
MA[e]	Cradle to processing	40	0.002	0.004	n.a.	n.a.	n.a.	n.a.

[a] Tang et al., 2024 ; [b] Siegrist et al., 2024 ; [c] Berardy et al., 2015 ; [d] Lie-Piang et al., 2021, with data from Geerts et al., 2017, Pelgrom et al., 2015 and Schutyser et al., 2015 ; [e] Rawindran et al., 2023
n.a. : not analyzed

1.2.2.1 Powdered protein isolates

Typical protein sources used for meat substitutes are pea, soy and wheat (Siegrist et al., 2024). Despite its high allergenicity, soy protein is frequently selected for its good digestibility, content in EAAs, high protein purity (up to 90% after extraction), good techno-functionality, availability and low cost (Tang et al., 2024). Concerning pea protein, it offers slightly lower textural performance compared to soy but shows low allergenic potential and is widely cultivated in Europe. Typically, the protein from soy or pea is being extracted via alkali solubilization and isoelectric precipitation, dried and used in the form of soy or pea protein isolate (SPI or PPI) powder, with a protein content of 75 – 90%, for the texturization process (Figure 1.2, left) (Schutyser et al., 2015). Such conventional fractionation processes, together with drying processes, require high water volume, energy, and chemical consumption, which compromises the native structure and functionality of the proteins (Lie-

Piang et al., 2021). Berardy et al. (2015) conducted an LCA to study the environmental impact of SPI manufacturing and compared it to published data for soybeans (Table 1.2). The GHG emissions for SPI (20.2 kg CO_2-eq/kg) was significantly higher compared to the value for soybeans (0.6 kg CO_2-eq/kg). Hence, the optimization of the manufacturing process of protein-rich ingredients is key to further reducing the environmental impact of meat substitutes. The potential of acting on the processing step was also validated by Lie-Pang et al. (2024), who reported a ~ two times higher GHG emissions for the processing of PPI compared to crop cultivation. Moreover, water consumption for processing was only slightly lower than for cultivation. Finally, Tang et al. (2024) also compared the impact of protein ingredient production (cultivation, processing to obtain texturized vegetable protein (TVP) and extrusion) to other steps across the product life cycle (packaging, distribution, storage and cooking). The percentage of land use and water consumption associated with production was ~ 92% and ~ 80%, respectively. GHG emissions were, in contrast, dominated by distribution (~ 68%) over production (~ 16%), packaging (~ 4%) and cooking (~ 12%).

Another alternative raw material that has recently attracted attention is microalgae. Its incorporation into soy-based meat substitutes has been associated with both nutritional and environmental benefits (Caporgno et al., 2020). Consistent with the potential sustainability advantage, Rawindran et al. (2023) conducted an LCA and reported low GHG emission associated with the cultivation, harvesting and protein extraction from microalgae biomass (Table 1.2).

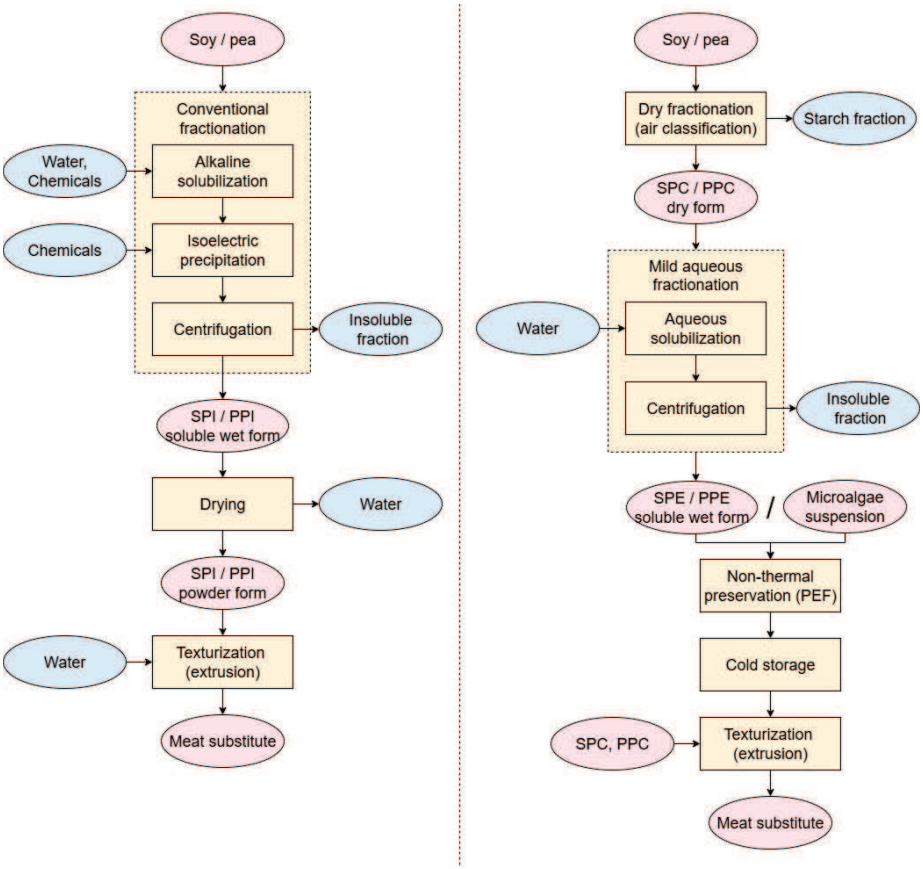

Figure 1.2: Flow chart of conventional (left) and mild processing (right) to produce meat substitutes. In this thesis, PPE was produced, and PEF was applied on PPE in soluble wet form and microalgae suspension. SPI: soy protein isolate, PPI: pea protein isolate, SPC: soy protein concentrate, PPC: pea protein concentrate, SPE: soy protein extract, PPE: pea protein extract, PEF: pulsed electric field.

1.2.2.2 Minimally processed protein concentrates and derivatives

Meat substitute impact can be reduced by using alternative plant- or algae-based proteins that 1) are derived from sustainable and locally sourced raw materials, and 2) are minimally processed. In this thesis, two model ingredients were selected based on real demand from the Swiss industry: the microalgae ***Chlorella vulgaris*** (*Cv*) and **yellow pea protein extract** (PPE), obtained through a mild fractionation process (Figure 1.2, right).

Cv stands out for its remarkable protein content (51 – 58%), nutritional value and rapid growth rate. Moreover, it can grow in saltwater and does not compete for arable land with conventional crops (Fu et al., 2021). However, its green color and mushy texture can negatively affect food quality, and this must be considered when formulating products. Mechanical disruption methods such as high-pressure homogenization (HPH) have proven

effective in breaking the cell wall, enabling the release of intracellular proteins for increased gelling capacity (Bernaerts et al., 2017). Furthermore, when cultivated under the right conditions, *Cv* can accumulate carotenoid pigments instead of chlorophylls, resulting in a yellow color that is more acceptable to consumers (Caporgno et al., 2019). In this thesis, wet, yellow, and HPH-disrupted *Cv* suspension was used.

Concerning **yellow pea**, as mentioned above, it shows low allergenicity potential and can grow in Switzerland. Additionally, it contains proteins (predominantly globulins and albumins) that exhibit strong gelling capacities (Lu et al., 2020). Previous studies investigated the potential of mild processing of peas to reduce the process environmental impact and negative alteration on protein functionality (Kornet et al., 2021a). In principle, mild processing involves dry fractionation to physically separate protein from starch, leading to a pea protein concentration (PPC) with ~ 50% protein content, potentially followed by a subsequent mild aqueous fractionation (at natural pH and room temperature) to further increase the protein content to ~ 60% (Möller et al., 2022; Pelgrom et al., 2015). The ingredient obtained through such hybrid fractionation is referred to as PPE. Lie-Piang et al. (2021) used published data to conduct an LCA and compare the impact of PPI (obtained through conventional fractionation), PPC (through dry fractionation), and PPE (through hybrid fractionation) (Geerts et al., 2017; Pelgrom et al., 2015; Schutyser et al., 2015). As shown in Table 1.2, GHG emission, land and water use were significantly lower for mild compared to conventional fractionation (< 1.7 vs 4.2 kg CO_2-eq/kg, < 3.6 vs 6.5 m^2year/kg and < 42.5 vs 79.3 L/kg, respectively). The decrease in all impact categories was mainly associated with the omission of the isoelectric precipitation step, with the associated acid use and heating. For this thesis, focus was brought to the PPE ingredient.

Besides mild fractionation, to further reduce energy and water use, and preserve protein functionality, the conventional drying step can be eliminated (Figure 1.2, right). Instead, the protein-rich ingredient (*Cv*, PPE) may be used **directly in its liquid form** for the texturization process. This strategy aligns with a global thinking of the production chain: avoid removing water and adding it back later in the texturization process. Moreover, from the LCA study, drying appears to be the most significant contributor for all the impact categories, in both conventional and hybrid fractionation (Lie-Piang et al., 2024; Schutyser et al., 2015). As a comparison, the energy use for the entire fractionation process is ~ ten times lower than the drying step. More precisely, while milling, air classification and centrifugation required 0.50, 0.23 and 0.15 MJ/kg processed material, respectively, spray drying uses 4.80 MJ/kg water

evaporated (or 5.42 MJ/kg wet material (10% dry matter (DM)) to obtain a powder (95% DM) (Schutyser et al., 2015). However, the elimination of drying and use of the protein extract in its liquid form brings additional challenges, particularly regarding transport, texture formation, food safety, and quality assurance. Transport might be minimized by gathering extraction and texturization processing in the same manufacturing site. Regarding meat-like texture formation, concentration steps or partial incorporation of plant-based protein powder may be required to achieve the minimal concentration at which a gel structure forms, referred as the least gelling concentration (Figure 1.2, right). Finally, an alternative preservation strategy needs to be implemented to maintain the quality and extend the shelf-life of liquid foods. To address this, **a hurdle approach combining non-thermal processing and refrigeration** is proposed in this thesis. One promising non-thermal method is the application of short, high-voltage pulses, referred to as **pulsed electric field (PEF)** treatment.

The energy (W) required for refrigeration at 4 °C can be estimated using the heat transfer Equation:

$$\dot{Q} = U \cdot A \cdot \Delta T \quad \text{(W)} \qquad (1.1)$$

Where U (W/(m^2·K)) is the heat transfer coefficient, A (m^2) is the surface area of the storage tank and ΔT (K) is the temperature difference between the room temperature and the temperature of storage (4 °C). For an insulated stainless-steel tank, U can be estimated to 0.25 W/m^2·K using Equation 1.2:

$$\frac{1}{U} = \frac{d_s}{\lambda_s} + \frac{d_i}{\lambda_i} = \frac{0.005}{15.9} + \frac{0.1}{0.025} \approx 4 \quad \text{(m}^2\text{·K/W)} \qquad (1.2)$$

With d_s and d_i (m) the thickness of the stainless-steel wall and insulation layer, respectively, and λ_s and λ_i (W/(m·K)) the respective thermal conductivity (Durmaz, 2018). For a 5'000 L storage tank (1.5 m diameter and 3 m length), A can be approximated to 14 m^2, and consequently $\dot{Q}$ equals 73.5 W (≈ 0.015 W/L). Hence, the energy consumption for PEF treatment (0.43 MJ/L, Aganovic et al., 2017) combined with storage (4 °C) (53 J/L per hour – 12.7 kJ/L for ten days) is ~ 12 times lower compared to drying (5.42 MJ/L). This validates the potential of minimal processing (Figure 1.2, right) to reduce the carbon footprint associated with conventional processing (Figure 1.2, left).

1.2.3 Microbial risk associated with plant-based liquids

Due to their high water activity and nutrient content, wet protein ingredients are particularly susceptible to germination of spores and microbial outgrowth. The level and type of microbial contamination in *Cv* and pea vary widely depending on cultivation practices, harvesting conditions and the form of the product (flours, concentrate or isolate). *Cv* has been associated with contamination by *Proteobacteria, Bacteroidetes, Actinobacteria* and *Planctomycetia* (Chegukrishnamurthi et al., 2020; Milana et al., 2024). Similarly, in peas, the presence of *Bacillus*, *Clostridium*, *Erwinia*, *Pantoea*, *Pseudomonas*, *Enterobacter,* and *Lysinibacillus* has been documented (Chartrel et al., 2021; Godebo et al., 2020; Kyrylenko et al., 2023). Most of the detected bacteria are harmless; however, some species, such as *Proteobacteria* (pathogenic *E. coli* and *Salmonella*)*, Bacillus cereus* and *Clostridium,* are pathogens and infect or produce potentially dangerous toxins for their host.

The texturization process used to produce meat substitutes typically involves high temperatures (T > 120 °C), which are effective in inactivating pathogens and microbial spores in the final food product. However, to maintain food quality and safety during earlier process stages and to prevent the spoilage (unpleasant odor or flavor, texture and color changes) of the intermediate substrate (*Cv* suspension, PPE in wet form – Figure 1.2, right), a preservation strategy is required. Conventional thermal pasteurization is potentially responsible for product deterioration, including the loss of fresh flavors and heat-sensitive vitamins, degradation of texture and color, development of off-flavors or browning, and alterations in techno-functional properties, making it an undesirable option. With the application of PEF combined with refrigeration, we target the inactivation of vegetative cells together with limited germination of spores and growth of psychrotrophic bacteria.

1.3 Preservation by pulsed electric fields

PEF treatment is based on the application of high-voltage short pulses to a sample (liquid or solid immersed in a liquid) placed between two electrodes. The short treatment time allows the preservation of heat-sensitive compounds, predominantly present in liquid foods, with minimal temperature increase (T < 60 °C), saving energy and consequently operational costs (Martin-Belloso et al., 2022; Toepfl et al., 2006). Additionally, PEF can be run in a continuous mode, allowing high product throughput. The use of electricity to kill bacteria in food dates from the end of the 19th century, and in the 1980s, the technology was commercialized in the USA for the preservation of dairy products, fruit juices and fluid egg. Since then, the technology has been applied to many foods not only for microbial inactivation

but also for valuable compounds extraction from cells or food structure modification. In the last decade, developments were mainly focused on improving productivity and sustainability, testing technology on new liquid foods and studying the impact of treatment on food functionalities. The efficacy of PEF treatment depends on many interconnected parameters, specifically those related to process equipment design, process conditions, food and microbial properties.

1.3.1 Interdependencies of PEF process parameters

Figure 1.3 illustrates the interdependencies of the PEF process parameters, and complexity of process optimization.

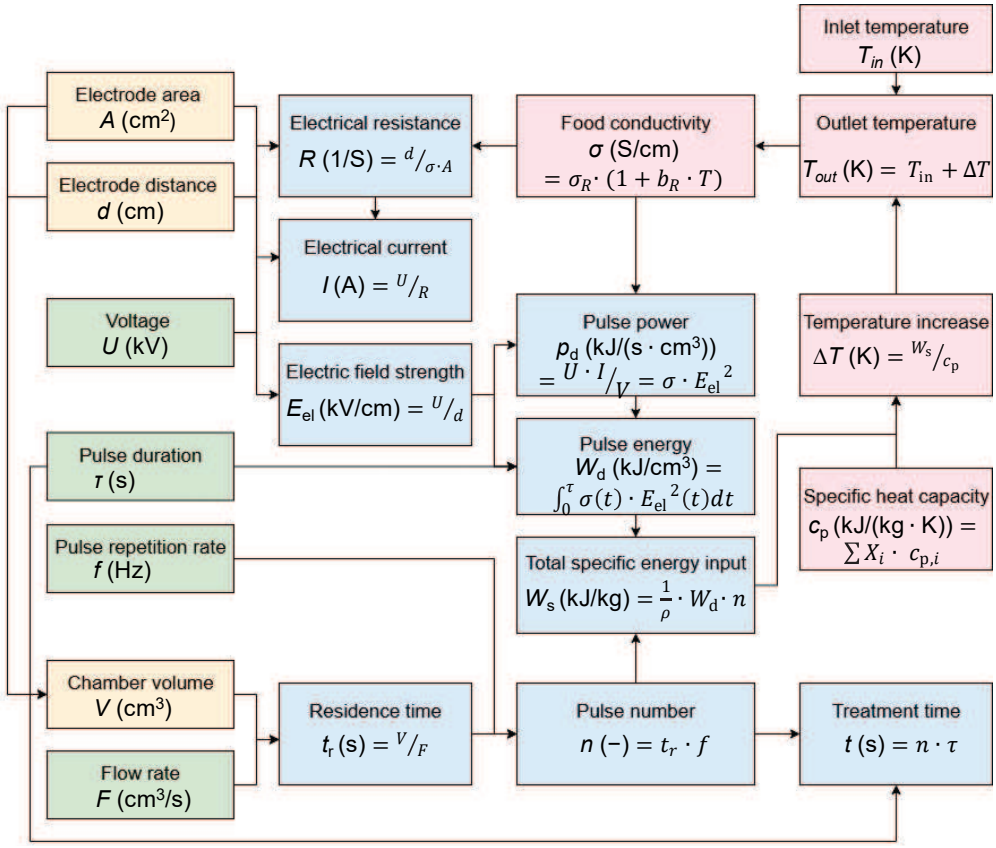

Figure 1.3: Interdependencies of PEF process parameters, chamber and food characteristics. The chamber characteristics are displayed in yellow: electrode area A (cm^2), distance between the electrodes d (cm) and chamber volume V (cm^3); the food characteristics in red: inlet temperature T_{in} (K), outlet temperature T_{out} (K), increase in temperature ΔT (K), specific heat capacity c_p (kJ/(kg·K)), electrical conductivity σ (S/cm) and density ρ (kg/cm3); and the process parameters with the independent process variables in green: voltage U (kV), pulse duration τ (s), pulse repetition rate f (Hz) and flow rate F (cm^3/s); and the dependent process variables in blue: electrical resistance R (1/S), electrical current I (A), electric field strength E_{el} (kV/cm), pulse power density p_d (kJ/(s·cm^3)), pulse energy density W_d (kJ/cm^3), total specific energy input W_s (kJ/kg), residence time t_r (s), pulse number n (-), and treatment time t (s). Adapted from Jaeger et al. (2022).

1.3.1.1 Equipment design

The two-electrode' systems are commonly designed as parallel plates, coaxial or co-linear cylinders, either in batch or continuous flow operation. Batch systems are preferred for laboratory-scale experiments, while continuous systems are necessary for high-volume treatment and for implementation in real industrial applications. In this thesis, most of the research was conducted using **a pilot plant co-linear continuous** system. In parallel, a batch PEF cell was developed internally and tested.

1.3.1.2 Process conditions

For bacterial inactivation, **electric field strengths** E_{el} and total **specific energy input** W_s commonly range within 15 – 40 kV/cm and 80 – 120 kJ/kg, respectively (Toepfl & Heinz, 2011). The **pulse power** p_d is expressed as a function of E_{el} (kV/cm) and the media **conductivity** σ (S/cm) (Equation 1.4), and the **energy input density** W_d is evaluated by the integral over pulse duration τ (s) to consider the change in electrical properties and deviation of the waveshape from the ideal case (Equation 1.5).

$$E_{\mathrm{el}} = {}^{U}/_{d} \qquad \text{(kV/cm)} \qquad (1.3)$$

$$p_{\mathrm{d}} = \frac{1}{V} \cdot U \cdot I = \frac{1}{V} \cdot \frac{U^2}{R} = \sigma \cdot {E_{\mathrm{el}}}^2 \qquad \text{(kJ/(s·cm}^3\text{))} \qquad (1.4)$$

$$W_{\mathrm{d}} = \int_0^{\tau} \sigma(t) \cdot {E_{\mathrm{el}}}^2(t) dt \qquad \text{(kJ/cm}^3\text{)} \qquad (1.5)$$

$$W_{\mathrm{s}} = \frac{1}{\rho} \cdot W_{\mathrm{d}} \cdot n \qquad \text{(kJ/kg)} \qquad (1.6)$$

With d the **distance between the electrodes** (cm), U the **voltage** (kV), I the **current** (A) and ρ the **density** (kg/cm^3), and n (-) the **number of pulses**. The typical conductivity value for liquid foods is $0.1 \cdot 10^{-3}$ – $2 \cdot 10^{-3}$ S/cm and increases with temperature (Equation 1.7) (Löffler, 2022).

$$\sigma = \sigma_{\mathrm{R}} \cdot (1 + b_{\mathrm{R}} \cdot T) \qquad \text{(S/cm)} \qquad (1.7)$$

With the referential conductivity σ_R (S/cm) and the temperature coefficient b_R (K^{-1}). The **electrical resistance** R (1/S) can be calculated as follows:

$$R = \frac{1}{\sigma} \cdot \frac{d}{A} \qquad \text{(1/S)} \qquad (1.8)$$

With *A,* the **electrode area** (cm^2). The **pulse duration** τ is very short, typically set at 1 – 100 µs. τ depends on the pulse shape, which is commonly either exponential decay or square wave for industrial applications. Square waves are often preferred because they allow more straightforward calculation of the **treatment time** t (s):

$$t = n \cdot \tau \quad \text{(s)} \quad (1.9)$$

Where n equals

$$n = t_r \cdot f \quad \text{(-)} \quad (1.10)$$

With t_r the **residence time** (s) and f the **pulse repetition rate** (Hz), which ranges from 0.5 to 500 Hz. Hence, the treatment time can be modified by varying either the number of pulses or the pulse duration. The **temperature increase** ΔT (K) due to ohmic heating can be estimated with W_s and the **specific heat capacity** c_p (kJ/(kg·K)) of the treated product (Equation 1.11), calculated using Equation 1.12, where X_i is the relative mass fraction of each component and the specific heat capacity for water, carbohydrates, protein, and fat approximated to 4.2, 1.4, 1.6 and 1.7 kJ/(kg·K), respectively (Kessler, 2002).

$$\Delta T = W_s / c_p \quad \text{(K)} \quad (1.11)$$

$$c_p = X_{water} \cdot c_{p,water} + X_{carb} \cdot c_{p,carb} + X_{prot} \cdot c_{p,prot} + X_{fat} \cdot c_{p,fat} \quad \text{(kJ/(kg·K))} \quad (1.12)$$

1.3.1.3 Food characteristics

Besides food **temperature**, the **conductivity** of the system influences the treatment efficacy strongly. The higher the conductivity of the medium, the higher the temperature increase (Equations 1.5 and 1.11), and consequently potential thermal inactivation effects. Moreover, variations in **pH** and **food composition** also affect the bacterial resistance to PEF. For example, Garcia et al. (2007) reported higher resistance of Gram-negative bacteria under acidic conditions than at neutral pH, while the opposite was observed for Gram-positive bacteria. Moreover, most of the research has been done on foods like fruit juice and milk (Cavalcanti et al., 2023; Timmermans et al., 2022). The microbial inactivation of plant-based protein-rich liquids is new and brings additional challenges, such as the **potential protective effect of proteins** against inactivation, as reported by Schottroff et al. (2019).

1.3.1.4 Microbial characteristics

The inactivation level or microbial resistance to PEF is strongly dependent on microbial characteristics, especially the **microbial strain, cell size** and **shape** as well as the **growth**

phase and conditions. In general, bigger cells are more sensitive compared to smaller cells, and spherical cells are more sensitive compared to nonspherical cells (Delso et al., 2022). Microbial culture conditions, i.e., growth temperature and growth phase, also influence the resistance to PEF. It has been reported that lower growth temperature leads to higher sensitivity, and that cells in the exponential phase are more sensitive than in the stationary phase (Wang et al., 2019). Some authors also studied the protective and sensitizing effects (adaptive response) when pre-exposing bacteria to acid or heat (Cebrián et al., 2012; Fernandez et al., 2018). Moreover, germinated and dormant spores are more resistant to PEF compared to the vegetative cells (Wu & Chang, 2022). Therefore PEF-treated liquids need to be stored in refrigerated conditions to limit spore germination (Soni et al., 2018).

1.3.2 Inactivation mechanism

1.3.2.1 Electroporation – cell injury level

Bacteria have a phospholipid bilayer membrane with low electrical conductivity, which prevents uncontrolled passage of charged particles. Typically, cells maintain an unequal distribution of ions across the membrane, creating a difference in electrical potential. When an external electric field is applied, ions redistribute and accumulate on both sides of the membrane and a progressive increase in the transmembrane potential occurs. When the critical transmembrane potential is reached (~ 1 V for bacteria), pores are formed in the membrane, increasing its permeability to water molecules (Martin-Belloso et al., 2022). The hydrophilic polar head groups of lipids are pushed to reorient toward these water molecules. Over time, the pores grow in both size and number. After the electric pulses stop, intracellular compounds may leak out of the cell, while external compounds may enter.

The bacterial cell injury caused by PEF can be categorised into four levels (Yarmush et al., 2014):

1) **no electroporation** – the cells are resistant to PEF, and the membrane stays intact,

2) **reversible electroporation** – the cells show a perforated membrane but retain viability. The pores can reseal, and the cells are considered sub-lethally injured,

3) **non-thermal irreversible electroporation** – the electroporation is too severe for the membrane to reseal, resulting in cell death,

4) **thermal irreversible electroporation** – cell death occurs due to denaturation of cellular molecules, primarily caused by ohmic heating.

The electric field strength required, at specific treatment time and temperature, to exceed the transmembrane potential threshold and cause the transition from stages 1) to 2) is referred to as the **critical electric field strength**, E_{crit} (Figure 1.4).

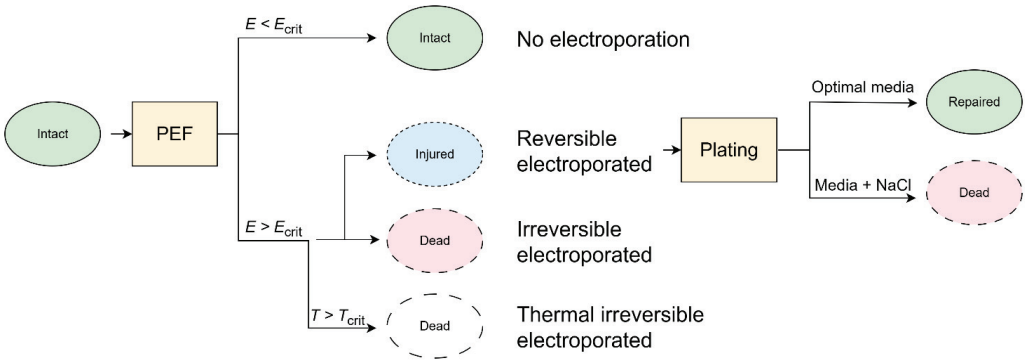

Figure 1.4: Different levels of cell injury after PEF treatment and detection of injured cells through selective plating. PEF: pulsed electric field, *E*: electric field strength, *T*: temperature. Adapted from Delso et al., 2022.

1.3.2.2 Methods to detect electroporation

Numerous techniques have been used to assess the cell injury level. In this thesis, **fluorescence flow cytometry** (FFC) using propidium iodide (PI) and SYTO 9 was applied to evaluate membrane integrity based on dye uptake. PI is a red-fluorescent nucleic acid stain that cannot penetrate cells with intact membranes, while SYTO 9 is a green-fluorescent dye that can penetrate both intact and electroporated cells due to its low molecular weight (Cal-Sabater et al., 2019).

In parallel, **selective plating on modified media** was used to quantify the sub-lethal injury. 6% w/v sodium chloride (NaCl) was added to plate count agar (PCA) to impose osmotic stress on PEF-treated cells. This additional challenge inhibits the growth of injured cells, allowing differentiation between intact and reversible electroporated cells (Jay, 1992) (Figure 1.4).

1.3.2.3 Synergistic effects between thermal and PEF treatments

The lethal effect of PEF can be enhanced through the application of mild heat, resulting in an additional or even synergistic effect between electric and thermal stresses. This synergy has been associated with a change in the phospholipid bilayer from a gel-like consistency to a more fluid state, thereby facilitating pore formation. Molecular dynamic simulations by Song et al. (2011) demonstrated a reduction of the electroporation threshold with temperature increase. Additionally, Cebrián et al. (2016) explained the phenomenon by the

thermal modification of membrane components and increased diffusion rates of ions and molecules across the membrane.

1.3.2.4 Shelf-life

The level of cell injury can provide valuable insights into predicting the shelf-life of food products. When the pores are reversible damaged, the time needed for the cells to repair and commence proliferation is referred to as the lag phase (λ) extension. Beside inactivation level, the λ extension significantly influences shelf-life (Selma et al., 2004). Previous research suggested that increasing PEF intensity leads to a prolonged duration of λ, ultimately resulting in an extended shelf-life for food products (Aronsson et al., 2004; Selma et al., 2004; Timmermans et al., 2016).

1.3.3 Effect on food properties

Thanks to its application at mild temperatures and short times, PEF enables effective microbial inactivation while preserving the sensory and nutritional quality attributes of foods. More interestingly, several studies have reported that PEF can even enhance functional properties and increase the concentration of health-promoting compounds (Sui et al., 2011; Vanga et al., 2021). An increasing number of review studies describe the potential of PEF to modify protein macrostructure (Ali et al., 2024; Giteru et al., 2018; Malik et al., 2024; Pereira et al., 2024; Rajeswari et al., 2024). Specifically, PEF induces partial unfolding of protein structures, which can significantly affect water-holding capacity, solubility and rheological behavior, as reported by Chen et al. (2022b) and Zhao et al. (2014) and for PPI and soy milk, respectively. These structural and consequent functional changes may result from a combination of electro-conformational effects and ohmic heating. To investigate these mechanisms, researchers have employed various analytical techniques, including spectroscopic, microscopic, chromatographic, electrophoretic, and rheological methods. To date, most studies have focused on fruit juices, egg and dairy proteins, whereas research on plant-based protein liquids remains limited.

1.4 Aim and outline of the thesis

This thesis aims to advance the development of plant-based protein ingredients specifically designed to produce meat substitutes. The research focuses on enhancing their functionality and nutritional value while reducing the environmental impact of processing. The ultimate goal is to propose an ingredient that is microbiologically stable, highly nutritious, exhibits high gelling capacity, and is derived from sustainable and locally sourced proteins. More

specifically, this research primarily aims to eliminate conventional, energy-intensive, and denaturing drying processes commonly applied to plant-based protein ingredients. In that context, pulsed electric field treatment combined with refrigerated storage is proposed, targeting shelf-life extension of microalgae suspensions and pea protein liquids (*Cv* and PPE).

1.4.1 Knowledge gap

PEF has been extensively optimized for preserving liquid foods such as fruit juices and milk (Cavalcanti et al., 2023; Nowosad et al., 2021; Šalaševičius et al., 2021; Timmermans et al., 2022). However, its application to plant-based, protein-rich liquids at neutral pH is relatively novel. Most of the existing PEF research focuses on simplified buffer systems using surrogate (model) bacteria. Studies that evaluate PEF effects within complex food matrices containing naturally occurring bacterial populations are limited. Furthermore, much of the research prioritizes microbial inactivation without distinguishing between the electrical and thermal effects of PEF.

Additionally, the implementation of PEF in producing extruded plant-based foods is unexplored so far. Extrusion is typically performed with powdered protein ingredients (Caporgno et al., 2019; Fu et al., 2021). PEF can enhance the functionality of protein-rich liquids, but its potential to improve protein behavior in extrusion has not been tested.

1.4.2 Research questions

The main research aim was to identify PEF windows for microbial reduction in protein-rich plant-based liquids (*Cv* and PPE) and shelf-life extension, while maintaining the protein techno-functionality. Several objectives were established:

1. Validate the possible use of liquids in extrusion processing
2. Identify the key psychrotrophic microbial contaminants in *Cv* and PPE
3. Apply PEF treatment combined with cold storage to control the identified contaminants
4. Study the PEF-induced microbial cell injury
5. Ensure that the PEF window for microbial reduction does not negatively alter protein functionality

1.4.3 Chapters

The outline of the thesis is displayed in Figure 1.5. The research questions are considered in **Chapters 2 – 6**.

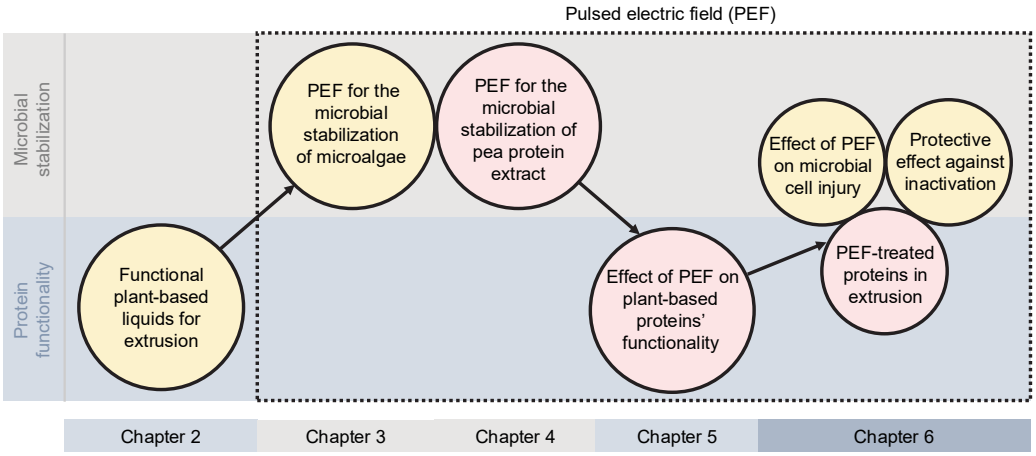

Figure 1.5: Illustration of the thesis chapters. The work conducted on *Cv* is shown in yellow, whereas the work on PPE is shown in pink.

Firstly, in **Chapter 2**, the incorporation of undried protein ingredient into extrusion was explored, to enhance the nutritional profile of meat substitutes and reduce the energy consumption of the process. Microalgae *Cv* suspension was selected as a local, sustainable protein source rich in essential nutrients. *Cv* was used in its liquid form and incorporated at a 10% w/w concentration into PPI. The impact of this supplementation on the texture and color properties of the final extrudates was analyzed. Additionally, HPH was investigated to disrupt microalgae cells and potentially influence gel network formation.

In **Chapter 3**, the microbial stability of *Cv* suspension was considered. Psychrotrophic bacteria, which grow at 10 °C in *Cv*, were isolated and identified as key contaminants. Three representative microorganisms were selected, inoculated into *Cv*, and subjected to challenge tests using PEF technology. The inactivation levels, the effects of PEF (electrical or thermal) and the *Cv* shelf-life extension were studied.

Similarly, in **Chapter 4**, the most predominant bacterial contaminants in PPE stored at 10 °C were isolated, purified and identified. PEF treatments were optimized for two specific bacteria. Inactivation levels, inactivation effects (electrical or thermal) and shelf-life studies were considered.

The impact of PEF treatments on the properties of pea proteins was studied in **Chapter 5.** PEF and thermal treatments that achieved comparable levels of microbial inactivation were compared. Protein functionalities, including thermal and gelling properties, were examined alongside structural characteristics at the secondary and tertiary structure levels.

In **Chapter 6**, first, a comprehensive review of the key findings from **Chapters 2 – 5** is presented. Second, deeper research on the electroporation mechanisms, particularly the extent of bacterial membrane injury caused by PEF, is discussed. Moreover, we address the challenge associated with protein-rich media and investigate the potential protective effects of proteins against inactivation. Additionally, the use of PEF-treated PPE in extrusion was tested. Furthermore, the carbon footprint of the obtained PPE is discussed through LCA data from partners. Finally, concluding remarks and an outlook for future research directions are provided.

2



Gelling capacity of cell-disrupted *Chlorella vulgaris* and its texture effect in extruded meat substitutes

This chapter is published as:

De Gol, C., Snel, S., Rodriguez, Y., & Beyrer, M. (2023). Gelling capacity of cell-disrupted Chlorella vulgaris and its texture effect in extruded meat substitutes. Food Structure, 37, 100332. https://doi.org/10.1016/j.foostr.2023.100332

Abstract

Microalgae attract increasing interest in enhancing the nutritional values of plant-based foods. However, alterations in the final product's color (by green algae) and mushy texture can be induced. In this study, we incorporated yellow *Chlorella vulgaris* (*Cv*) in pea protein-based meat substitutes and aimed to minimize properties alteration by using wet and disrupted *Cv* biomass. The cell wall disruption, done by high-pressure homogenization (HPH) at 150 MPa and initial biomass temperature below 10 °C, significantly increased the gelation capacity. The effect was confirmed by 1) ten times increase in the apparent viscosity of 14% (w/w) *Cv* suspensions, and 2) two times increase in the storage modulus *G'* of 9:1 (w/w) pea protein isolate - *Cv* gels. Furthermore, the HPH-treated *Cv* was successfully incorporated (10% (w/w)) into pea protein-based meat substitutes produced with high-moisture extrusion cooking without altering their visual appearance, hardness, or anisotropy index. Finally, spray drying or fractionation steps of the HPH-treated *Cv* did not improve protein gels, or meat substitutes produced thereof. This study demonstrated that disrupted *Cv* is a promising nutritious and sustainable ingredient for meat substitutes.

2.1 Introduction

Plant-based diets are gaining importance thanks to their lower environmental footprint and positive effect on overall consumer health. However, such diets increase the risks of deficiencies in certain nutrients such as vitamin B12, choline, and calcium (Chen et al., 2019). As a solution, microalgae emerge as promising candidates for fortifying plant-based foods (Caporgno & Mathys, 2018). They contain all essential amino acids (AA), vitamin B12, calcium, soluble fibers, and essential fatty acids (Barka & Blecker, 2016; Becker, 2007; Bito et al., 2020; Demarco et al., 2022; Grossmann et al., 2020). Moreover, microalgae have a low land requirement, high protein content, and a fast growth rate. Therefore, they are considered as promising raw material to produce sustainable food (Kusmayadi et al., 2021; Smetana et al., 2017).

Examples of microalgae that are currently used in food products are *Arthospira spp.* and *Chlorella spp.* (Lafarga, 2019). Interestingly, phototrophic, heterotrophic and mixotrophic cultivations of *Chlorella vulgaris* (*Cv*) are possible. The growth conditions, i.e., the light intensity and the agitation rate, influence the microorganism's protein content (Canelli et al., 2020a; Imamoglu, 2015; Seyfabadi et al., 2011). Typically, *Cv* contains 51 – 58% crude protein, 14 – 22% lipids, and 12 – 17% carbohydrates on dry basis (Oppen et al., 2022). Of the proteins, 50% are inside the cell, 20% are bound to the cell wall, and 30% can migrate in and out of the cell (Safi et al., 2014). *Cv* has quite rigid cell walls composed of chitosan, cellulose, hemicellulose, proteins, lipids, and minerals (Safi et al., 2014). Thus, to extract the intercellular proteins the cell walls must be disrupted. Several authors demonstrated that mechanical cell wall disruption like high-pressure homogenization (HPH) and bead milling results in the release of intracellular proteins, as well as an increase in protein digestibility, and bioavailability of vitamins and minerals, which were confirmed by *in vitro* assays (Bito et al., 2020; Canelli et al., 2020b; Demarco et al., 2022; Wang et al., 2020). Additionally, cell wall disruption modifies microalgae biomass functionality such as gelation capacity (Bernaerts et al., 2017). HPH has been proven to be the most effective technique, not only for achieving complete cell disruption (for *Cv* at 150 MPa, three passes) (Carullo et al., 2018) but also for being energy efficient (Grossmann et al., 2020; Safi et al., 2017). Following cell disruption, centrifugation can separate soluble from insoluble fractions (Grossmann et al., 2020). In general, the microalgae ingredient is dried to facilitate its storage and extend its shelf life. However, drying showed some limitations such as product quality degradation and

digestibility reduction, as well as high energy and cost requirements (Show et al., 2015). Cell disruption, centrifugation and drying are referred as downstream processing (DSP) steps.

The addition of microalgae to meat substitutes was identified as a promising route to improve their nutritional profile (Fu et al., 2021). Meat substitutes can be produced with high-moisture extrusion cooking (HMEC), among other techniques (Dekkers et al., 2018). Typically, HMEC involves the hydration and mixing of high protein powder ingredients with water (50 – 70% moisture), cooking under high shear, pressure, temperature, and cooling through a long die where elongated proteins align into a fibrous texture (Cornet et al., 2021). Ingredients that can be produced into fibrous meat substitutes include pea and soy protein isolates and concentrates, often in combination with starch, fibers, and gluten, due to their high functionality and texturizing capacity (Cornet et al., 2021; Yao et al., 2004). So far, the addition of *Arthrospira platensis* has been tested in soy and lupin meat substitutes produced with HMEC (Grahl et al., 2018; Palanisamy et al., 2019). However, the addition of *A. platensis* results in dark green-colored meat substitutes. The use of microalgae after chlorophyll removal was thus suggested to obtain a more acceptable color (Fu et al., 2021). Under the right cultivation conditions, *Chlorella spp.* can accumulate carotenoid pigments instead of chlorophylls, resulting in yellow biomass (Caporgno et al., 2019).

The focus of this study is to improve the heat-induced gelation properties of the *Cv* biomass by homogenization and incorporate the homogenized biomass without drying, into pea protein-based extruded meat substitutes. The goal is to obtain extrudates with unaltered texture but enriched with microalgae. To the best of the authors' knowledge, no studies have examined the incorporation of wet, yellow, and disrupted *Cv* biomass as an ingredient in HMEC.

2.2 Materials and methods

2.2.1 Materials

Two freshly produced *Cv* biomasses (C1 and C2) were kindly donated by Alver AG (Switzerland). Microalgae were heterotrophically cultivated in two different batches by Phycom (The Netherlands) using a patent-protected yellow *Cv UTEX 30* strain (Uran et al., 2021). Directly after harvesting, the biomasses were centrifuged, and the concentrated biomasses were packed in 5 kg bags, frozen and sent in insulation boxes. The frozen biomasses were stored at – 20 °C until use and transferred to a cooling chamber (4 °C) the day before the trial for defrosting. Their dry matter (DM) was 25.0 ± 0.2 and 26.0 ± 0.3%

(w/w), respectively. The defrosted biomasses were diluted with deionized water to 13.2 ± 0.0 and 13.8 ± 0.0% (w/w) DM. Their respective pH values were 6.4 ± 0.1 and 5.4 ± 0.0. Moisture content analysis was done using the rapid moisture analyzer (HC103 Mettler-Toledo) at the conditions of 120 °C, initial mass of 2 g, and stop criteria of 1 mg/50 s. The pH of the suspensions was measured with a pH meter 914 (Metrohm, Switzerland). C1 was used to optimize the HPH treatment, whereas C2 was intended for HMEC trials. The AA profile of C1 was analyzed by Eurofins Scientific (France) (Table 2.A.2) and was used to calculate the nitrogen-to-protein conversion factor (NPCF) (Equation 2.1). Using Equations 2.2 and 2.3, a value of 4.21 was obtained.

$$NPCF = \frac{1}{[N]_{protein}} \quad (-) \qquad (2.1)$$

With $[N]_{protein} = \sum_{i=1}^{18}[N]_{AA,i} = \sum_{i=1}^{18}[AA]_{protein,i} \cdot [N]_{AA,i}$ ($g_N/g_{protein}$) (2.2)

$$[N]_{AA,i} = \frac{n_N}{Mw_{AA,i} - Mw_{H_2O}} \cdot Mw_N \quad (g_N/g_{AA}) \qquad (2.3)$$

With n_N (-) the number of nitrogen atoms per AA, $[N]_{protein}$ ($g_N/g_{protein}$) the mass concentration of nitrogen in proteins, $[N]_{AA,i}$ (g_N/g_{AA}) the mass concentration of nitrogen in AAs and $[AA]_{protein,i}$ ($g_{AA}/g_{protein}$) the mass concentration of AA in proteins. M_W (g_N/mol) is the molecular weight.

Commercial pea protein isolate (PPI) (Nutralys® F85M) was obtained by Roquette Frères S.A. (Lestrem, France). The minimum protein content (NPCF = 6.25) on DM was given by the supplier and was 83% (w/w). The moisture content was 7.5% (w/w).

2.2.2 Cell disruption by HPH

Cv cell disruption was done by HPH using a NS3006L ARIETE homogenizer (GEA Niro Soavi, Italy) equipped with a radial diffuser homogenization valve. Different operating pressures and initial product temperatures were studied. C1 was used to find the HPH optimal conditions.

First, the effect of pressure (90, 120 or 150 MPa, one pass) at initial temperature T_{in} of 5 ± 1 °C was tested. Product flow rates were 64, 54 and 48 L/h for each pressure, respectively. A heat exchanger (cold tap water, 12 °C) was installed immediately after the homogenization valve to quickly cool down the product after HPH treatment. HPH-treated *Cv* suspensions were labeled as C1-H-90, C1-H-120 and C1-H-150. For each pressure, a second pass was

also tested. The product was cooled down between the passes using an ice bath to reach a temperature of 5 ± 2 °C.

Second, the effect of initial temperature T_{in} (5, 10, 15, 20 and 25 °C) at a fixed operating pressure Δp of 150 MPa and one pass was tested. The process temperature T_p (°C) during HPH treatment was estimated using Equation 2.4 (Osorio-Arias et al., 2020):

$$T_p = T_{in} + \delta \cdot \Delta p + \xi \cdot \Delta p - \sum heat\ loss \quad \text{(K)} \qquad (2.4)$$

The terms δ and ξ correspond to the temperature change due to the heat of compression and homogenization, respectively, and were approximated to 8 °C/100 MPa and 18 °C/100 MPa for a worst-case scenario. Heat losses were considered negligible (Osorio-Arias et al., 2020).

Third, cell disruption of C2 was done at the identified HPH optimal pressure and initial temperature conditions (150 MPa, 5 – 10 °C, one pass). The treated suspension was named C2-H. The protein, lipid, and carbohydrate content of C1-H-150 and C2-H were analyzed externally by the Swiss quality testing services (SQTS) (Switzerland).

2.2.3 Downstream processing (DSP) of microalgae biomass

To study the effect of DSP steps, namely centrifugation and spray-drying, on the gelation capacity of the HPH-treated *Cv* suspensions, C2-H was split into three parts. One part was centrifuged, another was spray-dried, and one was kept intact and used as a reference. All three preparations were used for rheological characterization, gel formation with PPI, and partial replacement of PPI in the production of extrudates by HMEC (Figure 2.1).

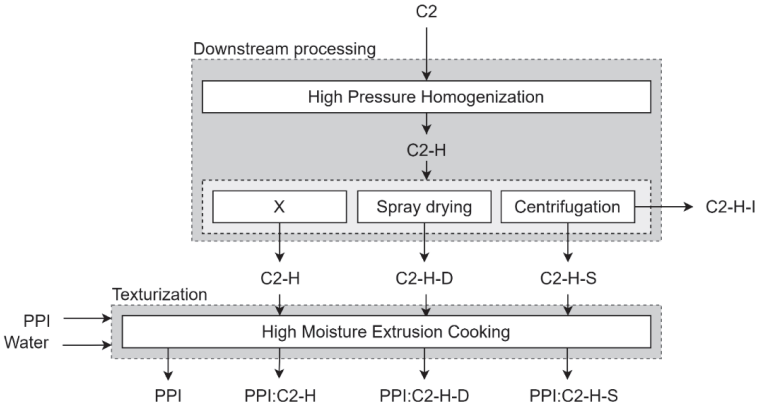

Figure 2.1: Schematic overview of the downstream processing of microalgae and application in high moisture extrusion cooking. C2: *Chlorella* batch 2, H: homogenized, X: no additional DSP, D: spray-dried, S: soluble fraction, I: insoluble fraction, PPI: pea protein isolate.

2.2.3.1 Centrifugation

Centrifugation was done at 8'000 x *g* at 4 °C for 10 min, using a lab-scale centrifuge Sigma 3-16KL (Adulf Kühner AG, Switzerland). The supernatant or soluble fraction (C2-H-S) was kept at 4 °C in closed containers until use. The insoluble fraction (C2-H-I) was discarded.

2.2.3.2 Spray drying

Spray drying was done using a mobile minor MM-PSR spray dryer (GEA Niro Soavi, Italy). The operating set conditions were 0.1 MPa pressure, 103 kg/h flow rate of drying air, 180 and 103 °C inlet and outlet air temperatures, respectively. The product was pumped using a peristaltic pump NEMA 4X IP66 (Watson Marlow, United Kingdom) at 9 rpm, corresponding to a product flow of 2 kg/h.

2.2.4 Characterization of microalgae preparations

2.2.4.1 Protein content and fraction of soluble protein

The protein content (dry basis) was calculated from the total nitrogen (TN) (mg/L) value obtained using a total organic carbon/total nitrogen (TOC/TN) analyzer (Shimadzu, Japan) (Equation 2.5). The auto dilution and injection volume were set at 2 and 100 µL, respectively. The dry weight is the DM of the sample before dilution expressed in mg/L. The NPCF used was 4.21 (Section 2.2.1).

$$Protein\ content\ = \frac{NPCF \cdot TN}{Dry\ weight} \cdot 100 \qquad \text{(\% w/w)} \qquad (2.5)$$

The fraction of soluble protein (Equation 2.6) was expressed as the amount of protein present in the supernatant (g) (Equation 2.5) with respect to the initial amount of protein in the suspensions before centrifugation (g) (from SQTS analysis). Centrifugation was done at 8'000 x *g* at 4 °C for 10 min on 5% (w/w) biomass and the supernatant was manually diluted 50 times with deionized water before the TOC/TN measurement.

$$Fraction\ of\ soluble\ protein\ (\%)\ = \frac{amount\ of\ protein\ in\ supernatant}{amount\ of\ initial\ protein} \cdot 100 \qquad \text{(\% w/w)} \qquad (2.6)$$

2.2.4.2 Imaging

An optical microscope (Zeiss Axioplan, Germany) was used to observe the cell disruption level after HPH at different operating pressures. The samples were diluted 100 times. The images were taken at a magnification of 40 times and with a differential interference contrast (DIC0.5-1.4) filter.

2.2.4.3 Differential scanning calorimetry (DSC)

Heat-induced protein denaturation was determined by DSC using a μDSC7 evo (Setaram Instrumentation, France). A standard Hastelloy cylinder was filled with 600 μL of the sample (14% (w/w) DM). The reference cell was loaded with 600 μL of deionized water. The system was purged with a constant nitrogen flow at around 0.1 MPa. The samples were scanned from 20 to 100 °C at a heating rate of 0.5 °C/min, held at 100 °C for 10 min, and subsequently cooled to 20 °C at the same rate. The peak maximum temperature T_{peak} and the reaction enthalpy ΔH (J/g suspension) were obtained from the baseline integration of the endothermic peaks observed in the thermograms using the Thermal Analysis® Software package V. 1.46 (Setaram Instrumentation). The peak area was divided by the DM content of the suspension to obtain the ΔH in J/g DM.

2.2.4.4 Enzymatic hydrolysis

An enzymatic treatment was applied on C2-H to better understand the role of polysaccharides in the gelation mechanism. To target cellulose and hemicellulose hydrolysis, two enzymes were used: a cellulase complex NS-22086 (Novozymes, Denmark) and an endo-xylanase NS-22083 (Novozymes, Denmark). The enzymatic treatment was done at 45 °C, for 2 h, at 120 rpm stirring speed, using 5.00% and 0.25% (w/w) cellulase and endo-xylanase, respectively. The pH of the biomass was not modified. The enzymatically hydrolyzed materials were studied by temperature sweep.

2.2.4.5 Temperature sweep (*T*-sweep)

The determination of the gelation capacity was done using the protocol described by Rodriguez & Beyrer (2023) with minor modifications. Briefly, the apparent viscosity μ_{app} as a function of temperature and time was obtained using a modular compact rheometer (MCR) model 302 (Anton Paar, Austria) equipped with an electrically heated temperature device, a counter-cooling concentric cylindrical system of 26 mm (C-ETD 160/ST) and a three-blade stirrer (ST24) measuring system. The *Cv* preparations were directly used at a DM of 14% (w/w) or diluted/rehydrated to 10.5% (w/w) with deionized water for better comparison with C2-H-S (due to DM reduction during centrifugation). The preparations were heated from 20 °C to 95 °C, held at this temperature for 5 min, and subsequently cooled to 20 °C. The heating and cooling rates were set at 6 °C/min and the stirring speed at 160 rpm. Data were obtained from the RheoCompass® software and firmware (Anton Paar, Austria) and treated to determine the initial viscosity $\mu_{app,\ initial}$, final viscosity $\mu_{app,\ final}$, and onset temperature

T_{onset}. Additionally, the peak viscosity $\mu_{app,\ peak}$ during the heating interval was also determined and used to compare the gelation capacity between the different preparations.

2.2.4.6 Gel preparation

PPI-*Cv* gels were prepared by thermal-mechanical treatment (Tanger et al., 2020) following the method used by Rodriguez & Beyrer (2023) with minor modifications. The minimal gelling concentration of pea protein was reported to be close to 12% (Batista et al., 2011), therefore aqueous dispersions of higher DM were prepared. 17% DM (w/w) dispersions of 90% (w/w) PPI and 10% (w/w) *Cv* preparation (C2, C2-H, C2-H-S or C2-H-D) were stirred at 400 rpm for 5 min to ensure homogeneity. 100% PPI was taken as a reference. The dispersions were heated to obtain PPI-*Cv* gels using a MCR 302 (Anton Paar, Austria) equipped with a pressure cell (C-ETD 160/ST) and a three-blade stirrer (ST24-Pr) measuring system. Compressed air at 0.2 MPa was used to prevent burning above 100 °C. The dispersions were first mixed at 400 rpm for 30 s, followed by a stabilization interval at 160 rpm for 60 s. The dispersions were subsequently heated from 20 °C to 120 °C at 7.9 °C/min, held at this temperature for 300 s, and then cooled down to 20 °C at 7.9 °C/min. All three steps were performed with a rotational speed of 160 rpm. The formed gels were stored at 4 °C for 24 h before their characterization.

2.2.4.7 Amplitude sweep

Amplitude sweeps were performed to characterize the obtained gel preparations. A modular compact rheometer (MCR) model 302 (Anton Paar, Austria) fitted with Peltier temperature devise (P-PTD200/56), plate-plate geometry and PP25 measuring system was used. Samples were placed onto the lower plate and compressed between the plates up to a gap of 1 mm. Strain amplitude sweeps were performed at increasing deformation from 0.01% to 100% (logarithmic ramp), with a constant angular frequency of 3 rad/s and constant temperature of 20 °C. RheoCompass® software and firmware (Anton Paar, Austria) provided the storage modulus *G'* (Pa), loss modulus *G"* (Pa), and shear stress *τ* (Pa) values for further analysis. For determining the linear viscoelastic (LVE) region, a limit of 3% of deviation of *G'* was used.

2.2.4.8 Confocal laser scanning microscopy (CLSM)

CLSM was used to visualize the microstructure of fresh gels. The gels were spread on a glass slide and stained with 0.002% Rhodamine B solution with ratio water:dye of 1:5 (v/v) (Sigma-Aldrich GmbH, Germany) over 24 h. The samples were analyzed with a CLSM type

510 (Carl Zeiss AG, Germany) using a 543-laser line. Images were taken at a magnification of 20 times and analyzed with LAS X software (version 4.5.25531) from Leica Microsystems CMS Gmbh (Germany).

2.2.5 HMEC

To test the applicability of *Cv* in PPI meat substitutes, the homogenized *Cv* biomass was added either in liquid form; C2-H and C2-H-S (soluble fraction), or in powder form; C2-H-D. The extrusion set-up was such that the final concentration of *Cv* in the extrudate was 10% (w/w) DM. To achieve this, C2-H and C2-H-S were diluted with demineralized water before extrusion. C2-H-D and PPI were mixed for 15 min with a MP50 screw mixer (Prodima Mixers SA, Switzerland) at the maximum speed. 100% PPI was taken as a reference. Meat substitutes were produced using a Clextral Evolum 25 twin-screw extruder (Clextral, Firminy, France) which has a screw diameter of 25 mm and a length/diameter ratio of 40. The barrel temperatures of the ten sections were set at 30, 50, 70, 90, 100, 120, 120, 125, 125 and 125 °C respectively. The screw speed was set at 240 rpm. A novel and patented rotating cooling die was coupled to the extruder (Beyrer et al., 2020). This rotating die consists of a rotating inner cylinder and a static outer cylinder, which enables well-defined shear in the cooling die (Snel et al., 2022). The rotating speed of this inner cylinder was set at 9 rpm, and the temperature at 85 °C. A twin-screw gravimetric feeder type KCM (K-tron, Niederlenz, Switzerland) was used to feed the dry ingredients into the extruder. Water, or diluted C2-H or C2-H-S, was injected in the second section with a peristaltic pump. Feeding rates were corrected to obtain a final moisture content in the extrudate of 58% and a total throughput of 15 kg/h. Samples were collected in plastic bags, sealed, and immediately frozen in a blast freezer (Electrolux, Sweden).

2.2.6 Meat substitutes characterization

The extrudates were defrosted overnight at ambient temperature (22 ± 2 °C) before the analysis. Moisture content was measured as a control with a rapid moisture analyzer (HC103 Mettler-Toledo, USA) at the conditions of 150 °C, initial mass of 2.5 g and stop criteria of 1 mg/50 s. The extrudates were cut into 2 mm-thick slices before the measurements. The crude nitrogen content of the meat substitutes was determined by the Kjeldahl method. A conversion factor of 5.5 was used to calculate the protein content. This conversion factor is appropriate for pea protein (Schlangen et al., 2022). The inner texture of the extrudates was exposed by making a small inclination with a sharp knife in the

direction of the flow (out of the die) and samples were broken along this cut. Pictures were taken with a digital camera (Nikon DS).

2.2.6.1 Texture profile analysis (TPA)

TPA was performed using a TA-XT2 texture analyzer (Stable Micro Systems, Surrey, UK) equipped with a 50 kg load cell. The samples were cut into cylinders of 20 mm in diameter and a height of 1 cm. Subsequently, samples were compressed twice with a 60 mm probe to 30% of the original height with a test speed of 1 mm/s and a waiting time between the two compressions of 5 s. The peak maximum force at first compression was taken as the hardness (Meulleneti, 1998).

2.2.6.2 Anisotropy index (AI)

The AI was measured to determine the degree of fiber formation of the extrudates. The method is based on the continuous time random walk (CTRW) theory and was developed by Ranasinghesagara et al. (2006). The method has been described by Snel et al. (2022.). Briefly, a red LED (λ = 600 nm) coupled to an optical fiber (diameter = 400 µm) was directed at the 2 x 2 cm sample at a 45 ° angle. The light reflectance was imaged by a digital camera (Nikon DS) and the AI was calculated based on the deviation from a circular reflection pattern. For an isotropic sample, the AI = 1, meaning the light reflectance was a perfect circle. For an anisotropic sample, the AI > 1.

2.2.7 Statistical analysis

All the analytical measurements were done in either duplicate (n = 2) or triplicate (n = 3). For duplicates, results were expressed as individual numbers, while triplicates were expressed as average ± standard deviation (SD). Regarding statistical analyses, first normality distribution (Shapiro-Wilk test) and equal variance (Chi-square test for variance) were checked (p = 0.05). Statistical significance was estimated by one-way ANOVA, followed by Tukey's post-hoc test. Dunn's test and Welch's ANOVA were used when normality and equal variance were rejected, respectively. When both were rejected, a Kruskal-Wallis test was performed, followed by a Dunn's test for pairwise comparisons. P-values < 0.05 were considered statistically significant. All statistical tests were performed with the software OriginLab® 2022b (OriginLab Corporation, USA).

2.3 Results and discussion

2.3.1 Influence of HPH on the microalgae suspension properties

The optimal HPH conditions were identified based on the fraction of soluble protein, gelation capacity, and thermal degradation degree of the 14% DM *Cv* suspensions. The effect of the operating pressure (90, 120, 150 MPa), the initial product temperature (5, 10, 15, 20, 25 °C), the number of HPH passes (one or two) as well as the microalgae composition (C1, C2) were considered.

2.3.1.1 Influence of pressure

First, the HPH-triggered cell disruption was confirmed using microscopic imaging. Consequently, increased extracellular organic matter concentration with increasing pressure was observed in the continuous phase (Figure 2.2).

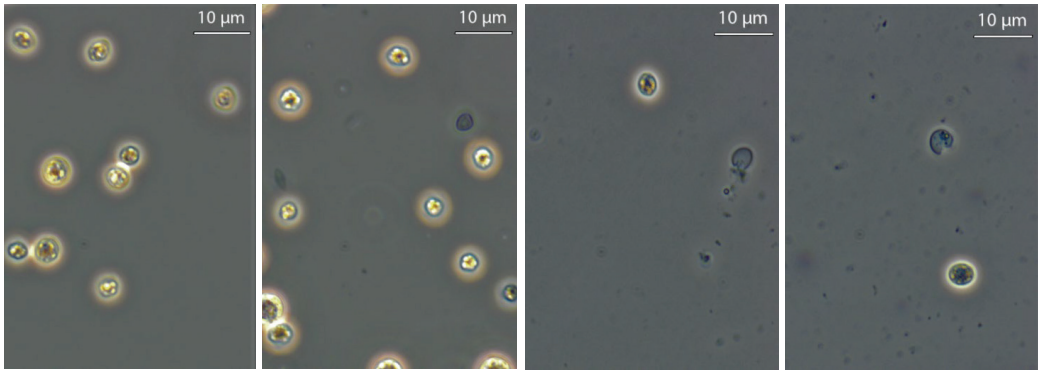

Figure 2.2: Microscopic images of untreated (C1) and microalgae suspensions treated at 90, 120 and 150 MPa (14% DM, 5°C, one pass) after dilution 100 times and magnification 40 times. From left to right: C1, C1-H-90, C1-H-120 and C1-H-150. C1: *Chlorella* batch 1, H: homogenized. Scale = 10 µm.

The fraction of soluble protein and the DM in the soluble fraction were measured for validation (Table 2.1). After HPH at 150 MPa, the respective values increased from 17.6 ± 0.2 (C1, untreated) to 25.3 ± 0.6% (C1-H-150), and from 3.3 to 5.0%. Spiden et al. (2013) used cell counting to quantitatively measure the cell disruption of *Chlorella* species (sp.) after HPH and found a yield of 50% at 107 MPa. Considering the higher pressure applied (150 MPa), we assumed a yield of cell disruption > 50% and, consequently, we were expecting a higher fraction of soluble protein (> 25.3%). The protein might stick to the cell debris or be organized in granules, explaining the observation.

Table 2.1: Chemical and thermal properties of intact and HPH-treated *Cv* suspensions. Fraction of soluble protein values are presented as average ± SD (n = 3), thermal properties are expressed as individual numbers (n = 2). The different letter means a significant difference $p < 0.05$. C1: *Chlorella* batch 1, H: homogenized, DM: dry matter

Samples	Chemical properties		Thermal properties			
	Fraction of soluble protein (% w/w)	DM in the soluble fraction (% w/w)	ΔH_1 (J/g DM)	$T_{peak,1}$ (°C)	ΔH_2 (J/g DM)	$T_{peak,2}$ (°C)
C1	17.6 ± 0.2[a]	3.3	1.6 / 1.8	63.9 / 64.1	0.1 / 0.4	90.4 / 94.8
C1-H-90	20.8 ± 0.1[b]	3.6	2.1 / 2.3	63.8 / 64.1	0.1 / 0.4	84.1 / 93.7
C1-H-120	22.8 ± 0.6[b]	4.0	2.3 / 2.3	63.9 / 63.9	0.2 / 0.8	92.1 / 93.5
C1-H-150	25.3 ± 0.6[c]	5.0	2.1 / 2.5	63.6 / 63.7	0.2 / 0.9	91.3 / 91.9

1 and 2 refer to the two main thermal events at 63.7 – 64.0 and 88.9 – 92.8 °C, respectively
The initial protein content (NPCF = 4.21) of the suspensions was obtained from the SQTS analysis.

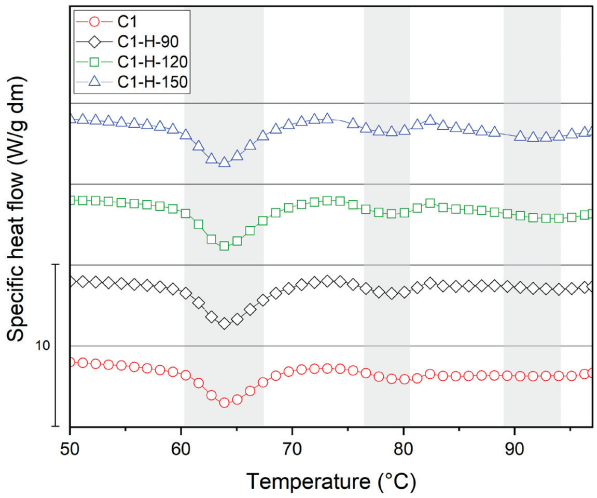

Figure 2.3: DSC thermograms of intact and HPH-treated suspensions (n = 2). C1: *Chlorella* batch 1, H: homogenized.

DSC was performed to evaluate the effect of HPH on the degree of modification of the *Cv* suspensions after HPH treatment. The reaction enthalpy was similar for untreated and HPH-treated suspensions at different pressures (Table 2.1, Figure 2.3), indicating that the applied HPH at the selected process conditions did not thermally degrade the *Cv* components. The thermal denaturation temperature, $T_{peak,1}$, of the *Cv* was detected at 64 °C (Table 2.1). Wagmare et al. (2016) reported a similar thermal denaturation temperature (60.1 °C) for *Chlorella pyrenoidosa*, mainly attributed to protein denaturation (78.1% (w/w) protein concentration), whereas Ahmed & Kumar (2022) found a temperature of 56.9 °C for *Cv*, associated with the denaturation of both proteins and carbohydrates. Moreover, other minor endothermic peaks were detected between 78 – 79 °C and 88.9 – 92.8 °C (Figure 2.3) suggesting that different fractions of biomolecules could be present. Furthermore, a second

DSC cycle revealed no peak confirming that these three thermal events were irreversible (data not shown).

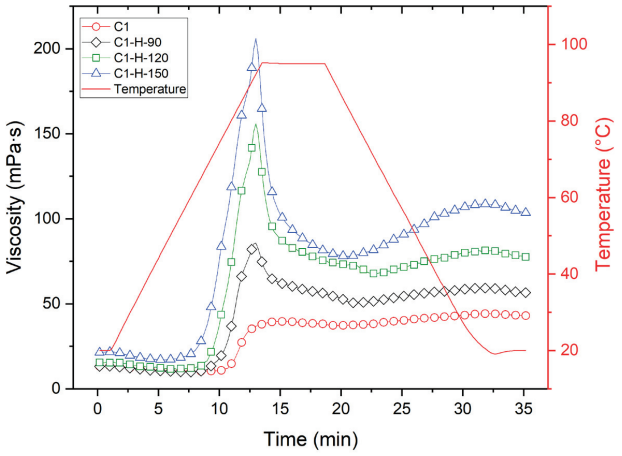

Figure 2.4: *T*-sweep viscosity curves of intact (C1) and HPH-treated suspensions (C1-H-90, C1-H-120, C1-H-150) at 14% DM (n = 3). The full red line indicates the temperature profile. C1: *Chlorella* batch 1, H: homogenized.

T-sweeps were carried out to determine the heat-induced gelation capacity of the *Cv* suspensions (Figure 2.4). In general, a minimum temperature of 62 °C or T_{onset} was required to induce a viscosity increase, which is also the onset value observed in the DSC. The T_{onset} was higher for the intact cells (76 °C) compared to the HPH-treated cells (62 – 67 °C), indicating a restricted impact on rheological phenomena when intracellular components are inside the cells. Upon heating, the apparent viscosity increased rapidly reaching a peak viscosity $\mu_{app,peak}$, which was detected at 92.2 °C (Table 2.2).

Table 2.2: Gelation properties of C1 and C2 before and after processing as measured with a *T*-sweep. Values are presented as averages ± SD (n = 3). The different letter means a significant difference $p < 0.05$. C1: *Chlorella* batch 1, C2: *Chlorella* batch 2, H: homogenized, S: soluble fraction, D: spray-dried

Samples	Pressure (MPa)	DM (% w/w)	$\mu_{app,\ initial}$ (mPa·s)	$\mu_{app,\ peak}$ (mPa·s)	T_{onset} (°C)	T_{peak} (°C)	$\mu_{app,\ final}$ (mPa·s)
C1	/	14	13.2 ± 0.3^{a}	36.9 ± 0.9^{a}	76	/	43.0 ± 0.6^{a}
C1-H-90	90	14	13.3 ± 0.2^{a}	85.7 ± 2.7^{b}	67	92.2	56.5 ± 1.1^{ab}
C1-H-120	120	14	15.5 ± 0.6^{b}	156.0 ± 9.3^{c}	67	92.2	77.6 ± 1.7^{ab}
C1-H-150	150	14	21.4 ± 1.4^{c}	206.0 ± 7.6^{d}	62	92.2	103.5 ± 2.5^{b}
C2	/	14	28.0 ± 0.2	36.7 ± 0.8	95.0	/	50.6 ± 0.4
C2-H	150	14	44.6 ± 1.2	404.6 ± 29.9	80.2	91.2	287.0 ± 17.5
C2-H	150	10	21.2 ± 0.8^{A}	145.6 ± 14.3^{A}	59.2	91.2	104.8 ± 5.0^{A}
C2-H-S	150	10	26.0 ± 0.4^{B}	108.7 ± 8.3^{B}	63.2	95.3	89.0 ± 2.2^{A}
C2-H-D	150	10	20.2 ± 0.6^{A}	118.6 ±1.9^{C}	63.2	95.0	91.7 ± 1.1^{A}

μ_{app} refers to the apparent viscosity, T_{onset} the onset temperature and T_{peak} the temperature at which μ_{app} is maximal

Looking at the $\mu_{app,peak}$ of the different treated *Cv* suspensions (Table 2.2), these values increased by at least a factor of two and up to a factor of five with increasing HPH pressure. Additionally, the final viscosity also increased by a factor of two and half (Table 2.2). The intracellular released proteins in combination with cell wall debris and other polysaccharides might swell and hydrate, gaining volume resulting in viscosity increase when reaching a temperature close to 64 °C. At 92 °C, the swollen granules might burst, reducing the viscosity, typically indicating the capacity of these granules to hold water as observed for corn starch (Rincon-Londono et al., 2016). Upon cooling, the viscosity starts to increase again, suggesting cross-linking between the different components, possibly proteins and polysaccharides. Similar viscosity curves were obtained for mixtures of chickpea starch and protein-rich fraction (Sayar et al., 2005). Bernaerts et al. (2017) also compared the viscosity (10.5 s^{-1}, 25 °C) between intact and HPH-treated *Cv* suspensions (8% DM, pH 6) at 100 MPa, one pass, and 4 °C. Although values were not significantly different, the authors measured a viscosity increase of a factor two after thermal treatment (121 °C, 5 min). In this study, results confirm that HPH treatment is essential to improve the heat-induced gelation properties of *Cv* suspensions, as observed with the increase in $\mu_{app,peak,}$ triggered by released intracellular components upon cell disruption.

From Table 2.2, a positive and linear correlation between the operating pressure and $\mu_{app,peak}$ (R^2 = 0.99) was obtained (Figure 2.A.1, Table 2.A.1). Similarly, Magpusao et al. (2021) detected a linear dependency of HPH pressure and cell disruption for *A. platensis, Isochrysis* sp.*,* and *Tetraselmis* sp. The authors explained their findings by an increase in dynamic viscosity detected in an isothermal measurement (0.1 s^{-1}, 20 °C) after HPH at 30, 60 and 90 MPa. From the linear regression and the intercept with the pressure axis, we estimated a critical pressure of 64 MPa for the HPH treatment to sufficiently disrupt the cells and enhance the heat-induced gelation capacity of 14% DM *Cv* suspensions.

2.3.1.2 Influence of the initial temperature and number of passes

Besides pressure, the effects of the initial product temperature (Table 2.A.3) and a second HPH pass were studied. HPH treatment at 150 MPa and one pass was applied on C1 at initial temperatures of 5, 10, 15, 20 and 25 °C. From Equation 2.4, an initial temperature equal to or above 25 °C was expected to result in a process temperature of 64 °C or higher, which is sufficient to induce thermal degradation in C1 as seen from the DSC results (Table 2.1). The highest $\mu_{app,peak}$ value (at 92.2 °C) was obtained for the HPH-treated suspension at an initial temperature of 5 °C (210 mPa·s) (Table 2.A.3). Results show a tendency for

lower $\mu_{app,peak}$ when higher initial temperatures are used. A gelation capacity reduction of up to 50% at 25 °C initial temperature (120 mPa·s) was observed when compared to 5 °C initial temperature. In conclusion, if thermal induced effects, such as a first protein denaturation step, are triggered by HPH, the gelation capacity will be reduced due to a lower protein solubility (Rodriguez & Beyrer, 2023). To prevent such reduction after HPH at 150 MPa and one pass, an initial temperature of 10 °C or lower is recommended. Finally, a second HPH pass at 150 MPa and 5 °C initial temperature was tested. The fraction of soluble protein and DM in the soluble fraction increased with the second pass and reached 35.8 ± 1.2 and 6.4%, respectively. However, $\mu_{app,peak}$ was not increased with the second pass (from 206.0 to 197.6 mPa·s). Thus, the optimal HPH conditions were found to be a pressure of 150 MPa, one pass, and 5 – 10 °C initial temperature to achieve sufficient cell disruption while avoiding thermal degradation and consequently optimizing the gelation capacity.

2.3.1.3 Influence of the composition of different microalgae batches

The biomass C1 and C2 were available in limited quantities. Pilot scale trials on HMEC were performed with C2, while C1 was used for optimization of DSP, and HPH specifically. For consistency and conclusiveness, some reference values are used to compare C1 and C2. The crude composition of C1-H-150 and C2-H is different, specifically C2-H has a higher protein (+ 4%) and carbohydrate content (+ 2%) (Table 2.3). On the other hand, the lipid content is reduced in C2-H (– 9%). This can be explained by differences in the fermentation process and suggest a process control improvement.

Table 2.3: Crude composition of HPH-treated *Cv* suspensions in % (w/w) and sodium content (mg/kg, wet basis). DM content of the suspensions was 14%. C1: *Chlorella* batch 1, C2: *Chlorella* batch 2, H: homogenized, NPCF: nitrogen-to-protein conversion factor

Samples	pH (-)	Protein (% w/w) (NPCF = 4.21)	Lipid (% w/w)	Carbohydrate (% w/w)	Sodium (mg/kg)
C1-H-150	6.4	36.6	25.8	29.6	110
C2-H	5.4	40.7	16.7	32.0	290

The values were analyzed by an ISO certified, external laboratory (SQTS)

The initial, peak, and final viscosities of homogenized C2 (C2-H) are twice those of C1 (C1-H-150) at the same DM concentration (Table 2.2). This can be explained by the higher protein and carbohydrate content of C2-H, but also with the lower pH of 5.4, which is close to the isoelectric point of *Cv* protein (4.5 – 5.5) (Ursu et al., 2014), where the protein net charge and electrostatic repulsion are minimal and protein aggregation is favored. The homogenization effect on the viscosities has the same trend for both batches, C1 and C2, but is more pronounced for C2 (Table 2.2). This could be once again due to the higher protein

and carbohydrate content. Also, the presence of fat reduces the hydrophilicity of the substrate and negatively affects crosslinking of biopolymers upon heating or cooling (Magpusao et al., 2021). C1 contains more fat, and 2.8 times lower final viscosity. It is interesting to mention that HPH enhanced the gelation capacity of both *Cv* suspensions despite their different compositions and pH. This suggests and confirms that HPH is indeed a robust cell wall disruption process, independently of possible batch variations. Besides composition and pH, the pre-handling of the biomass (concentration, freezing and dilution with demineralized water) may influence the disruption and consequently the *Cv*'s gelation properties.

2.3.2 Influence of further DSP steps on the gelation capacity

In general, DSP of microalgae includes centrifugation for separation of biomass from the fermentation broth, concentration of the biomass, and drying to obtain microbiologically stable products, as well as sometimes for protein extraction to obtain powdered microalgae protein isolates (Grossmann et al., 2020). Such processing is expected to impact the gelation capacity of microalgae ingredients. Two different DSP steps were performed after HPH, namely centrifugation and spray drying, and their effect on the gelation capacity was studied.

Upon centrifugation, the DM of the suspension was reduced from 13.8 ± 0.0% (C2-H) to 10.7 ± 0.1% (C2-H-S), however, the protein content and the nitrogen/carbon ratio were almost not affected (data not shown). In the *T*-sweep test, the C2-H-S showed significantly lower peak viscosity compared to C2-H at the same DM content (10% (w/w)) (Table 2.2). This might suggest that the insoluble fraction also contributes to the increase in the viscosity at heating. The aggregation of intact cells and cell wall material has previously been observed and can be explained by the presence of anionic particles in cell wall polysaccharides, such as sulfate groups and uronic acids (Bernaerts et al., 2017, 2018). Such anionic polymers can gel in the presence of salt, which was detected in the diluted suspension at a level of 220.7 mg sodium/kg (Table 2.3). To better understand the role of polysaccharides upon heat-induced gelation, a *T*-sweep was performed after enzymatic hydrolysis. C2-H was incubated with a cellulase complex as well as with an endo-xylanase. The $\mu_{app,\ peak}$ was reduced from 145.6 ± 14.3 to 103.3 ± 0.7 mPa·s, confirming that the peak viscosity is influenced by the presence of polysaccharide molecules.

Next to centrifugation, C2-H was also spray-dried at the pilot scale. The $\mu_{app,peak}$ of the C2-H reduced significantly from 145.6 ± 14.3 to 118.6 ± 1.9 mPa·s (Table 2.2) after spray drying. Drying (T > 100°C) might denature proteins and thus reduce the solubility during rehydration of the powder (Safi et al., 2013; Soto-Sierra et al., 2018). From these results, we conclude that the improvement of the gelation capacity triggered by the HPH treatment was partially diminished by further DSP. Thus, we anticipate higher gel strength of PPI:*Cv* blends when using HPH-treated *Cv* compared to gels made with untreated *Cv* or HPH-treated *Cv* submitted to further centrifugation or spray drying steps.

2.3.3 Influence of *Cv* addition on the rheological properties of heat-induced PPI gel

Amplitude sweeps were performed to better understand how the incorporation of HPH-treated *Cv* influenced PPI gel characteristics. Within the LVE region and up to the cross-over point, all preparations showed a *G'* > *G"* (Figure 2.5) indicating a viscoelastic gel or solid behavior (Mezger, 2014). The yield point at the end of the LVE region was detected at a strain 2.4 – 2.8% for the PPI-*Cv* gels, and 5.6% for the PPI gel (data not shown) suggesting a more brittle structure for PPI-*Cv* gels. Similarly, the *G'* plateau value at the LVE region was significantly reduced (60.8%) compared to PPI gel when substituting PPI with untreated biomass (PPI:C2) (Table 2.4). This *G'* reduction was not significant when HPH-treated biomass (PPI:C2-H) was used instead. The effect of HPH treatment on *G'* of microalgae has been shown previously (Ahmed & Kumar, 2022; Bernaerts et al., 2018; Nunes et al., 2020). Nunes et al. (2020) did a similar experiment where untreated *Cv* and HPH-treated *Cv* (at 340 MPa) were added to wheat dough observing that the overall *G'* decreased upon 1% (w/w) *Cv* addition, however, this decrease was less significant when using HPH-treated *Cv*. Similarly, Ahmed & Kumar (2022) observed an increase in *G'* of more than 1 log when *Cv* was treated with HPH, and Bernaerts et al. (2017) a four-time *G'* increase after HPH and thermal treatment of *Cv*. They attributed these findings to the effective cell disruption from the HPH treatment and the subsequent release of intracellular material, and protein aggregation after thermal treatment. These results correspond as well to the observations in viscosity increase (Section 2.3.1) after heat-induced gelation of the HPH-treated *Cv*.

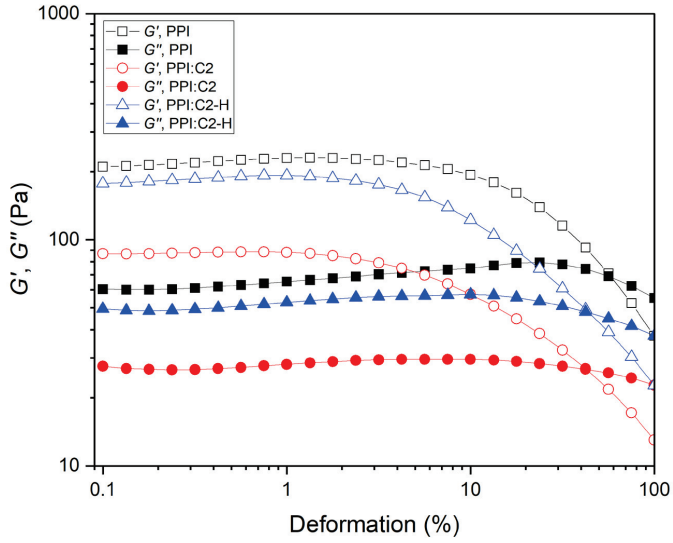

Figure 2.5: Storage *G'* and loss modulus *G''* of PPI and PPI-*Cv* gels (17% DM) (n = 3). PPI: pea protein isolate, C2: *Chlorella* batch 2, H: homogenized.

Removing the insoluble fraction in the centrifugation step (PPI:C2-H-S), resulted in a significant reduction (37%) of *G'*. However, the major gelling effect was provided by the soluble fraction. Also, spray-drying the whole homogenized biomass (PPI:C2-H-D) reduced the gelling ability by 38% compared to the non-homogenized, non-dried biomass. This could be possibly due to additional protein denaturation effects (Table 2.4). These values are in between the addition of fresh (C2, 60.8%) and wet HPH-treated biomass (C2-H, 16.0%) and correlate well with our previous observations that HPH alone was more prone to enhance gelation compared to further centrifugation or spray drying steps (Section 2.3.2). However, for all forms of *Cv*, the yield strain was reduced in a similar magnitude indicating that adding 10% (w/w) of *Cv* to PPI results in a more brittle gel, independent of the *Cv* treatment or DSP.

Table 2.4: Average storage modulus *G'* and loss modulus *G''* at the LVE region. Values are presented as averages ± SD (n = 3). The different letter means a significant difference $p < 0.05$. PPI: pea protein isolate, C2: *Chlorella* batch 2, H: homogenized, S: soluble fraction, D: spray-dried

Samples	*G'* at LVER (Pa)	*G''* at LVER (Pa)	Relative reduction of *G'* (%)
PPI	221.7 ± 6.9^{a}	64.9 ± 1.4^{a}	0.0
PPI:C2	86.9 ± 2.0^{b}	27.6 ± 0.5^{b}	60.8
PPI:C2-H	186.1 ± 19.6^{ac}	51.2 ± 3.7^{ac}	16.0
PPI:C2-H-S	140.5 ± 7.8^{c}	41.0 ± 1.9^{c}	36.7
PPI :C2-H-D	139.0 ± 18.5.3^{bc}	39.8 ± 4.9^{bc}	38.5

CLSM was done on PPI, PPI:C2 and PPI:C2-H gels to analyze their microstructure (Figure 2.6). The significant reduction of gel strength as a result of the addition of untreated *Cv* (C2) (60.8%) can be explained by a transition from a mono- toward a bi-phasic gel. Indeed, in the

PPI:C2 gel, pea protein aggregates (30 – 50 µm) were separated by a phase containing intact *Cv* cells (2 – 10 µm). In contrast, the microstructure of PPI:C2-H gel showed a more homogenous phase, like PPI gel, and therefore the least *G'* relative reduction (16.0%).

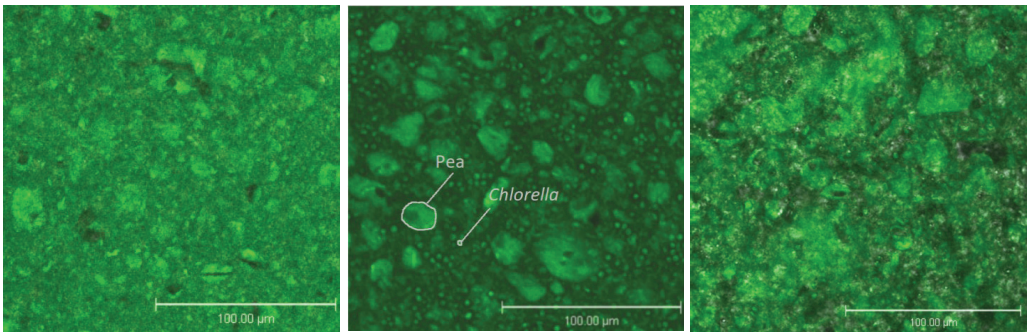

Figure 2.6: Gels' microstructure obtained by CLSM imaging. From left to right: PPI, PPI:C2 and PPI:C2-H gels after staining with Rhodamine B solution. PPI: pea protein isolate, C2: *Chlorella* batch 2, H: homogenized. Scale: 100 µm.

2.3.4 HMEC application

PPI and PPI-*Cv* meat substitutes were produced by HMEC and compared in terms of color, texture, and anisotropy. The addition of 10% (w/w) HPH-treated *Cv*, either in liquid or spray-dried forms, did not lead to instabilities during HMEC. The final moisture and protein content of the extrudates were reduced upon *Cv* addition (Table 2.5). This decrease was significant for extrudates PPI:C2-H and PPI:C2-H-D. The lower protein content in the PPI-*Cv* extrudates could be expected since the protein content of *Cv* (40.7% (w/w)) was approximately two times lower than in PPI. Visual observations showed no clear difference between the samples, although the PPI extrudate looked more fibrous and PPI:C2-H-D seemed slightly more yellow (Figure 2.7).

Despite the clear differences in *G'* observed previously after 10% (w/w) *Cv* incorporation in PPI gels (Section 2.3.3), no significant effect on hardness or AI was observed in the extrudates (Table 2.5). This is probably due to the much higher DM content of the extrudates, resulting in a more jammed gel, instead of the soft gel obtained at 17% DM as tested with rheology. In this jammed gel, *Cv* probably acts as a filler. This has been shown before for undisrupted microalgae and pea protein gels (Batista et al., 2011). Palanisamy et al. (2019) observed a similar effect for the addition of 15% dried *A. platensis* to lupin meat substitutes, for which no significant difference in cutting strength was measured. Apart from hardness, cohesiveness, springiness, and chewiness of the samples were also not significantly different (data not shown). Furthermore, the AIs were all above 1 and not significantly

different (Table 2.5), indicating that the anisotropic meat substitutes showed similar level of fibrousness.

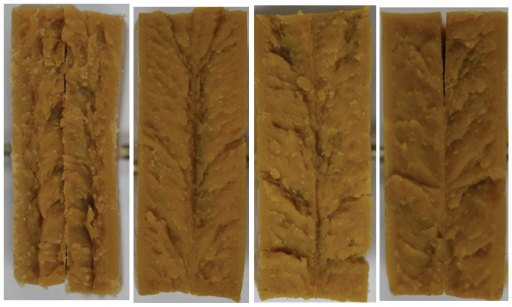

Figure 2.7: Visual appearance of meat substitutes after revealing the inner texture by folding the samples open. From left to right: PPI, PPI:C2-H, PPI:C2-H-D, PPI:C2-H-S. PPI: pea protein isolate, C2: *Chlorella* batch 2, H: HPH treatment, S: soluble fraction, D: spray-dried.

Table 2.5: Moisture content (% w/w) and protein content (% w/w, wet basis), hardness (N) and anisotropy index of PPI meat substitutes produced with *Cv*. Values are presented as averages ± SD (n = 3) or individual numbers (n = 2). Different letters indicate different significant groups $p < 0.05$. PPI: pea protein isolate, C2: *Chlorella* batch 2, H: HPH treatment, S: soluble fraction, D: spray-dried

Samples	Moisture content (% w/w)	Protein content (% w/w)	Hardness (N)	Anisotropy index (-)
PPI	58.0 ± 0.5^{a}	34.0 / 34.1	113.6 ± 16.0^{a}	1.19 ± 0.02^{a}
PPI:C2-H	57.2 ± 0.1^{b}	30.7 / 31.4	115.5 ± 2.8^{a}	1.13 ± 0.02^{a}
PPI:C2-H-S	57.5 ± 0.2^{ab}	31.5 / 31.9	112.0 ± 2.3^{a}	1.16 ± 0.02^{a}
PPI :C2-H-D	57.1 ± 0.3^{b}	30.1 / 31.5	107.6 ± 1.7^{a}	1.15 ± 0.02^{a}

2.4 Conclusions and perspectives

HPH-treated biomass from yellow *Cv* was studied as an ingredient for meat substitutes produced by HMEC. Optimal conditions for HPH were found at an operating pressure of 150 MPa and an initial product temperature below 10 °C. The heat-induced gelation capacity of both untreated and HPH-treated *Cv* suspensions was monitored by *T*-sweep measurements. We observed an up to ten-time increase in peak viscosity for HPH-treated, compared to the untreated *Cv* biomass. It is suggested that both soluble (released intracellular materials such as proteins) and insoluble fractions contribute to the development of viscosity upon heating. The positive impact of cell disruption by HPH on controlling PPI-*Cv* gels' structure was confirmed by strain sweeps and CLSM. Additional removal of insoluble matter from the *Cv* biomass or drying steps after HPH treatment did not lead to improved properties. The addition of 10% (w/w) HPH-treated *Cv*, wet or dry, to pea meat substitutes did not lead to significant differences in hardness, visual appearance or anisotropy index. HPH-treated *Cv* biomass is an interesting ingredient to consider when designing sustainable and nutritious plant-based meat substitutes.

2.5 Appendices

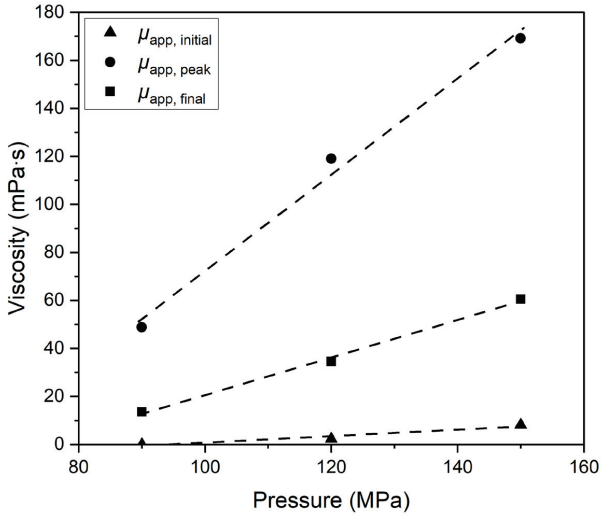

Figure 2.A.1: Linear regression analysis between pressure and initial, peak, and final viscosity. Values were obtained after subtracting μ_{app} of intact cell suspension. The intercept with the x-axis indicates the critical pressure of the cell disruption.

Table 2.A.1: Regression analysis parameters

	Viscosity		
	Initial	**Peak**	**Final**
Slope (mPa·s/MPa)	0.1	2.0	0.8
Critical pressure (MPa)	94.3	64.0	73.8
R^2	0.94	0.99	1.00

Table 2.A.2: Amino acids composition of C1 biomass

Amino acids	**Content (g/100 g powder)**	**Amino acids**	**Content (g/100 g powder)**
Alanine	1.53	Lysine	1.07
Arginine	9.99	Methionine	0.33
Aspartic acid	3.55	Phenylalanine	0.60
Cystein+Cystine	0.18	Proline	0.61
Glutamic acid	2.95	Serine	0.83
Glycine	0.80	Threonine	0.75
Histidine	0.35	Tryptophan	0.24
Isoleucine	0.51	Tyrosine	0.49
Leucine	1.21	Valine	0.92

Table 2.A.3: Initial and calculated (Equation 2.4) process temperatures at HPH treatment. $\mu_{app, peak}$ corresponds to the viscosity at 92.2 °C. Values are presented as individual numbers (n = 2)

T_{in} (°C)	T_p (°C)	$\mu_{app, peak}$ (mPa·s)
5	34	209.0 / 211.5
10	39	146.9 / 150.2
15	54	168.6 / 169.3
20	59	170.8 / 171.5
25	64	119.6 / 120.9

3



Pulsed electric field treatment for preservation of *Chlorella* suspensions and retention of gelling capacity

This chapter is published as:

De Gol, C., Moodycliffe, A., Den Besten, H. M. W., Zwietering, M. H., & Beyrer, M. (2024). Pulsed electric field treatment for preservation of Chlorella suspensions and retention of gelling capacity. Food Research International, 182, 114154. https://doi.org/10.1016/j.foodres.2024.114154

Abstract

Pulsed electric field (PEF) processing has emerged as an alternative to thermal pasteurization for the shelf-life extension of heat-sensitive liquids at industrial scale. It offers the advantage of minimal alteration in physicochemical characteristics and functional properties. In this study, pilot-scale continuous PEF processing (T_{outlet} < 55 °C) was applied to microalgae *Chlorella vulgaris* (*Cv*) suspensions (pH = 6.5), which was proposed as a functional ingredient for plant-based foods. *Cv* suspensions were inoculated with three distinct food spoilage microorganisms (*Pseudomonas guariconensis*, *Enterobacter soli* and *Lactococcus lactis*), isolated from the *Cv* biomass. PEF treatments were applied with varying electric field strength E_{el} of 16, to 28 kV/cm, pulse repetition rate f of 100 to 140 Hz, with a pulse duration τ of 20 µs and an inlet product temperature T_{in} of 30 °C. The aim was to evaluate the PEF-induced microbial reduction and monitor the microbial outgrowth during a ten-day cold storage period (10 °C). Maximum inactivation of 4.1, 3.7 and 3.6 logs was achieved (28 kV/cm and 120 Hz) for the investigated isolates, respectively. Under these conditions, the critical electric field strengths E_{crit} above which inactivation was observed, ranged from 22.6 to 24.6 kV/cm. Moreover, repeated PEF treatment resulted in similar inactivation efficiency, indicating its potential to enhance shelf-life further.

3.1 Introduction

While consumers demand safe and fresh food with high quality and organoleptic properties, there is an urgent need to mitigate the food processing impact on the environment. In this context, pulsed electric field (PEF) technology has emerged as an alternative to traditional pasteurization methods for achieving non-thermal microbial inactivation in heat-sensitive liquid foods (Toepfl et al., 2006), preserving the physicochemical characteristics of the product, such as color or functionality. The PEF preservation of foods such as fruit or vegetable juices, milk, liquid egg, and nutrient broth have been intensively studied and gave satisfying results, where microbial inactivation was achieved at temperatures below 60 °C (Cavalcanti et al., 2023; Garner, 2019; Roobab et al., 2018; Witt et al., 2020). Typically, PEF pasteurization involves 1) gentle pre-heating (20 – 55 °C), 2) exposing the liquid to an external electric field E_{el} of 10 – 40 kV/cm, 3) cooling and 4) aseptic packaging (Alirezalu et al., 2020; Yan et al., 2021). An electrical field is generated by applying high-voltage short pulses (1 – 100 µs), with energy input ranging within 50 – 8000 kJ/kg (Timmermans et al., 2022). This process induces a loss of microorganism viability by inducing membrane electroporation. The outcome of electroporation, whether reversible or irreversible, depends on numerous variables, including electric field strength, treatment duration, temperature, microbial strain, media composition, pH, and conductivity (García et al., 2006, 2007; Schottroff et al., 2019; Wang et al., 2018). Consequently, the efficiency of inactivation and the capability of the microbial cells to survive and recover from the treatment are affected. The implications of this phenomenon go beyond food safety considerations. PEF application is also used to preserve microbial stability and extend the shelf-life of liquid products while maintaining their native properties (Schilling et al., 2008). Nevertheless, PEF encounters limitations (Arshad et al., 2021). The treatment of liquids with a neutral pH and protein-rich composition is challenging since proteins might accumulate on electrode surfaces (Meneses et al., 2017) or play a protective role in the inactivation of microorganisms (Jaeger et al., 2009a; Schottroff et al., 2019; Schottroff & Jaeger, 2020). Recently, Alzahrani et al. (2022) investigated the preservation of neutral plant-based protein liquids containing whey protein concentrate and soy protein isolate. Furthermore, prior studies showed the advantages of PEF over thermal treatments in retaining the properties and nutritional quality of plant-based beverages (Elez-Martínez et al., 2017; Picart-Palmade et al., 2019). Nevertheless, to the best of the authors' knowledge, the application of PEF for the non-thermal pasteurization of neutral microalgae suspensions remains unexplored. This study introduces a novel approach for the intermediate preservation of microalgae suspensions, intended for use in

subsequent food formulations, as illustrated in Figure 3.1. Recently, De Gol et al. (2023) successfully incorporated fresh microalgae into pea-based formulations, resulting in a nutritionally enhanced and structurally non-significantly modified meat substitute. By utilizing the microalgae in its liquid form and eliminating the drying process, the final product's environmental footprint is reduced. This aligns with ongoing efforts to develop more sustainable foods, particularly high-quality meat substitutes (Fu et al., 2021; Grahl et al., 2018; Van der Goot et al., 2016). However, liquids are more prone to spoilage than powder due to their high water activity. We hypothesized that applying PEF on such microalgae suspensions could yield sufficient microbial reduction and minimal microbial growth during chilled storage.

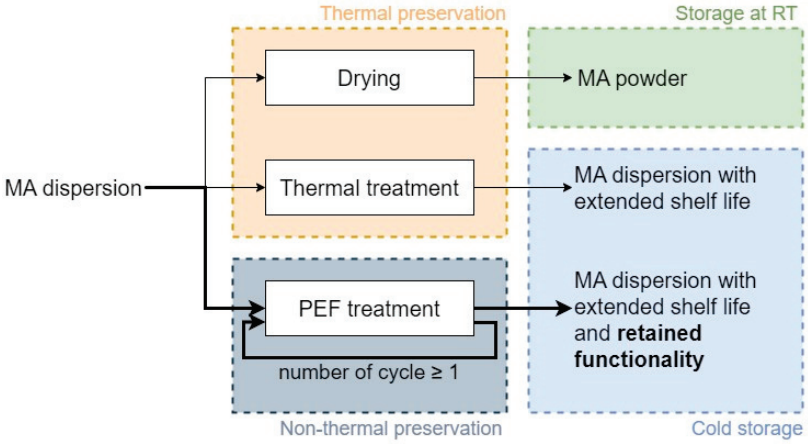

Figure 3.1: Preservation route proposed in this study (**tick arrows**) versus thermal processing (thin arrows). MA: microalgae, PEF: pulsed electric field, RT: room temperature.

3.2 Material and methods

3.2.1 Microalgal suspension

Microalgae were heterotrophically cultivated by Phycom (The Netherlands) using a patent-protected yellow *Chlorella vulgaris* (*Cv*) *UTEX 30* strain (Uran et al., 2021) and kindly donated by Alver AG (Switzerland). Directly after harvesting, the biomass was centrifuged for concentration, packed, frozen, and sent via refrigerated transport in insulated boxes (DHL Group, Germany). Microalgae biomass was received as a frozen slurry of 25.0 ± 0.2% dry matter (DM) and pH 6.4 ± 0.1. It was stored at – 20 °C until use and transferred to a cold room (4 °C) the day before the trial for defrosting. Moisture content was determined using a rapid moisture analyzer (HC103 Mettler-Toledo, Switzerland) at the conditions of 120 °C, initial mass of 2 g, and stop criteria of 1 mg/50 s. The biomass was diluted to 14% (w/w) DM with deionized water and used for characterizing its thermal properties (Sections 3.2.2.1 and

3.2.2.2). Additionally, the biomass was diluted to 2% (w/w) DM and pasteurized (85 °C, 5 min) using a custom-made tubular heat exchanger (three twisted tubes of 3 m long, 1 cm internal diameter). The pH and conductivity were measured using a pH/conductometer 914 (Metrohm, Switzerland). The variation of the conductivity at 2% (w/w) DM with temperature (20, 25, 30, 35, 40, 45, 50, 55 °C) was measured and expressed as:

$$\sigma(T) = \sigma_{\mathrm{R}} \cdot (1 + b_{\mathrm{R}} \cdot T) = 4 \cdot 10^{-4} \cdot (1 + 0.01 \cdot T) \quad \text{(S/cm)} \qquad (3.1)$$

With the referential conductivity σ_R (S/cm) and the temperature coefficient b_R (K^{-1}). Finally, the specific heat capacity c_p (kJ/(kg·K)) of the *Cv* suspension at 2% (w/w) DM was approximated using the compositional information provided by Alver AG (Switzerland) and Equation 3.2 (Kessler, 2002):

$$c_{\mathrm{p}} = 0.98 \cdot c_{\mathrm{p,water}} + 0.005 \cdot c_{\mathrm{p,carb}} + 0.011 \cdot c_{\mathrm{p,prot}} + 0.004 \cdot c_{\mathrm{p,fat}} = 4.13 \text{ (kJ/(kg·K))} \qquad (3.2)$$

With the specific heat capacity for water, carbohydrates, protein, and fat approximated to 4.2, 1.4, 1.6 and 1.7 kJ/(kg·K), respectively.

3.2.2 Thermal degradation of microalgae

3.2.2.1 Temperature sweep (*T*-sweep)

Thermal treatments followed by thermo-mechanical analysis were performed on functional microalgae suspensions, and the results were used to identify the temperature window for PEF trials. 14% (w/w) DM *Cv* suspensions were homogenized using a NS3006L ARIETE homogenizer (GEA Niro Soavi, Italy) (150 MPa, 5 °C, one pass) as described by De Gol et al. (2023) to enhance gelation capacity. A modular compact rheometer (MCR) model 302 (Anton Paar, Austria) equipped with a starch cell (C-ETD 160/ST) and a starch three-blade stirrer (ST24-2D/2V/2V-30) was used for thermal treatments. A solvent trap kit was used to minimize moisture loss during the measurements. The suspension was mixed at 160 rpm to ensure good homogeneity and heated at 20 °C/min up to the desired treatment temperature (50, 60, 70, 80 or 90 °C). The holding step was set for 30 s before cooling at 20 °C/min. The selected holding time was determined based on the duration required for the PEF-treated liquid to reach the cooling zone (20 s), with the inclusion of an additional safety margin (Section 3.2.8.3). The thermally treated suspensions were directly used for *T*-sweep measurements to study their functionality, i.e., gelation capacity. A similar protocol was reported before (Rodriguez & Beyrer, 2023). After reaching the equilibrium temperature at 20 °C, heating from 20 to 95 °C at a 6 °C/min heating rate, followed by a holding step at 95 °C for 5 min, and a cooling step back to 20 °C at 6 °C/min were performed. The

RheoCompass® software (Anton Paar, Austria) was used for data handling. The peak viscosity $\mu_{app,\ peak}$ during the heating interval was determined and used to compare the gelation capacity between the different thermally treated suspensions. The thermal treatments and *T*-sweep measurements were performed on the same *Cv* batch, in duplicates and on two different days.

3.2.2.2 Differential scanning calorimetry (DSC)

Heat-induced protein denaturation was determined by DSC using a µDSC7 evo microcalorimeter (Setaram Instrumentation, France), as explained by De Gol et al. (2023). Briefly, a standard Hastelloy cylinder was filled with a 14% (w/w) DM sample, and deionized water was used as the reference material. The system was purged with a constant nitrogen flow at around 0.1 MPa. The samples were scanned from 20 °C to 100 °C at a heating rate of 0.5 °C/min, held at 100 °C for 10 min, and subsequently cooled to 20 °C at the same rate. The Thermal Analysis® Software package V. 1.46 (Setaram Instrumentation) was used to evaluate the peak maximum temperature value, T_{peak}. The measurements were done on the same *Cv* batch in duplicate and on two different days.

3.2.3 Microorganism isolation and identification

The *Cv* suspension was diluted to 10% (w/w) DM with maximum recovery diluent (MRD) (peptone salt solution: 1.0 g enzymatic digest of casein and 8.5 g sodium chloride in 1 L water) (Biolife, Italy) to maintain the viability of organisms during dilution procedures and stored for six days in a constant climate chamber (10 °C) (ICH260 Memmert, Germany). Samples were collected at days 0, 3 and 6, serially diluted with MRD and inoculated on Petri dishes containing plate counting agar (PCA) (Biokar diagnostics, France). The plates were incubated at 10 °C for up to nine days. Single colonies with different colony morphology were selected in duplicate and purified (three subsequent streaking on PCA plates, incubation (IPP 110^{PLUS} Memmert, Germany) at 30 °C for 24 h). The plates containing pure colonies were sealed to avoid cross-contamination. Isolate identification was done by Mabritec SA (Switzerland) using matrix-assisted laser desorption/ionization - time of flight mass spectrometry (MALDI-TOF MS). The spectra were analyzed using the SARAMIS SuperSpectra (SSp) tool and matched with the putative assigned protein masses for the identification database (PAPMID). In parallel, isolated species were grown in tryptic-casein soy broth (TSB) (Biokar diagnostics, France) in a shaking incubator (Excella E24 New Brunswick Scientific, USA) at 30 °C, 150 rpm for 24 h, mixed with glycerol at a ratio of 1:1 and stored at – 80 °C for further use in challenge testing.

3.2.4 Microorganism selection

Three microorganisms were selected for the study, based on their capacity to grow in microalgae suspensions at low temperature (10 °C). The biosafety level and the Gram type were also considered. The isolated species were freshly inoculated on PCA plates. Single colonies were transferred from the plates to 100 mL TSB and cultivated at 30 °C, 150 rpm for 24 h. The initial inoculum size was estimated to be 10^9 cells/mL by microscopy (Olympus XC10, Carl Zeiss, Germany) using a Neubauer chamber of 0.02 mm depth and 0.0025 mm^2 (Assistant, Germany). For the detection of growth dynamics, the inocula were diluted 10^5 times into microalgae suspensions (14% (w/w) DM) and incubated at 10 °C for three days without shaking. Sampling, serial dilution and plating were performed on days 0 and 3. The plates were incubated at 30 °C for 24 h.

3.2.5 Deoxyribonucleic acid (DNA) extraction and whole-genome sequencing (WGS)

To validate the isolate identification, DNA extraction and WGS were performed to six microorganisms. The isolates were freshly inoculated on PCA plates. Single colonies were grown in TSB at 30 °C, 150 rpm for 24 h. Inocula of 8.0 – 18.2 mL were centrifuged (9'050 x *g*, 10 min, 20 °C) and approximately 350 mg pellets were collected. The pellets were resuspended in 978 µL sodium phosphate buffer and DNA was extracted using the FastDNA SPIN kit (MP Biomedicals, France), with a minor modification. After adding MT Buffer, the cells were lysed with Precellys 24 and centrifuged for 40 s at 2'500 x *g*. A quality control of the extracted DNA was done using Nanodrop and TapeStation. The sequencing reaction was performed on a Flongle flow cell (FLO-FLG001, ID AOJ319) and a GridION device (Oxford Nanopore Technology, UK). Super-accurate base-calling was done to obtain readable sequence data (FASTQ file). The latter was analyzed using the EPI2ME FASTQ WIMP classification tool for microbial genes (Oxford Nanopore Technology, UK) (Imai et al., 2020). The total classified reads and correctly classified species reads were recorded for species found with abundance > 1%.

3.2.6 Cultivation and viable cell count after thermal and PEF treatments

The isolates were freshly inoculated on PCA plates. Single colonies were grown in TSB at 30 °C, 150 rpm for 24 h, and inocula were diluted in microalgae suspensions (2% (w/w) DM) to reach an initial microbial load of approximately 10^6 colony forming units (CFU)/mL, noted as N_0 after enumeration. The samples were used to determine the thermal and PEF resistance of microorganisms (Sections 3.2.7 and 3.2.8.3). Each sample was stored in ice and plated within 2 h following thermal and PEF treatments. The serial dilutions were done

with MRD, and at least three dilutions (50 µL) were plated. The colonies were grown on PCA plates at 30 °C for 24 h. Enumeration of colonies allowed to determine the inactivation level for each treatment, calculated as $\log_{10}(N/N_0)$, where N and N_0 are the microbial concentrations (CFU/mL) in the treated and untreated samples, respectively. OriginLab® 2022b (OriginLab Corporation, USA) was used to generate logarithmic (log) reduction graphs. Cultivations, sample preparation, inactivation treatments and microbiological analysis were done in triplicate.

3.2.7 Thermal treatments

During PEF treatment, ohmic heating occurs, since the passage of the electric current in the liquid food generates heat. The thermal resistance of microorganisms was studied to control the ohmic effects and distinguish between electric and thermal inactivation effects. A modular micro reaction system (MMRS) (Ehrfeld Mikrotechnik GmbH, Germany) was used. The high surface-to-volume ratio of the system (2610 m^2/m^3) allowed very fast heating and cooling rates (Georget et al., 2013). Three coaxial heat exchangers (0.62 mL) in series allowed to reach the desired temperature (50, 55, 57, 59 and 61 °C) with a maximal heating rate of 2 °C/s. The treatment temperature was maintained in the meander reactor (1.5 mL) before cooling down to 25 °C in a further coaxial heat exchanger. The module configuration is depicted in Figure 3.2.

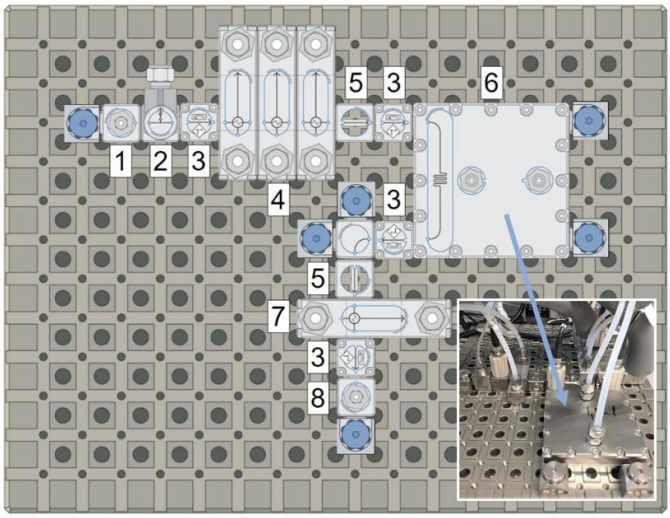

Figure 3.2: MMRS setup.1: inlet module, 2: pressure relief valve, 3: temperature sensor, 4: heat exchanger – heating (three modules in series), 5: insulation module, 6: meander reactor, 7: heat exchanger – cooling, 8: outlet module. The modules were attached to a heating base plate using clamping devices (blue) and separated by sealing plates. The figure was adapted from Ehrfeld Mikrotechnik GmbH, Germany.

The total dead volume, including the inlet/outlet of the heat exchangers, the temperature sensors, the insulation module, and the meander reactor, was calculated to be 2.5 mL. The liquid was pumped (Nikkiso pump, LEWA GmbH, Switzerland) at a flow rate of 7.4 mL/min (mini-Cori-Flow M14-ABD-22-0-S, Bronkhorst, Switzerland), leading to a total retention time of 20 s, corresponding to the holding time in the PEF system from the PEF cell to the cooling zone (Section 3.2.8.3). The temperatures and flow rate values were monitored using the software LabView. Cultivations, sample preparation, thermal treatments and microbiological analysis were performed on the same *Cv* batch in duplicate on two different days. The detection limit was 1 organism/mL sample. Disinfection with 2% (v/v) Deptil BC MAX (Kersia Schweiz AG, Switzerland) was conducted before each trial, and an alkaline solution of 2% (v/v) (sodium hydroxide, VC7, Clenebrite, Diversey, The Netherlands) was used for cleaning.

The log reduction was plotted as a function of the treatment temperature. The critical temperature T_{crit} was defined as the minimal value required to observe inactivation. It corresponds to the intercept between the x-axis and the regression line of the straight part of the inactivation curve and was used as an indicator of the thermal resistance of the microorganisms.

3.2.8 PEF treatments

3.2.8.1 PEF setup

The setup was composed of a pilot scale HVP-5 PEF machine (ELEA, Germany) containing a co-linear cell with a high-voltage electrode and two ground electrodes positioned down- and upstream of the powered high-voltage electrode (stainless steel 1.4301, inner diameter 1 cm). The electrodes were separated by spacers of 1 cm, resulting in a total treatment chamber volume of 1.57 mL. The liquid was pumped through the system using a screw pump (Mono pump 3NU10, Socsil-Inter SA, Switzerland) with a geared motor (RD11, Ströber, Germany). The flow rate was manually adjusted via the gearbox and measured by an electromagnetic flowmeter (OPTIFLUX 6100, Krohne, The Netherlands). The custom-made tubular heat exchanger (three twisted tubes of 3 m long, 1 cm inner diameter) was used to heat up and cool down the product. Tap water served as heating and cooling liquid in the shell of the heat exchanger, and the heating water temperature was controlled with a Hotbox (HB120, Huber Kältemaschinenbau AG, Germany). Thermosensors and a data acquisition system (LabView 2015) allowed to record the product's in and outlet temperatures. The generator displayed the temperatures before and after the PEF treatment

chamber. The flowchart of the setup, including heat exchangers, is represented in Figure 3.A.1.

3.2.8.2 PEF processing parameters

High-voltage square pulses were applied to the samples. Square pulses are considered the best option for the inactivation of microorganisms while minimizing ohmic effects (Li et al., 2023). The flow rate *F* was kept at 60 L/h, the microalgae concentration was kept at 2% (w/w) DM, inlet product temperature T_{in} at 30 °C and the pulse duration τ at 20 µs. For each selected microorganism (Section 3.2.4), 15 different PEF inactivation conditions were tested by varying the pulse repetition rate *f* (100, 120 and 140 Hz) and the output voltage (50, 60, 70, 80 and 90%). Samples were collected for 30 s to minimize the influence of process instabilities, such as fluctuation of the product flow rate. The Reynolds number was calculated using Equation 3.3:

$$Re = \rho v D / \mu \quad (-) \qquad (3.3)$$

With the approximated dynamic viscosity μ = 0.001 Pa·s and density ρ = 1000 kg/m^3 of *Cv* suspensions (2% (w/w) DM). The average fluid velocity v is given in m/s. *D* is the pipe hydraulic diameter in m.

Cultivations, sample preparation, PEF treatments and microbiological analysis were done three times in parallel experiments and using the same *Cv* batch. The detection limit was 20 organisms/mL sample. After each experiment, cleaning in place was conducted on the system using an alkaline solution of 2% (v/v) (sodium hydroxide, VC7, Clenebrite, Diversey, The Netherlands) and an acid solution of 1% (v/v) (nitric acid, VA5, Pascal, Diversey, The Netherlands). Disinfection with 2% (v/v) Deptil BC MAX (Kersia Schweiz AG, Switzerland) was conducted before each trial.

3.2.8.3 Electrical inactivation kinetics

The pulse amplitude (voltage *U* (V) and current *I* (A)), the electric field strength E_{el} (kV/cm) and the specific energy input W_s (kJ/kg) were monitored after 1 min treatment to ensure process stability. According to Raso et al. (2016), E_{el} and W_s are suitable parameters to consider when studying PEF-induced microbial inactivation. First, assuming a linear relation between the log reduction and E_{el} for a given treatment time *t*, the critical E_{el} value, E_{crit}, can be defined (Hülsheger et al., 1981). E_{crit} is the intercept between the x-axis and the linear regression line of the straight part of the inactivation profile. It corresponds to the E_{el} required, at specific treatment time and temperature, to exceed the transmembrane potential

threshold and cause electroporation (Puligundla et al., 2018). Moreover, W_s can be calculated from E_{el} using Equation 3.4 (Raso et al., 2016; Vaessen et al., 2019):

$$W_s = \frac{1}{m}\int_0^{\infty} U(t) \cdot I(t)dt = \frac{1}{\rho}\int_0^{\infty} \sigma(t) \cdot {E_{el}}^2(t)dt \quad \text{(kJ/kg)} \qquad (3.4)$$

With the mass of the treated product m (kg), the voltage U (kV), the current I (A), the density ρ (kg/m^3), the conductivity σ (S/m) and the treatment time t (s). Using Equation 3.5, t can be expressed as a function of the number of pulses n (-) and the pulse duration τ (µs).

$$t = n \cdot \tau = t_r \cdot f \cdot \tau \quad \text{(s)} \qquad (3.5)$$

With the pulse repetition rate f (Hz) and the residence time $t_r = V_{chamber}/F$ (s), calculated from the volume of the PEF chamber $V_{chamber}$ (m^3) and the flow rate F (m^3/s). t_r equals 0.094 s at a flow rate of 60 L/h. The time for the PEF-treated liquid to reach the cooling zone was 20 s. Finally, the temperature increase ΔT (K) due to ohmic heating can be calculated with Equation 3.6:

$$\Delta T = W_s/c_p \quad \text{(K)} \qquad (3.6)$$

3.2.8.4 Pulse monitoring

The PEF system measures the peak values of pulses (voltage and current). An oscilloscope (TDS 2024C Tektronix, USA) was connected to register the pulse shape. The pulse generator produces low voltage pulses (0 – 1.1 kV), while the transformer transforms initial pulses to high voltage (ratio of 1:24).

3.2.9 Storage control

Based on the results (Section 3.2.8.3), suited PEF conditions (90% output voltage, 120 Hz, 20 µs, 60 L/h, 30 °C) were chosen and used to study the microbial growth in PEF-treated suspensions during cold storage (10 °C). Microbiological analysis was performed each day for ten days. The untreated sample as well as an untreated and diluted (10^3 times, to achieve similar inactivation effects obtained after PEF treatment) sample were used as references to compare growth dynamics with PEF-treated samples. A second PEF treatment after two days of incubation was applied to evaluate the potential of applying several PEF cycles, thus allowing for further shelf-life extensions. Cultivations, sample preparation, PEF treatments and storage control were done two times in parallel experiments and on the same *Cv* batch. The detection limit was 1 organism/mL sample.

The growth curves were modelled using the “biogrowth R package” and an open-access interface (*https://foodmicrowur.shinyapps.io/biogrowth)* developed at Wageningen University (The Netherlands) (Garre et al., 2023). The primary reparametrized Gompertz model (Equation 3.7) was chosen to describe microbial growth with respect to time (Zwietering et al., 1990):

$$\log_{10}N = \log_{10}N_0 + A \cdot \left(\exp\left(-\exp\left(\frac{e\cdot\mu}{A}(\lambda - t) + 1\right)\right)\right) \quad \text{(CFU/mL)} \quad (3.7)$$

With the microbial concentration N (CFU/mL), the difference between $\log_{10}N_{max}$ and $\log_{10}N_0$ A ($\log_{10}$CFU/mL) and the storage time t (d). The maximum growth rate μ ($\log_{10}d^{-1}$) and the lag phase λ (d) values were used to compare the samples' growth capacity and cell injury level.

3.2.10 Process energy requirement

The energy required to reach a particular level of inactivation, i.e., 2 logs, was compared using PEF (E_{PEF}) versus thermal treatment (E_{TT}). Aganovic et al. (2017) calculated energy requirements for thermal processing using Equation 3.8. For the PEF treatment, the energy to pre-heat the product to 30 °C, combined with the specific energy at PEF treatment ($W_{s,2logs}$), was considered (Equation 3.9).

$$E_{\mathrm{TT}} = c_{\mathrm{p}} \cdot \Delta T = c_{\mathrm{p}} \cdot (T_{2\log} - T_{\mathrm{in}}) \quad \text{(kJ/kg)} \quad (3.8)$$

$$E_{\mathrm{PEF}} = c_{\mathrm{p}} \cdot \Delta T + W_{\mathrm{s}} = c_{\mathrm{p}} \cdot (T_{\mathrm{PH}} - T_{\mathrm{in}}) + W_{\mathrm{s,2logs}} \quad \text{(kJ/kg)} \quad (3.9)$$

With c_p = 4.13 kJ/(kg·K), obtained from Equation 3.2, the initial product temperature T_{in} = 20 °C and the product temperature after pre-heating T_{PH} = 30 °C.

3.2.11 Statistical analysis

All the analytical measurements were done in duplicate (n = 2) or triplicate (n = 3). Results were expressed as individual data points for duplicates, while triplicates were expressed as average ± standard deviation (SD). Regarding statistical analysis, first normality distribution (Shapiro-Wilk test) and equal variance (Chi-square test for variance) were checked (p = 0.05). Statistical significance was estimated by one-way ANOVA, followed by Tukey's post-hoc test. Dunn's test and Welch's ANOVA were used when normality and equal variance were rejected, respectively. P-values < 0.05 were considered statistically significant. All statistical tests were performed using OriginLab® 2022b (OriginLab Corporation, USA).

3.3 Results and discussion

3.3.1 Thermal sensitivity of the substrate

The microalgae substrate's thermal sensitivity was studied to mitigate the potential thermal modification of *Cv* caused by ohmic heating during PEF treatments and its subsequent decline in techno-functionality. The effect of various thermal treatments (50, 60, 70, 80 and 90 °C, 30 s) on the gelation capacity of *Cv* suspensions was measured (Figure 3.3A). Furthermore, DSC analysis was conducted, as illustrated in Figure 3.3B.

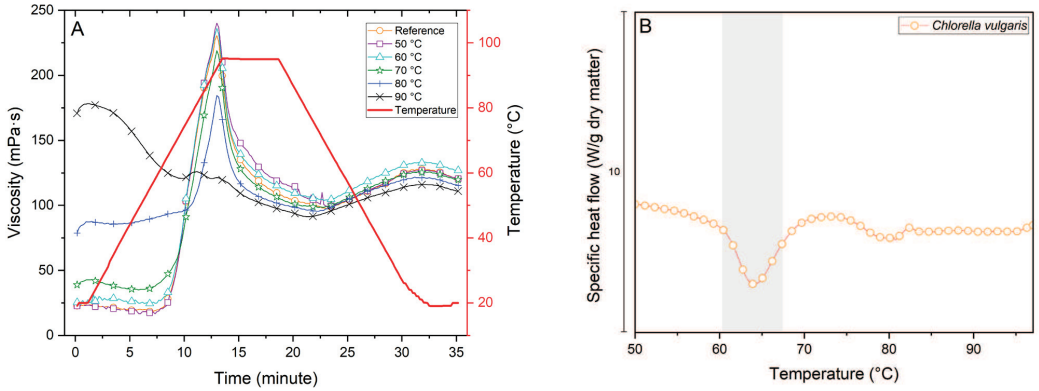

Figure 3.3: A. Temperature-sweep (20 to 95 °C, 6 °C/min) on 14% (w/w) DM *Cv* suspensions after thermal pre-treatments at 50, 60, 70, 80, and 90 °C for 30 s (n = 2), B. DSC thermogram (scanning from 20 °C to 100 °C at a heating rate of 0.5 °C/min) of *Cv* suspensions (n = 2). The grey zone indicates an endothermic reaction peak.

The gelation capacity, expressed as the apparent peak viscosity $\mu_{app,peak}$ during the heating interval, was slightly enhanced following mild heating (50 – 60 °C). Specifically, it increased from 230 to 240 mPa·s (+ 4%) after treatment at 50 °C. However, when subjected to higher temperatures (70 – 90 °C), a reduction of gelation capacity was observed, resulting in a decrease of $\mu_{app,peak}$ from 230 to 121 mPa·s (– 47%) (Figure 3.3A). Additionally, a treatment at 65 °C led to a similar $\mu_{app,peak}$ compared to the reference (229 mPa·s). A similar trend can be observed for the final viscosity. These results indicate that a PEF treatment threshold temperature of 65 °C can be established. Up to this point, temperature positively impacts suspension functionality, likely due to the swelling and hydration of microalgae components, particularly proteins and polysaccharides, as suggested by De Gol et al. (2023).

However, it is essential not only to assess the influence of caloric heating on *Cv*'s gelation capacity but also to consider the impact of the entire process sequence, encompassing PEF treatment, cell disruption, and intermediate storage. For instance, in a study by Bernaerts et al. (2018), the normalized viscosity of *Cv* suspensions (8% (w/w) DM, pH 6) was compared

after various combinations of mechanical and thermal processing. While thermally treated suspensions exhibited higher viscosity than unprocessed or cell-disrupted suspensions, the authors noted increased viscosity after the sequence of (cell disruption + thermal treatment) compared to (thermal treatment + cell disruption). Consequently, the DSC results, reflecting the thermal degradation of chemical bonds and protein structure, were considered a more reliable benchmark for assessing microalgae's thermal sensitivity. Notably, the denaturation peak temperature of fresh *Cv* suspension was measured at 64 °C, with an onset at 60 °C (see Figure 3.3B), establishing the critical temperature for the PEF treatments.

3.3.2 Identification and selection of microorganisms

The microbiological analysis of *Cv* suspension (storage at 10 °C for up to six days) resulted in the identification of 68 plates and the detection of 17 distinct species (Table 3.1). Marker microorganisms were selected based on their growth capacity in *Cv* suspensions at refrigerated conditions (10 °C) and quantified as the log increase after three days of cultivation. The biosafety level and Gram type were also considered selection criteria (Table 3.1).

Table 3.1: Selection criteria and identification level achieved through both MALDI-TOF MS and WGS. The grey highlight shows the selected microorganisms

Isolated species	log increase at 10 °C, 3 d	Biosafety level	Gram - or +	% id with MALDI-TOF-MS	% id with WGS
Citrobacter telavivensis	3.7	2	-	n.i.	79.2
Pseudomonas guariconensis	3.1	1	-	99.9	60.6
Enterobacter soli	2.8	1	-	84.0	85.2
Pseudomonas genomosp.	2.7	1	-	95.0	n.a.
Acinetobacter bereziniae	2.6	2	-	90.0	n.a.
Acinetobacter johnsonii	2.6	2	-	99.9	n.a.
Pseudomonas donghuensis	2.6	1	-	99.9	n.a.
Enterobacter ludwigii	2.5	2	-	99.9	n.a.
Microbacterium liquefaciens	2.0	1	+	84.0	89.2
Microbacterium oxydans	1.7	1	+	78.0	68.7
Acinetobacter radioresistens	1.7	1	-	99.9	n.a.
Lactococcus lactis	1.5	1	+	92.4	95.2
Stenotrophomonas maltophilia	1.2	2	-	n.i.	n.a.
Stenotrophomonas genomosp.	0.9	2	-	n.i.	n.a.
Enterococcus lactis	0.2	1	+	99.9	n.a.
Paenibacillus genomosp.	n.d.	1	+	n.i.	n.a.
Rhodococcus erythropolis/qingshengii	n.d.	1	+	84.0	n.a.

id: identification, n.i.: not identified, n.a.: not analyzed, n.d.: not detected
The biosafety levels were obtained from two main sources: Frey (2013) and the Bacdive platform referred as Reimer (2022)

Despite exhibiting the highest growth capacity, *Citrobacter telavivensis* was excluded from the study due to safety concerns (biosafety level 2). *Pseudomonas guariconensis* and *Enterobacter soli* were selected as relevant Gram-negative bacteria, showing a 3.1 and 2.8 log increase, respectively, in *Cv* at 10 °C after three days. Both species are aerobic mesophilic bacteria and grow well at neutral pH. Gram-negative bacteria are considered more susceptible to PEF than Gram-positive bacteria (Delso et al., 2022). Therefore, a Gram-positive bacterium was also selected to study the influence of generalized cell wall properties on PEF efficiency. *Lactococcus lactis* was chosen over *Microbacterium* for two main reasons. *Microbacterium* has been involved in human disease, and the identification level was low compared to *L. lactis.* More relevant for the study, *L. lactis* and *E. soli* likely induce acidification (data not shown) in microalgae suspensions, leading to undesired protein precipitation. Moreover, *P. guariconensis* exhibits aromatic compounds, which are likely unappealing to consumers.

3.3.3 Thermal sensitivity of marker microorganisms

The thermal sensitivity of the three selected microorganisms, *P. guariconensis, E. soli* and *L. lactis,* is illustrated through the thermal inactivation curves in Figure 3.4.

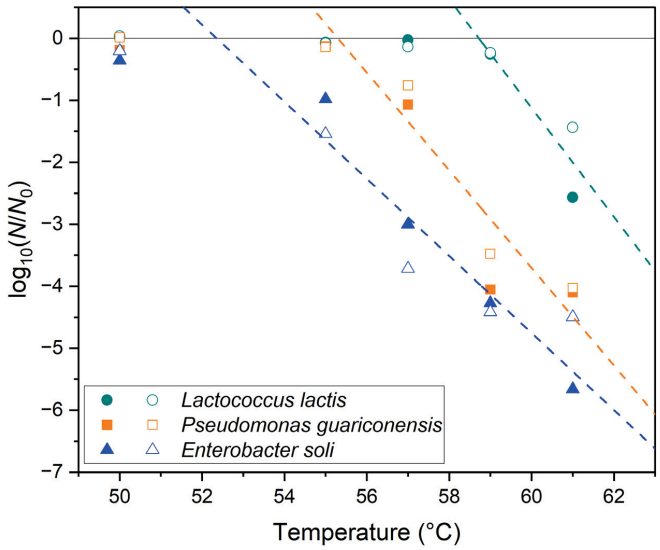

Figure 3.4: Thermal inactivation observed at MMRS treatments (n = 2). *P. guariconensis* (■), *E. soli* (▲) and *L. lactis* (●) at different treatment temperatures 50, 55, 57, 59 and 61 °C (exposure time = 20 s). The initial count N_0 was ~ 10^6 CFU/mL and detection limit – 6 logs. The dashed lines represent the regressions function of the thermal inactivation, and the intercept with the x-axis indicates T_{crit} values.

The critical inactivation temperature T_{crit} was used to rank the species from the more thermosensitive to the more thermoresistant ones: *E. soli* (T_{crit} = 52.4 [50.1 – 54.6] °C), *P. guariconensis* (T_{crit} = 55.3 [52.5 – 58.1] °C), *L. lactis* (T_{crit} = 58.7 [56.5 – 61.0] °C) (95% confidence intervals). As depicted in Figure 3.4, thermal treatment at 60 °C (for 20 s), a temperature found to be advantageous for the gelling of the microalgae substrate (see Section 3.3.1), induces inactivation of 4.8, 3.7 and 1.1 logs for the respective selected species. Inactivation effects at 50 °C or lower were considered negligible for all three species. Therefore, to investigate the effect of a non-thermal treatment on the inactivation, temperatures below 50 °C were tested.

3.3.4 PEF sensitivity of marker microorganisms

The influence of varying output voltage across different pulse repetition rates *f* was investigated (Figure 3.5). Output voltages of 50, 60, 70, 80 and 90% corresponded to electric field strengths E_{el} of 16, 19, 22, 25, and 28 kV/cm, respectively. E_{crit} values, indicating the minimal electric field strength for the inactivation of microbial cells for different pulse repetition rates, are the intercept with the x-axis.

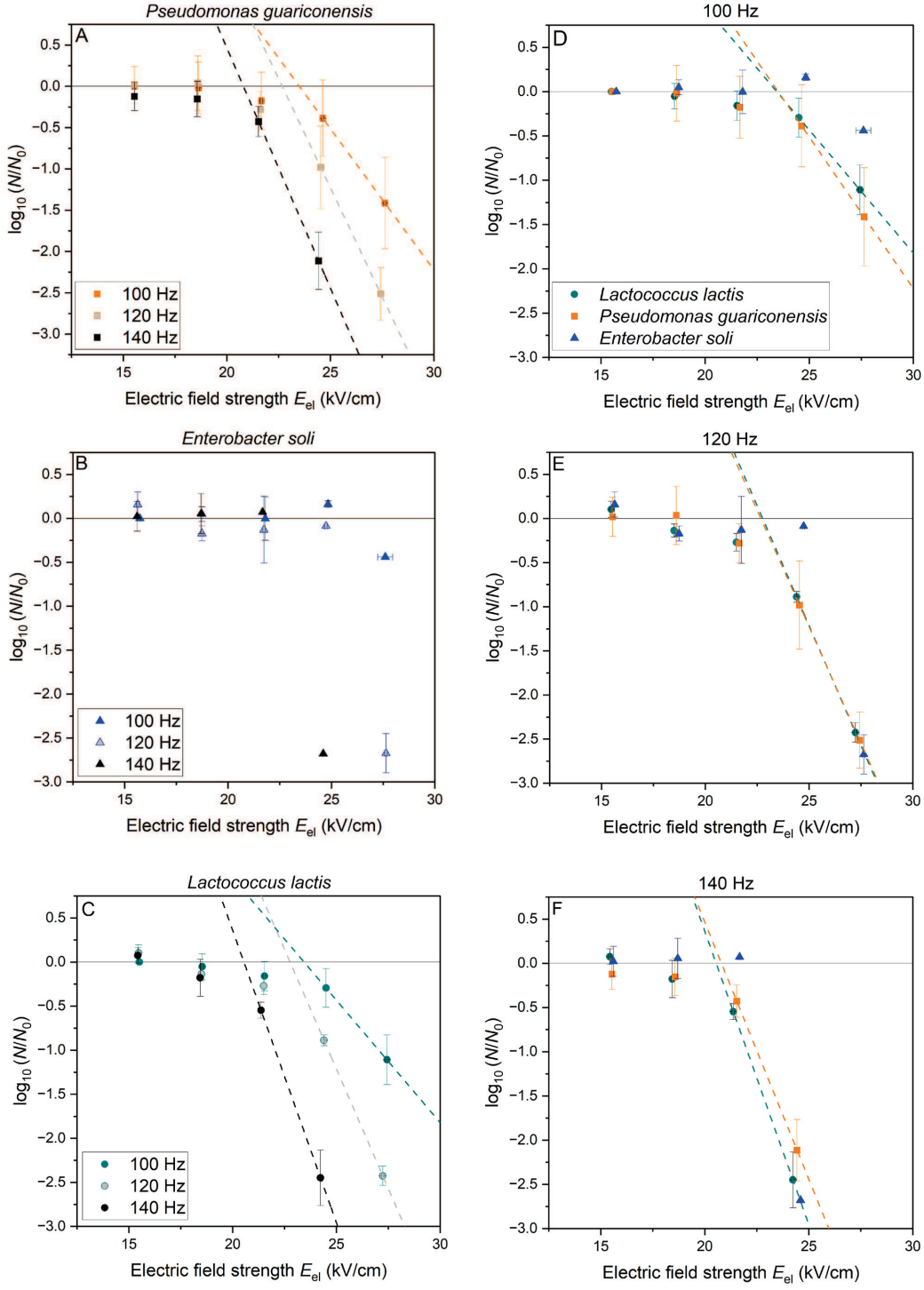

Figure 3.5 (*continued*)

Figure 3.5: Influence of the electric field strength E_{el} on the inactivation of *P. guariconensis* (■, A), *E. soli* (▲, B) and *L. lactis* (●, C) at different pulse repetition rates (100, 120 and 140 Hz), and comparison between the microorganisms at different pulse repetition rates 100 Hz (D), 120 Hz (E) and 140 Hz (F), for constant pulse duration (20 µs) and flow rate (60 L/h). The initial count N_0 was ~ 10^6 CFU/mL and detection limit – 4.7 logs. Plotted data points are averages of three repetitions (n = 3) ± SD. The dashed lines represent the regressions function of the inactivation and the intercept with the x-axis the E_{crit} values.

First, a minimum E_{el} of 20 kV/cm was required to induce microbial inactivation. The highest inactivation was recorded with 2.5 logs (90%, 120 Hz), 2.7 logs (90%, 120 Hz) and 2.5 logs (80%, 140 Hz) for *P. guariconensis, E. soli* and *L. lactis*, respectively. *E. soli* exhibited high E_{crit} of electroporation (25.6 kV/cm at 100 Hz, 24.6 kV/cm at 120 Hz, and 21.7 kV/cm at 140 Hz). However, the maximum inactivation is similar for the three microorganisms. As expected, a trend of increasing inactivation with increasing E_{el} (for a constant pulse repetition rate f) as well as with increasing pulse repetition rate f (for a constant E_{el}) was observed, which is in line with previous research (Flisar et al., 2014; Raso & Álvarez, 2016). Moreover, E_{crit} was lower at higher f, correlating with extended treatment durations. E_{crit} values for *P. guariconensis* (23.6 kV/cm at 100 Hz, 22.6 kV/cm at 120 Hz, and 20.8 kV/cm at 140 Hz) and *L. lactis* (23.4 kV/cm at 100 Hz, 22.8 kV/cm at 120 Hz, and 20.5 kV/cm at 140 Hz) were not significantly different ($p < 0.05$) despite their variance in morphology, different Gram type and estimated cell size and shape (2.5 µm in length and 0.85 µm in width versus 0.5 – 1.5 µm). In general, E_{crit} is lower for larger cells (Schottroff et al., 2017), and Gram-negative bacteria are more susceptible to PEF than Gram-positive bacteria (Delso et al., 2022). Additionally, it has been observed that Gram-negative bacteria are less resistant at neutral pH than in acidic conditions, whereas the opposite is valid for Gram-positive bacteria (García et al., 2005). In this study (pH = 6.5), *L. lactis*, despite its smaller cell size and Gram-positive nature, did not display higher resistance to PEF; instead, it exhibited a profile similar to that of *P. guariconensis*.

Trials involving *P. guariconensis* displayed considerable variability. A few samples from *E. soli* were excluded from further analysis due to process instability, and statistical analysis is not valid. Heterogenous inactivation effects and process instability can be attributed to several factors: 1) a non-uniform electric field in the co-linear PEF chamber, as reported by Raso et al. (2016), 2) a parabolic profile of flow velocity at laminar flow conditions (at a flow rate of 60 ± 1 L/h and using Equation 3.3, Re = 2088 – 2159, which falls below the critical value of 2300 for transition to turbulent flow), 3) a 10% variation of electric conductivities of batches (0.56 – 0.60 mS/cm), and 4) a 10% thermal energy losses within the system, discerned through the disparity between the theoretical c_p value (4.13 kJ/(kg·K), Equation

3.2) and the experimentally determined c_p value (4.60 kJ/(kg·K), Equation 3.6). To verify the robustness of the process, an evaluation of the pulse shape was conducted (Figure 3.6). For high output voltage (90%), the plateau value is reached later and an undershoot is observed at approximately 23.5 µs. Therefore, for higher E_{crit}, as observed for *E. soli,* such system-immanent behavior influences the process stability more importantly.

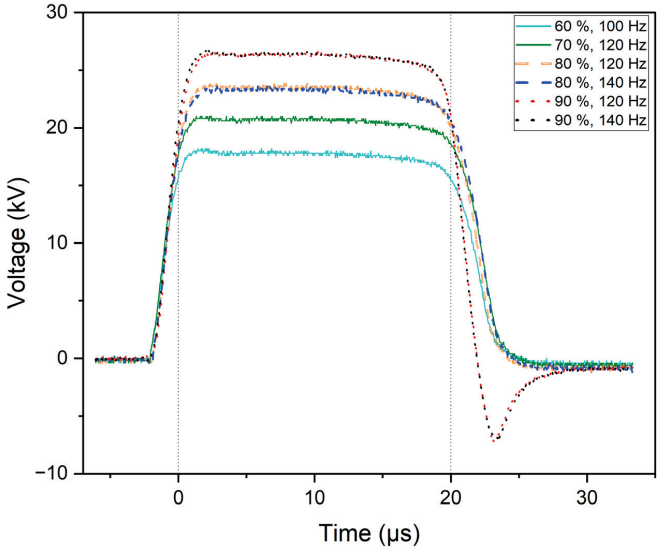

Figure 3.6: Monitoring of pulse shape for *Cv* suspensions (2% (w/w) DM, 30 °C inlet temperature, 60 L/h) and for different voltage output (60, 70, 80 and 90%) and pulse repetition rates *f* (100, 120 and 140 Hz).

In addition to the electric field strength E_{el}, it is imperative to consider the impact of the measured specific energy input W_s. This parameter considers the conductivity of the media and is crucial for the differentiation between electric and thermal inactivation effects. Figure 3.7 depicts both the PEF-induced log reduction in microbial load for the three species across various levels of specific energy inputs W_s, and the thermally induced logarithmic reduction at different temperatures (Section 3.3.3).

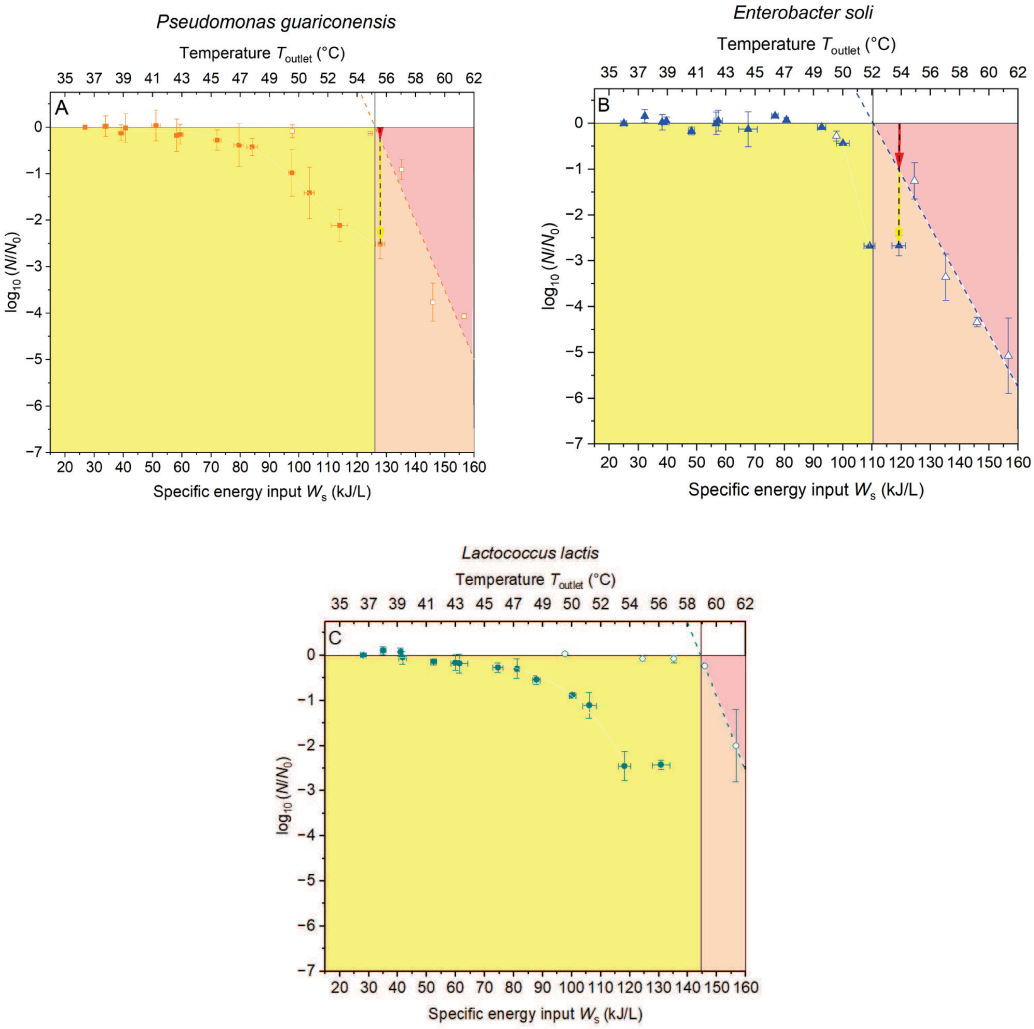

Figure 3.7: Influence of the specific energy input W_s on inactivation effects of *P. guariconensis* (■, A), *E. soli* (▲, B) and *L. lactis* (●, C) with constant pulse duration (20 µs) and flow rate (60 L/h). The initial count N_0 was ~ 10^6 CFU/mL. Data points are averages of three individual measurements (n = 3) ± SD. Dashed lines and open symbols represent the purely thermal inactivation effect (Section 3.3.3). Above this line, in the red zone, thermal effects are supposed to dominate the inactivation. The yellow zone expresses purely electric inactivation effects, whereas in the orange zone, combined effects are suggested.

Toepfl & Heinz (2011) reported that energy levels ranging between 80 and 120 kJ/kg are commonly applied to inactivate vegetative bacterial cells and shelf-life extension in heat-sensitive liquid foods using PEF. Accordingly, PEF-induced microbial inactivation was evident (> 0.5 log) for energy inputs exceeding 85 kJ/kg. An increase in the inactivation level was measured upon increasing the energy input (85 – 130 kJ/kg). The temperature increases during PEF treatments, attributed to ohmic heating. A positive correlation (n = 129,

R = 0.97) between the outlet product temperature T_{outlet} and the specific energy input W_s was found. From Section 3.3.3, the thermal inactivation curve for each species can be outlined (indicated by dashed lines in Figure 3.7). Furthermore, three distinct zones were defined to represent the inactivation dominated by electric effects (yellow), thermal effects (red) and combined effects (orange). The inactivation observed for *P. guariconensis* was predominantly caused by purely electric effects (Figure 3.7A, yellow zone). A reduction > 2.5 logs was explained by combined effects (Figure 3.7A, orange zone). In the case of *E. soli*, temperature as low as 52 °C is sufficient to cause thermal inactivation (Section 3.3.3), and PEF-induced inactivation was therefore explained by combined effects rather than purely electric effects (Figure 3.7B, orange zone). To acquire additional information on the sole impact of electric discharges, experiments at lower inlet product temperature T_{in} would be required. Finally, the inactivation of *L. lactis* was caused by purely electric effects (Figure 3.7C, yellow zone). In this case, experiments at higher T_{in} could give information on the potential synergistic effects of electric and thermal energy.

While the mechanisms of inactivation via heat and electric discharges are very different, particularly the denaturation of biomolecules versus electroporation of membranes, it has been reported that mild heating can enhance electroporation. This can be attributed to the cell membrane's fluidity increase at elevated temperatures, favoring local breakthroughs of the membranes (Coster & Zimmermann, 1975). The relationship between electric energy input and ohmic heating (Equation 3.6) makes the discernment of individual effects very complex. Consequently, microbial inactivation kinetics can be understood in a combination of both electric and thermal effects (Schottroff & Jaeger, 2020). Synergistic thermal-electric effects are more probable than overlaid independent effects, which sum up. In conclusion, reaction kinetics should differ in the three zones (Figure 3.7), depending on the thermal and electric resistances of the microorganisms. Above purely electric effects, thermal effects might have no accelerating influence for thermoresistant microorganisms with a high electro-sensitivity. In contrast, the opposite may be valid for thermosensitive microorganisms with low electro-sensitivity.

Finally, it is important to highlight the PEF treatment's generic effect at certain conditions, i.e., inactivation of ~ 1.5 logs at 105 kJ/L and ~ 2.5 logs at 120 kJ/L. In contrast, thermal inactivation levels are very species-specific (Figure 3.4). In addition to studying the effects at the bacterial level, further research is needed to investigate the advantageous changes in *Cv* functionality following PEF treatment in comparison to thermal pasteurization.

3.3.5 Deduction of a spoilage control concept with PEF treatments

Previous studies showed the potential of PEF technology to extend the shelf-life of liquid foods (Dziadek et al., 2019; Timmermans et al., 2016). Therefore, possible shelf-life extension of *Cv* suspensions was investigated with repetitive PEF treatments. In Figure 3.8, the measured data points and modelled growth curves demonstrate differences between untreated and PEF-treated inoculated *Cv* suspensions. One and two cycles of PEF processes were applied and observed growth parameters are displayed in Table 3.2.

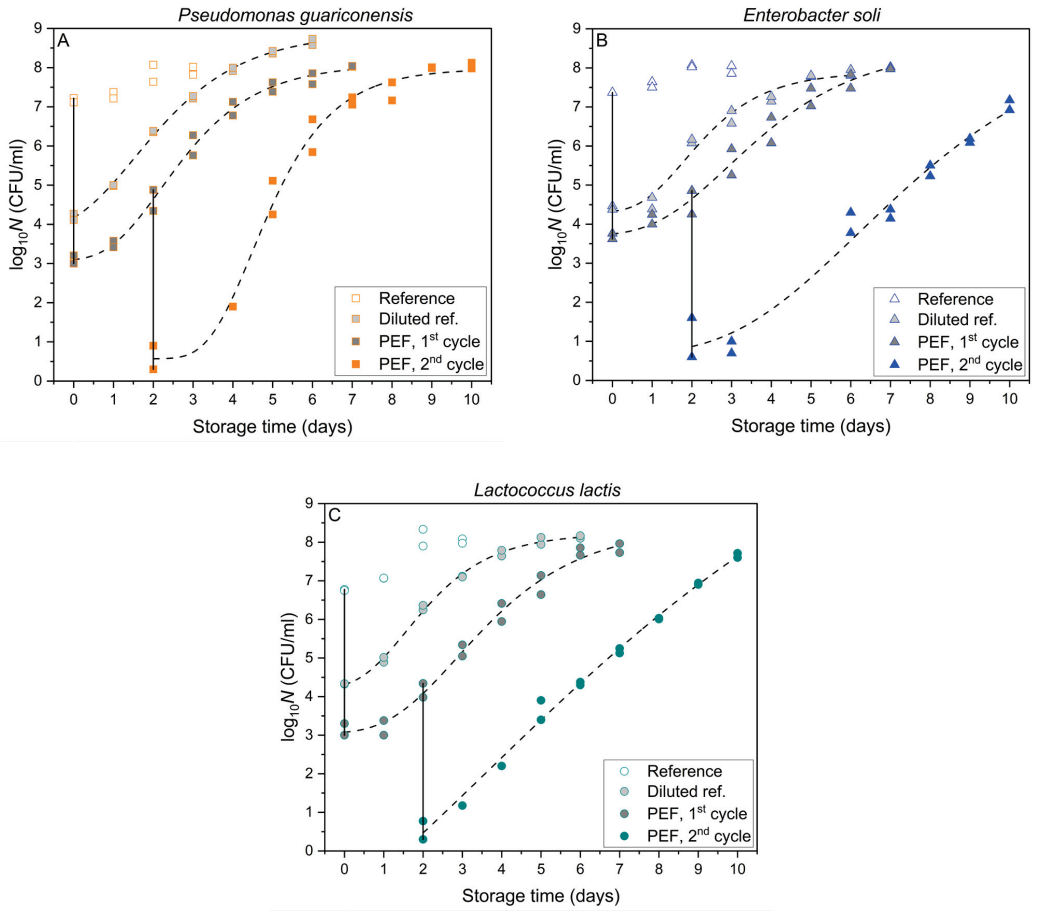

Figure 3.8: Microbial growth of untreated versus PEF-treated *Cv* suspensions inoculated with *P. guariconensis* (■, A), *E. soli* (▲, B) and *L. lactis* (●, C). Incubation at 10 °C for ten days. An untreated, diluted sample was included in the study for improved comparability of initial counts. PEF, 1st cycle corresponds to a single PEF treatment on day 0, whereas PEF, 2nd cycle corresponds to PEF, 1st cycle plus a second PEF treatment on day 2. PEF treatments were done at 90% output voltage (28 kV/cm), 120 Hz, 20 µs, 30 °C, 60 L/h (n = 2). The initial count N_0 was ~ 10^6 CFU/mL and detection limit 0 log. Growth fitting was done with biogrowth (Section 3.2.9).

Table 3.2: Growth parameters extracted from the biogrowth simulation as shown in Figure 3.8. Values are presented as averages ± SD

Isolates	***P. guariconensis***		***E. soli***		***L. lactis***	
Growth parameters	**μ ($log_{10}d^{-1}$)**	**λ (d)**	**μ ($log_{10}d^{-1}$)**	**λ (d)**	**μ ($log_{10}d^{-1}$)**	**λ (d)**
Diluted ref.	1.2 ± 0.0	Not significant	1.2 ± 0.2	0.7 ± 0.3	1.2 ± 0.1	0.4 ± 0.1
PEF, 1st cycle	1.4 ± 0.1	0.9 ± 0.2	0.9 ± 0.1	1.0 ± 0.5	1.1 ± 0.1	1.1 ± 0.3
PEF, 2nd cycle	2.4 ± 0.3	1.4 ± 0.2	1.0 ± 0.2	1.0 ± 1.4	1.0 ± 0.0	Not significant

A PEF-induced inactivation ≥ 3.5 logs was observed for all three species. Compared to the results in Section 3.3.4, the higher inactivation level can be explained by an elevated electric conductivity of the *Cv* suspension (0.73 mS/cm). The determined log reductions for an outlet product temperature $T_{outlet,av}$ of 53.4 °C were 4.1, 3.7 and 3.6 for *P. guariconensis, E. soli* and *L. lactis,* respectively.

Moreover, similar effects were achieved for the second PEF cycle (4.0, 3.5 and 3.6 log reductions for *P. guariconensis, E. soli* and *L. lactis,* respectively). These results emphasize the potential of PEF technology for shelf-life control in refrigerated tank storage of liquid food. The population's sensitivity to PEF treatments seems unaltered after passing the first PEF cycle. Regarding the growth parameters (Table 3.2), the growth rate μ and the lag phase λ increased after PEF treatment of *P. guariconensis.* Selma et al. (2004) observed a prolonged lag phase of PEF-treated cells. The lag phase extension was referred to as the time for the repair of damaged cells. The authors observed no effect of the initial cell concentration on the lag phase of untreated cells. Therefore, the possible effect of the initial cell concentration in untreated-diluted and PEF, 1st cycle samples was neglected. Furthermore, Zhao et al. (2009) suggested that cold storage (4 °C for seven days) following a PEF treatment can inhibit the repair of injured cells, thereby extending the shelf-life of tea infusions up to 90 days at 37 °C. Further work is required to study the level of cell injury and recovery at refrigerated storage.

3.3.6 Process energy requirement

Electricity is considered a sustainable energy if produced accordingly. In that respect, PEF treatment emerges as a sustainable alternative to thermal processing (Arshad et al., 2021). Arnal et al. (2018) conducted a life cycle assessment (LCA) for integrating PEF within the tomato peeling process and reported a reduction of 17 – 20% of the environmental footprint. In contrast, Aganovic et al. (2017) reported three times increase in energy requirements using PEF compared to thermal processing for fruit juice pasteurization. Moreover, Sampedro et al. (2014), estimated total costs of 1.5 and 3.7 ¢/L juice for thermal and PEF

pasteurization, respectively. In this study, the energy input required to achieve a 2-log reduction after PEF (E_{PEF}) or thermal treatment (E_{TT}) were calculated using Equations 3.8 and 3.9 and are displayed in Table 3.3. Cooling and energy losses were neglected.

Table 3.3: Process energy requirement comparison between thermal and PEF treatment to achieve a 2-log microbial reduction for three microorganisms inoculated in microalgae suspension

Isolates	Thermal treatment		PEF treatment		
	$T_{outlet,2logred}$ (°C)	E_{TT} (kJ/L)	W_s (kJ/L)	$T_{outlet,2logred}$ (°C)	E_{PEF} (kJ/L)
Pseudomonas guariconensis	57.7	155.6	113.6	53.0	154.9
Enterobacter soli	55.4	146.4	106.4	51.6	147.7
Lactococcus lactis	60.2	166.1	114.8	53.2	156.1

The same inactivation effects with PEF treatments require lower product temperatures T_{outlet}, and the temperature reduction was found to be 4.7, 3.8 and 7.0 °C for *P. guariconensis, E. soli* and *L. lactis*, respectively. The notably higher difference for *L. lactis* is aligned with its elevated thermal resistance (Section 3.3.3). However, the loss factors from the energy source, such as the sun, waterpower, or wind, to electric energy, energy transmission, and transformation of electric energy into thermal energy or high-voltage pulses must be considered for a meaningful comparison of the energy efficiency of thermal and non-thermal, electric treatments.

3.4 Conclusion

Microalgae are valuable ingredients in plant-based food, albeit their susceptibility to rapid spoilage, even under refrigerated storage conditions. Thermal pasteurization results in undesirable functionality losses. Applying high-intensity electric fields on *Cv* suspensions yielded up to 3.5-log cycle reduction for three substrate-specific psychrotropic bacteria and considerable shelf-life extension of the refrigerated substrate. The inactivation increased with an increased electrical field strength, and repeated (sequential) PEF treatments. These findings demonstrate PEF technology's potential within this specific application domain. Further investigation of the inactivation mechanism (cell injury) might trigger optimization of the inactivation effect. Also, the matrix composition, especially the soluble protein content and substrate conductivity, should be investigated to better understand the interconnectivity of parameters in PEF systems and improve the technology readiness level. In this study, PEF parameter settings were investigated which are considered not negatively influencing gelling properties of the protein rich substrate.

3.5 Appendix

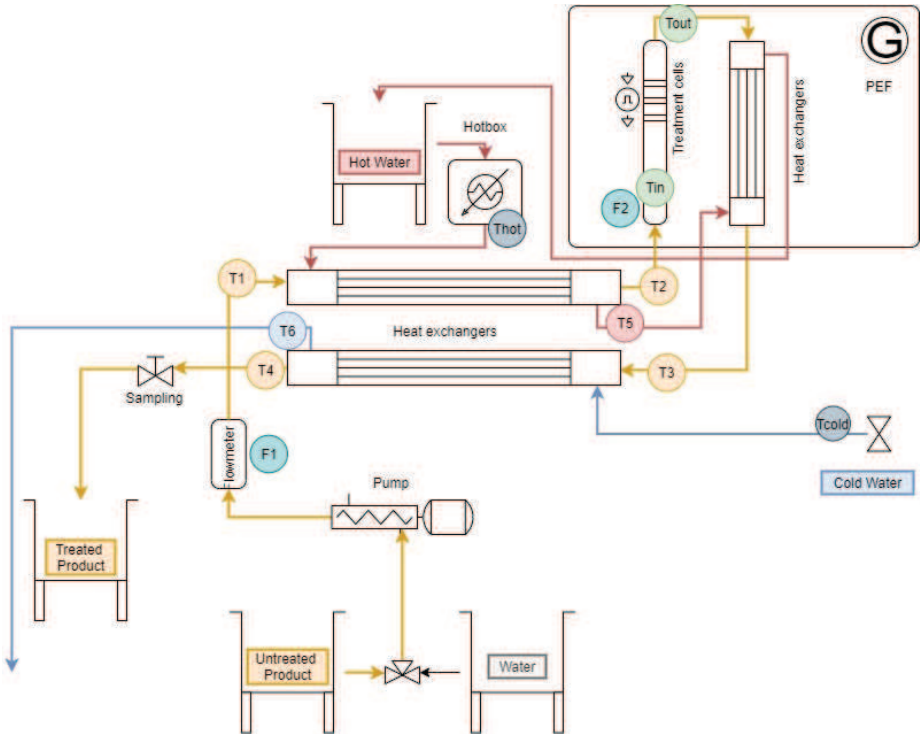

Figure 3.A.1: PEF setup. Product temperature at the inlet (T1) and outlet (T2) of the heating and inlet (T3) and outlet (T4) of the cooling. Water temperature at the outlets of the heating (T5) and cooling (T6). Product temperature at the inlet (Tin) and outlet (Tout) of the PEF chamber. F1 and F2, the flow rates.



Pulsed electric field combined with preheating to preserve mildly extracted pea protein

This chapter is published as:

De Gol, C., Etschmann, N., Zwietering, M. H., Den Besten, H. M. W., & Beyrer, M. (2024). Pulsed electric field combined with preheating to preserve mildly extracted pea protein. *LWT – Food Science and Technology*, *214*, 117100. https://doi.org/10.1016/j.lwt.2024.117100

Abstract

Innovative extraction methods involving dry fractionation and aqueous phase separation have been recently developed to obtain plant-based protein ingredients with high texturing functionality. Such a process was applied to yellow peas, and the microbial quality of the extract was assessed. *Pseudomonas trivalis* and *Erwinia gerundensis* were identified as critical microbial contaminants due to their high growth capacities (at 10 °C). As a preservation strategy, pulsed electric field (PEF) treatment (24 kV/cm, 50 Hz, 126 µs) was employed, combined with different product inlet temperatures (25 – 45 °C). Ohmic heating (ΔT = 20 °C) was measured. At 25 – 30 °C, the microbial reduction reached 3 logs, attributed solely to electrical effects. At 40 °C, the reduction exceeded 4 logs, where thermal effects dominated. Further increase to 45 °C resulted in thermal modification of pea proteins, potentially compromising its gelling capacity.

Additionally, the growth of PEF-treated contaminants at 5 and 10 °C were monitored, revealing rapid cell adaptation and proliferation. Finally, the extracts native microbiota showed an extension of the lag phase (four days at 5 °C) after PEF treatment, accompanied by a pH stability of ten days. The findings indicate improved microbial stability of the pea extract following PEF treatment.

4.1 Introduction

The shift from an animal-based to a plant-based diet is recognized as a key strategy for creating a more sustainable and healthy food system (Agyemang et al., 2022; Smetana et al., 2023). The development of plant-based meat substitutes, designed to mimic the taste, texture, and ease of preparation of meat, aims to facilitate this transition (Michel et al., 2021). The desired texture in these substitutes is typically achieved through extrusion, a thermomechanical process involving denaturation and intermolecular binding of biopolymers (proteins and potentially polysaccharides) at high temperatures combined with high shear stress. Van der Sman & Van der Goot (2023) and Guan et al. (2024) described the formation of fibrous structures through a multi-layer structuring theory, highlighting the critical role of the raw materials' viscoelastic properties in controlling gelation during extrusion.

Pea is a promising source for meat substitutes because of its low allergenicity, complete amino acid profile and the presence of proteins (predominantly globulins (~ 80%) and albumins (~ 20%) that exhibit strong gelling capacities (Lu et al., 2020). Additionally, substituting beef with pea protein has been shown to impact both human health positively and reduce carbon footprint (Saget et al., 2021). Typically, pea derivates as food ingredients come as powdered pea protein isolates (PPIs) with a protein content of 75 – 90% (Schutyser et al., 2015). PPIs are produced via wet extraction methods involving alkaline solubilization, isoelectric point precipitation, and mechanical separation followed by spray drying. While this process yields relatively pure protein ingredients, it comes at the cost of diminished protein nativity and high water, energy, and chemical consumption (Lie-Piang et al., 2021; Reinkensmeier et al., 2015; Schutyser & Van der Goot, 2011). Additionally, this process removes pea albumins, which are water-soluble at the isoelectric point of pea globulins, and which contribute to firmer and more elastic gels than pea globulins (Kornet et al., 2021b; Möller et al., 2022). The extraordinary texturizing effect of albumins was justified with its high content of sulfur-containing amino acids (Higgins et al., 1986), participating in disulfide binding and protein network formation at extrusion cooking.

Novel mild processing techniques, such as dry fractionation, are emerging as sustainable alternatives that prioritize protein functionality over purity (Kornet et al., 2021a; Möller et al., 2022; Pelgrom et al., 2015). Dry fractionation involves air classification, a physical separation of protein from starch, based on size and density, resulting in a pea protein concentrate (PPC) (Schutyser et al., 2015). Typically, PPC contains ~ 50% of proteins

(Reinkensmeier et al., 2015; Rodriguez & Beyrer, 2023). An additional step of aqueous phase separation and subsequent centrifugation can increase this protein content to ~ 60%, yielding pea protein extract (PPE) that contains both albumins and globulins (Lie-Piang et al., 2021; Möller et al., 2022; Pelgrom et al., 2015; Rodriguez & Beyrer, 2023). The higher functionality of these extracts compensates for their lower protein content in comparison to PPI. Indeed, Kornet et al. (2021a) showed that a lower degree of fractionation leads to an increased gelling capacity of the ingredient. Moreover, Rodriguez & Beyrer (2023) observed that partially substituting PPI with PPE enhanced the elasticity of the resulting gel. They also demonstrated that PPE could be directly used in the production of meat substitutes without the need for additional drying or concentration.

For storage and transportation purposes, ensuring PPE's microbiological stability is crucial. Pulsed electric fields (PEF) technology emerges as a sustainable alternative to thermal preservation. Despite showing higher estimated cost (0.037 EUR/L versus 0.015 EUR/L), PEF offers a non-denaturing, and low-energy preservation method suitable for heat-sensitive liquids at industrial scale (Jadhav et al., 2021; Sampedro et al., 2014; Toepfl et al., 2006). By subjecting the liquid to electric pulses of high voltage and short duration, the inactivation of microbial vegetative cells is possible at temperatures below 60 °C. The microbial inactivation is explained primarily by cell membrane permeabilization and can be facilitated by the additional thermal effect when combined with mild preheating (30 – 50 °C) (Alirezalu et al., 2020; Sharma et al., 2014; Yan et al., 2021; Zheng et al., 2024). The effectiveness of PEF depends strongly on factors such as electric field strength E_{el}, treatment time t, substrate inlet temperature T_{in}, pH, conductivity, composition, and microbial cell characteristics (Raso et al., 2016). PEF can be successfully used for the microbial reduction of low viscosity and low electrical conductivity liquid foods like fruit juice and milk (Cavalcanti et al., 2023; Nowosad et al., 2021; Šalaševičius et al., 2021; Schottroff et al., 2019; Sharma et al., 2014; Timmermans et al., 2022). Recent studies have also explored the application of PEF on plant protein ingredients such as microalgae (De Gol et al., 2024a), soy (Alzahrani et al., 2022), and oat milk (Thamsuaidee et al., 2024), as well as oat-based beverages enriched with pea protein (Horlacher et al., 2024). The authors highlighted challenges related to the protective effect of proteins and the high conductivity of the substrate (Schottroff et al., 2019). Conversely, PEF treatment not only achieves microbial inactivation but also has the potential to enhance protein solubility, thereby improving gelling characteristics (Malik et al., 2024; Taha et al., 2022). This dual benefit makes PEF an

appealing option for preserving plant-based ingredients intended for extruded meat substitutes.

This study aims to 1) identify relevant spoilage microorganisms able to grow in PPE under refrigerated conditions, 2) optimize PEF-induced inactivation of identified bacterial species at different product inlet temperatures, and 3) define a PEF treatment window for microbial inactivation and shelf-life extension of PPE.

4.2 Material and methods

4.2.1 Pea protein extract (PPE)

Air classified PPC was obtained from yellow pea (*Pisum sativum)* (GMSA, Switzerland). PPE was produced from PPC by aqueous extraction. PPC was dispersed in demineralized water (15 g PPC/100 g) and stirred at 200 rpm for 4 h at room temperature. This process avoided the use of solvents to maintain the natural pH of the PPE, thereby preserving protein functionalities. Moisture content was determined using a rapid moisture analyzer (HC103 Mettler-Toledo, Switzerland) at the conditions of 120 °C, initial mass of 2 g, and stop criteria of 1 mg/50 s. The pH and conductivity were measured using a pH/conductometer 914 (Metrohm, Switzerland). The extraction was done at lab scale in triplicate. The composition analyses and the microorganism selection (Sections 4.2.1.1, 4.2.1.2, 4.2.3 and 4.2.4) were done on multiple PPEs. The preservation treatments (Sections 4.2.5 to 4.2.8) were applied in biological triplicate on the same PPE, produced at pilot scale.

4.2.1.1 Sugar analysis by high performance liquid chromatography (HPLC)

Carrez I and Carrez II reagents were prepared from potassium hexacyanoferrate (II) (Sigma-Aldrich GmbH, Germany) and zinc sulphate (Sigma-Aldrich GmbH, Germany), respectively, and 200 µL of each reagent was added to the PPE (1 mL). After vortexing and incubation (10 min), the mixture was centrifuged (2'000 *x g*, room temperature, 5 min) using a microcentrifuge (Roth AG, Switzerland). The resulting supernatant was subjected to different purification steps: dilution with demineralized water (1:1), sonication for 10 min, centrifugation (7'500 *x g*, 20 °C, 8 min) and filtration through a 0.45 µm filter (Macherey-Nagel, Germany). Standards glucose, fructose and saccharose (Sigma-Aldrich GmbH, Germany) were dissolved in ultrapure water to prepare the stock solutions (10 g/L). The chromatographic analysis was conducted using an HPLC system 1220 Infinity LC system (Agilent Technologies, USA) equipped with the Aminex HPX-87H column (300 mm x 7.8 mm) from Bio-Rad Laboratories (USA) in conjunction with a Bio-Rad pre-column. Sulfuric

acid (Sigma-Aldrich GmbH, Germany) was used as the eluent solution (5 mmol/L) in isocratic mode and with a 0.6 mL/min flow rate. The sample injection volume was 5 µL and the column was maintained at 35 °C. Detection was accomplished using a refractive index detector (RID) at a wavelength of 210 nm. The peak areas were measured at 7.4, 8.8 and 9.6 min for saccharose, glucose and fructose, respectively. Four measurements were performed on multiple PPEs.

4.2.1.2 Protein content

The crude nitrogen content of the PPE was determined using the Kjeldahl method. The protein content was calculated using a conversion factor of 5.5, which is appropriate for pea proteins (Schlangen et al., 2022). The measurements were done in duplicate.

4.2.2 Microorganism isolation and identification

Fresh PPE was stored at 10 °C in a constant climate chamber (ICH260 Memmert, Germany), and was microbiologically analyzed at days 0, 3 and 6. For that, 1 mL of sample was decimally diluted using maximum recovery diluent (MRD, 1.0 g enzymatic digest of casein and 8.5 g sodium chloride in 1 L water) (Biolife, Italy), and different dilutions were plated on plate counting agar (PCA) (Biokar Diagnostics, France). The plates were incubated at 10 °C for up to nine days. The dilution showing an appropriate number of colonies was considered, and every single colony on the plate was isolated and purified for identification by three subsequent streaking on PCA plates and incubation (IPP 110^{PLUS} Memmert, Germany) at 30 °C for 24 h. The plates containing pure colonies were sealed to avoid cross-contamination and sent externally for identification (Mabritec SA, Switzerland) using MALDI-TOF MS technology. The spectra were analyzed using the SARAMIS SuperSpectra (SSp) tool and matched with the putative assigned protein masses for the identification database (PAPMID). Finally, the isolated species were grown in tryptic-casein soy broth (TSB) (Biokar Diagnostics, France) at 30 °C, 150 rpm for 24 h, mixed with glycerol at a ratio 1:1 and stored at – 80 °C for further use in challenge testing. The procedure was done on three different PPEs.

4.2.3 Microorganism selection

Based on the identification results (Section 4.2.2.), the three dominating species (*Erwinia gerundensis*, *Pseudomonas trivalis* and *Enterobacter amnigena*) were pre-selected and used for further growth tests. The isolated species were freshly inoculated on PCA plates. Single colonies were picked, transferred and grown in TSB at 30 °C at 150 rpm for 24 h, and

the cell concentration was estimated at 10^9 colony forming units (CFU)/mL by microscopy (Olympus XC10, Carl Zeiss, Germany) using a Neubauer chamber 0.02 mm depth and 0.0025 mm^2 (Assistant, Germany). The inocula were diluted into autoclaved (120 °C, 15 min) PPE and incubated at 10 °C, 150 rpm for six days in a shaking incubator (Excella E24 New Brunswick Scientific, USA). The microbial growth was monitored by sampling the PPE on days 0, 3 and 6 by preparing decimal dilution series and plating on PCA that were incubated at 30 °C for 24 h. Two microorganisms were selected for challenge tests based on their capacity to adapt and grow in refrigerated conditions.

4.2.4 Cultivation and viable cell count after PEF and thermal treatments

The selected species were freshly inoculated on PCA plates. Single colonies were grown in TSB at 30 °C, 150 rpm for 24 h, and inoculated in previously diluted PPE (dry matter (DM) content of 3 g/100 g sample) to reach an initial microbial load of approximately 10^6 CFU/mL, noted as N_0. The samples were used to determine the PEF and thermal resistance of the microorganisms (Sections 4.2.5 and 4.2.6). The treated samples were stored on ice and plated within 2 h following the treatment. The decimal dilutions were prepared with MRD, and at least three dilutions (50 µL) were plated. The colonies were grown on PCA plates at 30 °C for 24 h. Enumeration of colonies allowed us to determine the inactivation level for each treatment, calculated as $\log_{10}(N/N_0)$, where N and N_0 are the microbial concentrations (CFU/mL) in the treated and untreated samples, respectively. OriginLab® 2022b (OriginLab Corporation, USA) generated logarithmic (log) reduction graphs. Cultivations, sample preparation, inactivation treatments, and microbiological analysis were done in triplicate.

4.2.5 PEF treatments

During PEF treatment, the power required to apply a specific treatment is highly dependent on the conductivity of the substrate (Raso et al., 2022). Increased conductivity results in higher current in the PEF chamber, which can disrupt the generation of square pulses at high voltage and consequently decrease the intensity of the electric field strength. In this study, the conductivity of the PPE was reduced from 6 to 2 mS/cm by dilution with demineralized water to reach an E_{el} > 20 kV/cm. The PEF system was described by De Gol et al. (2024a). Briefly, the setup included a pilot-scale PEF machine (HVP-5, ELEA, Germany) with a co-linear flow cell with one high-voltage electrode in the middle and two ground electrodes (spacers of 1 cm), and a 1.57 mL treatment chamber. A screw pump (Mono pump 3NU10, Socsil-Inter SA, Switzerland) regulated the flow rate F of the diluted PPE (DM of 3 g/100 g sample, 2 mS/cm) at 45 L/h, corresponding to a residence time in the

PEF cell $t_r = V_{chamber}/F$ of 0.126 s. A customized tubular heat exchanger, with temperature control via a thermoregulator (HB120, Huber Kältemaschinenbau AG, Germany), was used for heating (T_{in} = 25, 30, 35, 40, 45 °C) and cooling the PPE. The time for the PEF-treated liquid to reach the cooling zone was 27 s at 45 L/h. Temperatures were monitored and recorded with PT100 TMR31 temperature sensors (Endress+Hauser Group Services AG, Switzerland) and LabView 2015 software. Square pulses of duration τ 20 µs and pulse repetition rate f 50 Hz were generated, with an output voltage set at 90%, resulting in an electric field strength E_{el} of 24 kV/cm and a treatment time $t = t_r \cdot f \cdot \tau$ of 126 µs. An oscilloscope (TDS 2024C Tektronix, USA) was connected to register the pulse shape. The pulse amplitude (voltage U (V) and current I (A)), the electric field strength E_{el} (kV/cm), the specific energy input W_s (kJ/kg) and the outlet temperature T_{out} (°C) were monitored after 1 min treatment to ensure process stability. Cultivations, sample preparation, PEF treatments and microbiological analysis were done in biological triplicate using the same PPE. The detection limit was 20 cells/mL sample.

4.2.6 Thermal treatments

As described by De Gol et al. (2024a), in addition to the PEF resistance, the thermal resistance of microorganisms was studied to distinguish between electrical and thermal inactivation effects. The temperature profile of both processes is similar. A modular micro reaction system (MMRS) (Ehrfeld Mikrotechnik GmbH, Germany) with a total treatment volume of 2.5 mL was used. The liquid was pumped (Nikkiso pump, LEWA GmbH, Switzerland) at a flow rate of 5.5 mL/min (mini-Cori-Flow M14-ABD-22-0-S, Bronkhorst, Switzerland), leading to a total retention time of 27 s, corresponding to the holding time in the PEF system from the PEF cell to the cooling zone (Section 4.2.5). The temperatures and flow rate values were monitored using the software LabView. Cultivations, sample preparation, thermal treatments and microbiological analysis were performed in biological triplicates. The detection limit was 1 cell/mL sample. The critical temperature T_{crit} was defined as the minimal temperature required to observe inactivation. It was calculated using Equation 4.1 on the straight part of the inactivation curve. The extracted T_{crit} mean value was used to determine the confidence intervals (95% confidence level) using the Student's t-distribution.

$$\log_{10} N/N_0 = a \cdot (T - T_{crit}) \quad \text{(-)} \qquad (4.1)$$

4.2.7 Thermal degradation of PPE – Differential scanning calorimetry (DSC)

Heat-induced denaturation was determined by DSC using a μDSC7 evo (Setaram Instrumentation, France), as explained by Rodriguez & Beyrer (2023). Briefly, the samples were scanned from 20 °C to 100 °C at a heating rate of 0.5 °C/ min, held at 100 °C for 10 min, and subsequently cooled to 20 °C at the same rate. The Thermal Analysis® Software package V. 1.46 (Setaram Instrumentation, France) was used to extract the reaction enthalpy ΔH and peak maximum temperature T_{peak} values. The measurements were done in triplicate on the reference and diluted PPE (DM of 3 g/100 g sample) and the PEF-treated PPE (T_{in} = 30, 40, 45 °C).

4.2.8 Storage control

P. trivalis and *E. gerundensis* were inoculated in diluted and pasteurized (85 °C, 5 min) PPE. Their microbial growth following PEF treatment (24 kV/cm, 50 Hz, 126 μs and 40 °C) was studied during cold storage (5 and 10 °C, 14 days). Additionally, the growth of the native microbiota of PPE (no pasteurization) after PEF treatment was also explored. Monitoring of the pH was done using a pH-meter 914 (Metrohm, Switzerland). Cultivations, sample preparation, PEF treatments and storage control were done in biological triplicates. The detection limit was 20 cells/mL sample.

Similarly to De Gol et al. (2024a), the growth curves were modelled using the primary reparametrized Gompertz model (Equation 4.2) (Garre et al., 2023; Zwietering et al., 1990):

$$\log_{10}N = \log_{10}N_0 + A \cdot \left(\exp\left(-\exp\left(\frac{e\cdot\mu}{A}(\lambda - t) + 1\right)\right)\right) \quad \text{(CFU/mL)} \quad (4.2)$$

With the microbial concentration N (CFU/mL), the difference between $\log_{10}N_{max}$ and $\log_{10}N_0$ A ($\log_{10}$CFU/mL), the storage time t (d), the maximum growth rate μ ($\log_{10}d^{-1}$) and the lag phase λ (d).

4.2.9 Statistical analysis

All the analytical measurements were done in duplicate (n = 2) or triplicate (n = 3). Results were expressed as individual data points for duplicates, while triplicates were expressed as average ± standard deviation (SD). Regarding statistical analysis, first, normality distribution (Shapiro-Wilk test) and equal variance (Chi-square test for variance) were checked (p = 0.05). Statistical significance was estimated by one-way ANOVA and Tukey's post hoc test. Dunn's test and Welch's ANOVA were used when normality and equal variance were rejected, respectively. P-values < 0.05 were considered statistically significant. All statistical tests were performed using OriginLab® 2022b (OriginLab Corporation, USA).

4.3 Results and discussion

4.3.1 Chemical properties of the substrate PPE

The DM content and pH of PPE were 10.6 ± 0.1 g/100 g and 6.7 ± 0.0, respectively. The protein content was 6.1 g/100 g PPE on a wet basis, corresponding to an average value of 57.7 g/100 g PPE on a dry basis. Free sugar analysis revealed saccharose, glucose and fructose concentrations at 3.1 ± 0.0, 0.5 ± 0.0, and 3.8 ± 0.3 g/L PPE, respectively. The substrate contains all the necessary nutrients (water, carbon and nitrogen sources, minerals and vitamins) for microbial growth, supported by its neutral pH (Campos-Vega et al., 2010; Millar et al., 2019; Vidal-Valverde et al., 2003). The dilution of the extract with demineralized water aiming to reduce the conductivity from 6 to 2 mS/cm and reach E_{el} > 20 kV/cm during PEF treatment led to a decrease of the DM to 3 g/100 g sample.

4.3.2 Microbial contaminants of PPE

4.3.2.1 Identification of marker microorganisms

The identification of bacterial species in PPE after three and six days was conducted to select the main microbial contaminants during cold storage (10 °C). A total of 69 species were purified and identified, leading to the detection of 20 different species, including *Erwinia* (*E. persicina, E. gerundensis, E. aphidicola*), *Pseudomonas* (*P. poae, P. trivalis, P. sivasensis, P. canadensis, P. reactans, P. synxantha, P. fluorescens*), *Pantoea* (*P. anthopila, P. agglomerans, P. pleuroti*) and *Enterobacter* (*E. cowanii, E. cloacae complex, E. amnigena*) species. *Myroides odoratimimus, Lysinibacillus capsici, Providencia stuartii* and *Bacillus cereus* were also detected. *E. persicina, E. gerundensis, P. agglomerans, P. fluorescens, E. amnigena, Lysinibacillus* and *B. cereus* were previously identified in pea (Chartrel et al., 2021; Godebo et al., 2020; Kyrylenko et al., 2023). During cold storage, the microbial load increased significantly from 3.4 to 9.1 logs CFU/mL, accompanied by a decrease in pH from 6.7 to 5.8, conceivable due to the production of organic acids (Table 4.1). Initially, *Erwinia* species dominated, comprising 64% of the microbial population on day 0 and 39% on day 3. However, by day 6, *Enterobacter* species became dominant, accounting for 65% of the population. *Pseudomonas* species were detected after three days of storage, constituting 25% of the microbial community at days 3 and 6.

Table 4.1: Microbial and pH evolution during incubation of PPE (DM of 10 g/100 g sample) at 10 °C for six days. Species (sp) identification was achieved through MALDI-TOF MS. Data are averages of biological triplicates (n = 3) ± SD [95% confidence intervals]. % indicates the proportion in % of total detected species

Description	Storage time (days)		
	0	**3**	**6**
N° colonies identified (-)	24	15	30
Total count (log CFU/ml)	3.4 ± 0.1	7.2 ± 0.1	9.1 ± 0.1
pH (-)	6.7 ± 0.0	6.7 ± 0.0	5.8 ± 0.5
Erwinia sp. (%)	64 ± 13 [47 – 82]	39 ± 8 [28 – 50]	n.d.
Pantoae sp. (%)	23 ± 14 [4 – 43]	14 ± 4 [8 – 19]	n.d.
Enterobacter sp. (%)	n.d.	n.d.	65 ± 14 [46 – 84]
Pseudomonas sp. (%)	n.d.	25 ± 19 [9 – 41]	25 ± 12 [9 – 41]
Other sp. (%)	12 ± 7 [2 – 22]	22 ± 8 [11 – 33]	10 ± 6 [2 – 18]

n.d. : not detected

4.3.2.2 Growth capacity of marker microorganisms

To eliminate competing effects between species, the three dominating species, i.e., *E. gerundensis, E. amnigena* and *P. trivalis,* were individually inoculated into autoclaved PPE and incubated at 10 °C for six days. The log increase after three- and six-days storage is presented in Figure 4.1. *P. trivalis* (2.5 and 2.9 log increase after three and six days, respectively) showed the highest growth capacity and was selected for the challenge tests. A second bacterial species (*E. gerundensis*) was also included in the study. Similarly, Chartrel et al. (2021) explored the microbial community composition of *Pisum sativum* after five days of soaking at 4 °C, identifying the *Proteobacteria* class (including *Erwinia, Pantoea, Pseudomonas and Sphingomonas*) as the most abundant, comprising 57% of the total community.

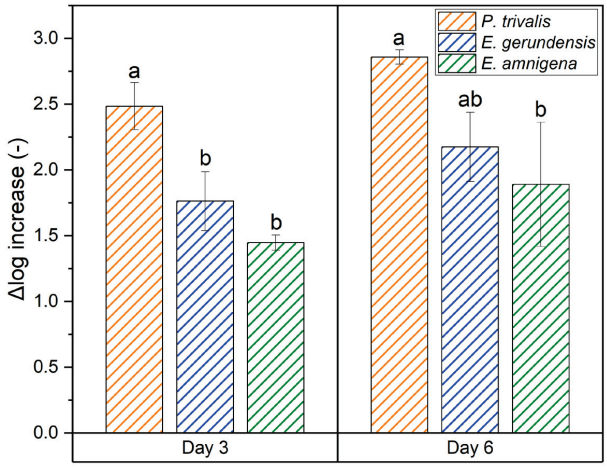

Figure 4.1: Growth kinetics of *P. trivalis, E. gerundensis* and *E. amnigena* shown as Δlog increase after three- and six-days storage at 10 °C. Different letters indicate significant differences ($p < 0.05$).

4.3.3 PEF and thermal sensitivity of marker microorganisms

P. trivalis and *E. gerundensis* were inoculated into diluted (DM of 3 g/100 g sample, 2 mS/cm, pH 6.7) and pasteurized (85 °C, 5 min) PPE and then subjected to PEF and thermal treatments. After optimization (data not shown), the selected PEF parameters were E_{el} = 24 kV/cm, f = 50 Hz, τ = 20 µs, t = 126 µs, corresponding to a measured specific input energy of W_s = 144 kJ/kg and reliable square-shape pulses (Figure 4.A.1). Various substrate inlet temperatures (T_{in} = 25, 30, 35, 40, and 45 °C) were tested. An increase in temperature of 20 °C due to ohmic heating was measured under these conditions. Therefore, thermal treatments at 45, 50, 55, 60, and 65 °C were conducted to study the thermal contribution during PEF treatments starting at inlet temperatures of 25, 30, 35, 40, and 45 °C, respectively.

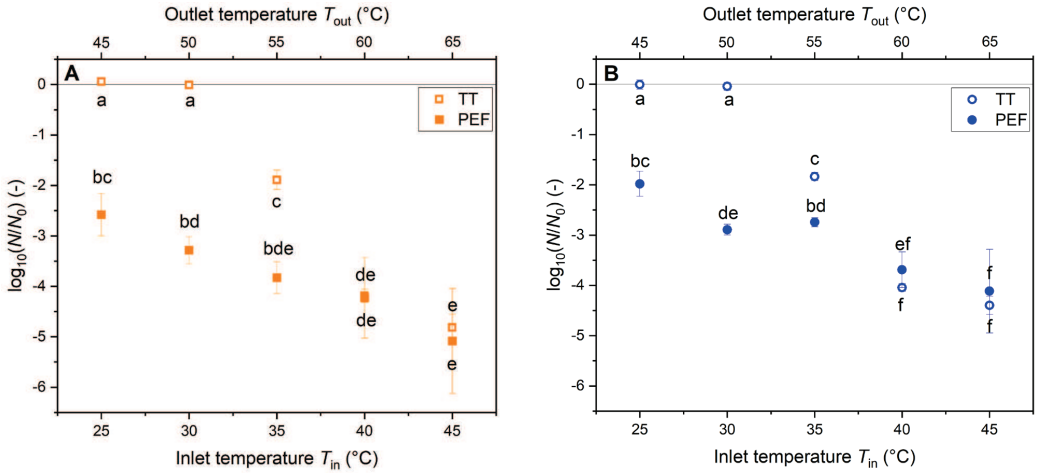

Figure 4.2: Influence of inlet temperature T_{in} on inactivation effects of *P. trivalis* (■, A) and *E. gerundensis* (●, B) for a PEF treatment of 24 kV/cm, 50 Hz, 126 µs in a PPE substrate of 2 mS/cm and pH 6.7. The initial count N_0 was ~ 10^6 CFU/mL. Data points are averages of three individual measurements (n = 3) ± SD. Filled and open symbols represent PEF (Section 4.2.5) and purely thermal (Section 4.2.6) inactivation effects, respectively. Different letters indicate significant differences ($p < 0.05$).

The levels of PEF inactivation increased with higher inlet temperatures for both *P. trivalis* (from 2.6 ± 0.4 to 5.1 ± 1.0 log reduction) and *E. gerundensis* (from 2.0 ± 0.3 to 4.1 ± 0.8 log reduction), as displayed in Figure 4.2. No thermal inactivation was detected at temperatures ≤ 50 °C for either species. However, PEF treatments at inlet temperatures T_{in} of 25 and 30 °C (resulting in an outlet temperature T_{out} of 45 and 50 °C, respectively) caused significant inactivation (≥ 2 logs), attributed solely to electrical effects. Both species exhibited thermal inactivation at 55 °C (1.9 ± 0.2 and 1.8 ± 0.1 log reduction for *P. trivalis* and *E. gerundensis*, respectively). They demonstrated similar thermal sensitivity, with critical inactivation

temperatures T_{crit} calculated at 50.9 ± 0.4 °C [95% confidence interval: 49.7 – 52.0] for *P. trivalis* and 50.8 ± 0.2 °C [95% confidence interval: 50.3 – 51.4] for *E. gerundensis*. Therefore, the inactivation observed at T_{in} = 35 °C can be attributed to both thermal and electrical effects. Previous studies also noted combined effects in the temperature range of 50 – 55 °C (Alirezalu et al., 2020; Schottroff & Jaeger, 2020; Sharma et al., 2014). At higher inlet temperatures (40 and 45 °C), the observed inactivation levels are ≥ 4 logs and thermal effects dominate electrical effects.

Horlacher et al. (2024) recently investigated a similar system with 5.1% plant-based protein content (oat and pea), a conductivity of 2.3 mS/cm and pH 7.0. They applied moderate field strengths (9 – 10 kV/cm, 50 Hz, 20 µs) combined with mild preheating (35, 40 and 45 °C) to a cocktail of surrogate bacteria (*E. coli* and *Listeria sp*). For a W_s of 96 – 102 kJ/L and an increase in temperature of ~ 15 °C, inactivation levels of 0.9, 1.6, and 4.8 logs were achieved for T_{in} of 35, 40 and 45 °C, respectively. At 35 and 40 °C, the reduction was likely attributed solely to electrical effects, with reduction levels (0.9 and 1.6 logs) slightly lower than those observed in the current study. These differences can be explained by the lower PEF intensity applied. At 45 °C and an increase of ~ 15 °C, the substantial jump to a similar reduction level (4.8 logs) as obtained in our study is most probably attributed to added thermal effects. Thamsuaidee et al. (2024) applied PEF treatment (24 kV/cm, 100 kJ/L, 30 °C) on an oat-based beverage (10 g/100 g, 2 mS/cm, pH 6.3) inoculated with *Lactiplantibacillus plantarum* and achieved higher reduction level (5.6 logs) compared to this study. Finally, Sharma et al. (2014) studied the effect of T_{in} (4, 30, 40, 45, 50 and 55 °C) on PEF-induced inactivation of *Pseudomonas aeruginosa* in whole milk (3.9 mS/cm). Using treatment parameters of 23 kV/cm, 60 Hz, 20 µs and 101 µs, they achieved lower reduction levels (0, 1.2, 2.3 and 3.0 log at 4, 30, 40 and 45 °C, respectively). The most probable explanation is the lower E_{el} and t values compared to this study.

4.3.4 Thermal properties of the substrate PPE before and after PEF

The DSC thermogram of the reference PPE reveals three distinct endothermic peaks (Figure 4.A.2.): a minor peak ΔH_1 (0.8 ± 0.2 J/g DM) detected at temperatures between 50 – 61 °C, a major peak ΔH_2 (4.2 ± 0.7 J/g DM) between 61 – 82 °C, and a second minor peak ΔH_3 (0.2 ± 0.1 J/g DM) between 82 – 88 °C (Table 4.2). Ma et al. (2017) analyzed DSC characteristics of yellow pea flour and coarse fibers, reporting a major peak (0.68 ± 0.05 J/g) at 81.9 ± 0.4 °C and a minor peak (0.02 ± 0.00 J/g) at 86.2 ± 0.2 °C for the flour. Specifically for the coarse fibers, next to a peak at 86 °C, an additional peak at 50 – 60 °C was detected.

Therefore, in Figure 4.A.2, the first peak ΔH_1 corresponds to fibers or pea starch gelatinization, whereas the second peak ΔH_2 is associated with protein denaturation (Zink et al., 2024). Moreover, Kuang et al. (2023) performed DSC analysis on PPI and attributed two characteristics denaturation endothermic peaks at 71 and 84 °C for 7S and 11S globulins, respectively. Similarly, O'Kane et al. (2004) reported denaturation temperatures of 69.9 – 71.8 °C and 87 °C for 7S and 11S globulins, respectively, and Pelgrom et al. (2015) found 87.7 ± 0.8 °C for PPI (NUTRALYS® F85G). Variations in temperature values may arise from different pea varieties or heating rates used during analyses (Li & Ganjyal, 2017; Mession et al., 2013).

Table 4.2 compares the thermal properties of PPE before and after dilution and PEF treatments. During PEF treatment, a temperature increase ΔT = 20 °C was measured due to ohmic heating. Consequently, PEF treatments at T_{in} = 35, 40 or 45 °C were selected for DSC analysis under the assumption that PEF at T_{in} = 25 and 30 °C would not significantly impact the thermal properties of PPE ($T_{out} \leq 50$ °C), PEF at T_{in} = 35 °C (T_{out} = 55 °C) would partially affect the first peak, PEF at T_{in} = 40 °C (T_{out} = 60 °C) would substantially affect the first peak, and PEF at T_{in} = 45 °C (T_{out} = 65 °C) would further impact the second peak. As expected, dilution had no significant impact on the thermal properties of PPE. Similarly, PEF treatment at T_{in} = 35 °C showed no significant influence. However, PEF treatment at T_{in} = 40 °C and 45 °C caused significant decreases in the reaction enthalpy values ΔH_1. Additionally, PEF treatment at T_{in} = 45 °C resulted in a significant reduction in ΔH_2 (– 39%), likely due to a T_{out} = 65 °C exceeding 61 °C, coupled with an observed decrease in gelling capacity during rheology tests (data not shown). Based on these findings, PEF treatment starting at a T_{in} of 40 °C was selected for further tests, showing high microbial inactivation (*P. trivalis*: 4.3 ± 0.8 log reduction and *E. gerundensis*: 3.7 ± 0.4 log reduction), while preserving the thermal properties of the PPE protein fraction (ΔH_2).

Table 4.2: Thermal properties of the substrate PPE at a DM of 10 g/100 g sample, after dilution to a DM of 3 g/100 g sample and after PEF treatments (T_{in} = 35, 40 or 45 °C). Data are averages of triplicates (n = 3) ± SD. Different letters indicate significant differences ($p < 0.05$)

Ingredients	ΔH_1 (J/g DM)	$T_{peak,1}$ (°C)	ΔH_2 (J/g DM)	$T_{peak,2}$ (°C)
PPE (DM of 10 g/100 g sample)	0.8 ± 0.2^{a}	53.8 ± 1.3^{a}	4.2 ± 0.7^{a}	73.9 ± 1.3^{a}
Diluted PPE (DM of 3 g/100 g sample)	0.6 ± 0.2^{ab}	54.4 ± 1.3^{a}	4.9 ± 1.1^{a}	77.3 ± 0.3^{a}
PEF-treated (T_{in} = 35 °C)	0.2 ± 0.1^{b}	55.3 ± 1.3^{a}	3.3 ± 0.3^{ab}	73.7 ± 0.5^{a}
PEF-treated (T_{in} = 40 °C)	n.d.	n.d.	3.0 ± 0.4^{ab}	72.9 ± 1.0^{a}
PEF-treated (T_{in} = 45 °C)	n.d.	n.d.	2.0 ± 0.7^{b}	72.6 ± 4.0^{a}

n.d.: not detected
ΔH_1 and ΔH_2 refer to the thermal events at 50 – 61 °C and 61 – 82 °C, respectively

4.3.5 Storage control and extract stability

The microbial growth of *P. trivialis* and *E. gerundensis* following PEF treatment (T_{in} = 40 °C) and subsequent storage under refrigerated conditions (5 and 10 °C for 14 days) is depicted in Figure 4.3. Growth parameters extracted from the model (Equation 4.2) are summarized in Table 4.3.

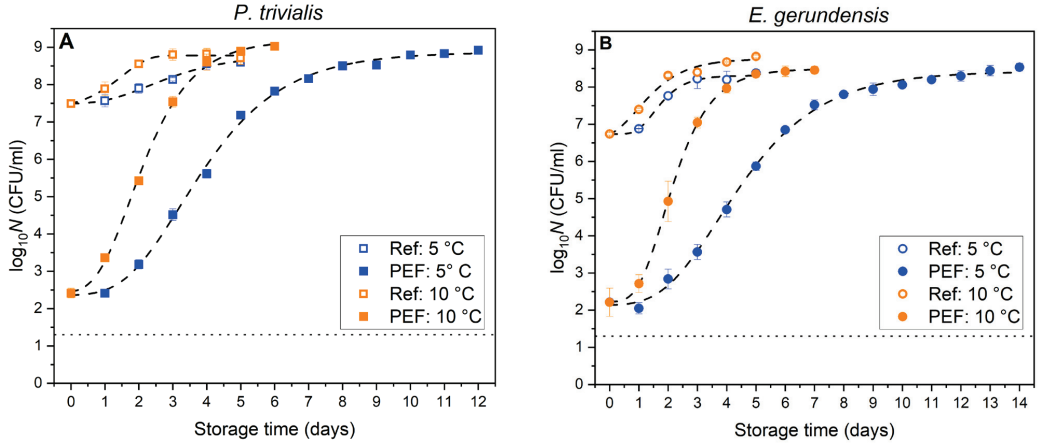

Figure 4.3: Microbial growth of untreated versus PEF-treated PPE inoculated with *P. trivialis* (A) and *E. gerundensis* (B) at T_{in} = 40 °C. Incubation was done at both 5 and 10 °C for 14 days. PEF treatments conditions were 24 kV/cm, 50 Hz, 126 µs in a PPE substrate of 2 mS/cm and pH 6.7. The initial count N_0 was ~ 10^6 CFU/mL, and the detection limit was 1.3 logs (dot lines). Data points are averages of three individual measurements (n = 3) ± SD. Open and Filled symbols represent references and PEF-treated samples, respectively. For visualization purposes, growth fitting was done on the average data points with biogrowth (dashed lines, Section 4.2.8).

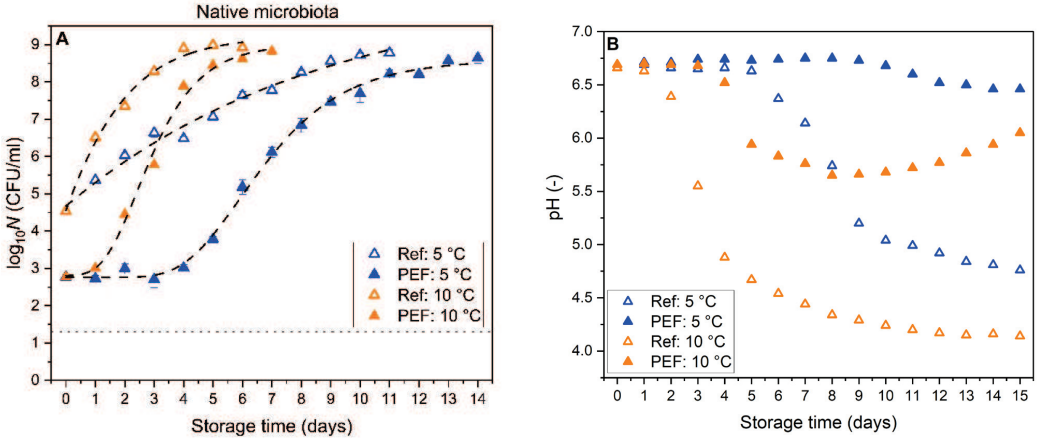

Figure 4.4: A: Microbial growth of untreated versus PEF-treated (T_{in} = 40 °C) PPE native microbiota. Incubation was done at both 5 (▲) and 10 °C (▲) for 14 days. PEF treatments conditions were 24 kV/cm, 50 Hz, 126 µs in a PPE substrate of 2 mS/cm and pH 6.7. The initial count N_0 was ~ 10^6 CFU/mL, and the detection limit was 1.3 logs (dot lines). Data points are averages of three individual measurements (n = 3) ± SD. Open and filled symbols represent references and PEF-treated samples, respectively. For visualization purposes, growth fitting was done on the average data points with biogrowth (dashed lines, Section 4.2.8). B: pH evolution during storage at 5 and 10 °C for 15 days.

As expected, the growth rate of both bacterial species increased at 10 °C in comparison to 5 °C, and a prolonged lag phase at lower temperatures was observed (Table 4.3). At 10 °C, both species exhibited similar growth rates and reached the spoilage level (i.e., 7 log/mL) within three days (Figure 4.3). In contrast, at 5 °C, *P. trivalis* grew faster and reached the spoilage level one day earlier than *E. gerundensis*. Previous studies have demonstrated the efficacy of PEF in extending the shelf-life of liquid foods. For instance, Timmermans et al. (2016) applied PEF (24 kV/cm, 100 Hz, 55 kJ/kg, 40 °C, ΔT = 18 °C) to yeast in fruit juice (3 mS/cm, pH 3.6) and observed an extension of the lag phase by 8.4 and 16 days at 7 and 4 °C, respectively. Additionally, De Gol et al. (2024a) applied PEF (28 kV/cm, 120 Hz, 226 µs, 115 – 120 kJ/kg, 30 °C) to bacteria inoculated into *Chlorella vulgaris* suspensions (2 g/100 g, 0.7 mS/cm, pH 6.5). They noted an increased lag phase for *Pseudomonas guariconensis* and *Lactococcus lactis* during storage at 10 °C. In the current study, the PEF treatment on *P. trivalis* and *E. gerundensis* appears to be ineffective for extending the lag phase and reducing the growth rate. Tests on reference samples with an initial cell concentration of 2 – 3 logs are recommended for improved comparability.

In addition to controlled challenge tests on *P. trivalis* and *E. gerundensis*, PEF treatment and storage control were also performed on the native microbiota of the PPE (Figure 4.4), with growth parameters shown in Table 4.3. The lag phase duration was significantly longer compared to the isolates. During storage at 5 °C, no growth was observed for the four first days, and the pH was stable for ten days (Figure 4.4). Additionally, the growth rate during storage at 10 °C was significantly lower than the data obtained for the isolates. The positive impact of PEF treatments on preservation was therefore more pronounced for the native microorganisms, making the psychrotrophic, substrate-isolated *P. trivalis* and *E. gerundensis* species relevant fast-growing candidates for challenge tests.

Table 4.3: Growth rate μ and lag phase duration λ after PEF treatment T_{in} = 40 °C, extracted from the biogrowth simulation as shown in Figures 4.3 and 4.4. Values are presented as averages of triplicates (n = 3) ± SD. Different letters indicate significant differences ($p < 0.05$)

Isolates	5 °C storage		10 °C storage	
	μ ($\log_{10}d^{-1}$)	λ (d)	μ ($\log_{10}d^{-1}$)	λ (d)
P. trivalis	1.5 ± 0.0^{a}	1.6 ± 0.2^{a}	2.5 ± 0.1^{a}	0.7 ± 0.0^{a}
E. gerundensis	1.2 ± 0.1^{b}	1.8 ± 0.2^{a}	2.6 ± 0.0^{a}	1.0 ± 0.1^{b}
Native microbiota	1.1 ± 0.1^{b}	4.0 ± 0.1^{b}	2.0 ± 0.0^{b}	1.3 ± 0.0^{c}

4.4 Conclusion and perspective

Mildly extracted and native pea proteins have significant potential for use in plant-based meat substitutes. However, they exhibit rapid spoilage even under refrigerated conditions. In this study, pilot-scale PEF treatments were applied to inactivate psychrotrophic spoilage microorganisms isolated from pea protein extract. The two studied species exhibited similar resistance at purely thermal or electrical treatments. PEF treatment effectively reduced microbial counts by approximately 3 logs, at processing peak temperatures below 50 °C, through purely electrical effects and without thermally modifying the pea proteins. However, to achieve inactivation levels higher than 4 logs, a processing peak temperature of 60 °C was necessary, where the inactivation was mainly attributed to thermal effects. Thus, the advantage of PEF over mild thermal treatment (at 60 °C) for higher inactivation levels remains to be demonstrated. While PEF may preserve or even improve protein functionality, further investigations are needed to confirm this potential benefit.

Additionally, pea protein extracts with the native microbiota were treated with PEF to validate the system in practical application. The lag phase of the native microbiota and general substrate stability were more extended compared to substrates inoculated with the isolated species, suggesting their suitability for challenge tests. Mild extraction, followed by temporary preservation of protein extracts, indicated energy savings and retention of protein functionality compared to traditional intense extraction and spray drying methods. Future research should focus on optimizing PEF treatments for higher concentration and higher electrical conductivity substrates, which is technically still challenging and essential for industrial scale implementation.

4.5 Appendices

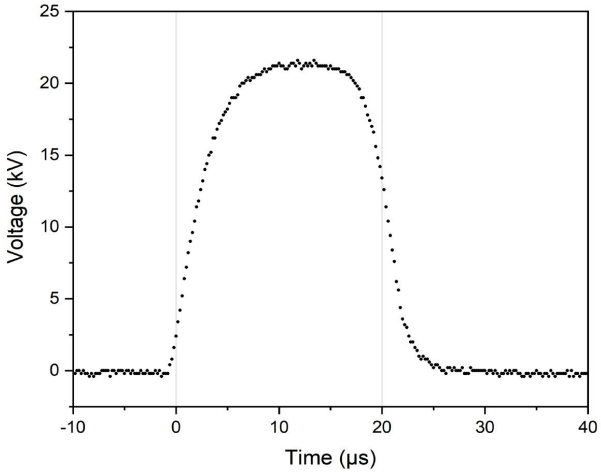

Figure 4.A.1: Monitoring of the pulse shape during PEF treatment at E_{el} = 24 kV/cm, f = 50 Hz, τ= 20 µs, t = 126 µs on the PPE substrate (DM of 3 g/100 g sample, 2 mS/cm, pH 6.7).

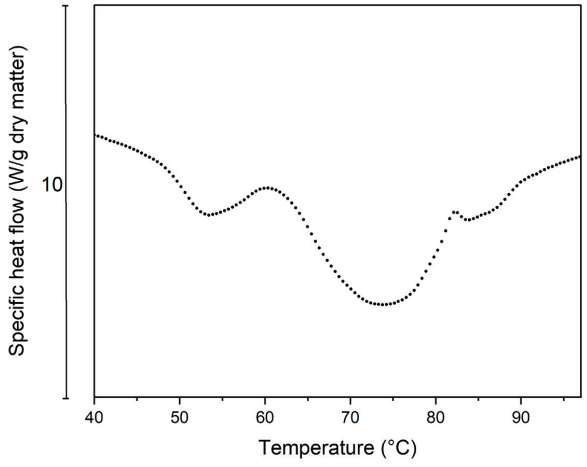

Figure 4.A.2: DSC thermogram (scanning from 20 °C to 100 °C at a heating rate of 0.5 °C/min) of the reference PPE (n = 3).

5



Effects of pulsed electric field and thermal treatment on the structural and techno-functional properties of mildly extracted pea proteins

This chapter is published as:

De Gol, C., De Ridder, V., Zwietering, M. H., Den Besten, H. M. W., & Beyrer, M. (2025). Effects of pulsed electric field and thermal treatment on the structural and techno-functional properties of mildly extracted pea proteins. *LWT – Food Science and Technology*, *238*, 118757. https://doi.org/10.1016/j.lwt.2025.118757

Abstract

Pulsed electric field (PEF) technology has gained interest for its potential to enhance the functional properties of food proteins. This study examined how PEF treatment, used to inactivate microorganisms, additionally affects the structure and functionality of mildly extracted pea proteins, and compared it to conventional heat pasteurization. PEF treatments of 24 kV/cm (f = 50 Hz, τ = 20 µs, t = 126 µs) combined with different product inlet temperatures (25, 30, 35 and 40 °C) were selected based on previously studied *Pseudomonas trivalis* and *Erwinia gerundensis* reductions, which ranged from 2.0 to 4.2 logs. Thermal treatments (TTs) of 51, 54, 57 and 60 °C for 27 s, leading to comparable microbial inactivation (from 0.1 up to 4.2 logarithmic reduction), were taken as reference and selected for comparison of protein modifications. Fluorescence and circular dichroism spectroscopy were performed on IEX-isolated pea albumins and globulins and revealed inverse impact on the structure for both proteins. While PEF-treatment led to protein unfolding (red shift of the Tryptophan (Trp) emission maxima), protein aggregation (blue shift) was observed for TT samples. Additionally, the impact of the treatments on the functionality of the extract was evaluated. While the gelling properties of pea extract were enhanced following PEF treatments (+ 35%), regardless of inlet temperature, the opposite was observed for the TTs, with a reduction of 60% compared to PEF-treated ingredients. The findings validated the advantage of PEF treatments over TTs for effective microbial reduction in pea protein extract while simultaneously enhancing the gelling properties.

5.1 Introduction

The diversification of protein sources towards more plant-based or algal proteins is crucial for reducing the environmental footprint and promoting healthier diets compared to traditional animal-based diets (Smetana et al., 2015; Springmann et al., 2018). Meat substitutes, particularly those produced from soy and pea proteins, support this transformation strategy (Ritchie et al., 2018). Yellow pea (*Pisum sativum*) is a promising source as it contains high protein content (~ 30%), low glycemic index, essential amino acids, and shows low allergenicity (Pereira et al., 2024). Additionally, pea seeds show strong growth yield and can be cultivated worldwide, meeting the sustainability criteria of local sourcing (Hall et al., 2017).

Typically, several processing steps, including milling, alkaline solubilization, isoelectric precipitation, mechanical separation and spray drying, are applied on the pea seeds to obtain a powdered pea protein isolate (PPI) containing 75 – 90% protein content, mainly consisting of globulins (Schutyser et al., 2015). PPI is often used to produce meat substitutes via extrusion (Cornet et al., 2021; Osen et al., 2014), a thermomechanical process involving high temperature and high shear stress. However, due to the intensity of the protein purification processes, PPI tends to be denatured and exhibits low functionality and solubility, which compromises the final texture of the meat substitute (Shanthakumar et al., 2022). Recently, researchers suggested the use of minimal extraction processing with no chemical and lower temperature (< 50 °C) to obtain mildly extracted protein-rich ingredients. Such extracts show better functionalities, including gelling capacity, and lower environmental footprint compared to PPI (Kornet et al., 2021; Möller et al., 2022; Zhu et al., 2021). More precisely, the protein extraction is done via dry fractionation to physically separate protein from starch, leading to a pea protein concentrate (PPC) with ~ 50% protein content. A potential subsequent aqueous phase separation can be applied to obtain a pea protein extract (PPE) with ~ 60% protein, composed of globulins and albumins (De Gol et al., 2024b; Pelgrom et al., 2015). The incorporation of such liquid pea extract in extrusion has been successfully achieved (Rodriguez & Beyrer, 2023), however it showed rapid spoilage, even under refrigeration conditions.

Conventional thermal pasteurization is effective for microbial inactivation and shelf-life extension but is energy intensive and often associated with a loss of nutritional quality and undesirable changes in protein structure (Pereira et al., 2024). To address these challenges, alternative pasteurization techniques, such as Pulsed Electric Field (PEF) treatment, have

been developed. PEF processing involves the application of electric pulses of high voltage and short duration (15 – 40 kV/cm, 1 – 100 µs), leading to microbial inactivation by cell electroporation without exceeding a temperature of 60 °C (Raso & Álvarez, 2016). Recently, PEF treatments (24 kV/cm, 50 Hz, 126 µs, inlet temperatures of 25 – 45 °C) have been successfully applied on mildly extracted pea proteins for microbial inactivation (De Gol et al., 2024b).

The distinct mechanisms of action underlying thermal and alternative pasteurization methods result in significantly different structural and functional modifications to proteins. Thermal pasteurization typically induces conformational shifts that lead to the formation of protein aggregates (Wijayanti et al., 2014). Due to the exposure of hydrophobic residues, the protein solubility and gelling capacity are reduced, compromising the desired food texture (Pereira et al., 2024). In contrast, PEF treatment can potentially enhance protein solubility, water-holding capacity, and gelling capacities. These effects arise from the polarization and disruption of non-covalent intermolecular bonds (Giteru et al., 2018; Liu et al., 2011; Zhao & Yang, 2008). However, at very high electric field strengths E_{el}, protein aggregation induced by PEF treatment has also been observed (Zhao & Yang, 2008). Some studies have suggested that PEF treatment generates free radicals, which can influence covalent intramolecular interactions within protein molecules (Han et al., 2018).

PEF's potential to modify the macrostructure of plant-based proteins has attracted growing interest and has been described in an increasing number of review studies (Ali et al., 2024; Giteru et al., 2018; Malik et al., 2024; Pereira et al., 2024; Rajeswari et al., 2024; Rodrigues et al., 2020; Taha et al., 2022; Vanga et al., 2021). To assess the structural (secondary and tertiary structures) and functional changes in proteins, researchers have employed various analytical techniques, including spectroscopic, microscopic, chromatographic, electrophoretic, and rheological methods. For example, PEF has been shown to influence the solubility, water- and oil-holding capacities, hydrophobicity and structural characteristics in wet gluten, soy, wheat, rice and canola proteins (Guo et al., 2023; Li, 2012; Liu et al., 2011, 2013; Qiu et al., 2021; Wang et al., 2023; Xiang et al., 2011; Zhang, C., et al., 2021; Zhang, L., et al., 2017). However, research on pea proteins remains limited, focusing primarily on PPI (Avelar et al., 2024; Chen et al., 2022; Guo et al., 2024; Melchior et al., 2020). To date, no studies have yet investigated the impact of PEF treatment on the structure and functionality of native pea proteins nor compared these effects with those of thermal pasteurization.

Therefore, this study's objective is to compare the effects of two pasteurization methods – PEF treatment and conventional thermal treatment (TT) – on the properties of mildly extracted and native pea proteins. Although both treatments can achieve similar levels of microbial inactivation, their distinct mechanisms of action are expected to affect protein characteristics differently. The authors hypothesized that PEF would induce minimal or positive alterations to proteins, offering a potential advantage over TT. Specifically, preservation by PEF might help preserve the gelling properties of pea proteins, which are crucial for applications such as plant-based meat substitutes. To test this hypothesis, structural changes in the proteins were first investigated, using intrinsic tryptophane fluorescence (ITF) and far-UV circular dichroism (CD) spectroscopy. Then, functional modifications were evaluated through differential scanning calorimetry (DSC) and rheological measurements.

5.2 Material and methods

5.2.1 Production of pea protein extract (PPE)

As described by De Gol et al. (2024b), PPE was obtained by aqueous extraction from air-classified PPC (*Pisum sativum*) (GMSA, Switzerland), which contains 49 g protein/100 g. Moisture content of the PPE was determined using a rapid moisture analyzer (HC103 Mettler-Toledo, Switzerland) at the conditions of 120 °C, initial mass of 2 g, and stop criteria of 1 mg/50 s. The pH and electric conductivity were measured using a pH/conductometer 914 (Metrohm, Switzerland). The crude nitrogen content of the PPE was determined using the Kjeldahl method with a nitrogen-to-protein conversion factor of 5.5, which is appropriate for pea proteins (Schlangen et al., 2022).

5.2.2 Preservation treatments

Two preservation technologies (PEF treatment and TT) were studied. Four different processing conditions were selected for each treatment, based on previous work (De Gol et al., 2024b), which demonstrated relevant inactivation of *Pseudomonas trivalis* and *Erwinia gerundensis* with reductions of up to 4.2 logs per treatment cycle (Table 5.A.1). These two bacteria were identified as critical microbial contaminants of PPE, with high growth capacities even in refrigerated conditions. Therefore, a total of eight preservation treatments were applied on the reference (REF) PPE and nine freeze-dried (FD) samples (FD-REF, FD-PEF25, FD-PEF30, FD-PEF35, FD-PEF40, FD-TT51, FD-TT54, FD-TT57 and FD-TT60) were produced and characterized as depicted in Figure 5.1.

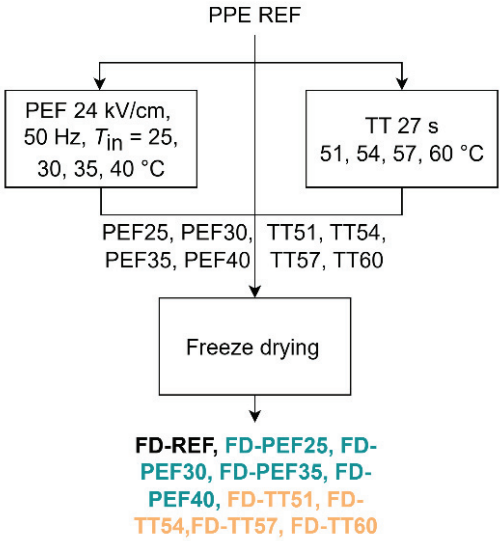

Figure 5.1: Schematic overview of the different preservation conditions applied to the pea extract. PPE: pea protein extract, REF: reference, PEF: pulsed electric field, TT: thermal treatment, FD: freeze dried. FD-REF, FD-PEF25, FD-PEF30, FD-PEF35, FD-PEF40 FD-TT51, FD-TT54, FD-TT57 and FD-TT60, correspond to the nine samples produced and characterized in the study.

PEF treatment was done on a pilot scale HVP-5 PEF machine (ELEA, Germany) containing a co-linear cell (treatment chamber of 1.57 mL) and combined with a tubular heat exchanger for preheating and cooling as described by De Gol et al. (2024a). PPE was diluted with demineralized water (~ PPE:water ratio of 1:3) to lower the conductivity to 2 mS/cm and reach an E_{el} > 20 kV/cm, as explained by De Gol et al. (2024b). The diluted PPE was pumped (45 L/h) through the system using a screw pump (Mono pump 3NU10, Socsil-Inter SA, Switzerland) with a geared motor (RD11, Ströber, Germany). The flow rate was manually adjusted via the gearbox and measured by an electromagnetic flowmeter (OPTIFLUX 6100, Krohne, The Netherlands). A custom-made tubular heat exchanger (three twisted tubes of 3 m long, 1 cm inner diameter, total treatment volume of 0.83 L) was used to heat (T_{in} = 25, 30, 35 and 40 °C) and cool down (20 °C) the product prior to and after PEF treatment, respectively. The residence time in the PEF cell $t_r = V_{chamber}/F$ was 0.126 s, and the time for the PEF-treated liquid to reach the cooling zone was 27 s. High-voltage square pulses of width τ of 20 µs at a frequency of 50 Hz were applied to the diluted PPE. E_{el} of 24 kV/cm and temperature increase of 20 °C were recorded. Besides PEF, PPE was thermally treated using the same custom-made tubular heat exchanger. Temperatures of 51, 54, 57 and 60 ± 1 °C were maintained for 27 s, corresponding to the holding time in the PEF system from

the PEF cell to the cooling zone. The temperature profiles during TT and PEF treatment are compared in Figure 5.A.1.

5.2.3 Characterization of FD-treated PPE

5.2.3.1 Freeze drying

Freeze drying was applied on reference and treated (PEF and TT) PPE samples prior to the different analyses. A Sublimator 25 freeze-dryer (Zirbus Technology GmbH, Germany) was used, and the freeze-drying process included seven different steps as depicted in Figure 5.A.2.

5.2.3.2 Solubility

FD samples were rehydrated in water at a dry matter (DM) content of 15 g/100 g and centrifuged at 6'000 x *g* at room temperature for 20 min using a micro centrifuge (Carl Roth Gmbh, Germany). The solubility of the samples was expressed as the mass of the supernatant with respect to the initial amount of sample before centrifugation.

5.2.3.3 Zeta potential

The zeta potential ζ was measured using a Zetasizer Nano ZS (Malvern Panalytical, UK) and a DTS1070 folded capillary cell (Malvern Panalytical, UK). The samples were rehydrated in demineralized water and diluted to reach a final concentration of 0.04 mg/mL. The instrument was set at 25 °C, measuring three runs per sample, each consisting of ten measurements.

5.2.3.4 Protein separation – Ion exchange (IEX) chromatography

FD samples were dissolved in 20 mM Tris-HCl buffer (Sigma-Aldrich, Switzerland) (pH adjusted to 8.5 with NaOH 1 M and filtered through a 0.22 µm syringe filter) to a concentration of 15 mg/mL (~ 7.5 mg protein/mL) and filtered through a 0.45 µm syringe filter (Macherey-Nagel, Germany). The chromatography was conducted using the ÄKTA Start protein purification system (Cytiva, USA) and a HiTrap Q HP anion exchange column of 1 mL (Cytiva, USA). Pea solutions were injected into the column after equilibration with 20 mM Tris-HCl (pH 8.5) and eluted at a flow rate of 1 mL/min using a linear gradient of NaCl, from 20 mM Tris-HCl (pH 8.5) to 20 mM Tris-HCl, 1 M NaCl (pH 8.5) (Sigma-Aldrich, Switzerland) over 30 column volumes. Chromatograms were obtained using the Unicorn software (Cytiva, USA) and protein fractions (presence of absorbance signal at 280 nm) were collected.

The collected fractions (0.9 mL) were desalted using Amicon centrifugal filters (3 kDa MWCO, Sigma-Aldrich, Switzerland) and centrifugation of 6'000 x *g* for 20 min at 4 °C. Washing with demineralized water (2 mL) at 6'000 x *g* for 30 min at 4 °C was done two times. The protein concentration of the desalted samples was estimated using a Nanodrop UV-Vis spectrophotometer (Thermo Fisher Scientific, USA), measuring purified proteins, which absorb at 280 nm. The protein concentration was adjusted using demineralized water to reach a final value of 0.2 mg/mL. Further analyses (Sections 5.2.3.5, 5.2.3.6 and 5.2.3.7) were done on desalted protein fractions (0.2 mg/mL).

5.2.3.5 Protein size distribution – Size exclusion chromatography (SEC)

The REF PPE and the different protein fractions collected from IEX chromatography were analyzed in high performance liquid chromatography (HPLC)-SEC to acquire information on the size of proteins. A 1220 Infinity DAD LC HPLC-SEC device (Agilent technologies, USA) with a TSKgel G3000SWXL column (30 cm × 7.8 mm, 5 µm particle size) (Sigma-Aldrich, Switzerland) was used. Phosphate-buffered saline (PBS) solution (137 mM NaCl, 2.7 mM KCl, 10 mM Na_2HPO_4, 1.76 mM KH_2PO_4) was used as the eluent at a flow rate of 0.75 mL/min. Samples were injected (80 µL), and the column was maintained at 20 °C. Detection was done using a UV detector (280 nm). A protein standard (Supelco 69385, Sigma-Aldrich, Switzerland) containing a lyophilized mixture of four proteins was used (Table 5.1).

Table 5.1: The four protein standards used for the HPLC-SEC and their respective concentration, molecular weight and retention time

Standards	Concentration (g/L)	Molecular weight (kDa)	Retention time (min)
Thyroglobulin bovine	0.5	670	7.6
γ-globulins from bovine blood	1.0	150	10.5
Albumin chicken egg grade VI	1.0	44.4	11.8
Ribonuclease A type I-A from bovine pancreas	1.0	13.7	14.5

5.2.3.6 Intrinsic tryptophane fluorescence (ITF) spectroscopy

To perform fluorescence spectroscopy, 200 µL of each fraction was transferred to a Nunc 96-well black plate (Thermo Fisher Scientific, USA). A SpectraMax ID3 microplate reader (Molecular Devices, USA) was used to measure the Tryptophan (Trp) fluorescence intensity (excitation 295 nm). Emission spectra 310 – 400 nm were obtained with an integration time of 500 ms and a read height of 1 mm. The fluorescence intensity values were normalized [0,1] using OriginLab® 2025b (OriginLab Corporation, USA).

5.2.3.7 Far-UV circular dichroism (CD) spectroscopy

CD measurements were conducted using a Chirascan V100 spectropolarimeter (Applied Photophysics, England) in the far-UV range with the following parameters: protein concentration of 0.2 g/L, temperature set at 20 °C, scanning speed of 20 nm/min, step size of 0.5 nm, intensity of 0.1 nm, and a digital integration time of 1 s. The range of measurements extended from 190 to 260 nm. Each sample was scanned four times, and the resulting spectra were averaged and smoothed. Quartz Suprasil cells (Hellma, Germany) with a 1 mm optical path length were employed. Data are presented in terms of ellipticity (mdeg) as a function of the wavelength (nm). Additionally, the CDNN 2.1 software (Applied Photophysics, England) was used to process the CD spectra and quantify the protein secondary structure content (percentage of α-helix, β-sheet, β-turn and random coil). Two protein fractions were considered, and the molecular weight and number of amino acids (AA) were estimated based on HPLC-SEC results (Section 5.2.3.5) and set at 40 kDa – 360 AA and 150 kDa – 1360 AA.

5.2.3.8 Thermal properties – Differential scanning calorimetry (DSC)

Heat-induced protein denaturation was determined by DSC using a μDSC7 evo machine (Setaram Instrumentation, France), as explained by De Gol et al. (2023). Briefly, the FD samples were rehydrated in demineralized water (15 g DM/100 g) and scanned from 20 to 100 °C at a heating rate of 0.5 °C/min, held at 100 °C for 10 min, and subsequently cooled to 20 °C at the same rate. The reaction enthalpy ΔH (J/g) and peak maximum temperature T_{peak} values were extracted using the Thermal Analysis® Software package V. 1.46 (Setaram Instrumentation). A second temperature cycle was applied to the REF sample. For each sample, the plotted data were obtained after subtracting the REF baseline curve.

5.2.3.9 Gelling properties – Temperature (*T*) sweep

The minimal gelling concentration of pea protein was reported to be close to 12% (Batista et al., 2011). Therefore, the FD samples were rehydrated in demineralized water (15 g DM/100 g) and analyzed through *T*-sweep measurements. The apparent viscosity μ_{app} as a function of temperature and time was obtained using a modular compact rheometer (MCR) model 302 (Anton Paar, Austria) equipped with an electrically heated temperature device, a counter-cooling concentric cylindrical system of 26 mm (C-ETD 160/ST) and a three-blade stirrer (ST24) measuring system. The solutions were heated from 20 °C to 95 °C, held at this temperature for 5 min, and subsequently cooled to 20 °C (Rodriguez & Beyrer, 2023). The heating and cooling rates were set at 6 °C/min and the stirring speed at 160 rpm. Data

were obtained from the RheoCompass® software and firmware (Anton Paar, Austria). The initial viscosity $\mu_{app,initial}$, final viscosity $\mu_{app,final}$ and the viscosity increase $\Delta\mu_{app}$ were used to compare the gelling properties of the different samples.

5.2.4 Statistical analysis

The production, preservation and fractionation (IEX) processes were done once, while all the analytical measurements were done at least in triplicate (n ≥ 3). Results were expressed as average ± standard deviation (SD). Regarding statistical analysis, first normality distribution (Shapiro-Wilk test) and equal variance (Chi-square test for variance) were checked. Statistical significance was estimated by one-way ANOVA, followed by Tukey's post-hoc test. Dunn's test and Welch's ANOVA were used when normality and equal variance were rejected, respectively. P-values < 0.05 were considered statistically significant. All statistical tests were performed using OriginLab® 2025b (OriginLab Corporation, USA).

5.3 Results and discussion

The pea extract used in the study had a DM content of 11.1 ± 0.2 g/100 g, a pH of 6.3 ± 0.0 and a conductivity of 5.7 ± 0.0 mS/cm. Prior to PEF treatments, PPE was diluted to 2.6 ± 0.1 g/100 g with demineralized water to reach a conductivity of 2.0 ± 0.0 mS/cm. The PEF and TT conditions (Figure 5.1) were selected to achieve comparable microbial logarithmic (log) reductions, namely 2.0 – 4.2 and 0.1 – 4.2 logs, respectively (Table 5.A.1), though PEF enabled a shorter heating time (Figure 5.A.1), and lower process temperatures (Table 5.A.1) compared to TT. Following PEF or TT treatments, the samples were freeze-dried to ensure standardization prior to further functionality analysis. Freeze-drying had a proofed, negligible impact on structural and functional properties (Tables 5.5 and 5.6, Figure 5.A.3).

5.3.1 Molecular structure of albumins and globulins

First, the presence of albumins and globulins in the PPE was confirmed using HPLC-SEC (Figure 5.2). For accurate structural characterization and clearer interpretation of spectroscopic data, pea proteins were further purified, and the soluble globulin and albumin fraction were collected. For that, IEX was employed to purify and fractionate proteins based on similar surface charge characteristics, and a second HPLC-SEC analysis of the IEX fractions was performed to validate the separation of albumins and globulins (Section 5.3.1.2). Finally, the tertiary and secondary structure of IEX-isolated albumins and globulins were characterized using ITF (Section 5.3.1.3) and CD spectroscopy (Section 5.3.1.4).

5.3.1.1 Protein composition of PPE

PPE contained primarily proteins (56.5 ± 0.5 g/100 g PPE), indicating that the protein content shifted through centrifugation of the PPC dispersion to a 7% higher level. The molecular mass distribution of the PPE proteins (FD-REF) obtained from HPLC-SEC is displayed in Figure 5.2. Bands from 2 – 960 kDa were detected, indicating the presence of both globulins and albumins. More precisely, the bands revealed the presence of legumins (404 kDa), native convicilins and their subunits (226 and 71 kDa), vicilins (127 kDa), and albumins (19, 8 and 5 kDa). The bands at extreme molecular mass values (960 and 2 – 3 kDa) were attributed to protein aggregates and fragments, respectively (Kornet, 2020; Lu et al., 2020; Tzitzikas et al., 2006; Zhao 2024).

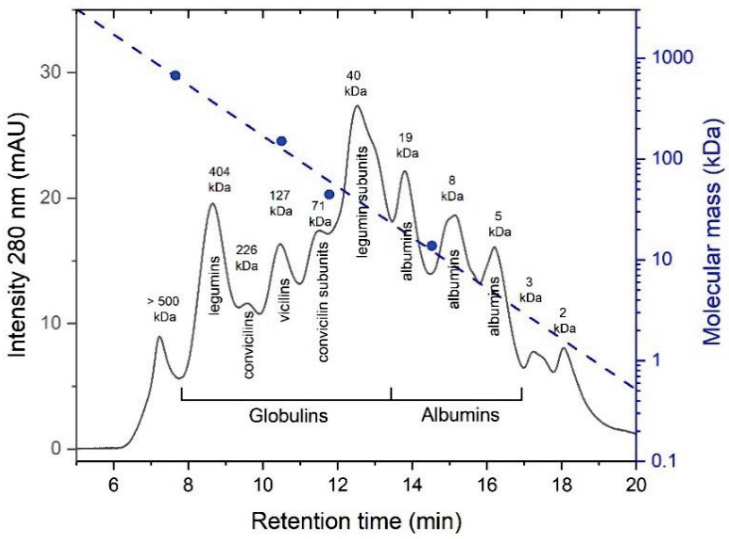

Figure 5.2: HPLC-SEC chromatogram of FD-REF, showing the UV absorption intensity as a function of retention time. The dashed line represents the molecular mass as a function of retention time, obtained from the size distribution of the protein standards (●).

Interestingly, Kornet et al. (2020) used HPLC-SEC to study the protein distribution of yellow pea flour and derived protein extract obtained through aqueous extraction at natural pH. The HPLC-SEC chromatograms for both the flour and the extract were similar, closely resembled those obtained in the present study, with seven major protein bands detected, which were attributed to legumin hexamers (487 kDa), convicilins (283 kDa), trimeric vicilins (150 – 190 kDa), vicilin subunits, and albumins (77, 30, 9 and 3.7 kDa). In addition, Shrestha et al. (2023) reported a similar protein composition in PPI from yellow peas, with bands observed at 713, 403, 250, 166, 39, 12 and 4 kDa. Our results suggest that the albumin/globulin ratio is preserved during mild purification.

5.3.1.2 PPE protein purification for molecular structure analyses

IEX was applied to purify albumins and globulins by removing matrix components such as fibers, starch and oil from the rehydrated FD-PPE. Figure 5.3A presents the IEX chromatograms for the nine different samples (REF, PEF-treated and thermally treated). The first band, occurring at an elution volume of 2 mL, corresponds to the flow-through containing proteins that show no affinity for the column. The zoomed-in view in Figure 5.3B highlights the different protein fractions, which exhibit varying affinities for the column. The band intensities varied slightly, but the profile was maintained. This indicates that the treatments have a neutral effect on the surface charges of soluble proteins.

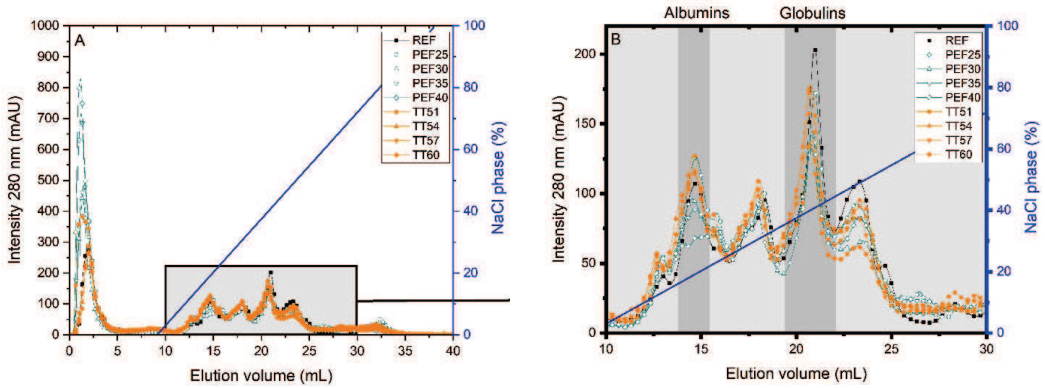

Figure 5.3: A. IEX chromatogram of the FD pea samples before (REF) and after preservation processes (PEF and TT), showing the UV response in function of elution volume. The blue line shows the linear gradient of the eluent phase. B. Zoomed-in view of the IEX chromatogram in the elution volume range 10 – 30 mL. The two highlighted bands in dark grey represent the protein fractions (albumin and globulin) selected for fluorescence and CD spectroscopy. REF: reference, PEF: pulsed electric field, TT: thermal treatment.

The three leading bands observed on the IEX chromatogram (Figure 5.3), corresponding to the respective elution volumes of ~ 2, 15 and 21 mL, were collected and individually analyzed by HPLC-SEC (Figure 5.4). The first HPLC-SEC band (elution volume of 2 mL) is assigned to proteins that are either albumin subunits or even smaller protein fragments (< 10 kDa) (Figure 5.4A). As shown in Figure 5.3A, a greater concentration of smaller protein was measured after PEF treatments. The second band (elution volume of 15 mL) represents albumins, while the third band (elution volume of 21 mL) corresponds to globulins, which are larger and have a higher surface charge compared to albumins, giving them a greater affinity for the IEX column (Figures 5.4B and 5.4C). Previous studies have reported similar HPLC-SEC chromatograms for pea albumins and globulins, with albumins displaying two leading bands corresponding to two native forms of albumins (Figure 5.4B) and globulins including bands of legumins, convicilins and vicilins (Figure 5.4C) (Kornet et al., 2022; Li et al., 2024).

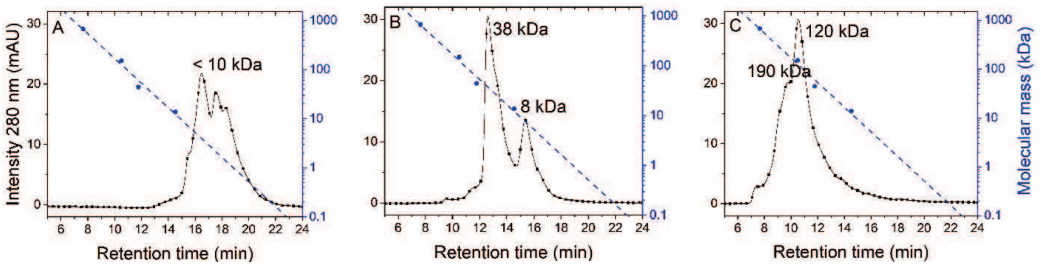

Figure 5.4: HPLC-SEC chromatograms of the REF after protein separation by IEX, showing the UV response as a function of retention time. The dashed line represents the molecular mass as a function of retention time, obtained from the size distribution of the protein standards (●). A: protein fraction eluted at 2 mL, B: albumin fraction eluted at 15 mL, C: globulin fraction eluted at 21 mL as seen in Figure 5.3B.

The IEX albumin and globulin fractions (highlighted in Figure 5.3B) were collected, desalted by dialysis, diluted to a protein concentration of 0.2 mg/mL, and subsequently analyzed by fluorescence and CD spectroscopy.

5.3.1.3 Intrinsic tryptophane fluorescence spectroscopy

A fluorescence analysis of Trp was carried out to investigate the impact of PEF treatment and TT on the spatial structure of PPE-derived albumins and globulins. When excited by UV light, the aromatic amino acid Trp emits fluorescence in the range 330 – 350 nm. The emission maximum is highly sensitive to the Trp's microenvironment within the protein's three-dimensional structure, making it a suitable sensor for detecting protein conformational changes.

Although the shape of the normalized fluorescence curves was similar for all samples (Figures 5.5A and 5.5B), distinct spectral shifts were observed depending on the treatment. PEF-treated samples exhibited a red shift (toward longer wavelengths), whereas thermally treated samples showed a blue shift (toward shorter wavelengths). The red shift induced by PEF suggests that Trp is more exposed at the protein-solvent interface which is indicative of protein unfolding or disaggregation. In contrast, the blue shift caused by TT indicates that Trp residues are more hidden from the surface exposure, likely due to protein aggregation. Chen et al. (2022) noted a red shift (from 334 to 340 nm) in the Trp emission spectrum for PPI subjected to ohmic heating (20 V/cm, 50 Hz, 95 °C, 10 min), a process that combines thermal and electric effects. Conversely, Avelar et al. (2024) observed a blue shift (from 346 to 342 nm) in pea protein after ohmic heating at higher temperatures (90 – 150 °C) under similar electric field strength (25 V/cm). In this case, the thermal effect might have become dominant.

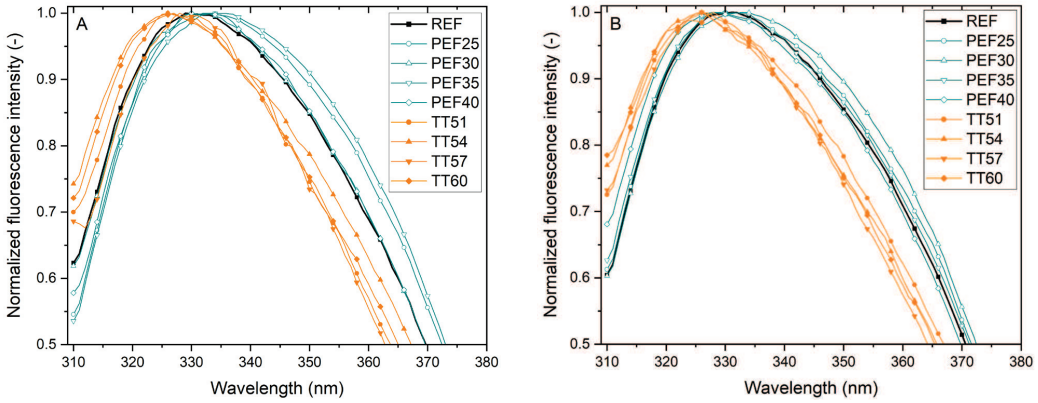

Figure 5.5: Intrinsic fluorescence emission spectra after excitation at 275 nm of the REF PPE before and after preservation by PEF and TT. A: albumin fraction, B: globulin fraction. Data points are averages of three individual measurements (n = 3). REF: reference, PEF: pulsed electric field, TT: thermal treatment.

The PEF-treated samples exhibited significantly higher average emission maxima compared to TT-treated samples for both albumins and globulins, as determined quantitatively in Table 5.2. This suggests greater exposure of Trp in PEF samples due to protein unfolding, whereas TT may promote aggregation.

Table 5.2: Tertiary protein structure of the FD pea albumins and globulins before (REF) and after preservation processes (PEF and TT). The wavelength values corresponding to the average emission maxima were extracted from the intrinsic fluorescence spectra (Figure 5.5). Data are presented as averages ± SD of the REF (n = 3), PEF-treated (n = 12) and thermally treated (n = 12) samples. A different letter means a significant difference $p < 0.05$. REF: reference, PEF: pulsed electric field, TT: thermal treatment, FD: freeze-dried

Samples		Wavelength at emission maxima (nm)	Samples		Wavelength at emission maxima (nm)
Albumins	FD-REF	331.0 ± 2.0^{ab}	Globulins	FD-REF	329.0 ± 1.7^{AB}
	FD-PEF	332.7 ± 3.1^{a}		FD-PEF	330.3 ± 3.3^{A}
	FD-TT	327.9 ± 2.0^{b}		FD-TT	326.7 ± 1.2^{B}

5.3.1.4 Circular dichroism spectroscopy

CD spectroscopy was used to evaluate the impact of PEF treatment and TT on the secondary structure of albumins and globulins. As illustrated in Figure 5.6, both treatments induced alterations in the CD spectra compared to the reference, with distinct signatures for the albumin and globulin fractions (Hou et al., 2017; Miranda et al., 2023). For both preservation treatments (Figures 5.6A and 5.6B), the albumin spectra displayed a hybrid profile characterized by a combination of random coil and β-structures, highlighted by two negative bands centered at 203 and 218 nm, respectively. Interestingly, PEF35 and PEF40 treatments revealed an α-type signature featuring two negative bands at 206 and 222 nm. In the case of globulins (Figures 5.6C and 5.6D), which are larger than albumins, the spectra exhibited predominantly mixed fingerprint (α-helices, β-sheets, and random coil) irrespective

of the treatment. Similar findings have been reported in the literature for PPI, where the slight variation in the results may be attributed to differences in cultivation conditions and extraction processes (Avelar et al., 2024; Chen et al., 2022; D'Alessio et al., 2023; Guo et al., 2024; Shrestha et al., 2023; Zhi et al., 2022). For both treatments (PEF and TT), slight shifts toward longer wavelengths were observed, suggesting an enrichment in β-sheets and potential protein aggregation, also reported by Chen et al. (2022). Moreover, Guo et al. (2024) reported no impact of PEF at E_{el} of 5 – 12.5 kV/cm (f = 600 Hz, τ = 6 µs, t = 3 min) but observed a reduction of α-helix content at higher E_{el} (15 kV/cm). At the molecular level, this α-helix disruption can be explained by the influence of the electric field on the strong dipole moment of the helical structure (Zhao et al., 2012).

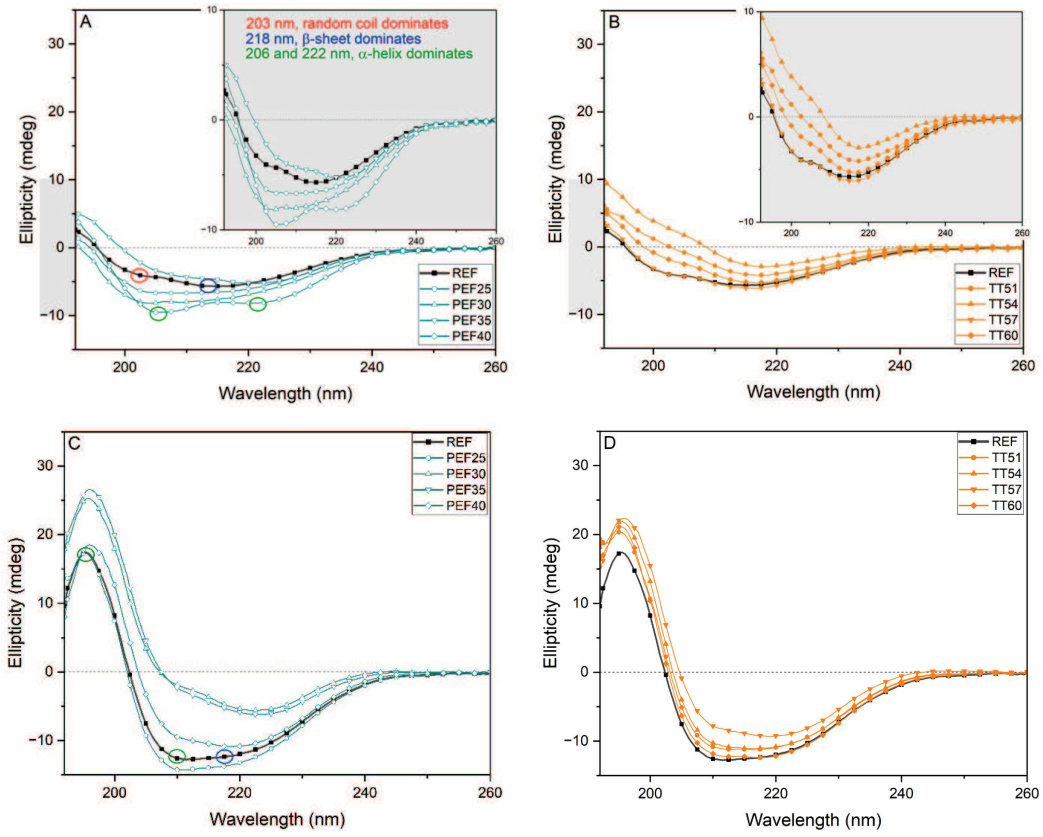

Figure 5.6: Circular dichroism spectra of the FD pea samples before (REF) and after preservation processes (PEF and TT). A: albumin fraction for PEF-treated samples, B: albumin fraction for thermally treated samples, C: globulin fraction for PEF-treated samples, D: globulin fraction for thermally treated samples. The graphs highlighted in grey represent the zoom-in view for the albumin signals. Colored circles showed positive and negative bands corresponding to specific structures. Curves are averages of four individual measurements (n = 4). REF: reference, PEF: pulsed electric field, TT: thermal treatment.

As an indication, CDNN 2.1 software was used to extract the percentage distribution of the different configurations. The results are presented in Table 5.3. While the preservation treatments did not significantly impact the albumin structure compared to the reference, the rearrangement of globulins into parallel β-sheets (increase from 10.6 to 13.0%) induced by PEF was confirmed. It is important to interpret these findings with caution, as they were based on estimates of molecular weight and the number of AA (see Section 5.2.3.7).

Table 5.3: Secondary protein structure of the FD pea albumins and globulins before (REF) and after preservation processes (PEF and TT). The secondary structure configuration contents were extracted from CD spectra (Figure 5.6) using the CDNN 2.1 software. Data are presented as averages ± SD of the REF (n = 3), PEF-treated (n = 12) and thermally treated (n = 12) samples. A different letter means a significant difference $p < 0.05$. REF: reference, PEF: pulsed electric field, TT: thermal treatment, FD: freeze-dried, CD: circular dichroism

	Samples	CD – Secondary structure content (%)				
		α-Helix	β-Sheet		β-Turn	Random coil
			Antiparallel	Parallel		
Albumins	FD-REF	14.6 ± 0.1^{ab}	29.1 ± 0.2^{ab}	9.3 ± 0.0^{ab}	15.9 ± 0.0^{ab}	31.1 ± 0.1^{ab}
	FD-PEF	15.2 ± 1.0^{a}	28.8 ± 1.7^{a}	9.2 ± 0.3^{b}	16.1 ± 0.3^{a}	30.7 ± 1.4^{b}
	FD-TT	14.4 ± 0.3^{b}	27.3 ± 1.2^{b}	9.7 ± 0.3^{a}	15.7 ± 0.2^{b}	32.9 ± 1.3^{a}
Globulins	FD-REF	22.1 ± 0.3^{A}	14.0 ± 0.1^{A}	10.6 ± 0.1^{B}	17.0 ± 0.0^{AB}	36.3 ± 0.1^{B}
	FD-PEF	16.6 ± 5.9^{A}	13.2 ± 1.0^{A}	13.0 ± 2.1^{A}	16.9 ± 0.3^{B}	40.3 ± 3.5^{A}
	FD-TT	19.1 ± 1.9^{A}	11.8 ± 0.5^{B}	12.1 ± 0.6^{AB}	17.3 ± 0.1^{A}	39.7 ± 1.0^{AB}

To conclude, spectroscopic measurements suggest that the preservation treatments induce slight modifications to the tertiary and secondary structures of the proteins. Further analyses are needed to elucidate the mechanisms underlying these modifications. However, besides thermal effects through ohmic heating, molecular dissociation and migration of charged particles in electric fields create overlapping effects of temperature, ionic-strength, and pH (Axelrod et al., 2022). Surprisingly, already short residence time in the electric field induced changes in the properties of native pea proteins as has been used for this study.

5.3.2 Techno-functionality of PPE

The impact of PEF and TT on techno-functional properties of PPE was evaluated using freeze-dried and rehydrated PPE.

5.3.2.1 Solubility and zeta potential

PEF treatments significantly increased the mass solubility of PPE with 6%, whereas no changes were observed following mild TTs (Table 5.4). However, a marked decrease of 35% in solubility was observed following more intense heating (boiling temperature, 5 min) (data not shown), likely due to heat-induced protein aggregation.

Table 5.4: Solubility of the FD pea samples before (REF) and after preservation processes (PEF and TT). Data are presented as averages ± SD (n = 3). A different letter means a significant difference $p < 0.05$. REF: reference, PEF: pulsed electric field, TT: thermal treatment, FD: freeze-dried

Samples	Soluble mass fraction (%)
FD-REF	79.0 ± 2.1^{cd}
FD-PEF25	83.2 ± 0.7^{ab}
FD-PEF30	85.5 ± 1.9^{a}
FD-PEF35	82.4 ± 1.0^{abc}
FD-PEF40	83.5 ± 0.2^{ab}
FD-TT51	76.0 ± 2.5^{d}
FD-TT54	76.6 ± 0.8^{d}
FD-TT57	79.6 ± 1.2^{bcd}
FD-TT60	79.5 ± 1.1^{bcd}

Moreover, zeta potential ζ measurements were conducted to study the impact of processing on the surface charge of proteins and, consequently, on the electrostatic interactions between particles (Kornet et al., 2022). At pH 6.3, PPE proteins are negatively charged, resulting in a negative ζ. The isoelectric point (pI) value (measured in previous experiments, data not shown) aligns with literature-reported values for albumins and globulins of 6.0 and 4.5, respectively (Dziuba et al., 2014; Kornet et al., 2020). The average values of ζ were measured as – 14.1 ± 1.8, – 22.6 ± 0.9 and – 11.1 ± 0.3 mV for REF, PEF-treated and thermally treated samples, respectively. The increase of surface charge induced by PEF is consistent with increased solubility.

5.3.2.2 Thermal properties

As reported by De Gol et al. (2024b) and confirmed by several studies on pea ingredients (Kuang et al., 2023; Ma et al., 2017; Zink et al., 2024) the DSC thermogram of PPE reveals two prominent peaks; a first endothermic peak ΔH_1 at 50 – 61 °C corresponding to fiber or starch gelatinization and a second endothermic peak ΔH_2 at 61 – 82 °C associated with protein modifications. As expected, PEF treatments at low inlet temperatures (T_{in} = 25 °C and 30 °C) did not affect the DSC signal (Figure 5.7A). In contrast, higher inlet temperatures (T_{in} = 35 °C and 40 °C) resulted in a reduction of the first peak, due to combined thermal and electric effects. Concerning TT, all temperatures affected the first peak, and the highest temperature (60 °C) affected both peaks (Figure 5.7B).

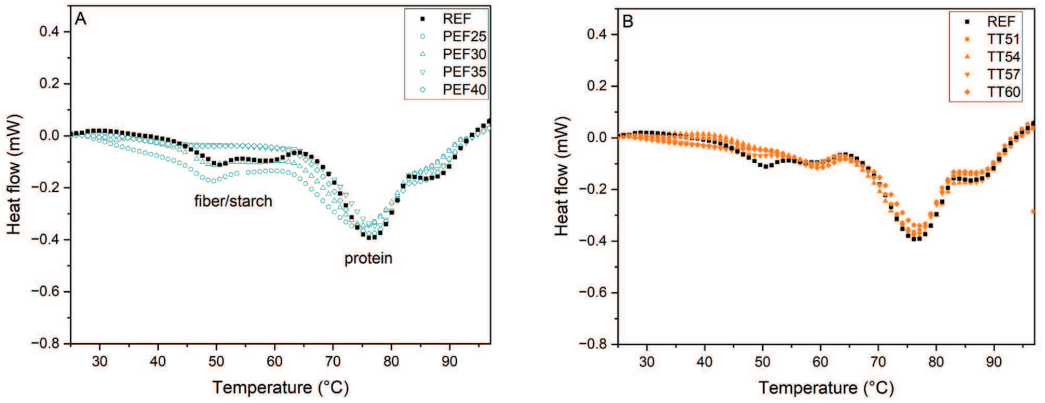

Figure 5.7: DSC thermogram (scanning from 20 °C to 100 °C at a heating rate of 0.5 °C/min) of the FD and rehydrated (15 g/100 g DM) pea samples before (REF) and after preservation processes, A: PEF, B: TT. Data points are averages of three individual measurements (n = 3). REF: reference, PEF: pulsed electric field, TT: thermal treatment.

Such observations are reported in Table 5.5. The first peak was significantly reduced after PEF treatments at T_{in} = 35 °C and 40 °C (T_{out} = 55 °C and 60 °C), and TT at temperature ≥ 54 °C. The second peak remained unaffected, except for TT at 60 °C, where a reduced reaction enthalpy was observed. Moreover, shifts of the first peak maxima toward lower values for the PEF-treated samples, and higher for the thermally treated samples were observed, indicating a shift in the samples' thermal properties.

Table 5.5: Thermal properties of the FD pea samples before (REF) and after preservation processes (PEF and TT). Data are presented as averages ± SD (n = 3). A different letter means a significant difference $p < 0.05$. REF: reference, PEF: pulsed electric field, TT: thermal treatment, FD: freeze-dried, DM: dry matter

Samples	ΔH_1 (J/g DM)	$T_{peak,1}$ (°C)	ΔH_2 (J/g DM)	$T_{peak,2}$ (°C)
FD-REF	0.9 ± 0.1^{a}	50.7 ± 0.5^{bcd}	2.8 ± 0.3^{a}	77.0 ± 2.0^{a}
FD-PEF25	0.8 ± 0.0^{ab}	49.7 ± 0.1^{bcd}	2.7 ± 0.1^{a}	76.0 ± 0.5^{a}
FD-PEF30	0.8 ± 0.1^{abc}	49.6 ± 0.1^{bcd}	2.7 ± 0.0^{a}	75.8 ± 1.0^{a}
FD-PEF35	n.d.	45.2 ± 1.0^{d}	2.8 ± 0.0^{a}	76.5 ± 1.6^{a}
FD-PEF40	n.d.	46.2 ± 0.9^{cd}	2.7 ± 0.1^{a}	76.1 ± 0.6^{a}
FD-TT51	0.7 ± 0.2^{abc}	54.5 ± 4.9^{abc}	2.7 ± 0.2^{a}	77.2 ± 0.5^{a}
FD-TT54	0.5 ± 0.1^{bcd}	52.1 ± 4.7^{abcd}	2.8 ± 0.1^{a}	76.3 ± 0.7^{a}
FD-TT57	0.5 ± 0.1^{cd}	55.5 ± 5.3^{ab}	2.6 ± 0.0^{ab}	76.0 ± 0.0^{a}
FD-TT60	0.3 ± 0.0^{d}	59.0 ± 0.7^{a}	2.3 ± 0.0^{b}	76.3 ± 0.9^{a}
Fresh REF2	0.5 ± 0.2^{A}	54.4 ± 1.3^{A}	4.3 ± 0.5^{A}	77.3 ± 0.3^{A}
FD-REF2	0.6 ± 0.3^{A}	55.3 ± 2.4^{A}	3.8 ± 0.7^{A}	74.9 ± 2.8^{A}

ΔH_1 and ΔH_2 refer to the thermal events at 50 – 61 °C and 61 – 82 °C, respectively.
n.d.:not detected.

5.3.2.3 Rheological properties

Gelling properties were investigated using *T*-sweep measurements (Figure 5.8), with the resulting shape parameters $\mu_{app,initial}$, $\mu_{app,final}$ and $\Delta\mu_{app}$ of the viscosity curve summarized in

Table 5.6. At a concentration of 15 g/100 g, the samples exhibited visco-elastic behavior (*G'* > *G"*), which was confirmed by an amplitude sweep test conducted at 20 °C within the linear visco-elastic region (LVER) (data not shown).

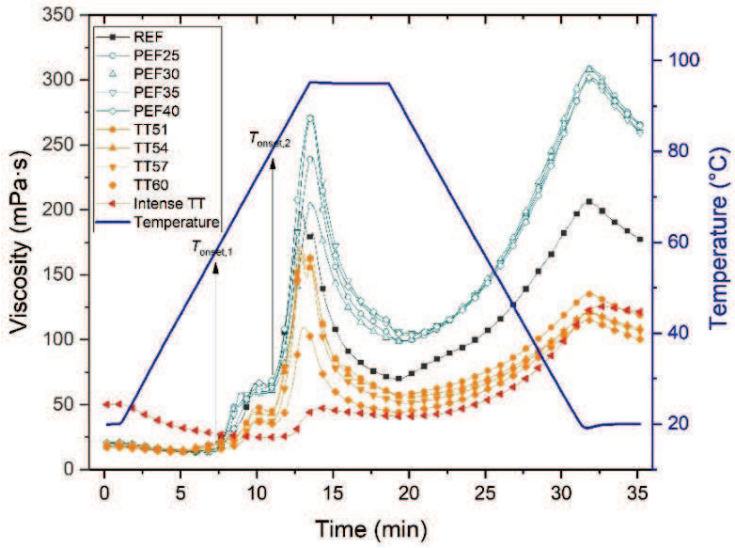

Figure 5.8: Temperature-sweep viscosity curves of the FD and rehydrated (15 g DM/100 g) pea samples before (REF) and after preservation processes (PEF and TT). The full blue line indicates the temperature profile. Data points are averages of three individual measurements (n = 3). REF: reference, PEF: pulsed electric field, TT: thermal treatment.

Peaks at $T_{onset,1}$ = ~ 55 °C and $T_{onset,2}$ = ~ 80 °C were attributed to starch gelatinization and protein aggregation, respectively, consistent with the DSC results (Section 5.3.2.2). PEF treatments and TTs had a distinct influence on the viscosity function. While PEF treatments significantly enhanced viscosity, as indicated by an increase of 53% in the average value of $\Delta\mu_{app}$, TTs caused a significant reduction of 44% in $\Delta\mu_{app}$, suggesting impaired gelling properties. The onset temperature for the viscosity increase is higher for thermally treated samples compared to PEF-treated samples and correlates well with the increase in peak temperature values from DSC (Table 5.5). An intense heating step (boiling temperature, 5 min) was also tested to confirm the negative impact of TT on the gelling properties, with significant reduction of 32% for $\mu_{app,final}$ and 55% for $\Delta\mu_{app}$ (red profile in Figure 5.8). The increase of 179% in $\mu_{app,initial}$ is aligned with a loss of solubility (Section 5.3.2.1).

Table 5.6: Gelling properties of the PPE before (REF) and after preservation processes (PEF and TT). Data are presented as averages ± SD of the REF (n = 3), PEF-treated (n = 12) and thermally treated (n = 12) samples. A different letter means a significant difference $p < 0.05$. REF: reference, PEF: pulsed electric field, TT: thermal treatment, FD: freeze-dried. The individual values are displayed in Table 5.A.2

Samples	% DM	$\mu_{app,initial}$ (mPa·s)	$\mu_{app,final}$ (mPa·s)	$\Delta\mu_{app}$ (mPa·s)	$\mu_{app,peak}$ (mPa·s)
FD-REF	15.0	18.0 ± 0.9^{a}	178.4 ± 11.6^{b}	160.5 ± 12.4^{b}	199.8 ± 10.5^{b}
FD-PEF	15.0	19.5 ± 1.4^{a}	264.4 ± 19.4^{a}	244.9 ± 20.0^{a}	246.7 ± 29.8^{a}
FD-TT	15.0	18.4 ± 1.1^{a}	109.1 ± 12.2^{c}	90.6 ± 12.1^{c}	155.1 ± 28.2^{b}
Fresh REF2	10.4 ± 0.1^{A}	13.3 ± 0.2^{A}	124.1 ± 1.0^{A}	110.8 ± 0.5^{A}	50.6 ± 0.5^{A}
FD-REF2	10.5 ± 0.2^{A}	13.7 ± 1.2^{A}	128.2 ± 3.4^{A}	114.5 ± 4.1^{A}	47.4 ± 1.8^{B}

The observed enhancement of gelling properties could be attributed to the PEF-induced conformational changes in the proteins, resulting in increased solubility, a higher surface charge (zeta potential) and altered polarity. The red shift in the ITF spectrum and the shift toward a more disordered secondary structure (increase in β-sheet and random coil content) are also indicative of protein chain dispersion in the solvent. This facilitates unfolding of the proteins during heating (*T*-sweep), promoting intermolecular interactions and stronger network formation. Similarly, Tolkach & Kulozik (2007) identified protein unfolding as the first step in thermally induced beta-lactoglobulin denaturation, followed by aggregation. To summarize, the changes induced by PEF create a more favorable environment for gel formation, highlighting the relationship between protein structural modification, surface charge, solubility, and functional gelling behavior.

5.4 Conclusions

This study demonstrates that PEF treatments and TTs with equivalent microbial inactivation levels induce clearly distinct structural and functional modifications of pea proteins. For TT, protein aggregation was seen, what could be concluded from ITF analysis (blue shift), reduced solubility, and ability of thermally induced gelation. In contrast, for PEF treatment, protein unfolding was found, what was shown by increased protein solubility (+ 8%), Trp exposure as evidenced by ITF results (red shift), and ability of thermally induced gelation. The results of thermomechanical tests (temperature-dependent viscosity) indicated an increase of 35% in the gelling properties of PEF-treated pea proteins, which could be justified by stronger intermolecular protein interactions. More interestingly, for a similar microbial inactivation level, TT led to a reduction of 60% in gelling properties compared to the PEF-treated ingredient. Therefore, PEF offers an effective alternative to thermal treatment, achieving comparable microbial inactivation while also enhancing the gelling properties of the pea extract. Such improvement in techno-functionality can be purposeful in added-value food ingredients by significantly influencing the dosage or reducing water

exudation in plant-based foods. For an advanced proof of concept in plant-based food production and to increase technology readiness levels, process validation in an industrially relevant environment, as well as the application of PEF equipment for handling more concentrated protein extracts than in this study, are recommended.

5.5 Appendices

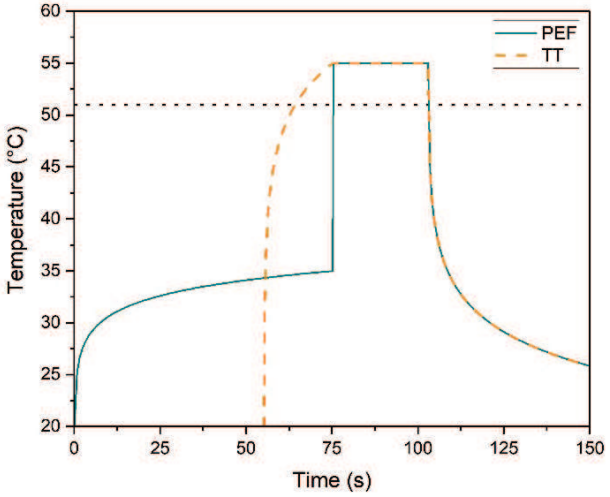

Figure 5.A.1: Typical temperature profiles for the two different preservation processes (PEF and TT), PEF: Pulsed electric field, TT: thermal treatment. The dotted line represents the critical temperature for starch modification and thermal inactivation of *Pseudomonas trivalis* and *Erwinia gerundensis.*

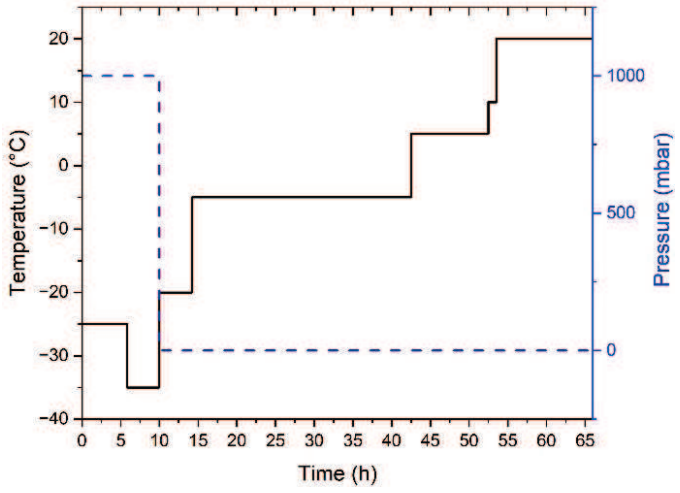

Figure 5.A.2: Temperature and pressure profile for freeze-drying.

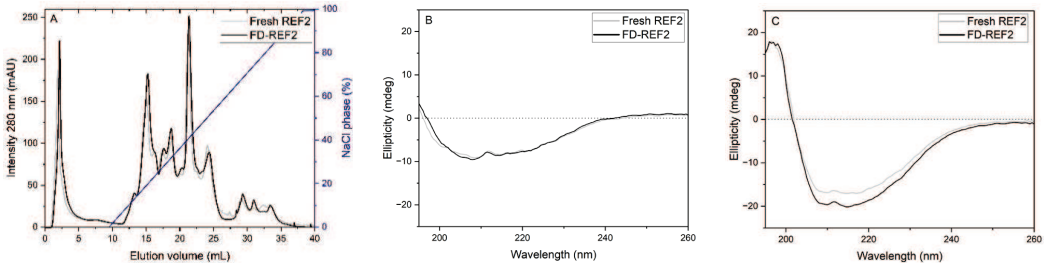

Figure 5.A.3: Effect of FD process on the structure of PPE proteins. A. IEX chromatogram, B. CD spectra for albumins, C. CD spectra for globulins.

Table 5.A.1. Microbial inactivation level (log reduction) of *Pseudomonas trivalis* and *Erwinia gerundensis* obtained in previous work (De Gol et al., 2024b) for the different preservation treatments applied in this study. PEF reductions were measured, while TT reductions were calculated from the average inactivation curves

Preservation treatments		**log reduction (-)**	
Treatments	**T_{out} (°C)**	***Pseudomonas trivalis***	***Erwinia gerundensis***
PEF25	45	2.6 ± 0.4	2.0 ± 0.3
PEF30	50	3.3 ± 0.3	2.9 ± 0.1
PEF35	55	3.8 ± 0.3	2.7 ± 0.1
PEF40	60	4.2 ± 0.8*	3.7 ± 0.4
TT51	51	0.1 ± 0.2	0.1 ± 0.1
TT54	54	1.4 ± 0.2	1.4 ± 0.1
TT57	57	2.8 ± 0.2	2.7 ± 0.1
TT60	60	4.2 ± 0.1*	4.0 ± 0.1

*Due to TT's longer heating time compared to PEF (Figure 5.A.1), the inactivation level achieved for PEF40 is also attributed to electrical effects

Table 5.A.2. Gelling properties of the PPE before (REF) and after preservation processes (PEF and TT). Data are presented as averages ± SD (n = 3). A different letter means a significant difference $p < 0.05$. REF: reference, PEF: pulsed electric field, TT: thermal treatment, FD: freeze-dried, DM: dry matter

Samples	**% DM**	**$\mu_{app,initial}$ (mPa·s)**	**$\mu_{app,final}$ (mPa·s)**	**$\Delta\mu_{app}$ (mPa·s)**	**$\mu_{app,peak}$ (mPa·s)**
FD-REF	15.0	18.0 ± 0.9^{a}	178.4 ± 11.6^{b}	160.5 ± 12.4^{b}	199.8 ± 10.5^{c}
FD-PEF25	15.0	18.4 ± 0.9^{a}	267.7 ± 7.3^{a}	249.2 ± 8.1^{a}	240.4 ± 7.0^{b}
FD-PEF30	15.0	18.6 ± 1.5^{a}	262.0 ± 23.4^{a}	243.4 ± 24.7^{a}	204.0 ± 14.9^{c}
FD-PEF35	15.0	20.2 ± 0.9^{a}	261.4 ± 17.1^{a}	241.1 ± 17.5^{a}	271.9 ± 4.8^{a}
FD-PEF40	15.0	20.8 ± 0.6^{a}	266.7 ± 33.7^{a}	245.9 ± 34.0^{a}	270.5 ± 1.1^{a}
FD-TT51	15.0	18.6 ± 0.1^{a}	119.2 ± 9.5^{b}	100.7 ± 9.4^{c}	169.8 ± 5.6^{d}
FD-TT54	15.0	19.7 ± 0.7^{a}	109.1 ± 4.5^{c}	89.4 ± 4.8^{c}	173.8 ± 8.5^{d}
FD-TT57	15.0	18.6 ± 0.5^{a}	107.2 ± 2.3^{c}	88.6 ± 2.7^{c}	166.9 ± 7.6^{d}
FD-TT60	15.0	16.9 ± 0.5^{a}	100.8 ± 20.9^{c}	83.9 ± 21.4^{c}	109.8 ± 9.1^{e}
Fresh REF2	10.4 ± 0.1^{A}	13.3 ± 0.2^{A}	124.1 ± 1.0^{A}	110.8 ± 0.5^{A}	50.6 ± 0.5^{A}
FD-REF2	10.5 ± 0.2^{A}	13.7 ± 1.2^{A}	128.2 ± 3.4^{A}	114.5 ± 4.1^{A}	47.4 ± 1.8^{B}

6



General discussion

6.1 Outline

Sustainable and healthy diets are essential for promoting good health and reducing the environmental impact of the food system (IPPC, 2023). In this context, meat substitutes have been developed to help consumers shift from animal-based proteins to plant-based alternatives. These products are typically made from plant-based protein ingredients, most commonly imported soy protein isolate (SPI) powder, which are texturized via extrusion into a gelled, meat-like structure. However, conventional protein extraction and drying steps used to obtain SPI powder are energy intensive and can negatively alter the gelling properties required for developing the final texture.

The main objective of this thesis was to rethink current meat substitute manufacturing by using **locally sourced plant-based proteins, minimizing processing for protein extraction and eliminating the conventional drying step.** The research further focused on the application of pulsed electric field (PEF) treatment for short-term microbial preservation of plant-based liquids, enabling intermediate storage and transport prior to extrusion. PEF was chosen as a mild preservation strategy to avoid thermally induced protein modifications, as observed in conventional drying and heat pasteurization. Overall, the approach was designed to achieve a lower carbon footprint and improved functionality of the minimally processed, non-dried and PEF-treated ingredients compared to conventionally fractionated and dried or thermally treated protein ingredients.

To address the research questions as described in Section 1.4.2, two raw materials were used: the microalgae *Chlorella vulgaris* (*Cv*) (**Chapters 2 – 3**) and yellow pea protein extract (PPE) (**Chapters 4 – 5**), which correspond to real demands from the food industry. First, **Chapter 2** examined the feasibility of incorporating plant-based liquids into extrusion, which is typically performed using protein powders. Then, the identification of microbial contaminants, together with the application of PEF treatments for the preservation of *Cv* and PPE are discussed (**Chapters 3** and **4**). **Chapter 5** aimed to ensure that PEF conditions, optimized for microbial inactivation, is a viable preservation method and do not negatively alter protein functionality. The main findings from **Chapters 2 – 5** are discussed in **Chapter 6** (Section 6.2). Moreover, **Chapter 6** discusses unpublished findings to further explore the use of PEF for the microbial inactivation of plant-based liquids (Section 6.3). More precisely, Section 6.3.1 gives general observations regarding microbial contamination, sensitivity to PEF and potential shelf-life extension. Then, investigations at the molecular level are described, with the potential correlation between the extent of bacterial cell membranes

electroporation and lag phase duration during shelf-life (Section 6.3.2), and the potential protective effect of proteins against inactivation (Section 6.3.3). Moreover, the advantage of PEF over thermal treatment (TT) to maintain protein functionality is described in Section 6.4. Furthermore, life cycle assessment (LCA) data are presented to compare the carbon footprint of conventional (from literature) and minimally processed ingredients (this thesis) (Section 6.5). This discussion chapter ends with the main conclusions from the thesis (Section 6.6) and suggestions for future research (Section 6.7).

6.2 Main findings – PEF to inactivate bacteria and simultaneously enhance protein functionality

In **Chapter 2**, the feasibility of using protein liquids is described, instead of powdered proteins, to produce extrudates of similar quality. More precisely, liquid (suspension) and dried *Cv* ingredients were incorporated (10% (w/w) on a dry basis) into pea protein isolate (PPI) during extrusion, and the final products were compared. The drawback of using liquid ingredients is the minimal action on protein and dry matter (DM) contents. Indeed, the cell concentration of microalgae suspensions is in general of 2 – 3% (w/w) after cultivation and can be increased to 20 – 25% (w/w) through centrifugation. In **Chapter 2**, the concentration of microalgae was 10% (w/w), and therefore, its incorporation rate in PPI was limited, knowing that high-moisture extrusion is typically run at 60% water. To compensate for lower protein and DM contents, higher functionality is desired. Hence, cell disruption was applied during downstream processing of *Cv* to release intracellular proteins from the microalgae cells and make them available for better gel formation. PEF-induced cell disruption was tested (data not shown) but proved inefficient. However, high-pressure homogenization (HPH) (150 MPa, inlet temperature T_{in} = 30 °C) effectively disrupted the cells and promoted protein release, as validated by imaging. The outlet temperature T_{out} was maintained below 60 °C, to avoid thermal degradation of proteins as measured in differential scanning calorimetry (DSC). The gelling properties of the ingredients were enhanced as observed with an increase in final viscosity and gel strength after Temperature-sweep (*T*-sweep). Confocal laser scanning microscopy (CLSM) also showed a more homogeneous gel network after HPH. To conclude, the addition of 10% (w/w) HPH-treated *Cv*, wet or dry, did not compromise the process efficiency, final color and texture properties of PPI-based extrudates, while improving their nutritional and sustainability aspects.

Chapter 2 demonstrated the feasibility of using protein-rich plant-based liquids in extrusion. However, liquids are more prone to spoilage than their powdered counterparts due to their

high water activity. Therefore, in **Chapter 3**, the microbial preservation strategy for protein liquids was investigated, enabling their intermediate storage and transport prior to extrusion. First, microorganisms were isolated from a *Cv* suspension (10% w/w, pH 6.5, 10 °C), and three fast-growing psychrotolerant bacteria (***Pseudomonas guariconensis, Enterobacter soli*** and ***Lactococcus lactis***) *were selected for the study.* The isolates were inoculated in the *Cv* suspension (2% w/w, 0.6 mS/cm) and subjected to challenge tests using PEF treatment combined with cold storage. The PEF conditions were optimized by varying electric field strength and pulse repetition rate values. Maximum inactivation of 4.1, 3.7 and 3.6 logs was achieved at E_{el} = 28 kV/cm, f = 120 Hz, τ = 20 µs, t = 225 µs, T_{in} = 30°C, and T_{out} < 55°C, for the investigated isolates, respectively. Additionally, shelf-life studies in refrigerated conditions (10 °C) were conducted over a period of ten days. Due to the significant reduction of the microbial load, shelf-life was extended; however, the lag phase duration and growth rate were not affected by PEF, suggesting no sub-lethal damage or very fast recovery. Thus, sequential PEF treatments were tested, with a second PEF treatment showing similar inactivation efficiency compared to the first PEF treatment. To summarize, **Chapter 3** showed the potential of PEF to reduce key contaminants in *Cv* suspension and the possibility to extend shelf-life further with repetitive PEF cycles, resulting in larger process flexibility.

In **Chapter 4**, the preservation strategy was applied to a second protein liquid, a PPE, to validate that the concept is not ingredient-specific and can be extended to a multitude of protein-rich plant-based ingredients. The work was done on PPE obtained by dry fractionation of pea protein concentrate (PPC) followed by a mild aqueous fractionation as illustrated in Figure 1.2. Such ingredients showed promising gelling capacity. Similar to **Chapter 3**, psychrotrophic bacteria were first isolated from the PPE, purified and identified. ***Pseudomonas trivalis*** and ***Erwinia gerundensis*** were selected based on their high growth capacities in PPE (10% w/w, pH 6.7, 10 °C). The isolates were inoculated in diluted PPE (3% w/w, 2 mS/cm), and PEF treatment conditions were optimized by varying the initial product temperature. At a T_{in} of 25 – 30 °C (24 kV/cm, 50 Hz, 20 µs, ΔT = 20 °C), inactivation of 3 logs was reached and explained solely by the electrical effect. Increasing the T_{in} to 40 °C enabled an inactivation of 4 logs, where thermal effects dominated. At a T_{in} of 45 °C, thermal modification of pea proteins was observed in DSC measurements (endothermic peak between 61 and 82 °C), potentially compromising the pea extract's gelling properties. Shelf-life studies on *P. trivalis*, *E. gerundensis* and the native microbiota of the PPE were

conducted at 5 °C and 10 °C storage. Notably, an extension of the lag phase (four days at 5 °C) was observed for the native microbiota and was accompanied by a pH stability of ten days. Such findings validated the promising use of PEF to extend the shelf-life of different plant-based liquids.

In **Chapters 3 and 4**, the primary focus was to study the impact of PEF treatment on the microbial inactivation and shelf-life extension of the plant-based ingredients. Process windows for microbial reduction were defined for both microalgae suspension and pea extract. In **Chapter 5**, the focus shifted toward **the impact of PEF treatment on the functionality and structure of the treated ingredients**, more specifically, the properties of pea proteins, i.e. albumins and globulins. The optimized PEF parameters (24 kV/cm, 50 Hz, 20 µs, T_{in} 25 – 40 °C) obtained from **Chapter 4** were selected, and TTs (51 – 60 °C, 27 s) leading to similar microbial inactivation were added to the study. Characterization of the reference, PEF-treated and thermally treated ingredients was conducted. While the PEF treatment led to an increase in solubility, surface charge and polarity of the proteins, thermal treatments induced inverse effects. Moreover, different protein modification pathways were observed for PEF versus TTs, which could explain the difference in gelling properties. While the gelling properties of pea extract were enhanced following PEF treatments, regardless of inlet temperature, the opposite was observed for the TTs.

Overall, it was possible to produce plant-based extrudates partially formulated with protein extracts in their liquid form. Moreover, PEF treatment allowed the microbial inactivation (up to 5 logs) of substrate-specific psychrotolerant bacteria inoculated in such liquids, with a combined increase of 35% in gelling properties compared to the untreated ingredient. Beyond this, for a similar microbial inactivation level, TT led to a reduction of 60% in gelling properties compared to the PEF-treated ingredient. Therefore, besides efficient microbial inactivation, **PEF also showed potential for enhancing the gelling capacity of protein extracts.**

6.3 PEF to inactivate bacteria – generalities and limitations

6.3.1 Plant-based microbial contaminants, sensitivity to PEF and potential shelf-life extension

Plant products and algae are prone to contamination from contact with soil, air, water or human skin during harvesting and processing (Gräfenhahn & Beyrer, 2024). Conventional extraction processes and drying, done at elevated temperatures, reduce the contaminant load. In contrast, microbial reduction in minimally processed and liquid protein extracts is limited. For validation, the microbial loads (total plate count (TPC)) in PPC, PPE and PPI were measured (unpublished data). The microbial loads in PPC (3.8 log colony forming unit (CFU)/g) and PPE (3.7 log CFU/g) were significantly higher compared to PPI (< detection limit (1 log CFU/g)), which was obtained by a more intense (temperature and chemicals) extraction process. Additionally, the microbial load of PPI-based extrudates obtained internally (unpublished data) was lower than the detection limit (1 log CFU/g). According to Wild et al. (2014), extrusion processing conditions (T > 90 °C, pressures > 1 bar, residence times up to minutes) allow very high inactivation of vegetative cells. Therefore, in this thesis, the objective was to maintain acceptable food quality during intermediate storage, while extrusion allowed controlling the microbial load in the final food product.

In **Chapters 3 and 4**, microbial isolation and identification allowed the detection of 17 different species in *Cv* and 20 in PPE, including pathogens and spore formers. Four Gram-negative (-) and one Gram-positive (+) non-pathogenic bacteria were selected for the study (*P. guariconensis* (-)*, E. soli* (-)*, P. trivalis* (-)*, E. gerundensis* (-) and *L. lactis* (+)) based on their capacity to grow in the substrate (*Cv* or PPE) at 10 °C. PEF treatment enabled significant inactivation level (> 2 logs of reduction) for the five studied bacteria. In **Chapter 3**, the considerable influence of media conductivity on process efficacy reflects the complex interdependence of PEF parameters (Figure 1.3) and was explained by a combination of electrical and thermal effects. Moreover, in **Chapter 3**, while thermal inactivation is considerably species-specific (Figure 3.4), PEF treatment showed generic effects with similar inactivation tendencies for the three species (Figure 3.5). In PEF, it seems that the higher electrical resistance (E_{crit}) of bacteria (*E. soli* > *L. lactis* > *P. guariconensis*) is partially compensated by their lower heat resistance (T_{crit}) (*E. soli* < *P. guariconensis* < *L. lactis*).

Besides challenge tests, spoilage control studies were conducted to assess the impact of PEF on the shelf-life of plant-based liquids and the potential extension of lag phase duration during storage at 10 °C. For the isolates, PEF did not lead to a significant extension of lag

phase duration and a reduction of growth rate. The observations in *Cv* and PPE were similar. In contrast, for the native microbiota, lag phase duration was significantly extended after PEF treatment (**Chapter 4**). For feasibility reasons, shelf-life studies, as conducted in **Chapters 3 and 4**, were done for only one PEF condition. Further investigations of the effect of increasing PEF intensity on the lag phase duration are presented in Section 6.3.2.

Furthermore, **the implementation of PEF** within the supply chain was evaluated using two case-scenarios: immediately after microalgae cultivation (or protein extraction), and one day later to simulate storage or transport conditions. Two implementations were therefore considered and compared: 1) cultivation (at 30 °C) – PEF – shelf-life (10 °C), and 2) cultivation (at 30 °C) – one day storage (at 10 °C) – PEF – shelf-life (10 °C). The microbial cultivation done at 30 °C was aligned with the cultivation of *Cv*, typically done at 20 – 30 °C (Cai et al., 2021), and the production of the PPE done at room temperature (**Chapter 4**). For both scenarios, PEF-induced inactivation and microbial growth during storage at 10 °C were measured to acquire information on the potential adaptive response of the cells. Cultivation, PEF treatments, microbial analyses and growth modelling were done as described in **Chapter 3**. Figure 6.1 shows the effect of one day storage (at 10 °C) on subsequent PEF treatment efficiency and growth dynamics. Reductions of 3.5 and 4.1 logs were obtained for *P. guariconensis* and *E. soli*, respectively. It is worth noting that the shelf-life of *E. soli* was positively affected by cold storage prior to the PEF treatment. This was reflected in a significantly reduced specific growth rate and a more extended lag phase (Table 6.1). These promising outcomes signify the potential efficiency of this approach. However, it was not possible to PEF-treat *L. lactis* following one-day storage at 10 °C. Lactic acid fermentation was indicated by a pH reduction (up to 4.5) as well as a conductivity increase (up to 0.93 mS/cm), caused by the accumulation of lactate ions. The strong influence of bacterial species on the outcome showed the importance of considering the native microbiota of the ingredient when determining the most effective implementation strategy for PEF treatment.

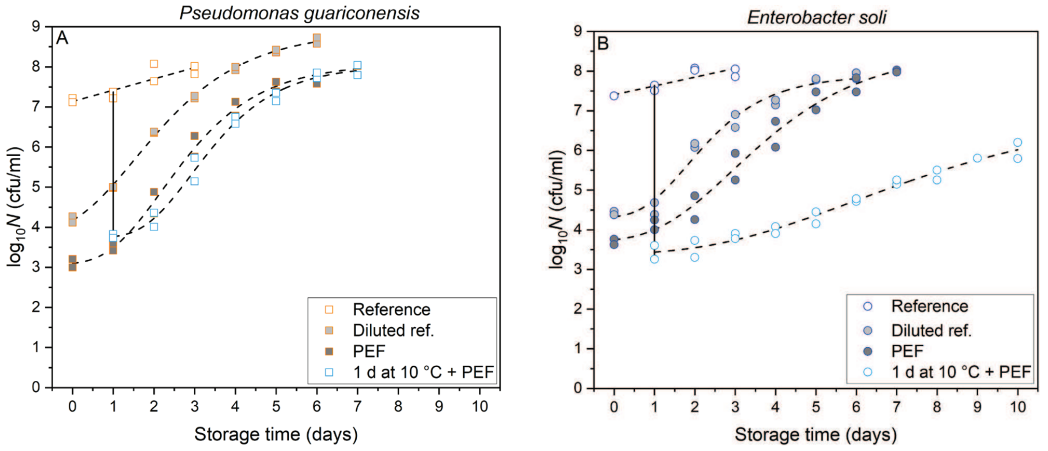

Figure 6.1: Microbial evolution of untreated versus PEF-treated cells for different isolates *P. guariconensis* (A) and *E. soli* (B) in *Cv* suspensions during storage at 10 °C until ten days. PEF corresponds to the treatment directly after inoculation, whereas 1 d at 10 °C + PEF corresponds to the treatment after one day of storage at 10 °C. PEF treatments were done at 90% output voltage (28 kV/cm), 120 Hz, 20 µs, 30 °C, 60 L/h (n = 2). An untreated, diluted sample was included in the study for improved comparability of initial counts. For visualization purposes, growth fitting was done on the average data points with biogrowth (dashed lines).

Table 6.1: Growth parameters extracted from the biogrowth simulations (https://foodmicrowur.shinyapps.io/biogrowth) as shown in Figure 6.1. Values are presented as averages (n = 2) ± SD. 10 °C + PEF treatment on *Lactococcus lactis* was not feasible at the selected PEF conditions

Isolates	***P. guariconensis***		***E. soli***		***L. lactis***	
Growth parameters	**μ ($\log_{10}d^{-1}$)**	**λ (d)**	**μ ($\log_{10}d^{-1}$)**	**λ (d)**	**μ ($\log_{10}d^{-1}$)**	**λ (d)**
Diluted ref.	1.2 ± 0.0	Not significant	1.2 ± 0.2	0.7 ± 0.3	1.2 ± 0.1	0.4 ± 0.1
PEF	1.4 ± 0.1	0.9 ± 0.2	0.9 ± 0.1	1.0 ± 0.5	1.1 ± 0.1	1.1 ± 0.3
10°C + PEF	1.3 ± 0.1	0.7 ± 0.2	0.4 ± 0.0	1.4 ± 0.8	Not feasible *	

*it was not possible to PEF-treat *L. lactis* at the selected PEF conditions. The sample exhibited a reduction in pH (to 4.5) and an increase in conductivity (to 0.93 mS/cm) following one-day storage at 10 °C

Finally, the possibility of extending the storage with a second PEF cycle was tested in **Chapter 3**. It showed promising results, with similar levels of inactivation compared to the first treatment, and even an extension of the lag phase duration for *P. guariconensis* (Figure 3.8). The development of a concept for repetitive PEF treatments to extend shelf-life is of interest. A better understanding of the outcomes of electroporation was provided in the next Section (6.3.2) to consistently influence lag phase extension. First, it was verified that the lag phase extension observed in this work cannot be attributed to the reduced bacterial cell concentration following PEF treatment. For this, *E. soli* was inoculated in *Cv* at an initial count N_0 of ~ 10^6 CFU/mL and serially diluted in sterile *Cv*. Microbial growth fitting and lag phase duration calculation were done as described in **Chapter 3**. Shelf-life study was conducted for five different initial cell concentrations (10^6 to 10^2 CFU/mL) (Figure 6.2). The lag phase durations were not significantly different, suggesting that the lag phase extensions

reported in this thesis were rather explained by PEF-induced microbial cell injury. However, additional data points would be beneficial to validate this observation.

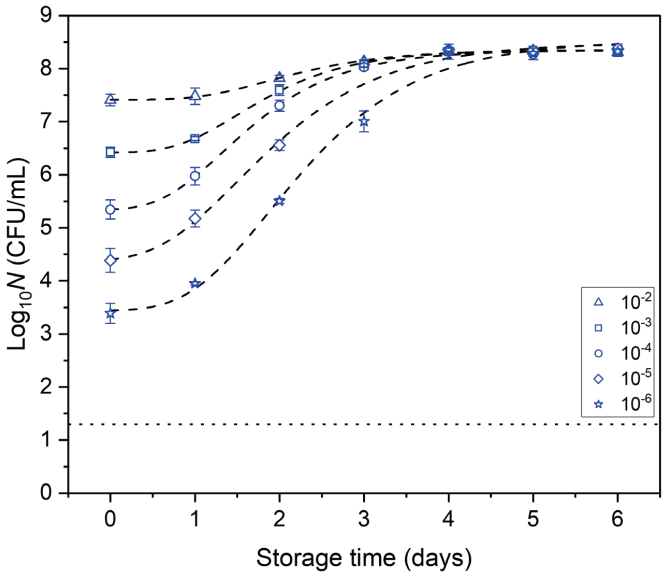

Figure 6.2: Microbial growth of *Enterobacter soli* inoculated in *Cv* suspension and serially diluted (10^{-2} to 10^{-6}) with *Cv* suspension. Incubation was done at 10 °C for six days. The initial count N_0 was ~ 10^6 CFU/mL, and the detection limit was 1.3 log (dot lines). Data points are averages of three individual measurements (n = 3) ± SD. For visualization purposes, growth fitting was done on the average data points with biogrowth (dashed lines).

6.3.2 Insight into microbial cell injury

In **Chapter 3**, PEF treatment was optimized for the microbial preservation of *Cv*, focusing on both logarithmic (log) reduction and shelf-life extension. However, further research was conducted to investigate the outcome of electroporation on bacterial membrane permeabilization, whether this process is reversible or irreversible (unpublished data). In theory, PEF treatment at E_{el} > 25 kV/cm (28 kV/cm in **Chapter 3**) leads to irreversible electroporation, causing cell death. However, due to the varying susceptibility to PEF, not all cells succumb to inactivation; some remain intact, while others experience sublethal injury, showing a loss of membrane integrity but retaining metabolic activity and repair capacity (Jaeger et al., 2009b; Wang et al., 2018). The time needed for cells to repair damage and to adapt for growth, referred to as lag phase, significantly influences shelf-life (Selma et al., 2004). Thus, understanding the extent of cell injury can provide valuable insights into predicting and potentially controlling the shelf-life of food products. In this part of **Chapter 6**, the cell injury level of *E. soli* treated by varying PEF intensities (19 – 28 kV/cm, 120 Hz, 20 µs) was assessed, focusing on the sublethal injury. A shelf-life study (at 10 °C) was

conducted to investigate the correlation between cell injury level and lag phase duration. The PEF setup and parameters, the cultivation of *E. soli* and the shelf-life study methods are detailed in **Chapter 3**. Only PEF treatments at a frequency of 120 Hz and T_{out} below 52 °C were conducted to ensure that all observed effects were caused by electroporation and not thermal effects (T_{crit} for *E. soli* = 52.4 °C, Figure 3.4). Different analytical methods, namely, **viable cell count** on plate counting agar (PCA), **fluorescence flow cytometry** (FFC)**, selective plating**, and **colony size distribution imaging**, were used for the investigation.

In parallel to viable cell count, FFC was used to distinguish between intact cells and cells with compromised membranes integrity after PEF treatments (19 – 28 kV/cm). FFC was performed using a double staining with the competitive nucleic acid dyes Propidium Iodide (PI) and SYTO 9. The red-fluorescent dye PI penetrates only cells with permeable membranes, while the green-fluorescent dye SYTO 9 penetrates both intact and permeabilized cells (Cal-Sabater et al., 2019). The FFC method is described in Section 6.8.1. FFC has previously been used for the characterization of bacteria in liquid foods such as milk, tea, juice, and wine (Zand et al., 2021). However, in most cases, pre-processing of the food samples, such as filtration or centrifugation, is necessary for the adequate enumeration of bacterial populations (Marcos-Fernández et al., 2022). The use of FFC directly within food matrices presents significant challenges, such as significant background noise and competition of the matrix components for the binding of the dyes. For these reasons, analyses were conducted using **Ringer's solution** as the background substrate. The recipe is described in Section 6.8.2.

Increasing PEF intensity led to a shift from intact to electroporated cells, which can be observed through the shift from the green fluorescence signal (SYTO 9) to the red fluorescence signal (PI) (Figure A.6.1). The inactivation level measured in FFC followed the same tendency as in viable cell count (PCA) (Table 6.2, Figure A.6.2). In both methods, the reversibly electroporated cells recovered and were detected as intact cells. A second FFC analysis with staining done before PEF would allow differentiation between reversible and irreversible electroporation (Vaessen et al., 2019). As seen in Figure 6.3, intact and irreversibly perforated cells are stained in green and red, respectively, independently of the staining procedure. However, reversibly perforated cells are stained in green if the staining is done after the PEF treatment (A), and in red if the staining is done before the PEF

treatment (B). Therefore, the difference in PI uptake between the two procedures (A and B) gives the reversibility of membrane integrity.

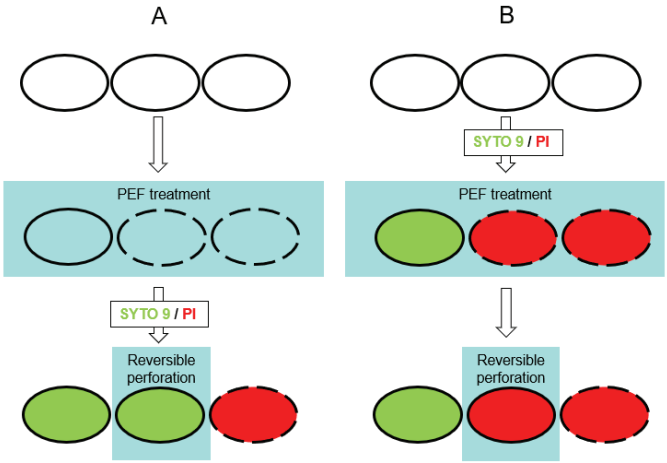

Figure 6.3: Schematic overview of the FFC method used in this work (A) to detect the population of live (green) and dead (red) cells. Intact black lines represent intact cell membranes while dashed lines represent perforated membranes. A second method (B) is necessary to study the reversibility of electroporation. Adapted from Vaessen et al., 2019.

Additionally, a thermally treated sample (80 °C, 10 min) referred as “dead” cells was analyzed and the density plots is displayed in Figure A.6.1. While the percentage of dead cells after PEF treatment at 28 kV/cm and heat treatment are very similar (97.0 versus 98.6%), the SYTO 9 (green) intensity signals differ. Such findings can be explained by the different inactivation mechanisms of heat (denaturation of biomolecules) and PEF (electroporation of membrane) treatments. Intense heating can lead to partial denaturation of nucleic acid and consequently a reduction of the dye binding sites. Such a graph could help with distinguishing between electrical and thermal effects.

Moreover, non-selective (PCA) and selective (PCA + **sodium chloride NaCl**) media were used to distinguish between intact, injured and dead cells. PCA plates allowed the growth of both intact and PEF-injured cells, while on PCA + NaCl plates, only intact cells grow due to the inability of injured cells to form colonies under additional stress conditions. First, *E. soli* inoculum was serially diluted and plated on PCA with 2, 4, 6, 8, 10% (w/v) NaCl (ITW Reagents, Italy) and 6% was set as the critical inhibitory NaCl concentration (Saldaña et al., 2009). Untreated and PEF-treated samples were plated on PCA and PCA + 6% (w/v) NaCl plates and incubated at 30 ˚C for up to 72 h. The percentages of intact and injured cells were calculated using Equations 6.1 and 6.2, respectively. The percentage of dead cells was indirectly derived from CFU of the untreated sample on non-selective media and the PEF-

treated sample using Equation 6.3. Finally, the sublethal injury ratio was calculated using Equation 6.4 (Siderakou et al., 2021).

$$\text{Intact cells} = \frac{\text{CFU}_{\text{PCA+6 \% NaCl}} \text{ of PEF-treated sample} \cdot 100}{\text{CFU}_{\text{PCA}} \text{ of untreated sample}} \quad (\%) \quad (6.1)$$

$$\text{Injured cells} = \frac{\{(\text{CFU}_{\text{PCA}} \text{ of PEF-treated sample} - \text{CFU}_{\text{PCA+6 \% NaCl}} \text{ of PEF-treated sample}) \cdot 100\}}{\text{CFU}_{\text{PCA}} \text{ of untreated sample}} \quad (\%) \quad (6.2)$$

$$\text{Dead cells} = \frac{\{(\text{CFU}_{\text{PCA}} \text{ of untreated sample} - \text{CFU}_{\text{PCA}} \text{ of PEF-treated sample}) \cdot 100\}}{\text{CFU}_{\text{PCA}} \text{ of untreated sample}} \quad (\%) \quad (6.3)$$

$$\text{Sublethal injury log ratio} = \log_{10}\left(\frac{\text{CFU}_{\text{PCA}} \text{ of PEF-treated sample}}{\text{CFU}_{\text{PCA + 6 \% NaCl}} \text{ of PEF-treated sample}}\right) \quad (-) \quad (6.4)$$

The percentage of each subpopulation (intact, injured and dead cells) after PEF treatments (19 – 28 kV/cm) is displayed in Figure A.6.3, and the sublethal injury ratio in Table 6.2. A significant increase in the sublethal injury ratio was observed only following PEF treatment at 28 kV/cm, indicating that the cells damage caused by PEF was primarily irreversible.

Table 6.2: Summary of the different results obtained through the investigation of PEF-induced cell injury level of *E. soli* inoculated in Ringer's solution. Log reductions were obtained from viable cell counting on PCA (n = 3) and FFC (n = 1), sublethal injury ratio from selective plating (PCA + 6% (w/v) NaCl), average size of colonies from image processing (n=3) and lag phase duration from shelf-life in *Cv* at 10 °C for six days (n = 3). Values are presented as averages ± SD. Different letters indicate significant differences ($p < 0.05$)

PEF treatment	PCA	FFC	Selective plating	Imaging	Shelf-life
	log reduction (-)	log reduction (-)	Sublethal injury ratio (-)	Average size of colonies (pixels)	Lag phase duration (d)
Untreated		0.0	0.05 ± 0.04^{a}	894.5 ± 52.7^{ab}	1.4 ± 0.4^{a}
19 kV/cm	0.4 ± 0.1	0.3	Not consistent*	1050.4 ± 143.3^{a}	1.1 ± 0.5^{a}
22 kV/cm	0.5 ± 0.1	0.5	0.02 ± 0.01^{a}	747.8 ± 79.1^{bc}	1.3 ± 0.5^{a}
25 kV/cm	0.6 ± 0.3	0.9	0.09 ± 0.15^{a}	581.8 ± 3.7^{cd}	0.9 ± 0.1^{a}
28 kV/cm	1.8 ± 0.4	1.6	1.01 ± 0.20^{b}	427.5 ± 50.0^{d}	1.4 ± 0.3^{a}

* More cells were counted on PCA + 6% (w/v) NaCl than on PCA, resulting in a negative number of injured cells (Table A.6.1)

Furthermore, plate image processing was conducted to measure the size of the colonies. The method is described in Section 6.8.3. We assumed that injured cells need an adaptation and recovery period, leading to a delay in colony formation, which is detected through a different colony size compared to intact cells that immediately initiate colony growth upon plating. Figure 6.4 shows the difference in *E. soli* colonies formed on PCA plates before (A) and after PEF treatment at 28 kV/cm (B). PEF treatment at 28 kV/cm led to a reduction in the average colony size (in pixels) accompanied by a broader size distribution, suggesting variability in microbial susceptibility to PEF (Figure 6.4.B). Moreover, at 22 kV/cm and above, a gradual decrease in the colony size with increasing PEF intensity was observed (Figure

6.4.C). The colony size at 25 kV/cm (581.8 pixels) and at 28 kV/cm (427.5 pixels) was significantly lower compared to the untreated sample (894.5 pixels) (Table 6.2), indicating a longer time to adapt before proliferation and consequently potential cell injury. Such findings correlate well with the calculated sublethal injury ratio.

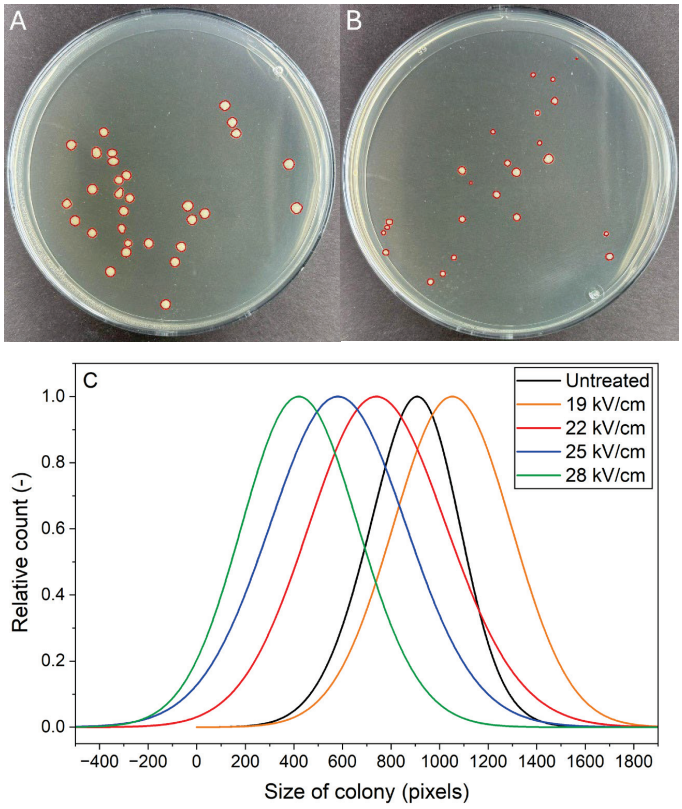

Figure 6.4: Image segmentation obtained with the AutocellSeg analysis to determine the colony size distribution before (A) and after PEF treatment at 28 kV/cm (B). C: Normalized colony size distribution of the untreated and PEF-treated samples. Data are presented as averages (n = 3) ± SD.

Finally, shelf-life studies were conducted to see if the observed increase in sublethal injury ratio and reduction of colony size at 28 kV/cm correlate with the hypothesized longer lag phase duration. *E. soli* was inoculated in Ringer's solution, PEF-treated and diluted in *Cv* to allow cell growth. Shelf-life and growth fitting were done as described in **Chapter 3**. Although shelf life was extended due to microbial inactivation, no additional effect of sublethal injury on the hypothesized prolongation of the lag phase duration was observed (Table 6.2).

To conclude, PEF treatment at 28 kV/cm caused sublethal injury in *E. soli* inoculated in Ringer's solution, as indicated by a sublethal injury ratio of 1 log and smaller colony size

upon plating. Unexpectedly, in condition without stress, these sublethally injured cells did not require additional adaptation time in *Cv* and exhibited a lag phase duration comparable to that of untreated cells. Further investigation is essential to understand the recovery conditions of injured PEF-treated cells and limit their regrowth. Experiments exploring different recovery conditions, combined with proteome analyses, could provide valuable insights into the repair mechanisms and help delay or inhibit the repair process (Emanuel et al., 2021; Zhao et al., 2009). In addition, measuring the sublethal injury ratio of the native microbiota in the real food system would provide valuable insights.

6.3.3 Potential protective effect of proteins against inactivation

In this thesis, to reach maximal irreversible electroporation, PEF at high E_{el} values were applied. To minimize the specific energy input W_s, and consequently an important increase in temperature, the conductivities of the substrates were reduced to 0.7 mS/cm for *Cv* (2% DM) and 2 mS/cm for PPE (3% DM) (**Chapters 3 and 4**) (Equation 1.5). However, it is important to consider real case scenarios. Even though the DM of *Cv* after cultivation is generally low (2%), the implementation of PEF as far as possible in the production chain is preferred to avoid post-contamination. Concerning PPE, it is typically produced at 10% DM and 6 mS/cm, and diluting required to reduce the conductivity is not desired. Therefore, it is important to validate if the inactivation levels achieved in **Chapters 3 and 4** are also possible at higher DM and protein content. Indeed, protein-rich media pose challenges since proteins may play a protective role in the inactivation of microorganisms, explained by their ability to absorb thermal or electrical stress or physically shield bacteria from the electric field (Jaeger et al., 2009b; Schottroff et al., 2020). In this part of **Chapter 6**, the effect of substrate concentration on the PEF-induced inactivation of previously isolated microorganisms (*P. guariconensis*, *P. trivialis* and *E. gerundensis*) was assessed. For this, *Cv* at 25% DM (**Chapter 3**) was diluted to 5, 10 and 15 g/100 g and standardized to a conductivity of 4.0 ± 0.0 mS/cm and pH 5.9 ± 0.1 using Ringer's solution, NaOH (3%) and HCl (1 M), respectively. The ingredients were stored at 4 °C until use.

Moreover, to minimize the time and quantity of substrate required for the experiment, as well as to obtain more accurate data compared to the non-uniform electric field in continuous cell (Delso et al., 2022), a parallel plate (round shape electrodes) batch cell compatible with PEF HVP-5 pilot-scale machine (ELEA, Germany) was designed and constructed internally. The distance between the electrodes was set at 10 mm, and the diameter of the electrodes 16 mm, resulting in a total chamber volume of 2.01 mL (Figure 6.5).

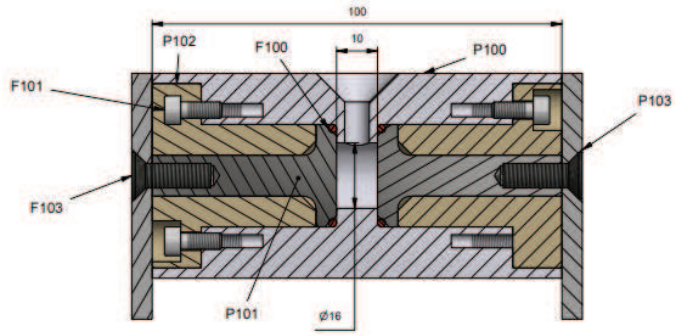

Figure 6.5: Drawing of the internally designed batch PEF cell. P103: feed plates (stainless steel 1.4301), P102: electrode plug (polyoxymethylene), P101: electrodes (stainless steel 1.4435), P100: base (polyoxymethylene), F103: flat screw (steel), F101: socket head cap screw (PC/ABS plastic), F100: O-ring seal (silicone rubber).

Square pulses of output voltage 90%, pulse width 20 µs, pulse repetition rate of 50 Hz were applied to the samples. Three treatment intensities were tested by varying the number of pulses *n* (6, 8 and 10). T_{in} was kept at 24 ± 2 °C, and the c_p of *Cv* was 4.06 kJ/(kg·K). Pulses up to 24 kV were monitored when treating water (data not shown). When treating samples at 4 mS/cm, the maximum E_{el} value decreased to 15 kV/cm (Figure A.6.4). The discrepancy from the square wave shape, with a smooth rise to 15 kV around 10 µs and almost non-existent plateau, can be explained by the high conductivity media and limited capacity of the pulse generator. The long rise and fall time can influence the "effective treatment energy" as reported by Zare et al. (2023). Figure 6.6 displays the PEF-induced inactivation of the three studied bacteria inoculated in *Cv* of different concentrations.

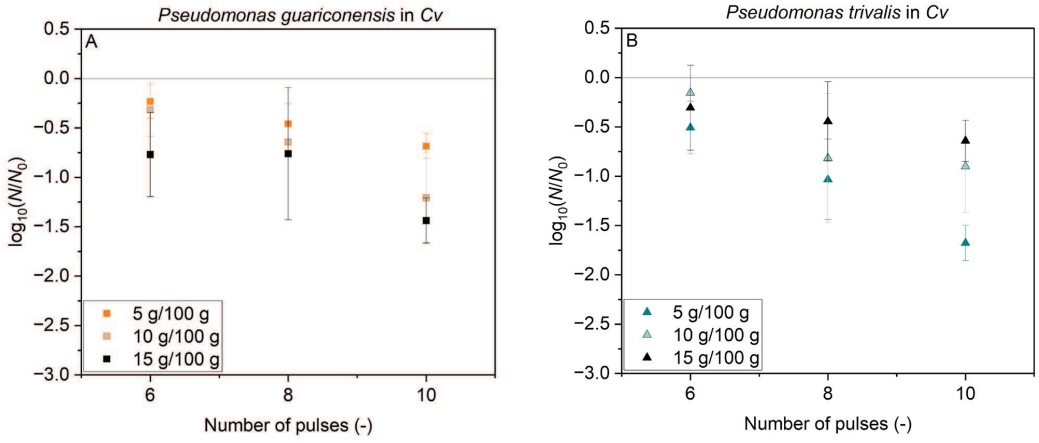

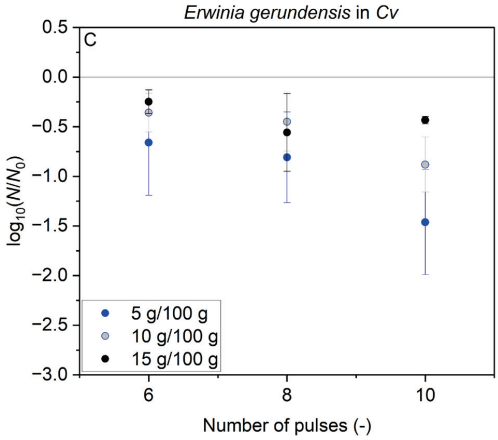

Figure 6.6: Influence of the number of pulses on the inactivation of *P. guariconensis* (A), *P. trivalis* (B) *and E. gerundensis* (C) inoculated in *Cv* at different DM concentration (5, 10 and 15 g/100 g sample), for constant output voltage (90%, 15 kV/cm), pulse repetition rate (50 Hz) and pulse width (20 µs). The initial count N_0 was ~ 10^6 CFU/mL. Plotted data points are averages of three repetitions (n = 3) ± SD.

For PEF treatments of 6 and 8 pulses, the substrate concentration did not significantly impact microbial inactivation levels. In contrast, for a 10-pulse treatment, the inactivation of both *P. trivalis* and *E. gerundensis* was significantly higher in the substrate of 5 g/100 g concentration compared to 15 g/100 g (Table 6.3). This suggests that the influence of substrate concentration becomes apparent under more intensive treatment. Further investigations are needed to elucidate the potential protective effect of proteins against microbial inactivation. It is worth noting that doubling the concentration from 5 to 10 g/100 g did not lead to a significantly lower inactivation, indicating that the treatment of 10 g/100 g substrate, as proposed in this thesis, remains promising.

Table 6.3: Influence of the substrate concentration (5, 10 and 15 g/100 g) on the PEF-induced inactivation of *P. guariconensis, P. trivalis and E. gerundensis* inoculated in *Cv* for PEF treatments of 6, 8 or 10 pulses. Values are presented as averages (n = 3) ± SD. Different letters indicate significant differences ($p < 0.05$) between the substrate concentrations for each microorganism (for each PEF condition)

Isolates	***Cv* concentration (g/100g)**	**log reduction (-)**		
		6 pulses	**8 pulses**	**10 pulses**
P. guariconensis	5	0.2 ± 0.2^{a}	0.5 ± 0.2^{a}	0.7 ± 0.1^{a}
	10	0.3 ± 0.3^{a}	0.6 ± 0.2^{a}	1.2 ± 0.5^{a}
	15	0.8 ± 0.4^{a}	0.8 ± 0.7^{a}	1.4 ± 0.2^{a}
P. trivalis	5	0.5 ± 0.3^{a}	1.0 ± 0.4^{a}	1.7 ± 0.2^{b}
	10	0.2 ± 0.2^{a}	0.8 ± 0.7^{a}	0.9 ± 0.5^{ab}
	15	0.3 ± 0.4^{a}	0.4 ± 0.4^{a}	0.6 ± 0.2^{a}
E. gerundensis	5	0.7 ± 0.5^{a}	0.8 ± 0.5^{a}	1.5 ± 0.5^{b}
	10	0.4 ± 0.2^{a}	0.5 ± 0.3^{a}	0.9 ± 0.3^{ab}
	15	0.2 ± 0.1^{a}	0.6 ± 0.4^{a}	0.4 ± 0.0^{a}

Furthermore, homogenized *Cv*, as obtained in **Chapter 2**, was tested to study the impact of protein state (soluble versus trapped inside the *Cv* cells) on inactivation (Figure 6.7).

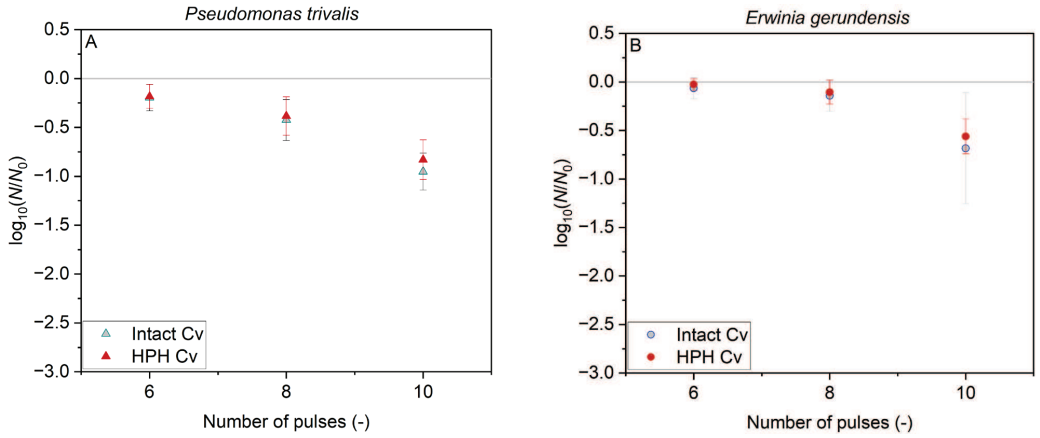

Figure 6.7: Influence of the number of pulses on the inactivation of *P. trivalis* (A) and *E. gerundensis* (B) inoculated in intact or HPH-treated *Cv* at a DM concentration of 10 g/100 g sample, for constant output voltage (90%, 15 kV/cm), pulse repetition rate (50 Hz) and pulse width (20 µs). The initial count N_0 was ~ 10^6 CFU/mL. Plotted data points are averages of three repetitions (n = 3) ± SD.

We hypothesized that soluble, released proteins would form a protective layer around the bacterial cells and play a more pronounced role against inactivation. However, the inactivation of *P. trivialis and E. gerundensis* in HPH-*Cv* was comparable to the intact *Cv* at the tested concentration of 10 g/100 g. Visually, the difference between intact and HPH-*Cv* appeared to increase with treatment intensity. Further studies under more intensive treatment and at different concentrations would be valuable to better understand the influence of released protein on microbial inactivation.

6.4 PEF to enhance the functionality of plant-based extracts

6.4.1 PEF advantage over TT to enhance gelling properties

Beside energy reduction, the primary motivation for developing alternatives to thermal processes is to prevent the degradation of heat-sensitive compounds present in liquid foods. In this work, PEF is considered a viable microbial preservation method only if protein functionality is maintained. Pre-trials on the impact of PEF treatment on the gelling properties of HPH-*Cv* as used in **Chapter 2** have been conducted and revealed a potential enhancement of the properties (unpublished data). Figure A.6.5 showed an increase in the peak viscosity $\mu_{app,\ peak}$ from 604 to 744 mPa·s. The difference in the viscosity curve from the results displayed in **Chapter 2** (Figure 2.4) can be explained by the variation of the *Cv* batch and the isoelectric precipitation step required to increase the concentration of the

samples from 2 to 14% DM. It would be interesting to validate these observations across multiple *Cv* batches to account for batch-to-batch variability, as well as on freeze-dried and rehydrated biomass to eliminate the potential effects arising from concentration step.

In the case of PPE, in **Chapter 5**, the negative impact of TT on gelling properties of PPE was validated through *T*-sweep measurements of thermally treated (at 51 – 60 °C) PPE samples. The peak viscosity $\mu_{app,\ peak}$ was significantly reduced for thermally treated ingredients compared to the untreated ingredient, with a reduction by a factor two for the TT at 60 °C (Table 5.A.2). In contrast, PEF treatments at T_{in} 25 °C and above induced an enhancement of the gelling properties with an increase of the peak viscosity $\mu_{app,\ peak}$ up to 35% for PEF treatment at T_{in} 40 °C (T_{out} 60 °C). Therefore, such PEF treatment (24 kV/cm, 50 Hz, 20 µs, T_{in} 40 °C) seems to be a suitable process window for microbial inactivation (5.1 logs of reduction for *P. trivalis* and 4.5 logs of reduction for *E. gerundensis*, Figure 4.3) thus potential shelf-life extension (Figure 4.4), while enhancing functionality. It is interesting to note that for the same T_{out} (60 °C), both treatments (PEF and TT) induced an inverse effect on functionality, validating their different mechanisms of action. It would be interesting to determine the maximal T_{out} for PEF before functionality reduction. In fact, higher T_{out} induces higher microbial reduction and shelf-life extension, and beyond this, a higher specific energy input, W_s, also implies the possibility of treating higher conductive ingredients, as tested in Section 6.3.3.

6.4.2 Extrusion with PEF-treated PPE

The impact of processing on the texture formation during extrusion was also investigated. Freeze-dried reference and PEF- or TT-processed PPE ingredients were incorporated (30 g/100 g) in PPI and texturized using a co-rotating twin-screw extruder (Process 11, Thermo Fisher, UK). The method is described in Section 6.8.4. A texture profile analysis (TPA) allowed to extract six parameters including hardness, gumminess, chewiness, springiness, cohesiveness and resilience of the obtained extrudates. The textural parameters are described in Section 6.8.9. Figure 6.9 shows the impact of PEF- or TT-processed ingredients on the extrudates' final textural properties.

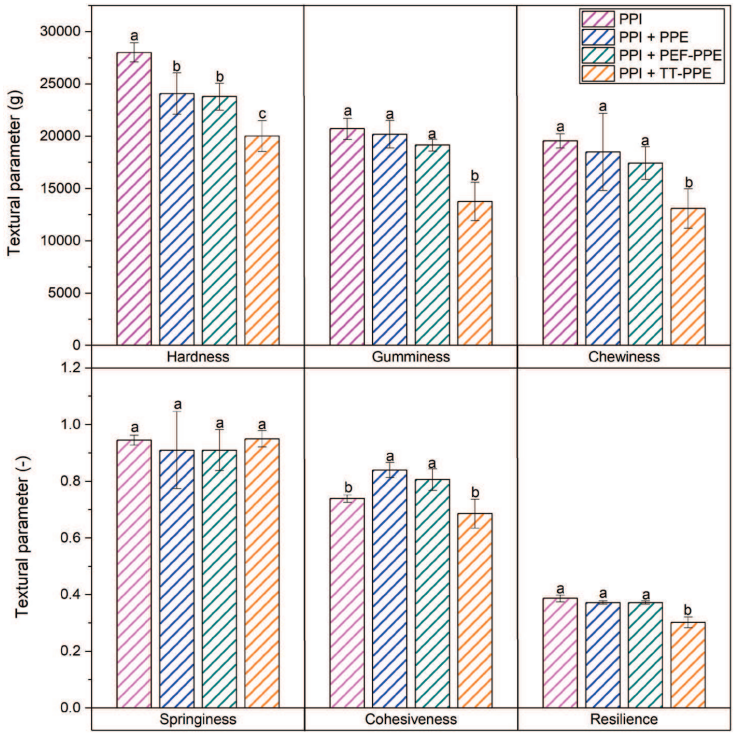

Figure 6.9: Hardness, gumminess, chewiness, springiness, cohesiveness and resilience of PPI and PPI-PPE extrudates as measured with TPA. PPI (pink) extrudates were supplemented with 30% (w/w dry basis) PPE either untreated (blue), PEF-treated at inlet temperature of 30 °C (turquoise) and thermally treated (boiling temperature, 5 min) (orange). Moisture content was 64% DM and data are expressed as averages (n = 5) ± SD. Different letters indicate significant differences ($p < 0.05$). g stands for gram-force.

The incorporation of PPE into PPI resulted in decreased hardness and increased cohesiveness of the extrudates, without significantly affecting the other textural parameters. The differences could be explained by a lower protein content in PPE compared to PPI. Moreover, while PEF treatment did not significantly influence extrudate texture, intense TT reduced all the textural parameters except springiness. These findings are consistent with those presented in Section 6.4.1 and further validate the advantages of PEF over TT regarding protein functionalities.

6.5 Minimally processed plant-based proteins for carbon footprint reduction

Shifting from animal-based to plant-based protein diet allows carbon footprint and land-transformation reduction as previously reported. For example, Smetana et al. (2015) obtained a reduction of at least 50% when replacing chicken (5.2 – 5.8 kg CO_2-eq/kg product) with soy-based meat substitutes (2.6 – 2.8 kg CO_2-eq/kg product). When emissions are expressed per kilo digestible protein, however, the difference became less pronounced

(16.8 – 18.7 kg CO_2-eq/kg digestible chicken protein versus 15.8 – 17.0 kg CO_2-eq/kg digestible soy protein). Similarly, Tang et al. (2024) calculated a 65% reduction when shifting from one kilo beef burgers to one kilo plant-based burgers. However, the added benefits of using **alternative minimally processed** plant-based proteins for meat substitute production are less documented. In parallel to the thesis study, an LCA study conducted by international partners (CIRAIG, Polytechnique Montréal, UQAM, EPFL and HEI) compared the carbon footprint of soy protein concentrate (SPC), PPC, PPI and PPE as produced in this work (unpublished data). The method is described in Section 6.8.6. While the production of SPC emits 11.1 kg CO_2-eq/kg protein, the production of PPC emits only 2.0 kg CO_2-eq/kg protein, confirming the potential of pea proteins to reduce the environmental impact compared to typical soy-based meat substitutes (Figure 6.10).

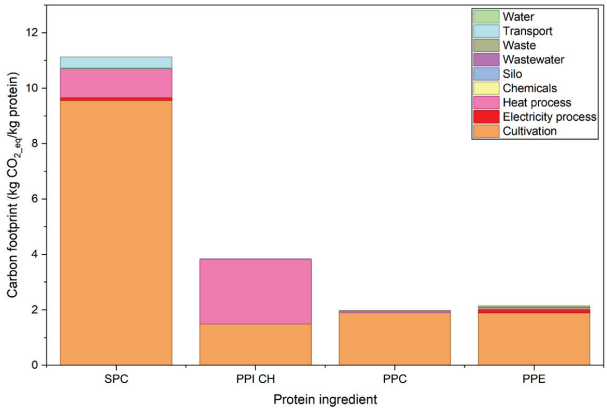

Figure 6.10: Carbon footprint comparison (kg CO_2-eq/kg protein) of the soy and pea protein ingredients across production stages (cradle to gate). SPC: soy protein concentrate, PPI CH: pea protein isolate produced in Switzerland, PPC: pea protein concentrate, PPE: pea protein extract as produced in **Chapter 4**.

The marked difference in cultivation impacts between soy and peas can be explained by land-use and supply chain factors. Soy production is often associated with deforestation, large-scale monoculture, and global exportation. In contrast, peas are typically grown on existing farmland in rotation with other crops, and potentially cultivated locally, closer to consumers (Kogar et al., 2024). Moreover, liming and fertilization also contribute to CO_2 emission (Lucić et al., 2025). Additionally, the carbon footprint of PPI, PPC and PPE was also compared. As expected, PPI showed significantly higher footprint (3.8 kg CO_2-eq/kg protein) compared to the minimally processed ingredients (2.0 kg CO_2-eq/kg protein for PPC and 2.1 kg CO_2-eq/kg protein for PPE). Such results emphasized the need to further develop alternative, minimally processed ingredients to reduce further the environmental footprint of the food system.

Besides raw materials and protein extraction processes, the energy required for the preservation treatment was also considered. In **Chapter 3**, the process energy demand of PEF and TT for achieving similar inactivation was compared, with no evident advantage of PEF over conventional heat pasteurization. However, as reported in **Chapter 1**, the energy requirements for PEF treatment combined with cold storage are unquestionable lower than for spray drying.

6.6 Concluding remarks

This work demonstrated the potential of PEF technology for preserving protein-rich plant-based liquids during intermediate storage, prior to further texturization or formulation into meat or dairy substitutes. Unlike conventional heat pasteurization, PEF treatment achieved microbial inactivation without compromising ingredient gelling properties and, more importantly, enhanced functionality. This thesis therefore illustrates how food product and process development can meet consumer demand for minimally processed and sustainable food products, without compromising the final product quality.

PEF-induced microbial inactivation appeared to have a generic rather than a species-specific effect, which is advantageous as a broadly effective process reduces the complexity and costs of its implementation. Moreover, PEF treatment had an even stronger effect on the native microbiota compared to isolated species, with a pronounced lag phase extension during shelf-life, which is promising for the application of PEF in real conditions. Additionally, storage time can be easily extended by repeating PEF treatments, which maintained comparable efficacy when applied in cycles. From an energy perspective, repeated PEF treatments combined with cold storage remain considerably less energy-intensive than conventional drying, while being relatively easy to implement at industrial scale. Overall, PEF technology enables continuous, effective and tuneable processing that is easy to implement and offers meaningful energy savings.

Finally, beyond technological advantages, the use of local, sustainable and minimally processed protein ingredients aligns with broader societal goals, including the relocalization of food supply chains, the reduction of resource-intensive processing and the development of a more sustainable food system.

6.7 Suggestions for future research

In this thesis, pilot-scale PEF process windows were established for reducing the microbial load (up to 5 logs of reduction) of plant-based liquids *Cv* and PPE at low concentrations (2

– 3% DM) and low conductivity (0.5 – 2 mS/cm). However, PEF treatment of *Cv* at higher concentrations (up to 15 g/100 g) and higher conductivity (4 mS/cm) was tested at laboratory scale and resulted in lower microbial inactivation, reduced electric field strength and increased ohmic heating. The direct application of PEF on the PPE as obtained in this work (10% DM, 6 mS/cm) was not feasible, and dilution prior to PEF treatment was required. To reach the least gelling concentration or a DM content of ~ 40% in extrusion (**Chapter 1**, Section 1.2.2.2), the diluted and PEF-treated extract would need to be recombined with plant-based powders. Ideally, such dilution should be avoided, emphasizing the need for optimized PEF treatment for higher conductivity liquids. Alternatively, diluted extracts may find other applications such as plant-based yoghurts, where lower solids content is acceptable.

Moreover, considering raw material variability is essential. As illustrated in Figure 1.3, food characteristics and PEF process parameters are closely interconnected, and changes in biomass properties can directly influence process efficacy. In **Chapter 3**, batch-to-batch variability of *Cv* was identified, and an increase in conductivity resulted in different levels of microbial inactivation. Extending the research to other plant-based liquids and microorganisms would also be valuable. The work focused on key contaminants that can grow at 10 °C. This temperature was selected for time efficiency, but variations in growth and incubation temperature may influence microbial populations in the liquids. Colder storage conditions may prevent the recovery of sublethally injured cells. The presence of toxicogenic pathogens also needs to be considered. Infective pathogens are less relevant since they will generally be inactivated in subsequent heat treatments, but the prevention of spoilage and toxin formation within the raw material is relevant. In **Chapters 3 and 4**, shelf-life extension was explained solely by a microbial load reduction by PEF. However, lag phase extension was observed with pre-cold storage or during sequential PEF, which calls for further investigations in that direction. Finally, the PEF-induced modifications of plant protein and their positive effects on functionality, as observed in this work, highlight the potential for further research in this field.

6.8 Appendices

6.8.1 Fluorescence flow cytometry

FFC was performed using the LIVE/DEAD BacLight Bacterial Viability Kit (Molecular Probes, Invitrogen, USA) and a double staining with PI and SYTO 9 dyes. The red-fluorescent dye PI penetrates only cells with permeable membranes, while the green-fluorescent dye SYTO 9 penetrates both intact and permeabilized cells (Cal-Sabater et al., 2019). Prior to the analysis, fresh dye solutions were prepared by dissolving the contents of one pipette in 5 mL of dH_2O, thoroughly mixed using a vortex, and always protected from light. Background, untreated and PEF-treated samples were stored on ice and incubated within two hours after PEF treatments with a mixture of PI and SYTO 9 (1:1). The staining was done at a ratio dye: sample of 1:1 for 15 min in the dark at room temperature. The final concentration of the dyes was 30 µM for PI and 6 µM for SYTO 9. The analysis was conducted using the CytoFLEX flow cytometer device (Beckman Coulter, USA) equipped with three lasers—violet (405 nm), blue (488 nm), and red (638 nm). Data were acquired using the blue laser (488 nm) for both dyes, with filters 610/20 and 525/40 nm used for detecting PI and SYTO 9, respectively. PI stain excites/emits at a maximum wavelength of 490/635 nm, while stain SYTO 9 at 480/500 nm. The peak intensity and the duration of each fluorescence signal were considered. The threshold values were set at 1218 for the forward scatter (FSC – information about cell size) and at 1125 for the side scatter (SSC – information about cell granularity and internal complexity) lights. PI and SYTO 9 threshold values were 785 and 844, respectively. The sample flow rate was 60 µL/min, and the results were derived from the analysis of 20'000 cells (events). Gating was done on the acquisition data software CytExpert (Beckman Coulter, USA) with background, live, and dead subpopulations.

6.8.2 Ringer's solution

Calcium chloride dihydrate, potassium chloride, sodium bicarbonate and sodium chloride were dissolved into demineralized water (dH_2O) at the respective concentrations of 1.9, 1.3, 0.6 and 27.0 g/L. Prior to use, the solution was autoclaved and its conductivity adjusted with dH_2O to 0.7 mS/cm.

6.8.3 Colony size distribution imaging

Samples were serially diluted, spread on PCA plates and incubated at 30 °C for 24 h. Subsequently, pictures of the plates were taken using an iPhone 14 with a 12 MB primary camera. The images were processed using the AutoCellSeg segmentation method, based on MATLAB runtime v9.1 (Khan et al., 2018). Experiments were conducted in biological

triplicate and data were expressed as average colony count in pixel and normalized colony size distribution after normalization in OriginLab® 2022b (OriginLab Corporation, USA).

6.8.4 High-moisture extrusion

The screw and barrel diameter were 11 mm and the length-to-diameter ratio 40. The extruder barrel comprised 8 temperature-controlled zones (30, 45, 60, 75, 90, 105, and 120 °C). Transition die temperature and cooling die temperature were kept at 100 °C and 60 °C, respectively. The screw rotation speed was maintained at 175 rpm. Freeze-dried ingredients were fed into the extruder using a twin-screw gravimetric feeder (Gravimetric MiniTwin MT0, Brabender Technologie, Germany) at a rate of 250 g/h. Water was introduced into the third barrel zone via a water pump (Masterflex® L/S®, Intertek, USA) at 391 mL/h, targeting a final extrudate moisture content of 64%. The extrudates were stored under refrigerated conditions and subjected to TPA. A texture analyzer (TA-XT2*i*, Stable microsystem, UK) equipped with a 30 kg load cell was used. The samples were cut into cuboidal shape (20 x 20 mm) and compressed at room temperature twice with a P/36R probe to target strain of 70% with a test speed of 2 mm/s and a waiting time in between the two compressions of 5 s. Six textural parameters were extracted from the TPA curve. For each treatment, at least five samples were measured and averaged.

6.8.5 Textural parameters

Hardness is the force required to deform the extrudate to a certain deformation and corresponds to the peak maximum force at first compression. Springiness is the time required for deformation recovery, calculated as the time between the start and the peak of the second compression over the time between the start and the peak of the first compression. Cohesiveness gives information about the internal structure and was calculated as the area of the second compression over the area of the first compression. Gumminess is the product of hardness and cohesiveness and describes how dense the extrudate is. Chewiness is the product of gumminess and springiness, and finally resilience gives the ability to recover deformation right after the compression and was calculated as the area under curve after peak maxima over the area under curve before peak maxima for the first compression (Funami & Nakauma, 2022; Meulleneti, 1998).

6.8.6 LCA

The results were obtained through a cradle-to-gate study using the Impact World +2.01 LCIA method, the ecoinvent v3.8 and Agrifootprint 6.3 databases and the openLCA v2.02

software. The functional unit was 1 kg of protein produced in 2024, in Switzerland concerning pea and worldwide for soy. The assessment covers nine fields: crop cultivation (including fertilizers, machinery use and on-farm emissions), electricity and heat process, chemicals, silo, wastewater, waste, transport and water.

6.8.7 Supplementary Figures and Table

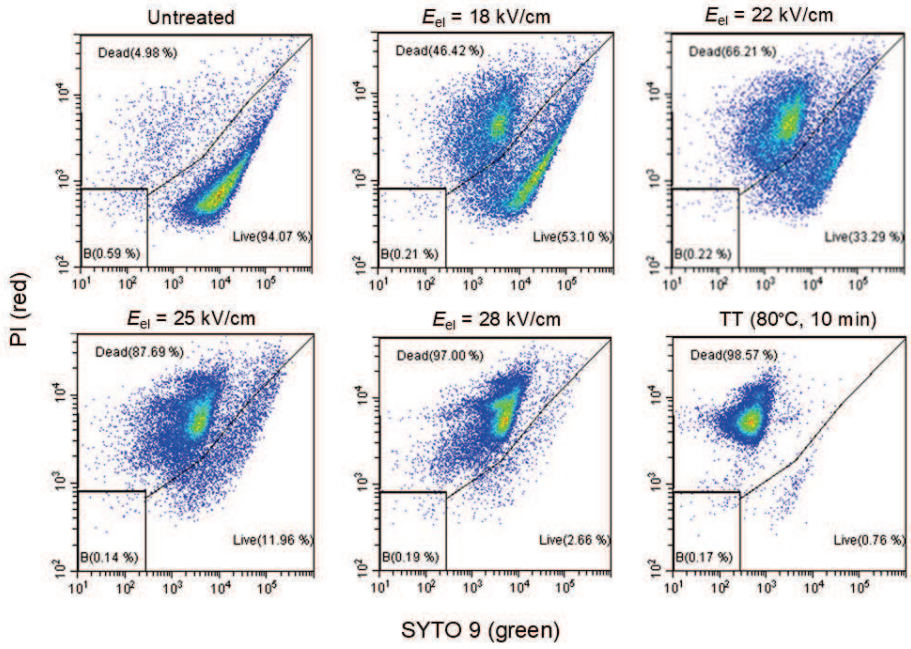

Figure A.6.1: Fluorescence density plots depicting the population of *E. soli*, stained with PI and SYTO 9, as analyzed using the flow cytometry. Each dot represents a single cell of *E. soli*, and in total, 20'000 events are being displayed. Different colors represent a scale of densities from low cell density (blue) to high (red). The three distinct areas of each dot plot represent different fractions of the population: B: Background, Live: cells with intact membrane, Dead: cells with compromised membrane. Density plots show the impact of processing (PEF and TT) on the ratio of live/dead cells. X-axis represents the signal intensity of the SYTO 9 stain, while y-axis the signal intensity of the PI stain.

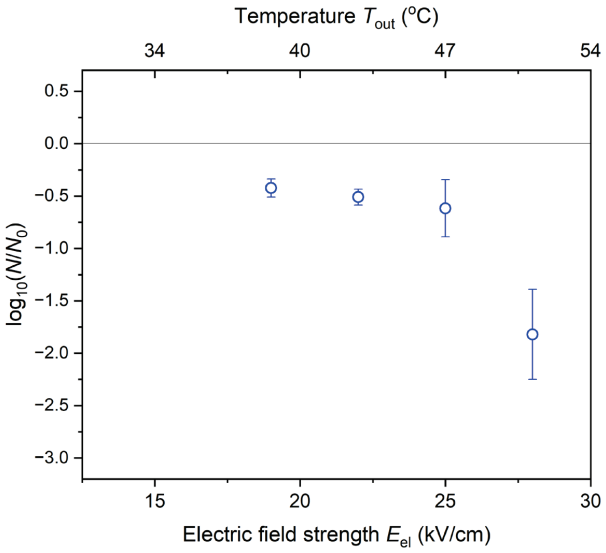

Figure A.6.2: Influence of the electric field strength E_{el} on the inactivation of *E. soli* inoculated in Ringer's solution, at pulse repetition rate 120 Hz, pulse width 20 µs and flow rate 60 L/h. The initial count N_0 was ~ 10^6 CFU/mL, and the detection limit was 1.3 log CFU/mL. Plotted data points are averages of three repetitions (n = 3) ± SD. The top x-axis represents the temperature at the exit of the PEF cell, T_{out}.

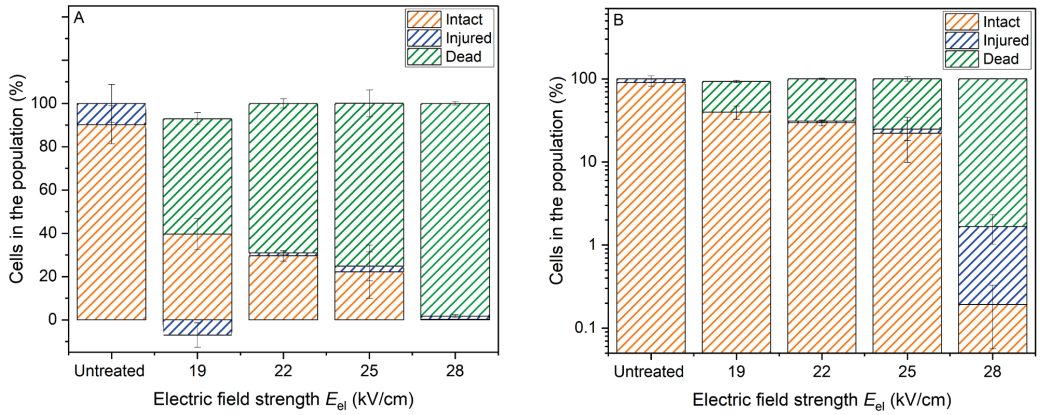

Figure A.6.3: Cell injury level investigation showing the relative percentage of intact (orange), injured (blue) and dead (green) cells, in linear (A) and log (B) scales. Data are presented as averages of three individual measurements (n = 3) ± SD.

Table A.6.1: Microbial cell count on PCA and PCA + 6% (w/v) NaCl, and percentage of each subpopulation (intact, injured and dead cells). Values are presented as averages (n = 3) ± SD

PEF treatment	Selective plating				
	Count on PCA (CFU/mL)	Count on PCA + 6% (w/v) NaCl (CFU/mL)	Intact cells (%)	Injured cells (%)	Dead cells (%)
Untreated	7.6 ± 0.1	7.6 ± 0.1	90.1 ± 8.8	9.9 ± 8.8	0.0 ± 0.0
19 kV/cm	7.2 ± 0.0	7.3 ± 0.0	46.1 ± 8.4	Not consistent	62.1 ± 3.3
22 kV/cm	7.1 ± 0.0	7.1 ± 0.1	29.6 ± 2.5	1.4 ± 0.7	69.1 ± 2.1
25 kV/cm	7.0 ± 0.1	6.9 ± 0.2	22.2 ± 12.3	2.6 ± 6.6	75.3 ± 6.2
28 kV/cm	5.8 ± 0.2	4.8 ± 0.4	0.2 ± 0.1	1.5 ± 0.6	98.3 ± 0.8

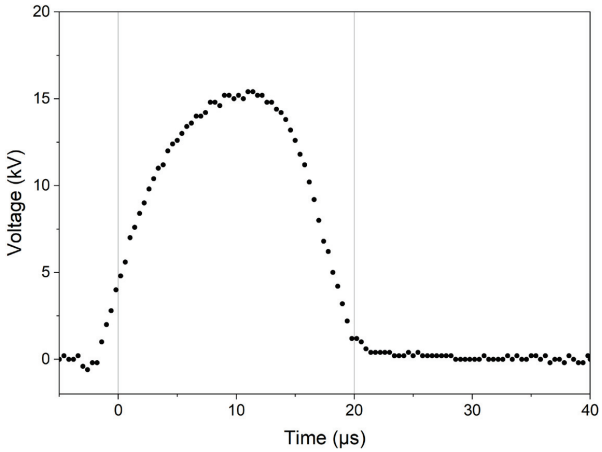

Figure A.6.4: Monitoring of the pulse shape during PEF treatment at output voltage 90%, f = 50 Hz, τ = 20 µs on the PPE substrate (5 g/100 g, 4 mS/cm, pH 5.9).

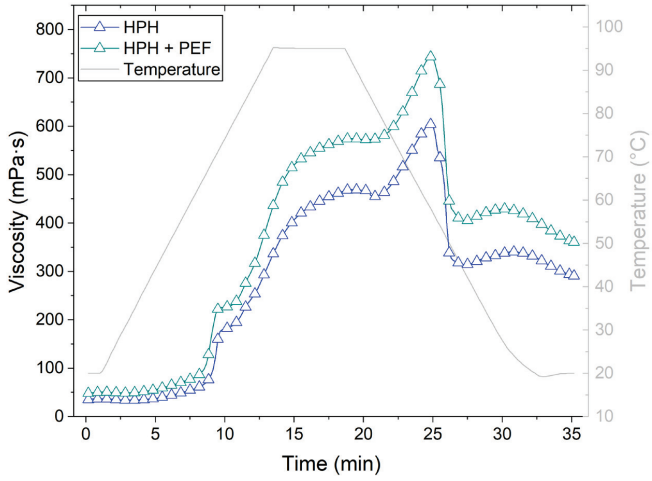

Figure A.6.5: *T*-sweep viscosity curves of HPH-treated *Cv* suspension (150 MPa, one pass and T_{in} 5 °C) before and after PEF (90% voltage, 100 Hz, 20 µs, T_{in} 30°C, 0.7 mS/cm) (n = 2). To increase the mass concentration to 14% DM for *T*-sweep, isoelectric precipitation (pH adjusted to 4.5 with HCl 1 M) and centrifugation (6'000 x g, 10 min, 4 °C) were applied to the samples. The full grey line indicates the temperature profile.

References

Aganovic, K., Smetana, S., Grauwet, T., Toepfl, S., Mathys, A., Van Loey, A., & Heinz, V. (2017). Pilot scale thermal and alternative pasteurization of tomato and watermelon juice: an energy comparison and life cycle assessment. *Journal of Cleaner Production, 141*, 514–525. https://doi.org/10.1016/j.jclepro.2016.09.015

Agyemang, P., Kwofie, E. M., & Baum, J. I. (2022). Transitioning to sustainable healthy diets: a model-based and conceptual system thinking approach to optimized sustainable diet concepts in the United States. *Frontiers in Nutrition, 9*, 874721. https://doi.org/10.3389/fnut.2022.874721

Ahmed, J., & Kumar, V. (2022). Effect of high-pressure treatment on oscillatory rheology, particle size distribution and microstructure of microalgae *Chlorella vulgaris* and *Arthospira platensis*. *Algal Research*, *62,* 102617. https://doi.org/10.1016/j.algal.2021.102617

Ali, M., Liao, L., Zeng, X. A., Manzoor, M. F., & Mazahir, M. (2024). Impact of sustainable emerging pulsed electric field processing on textural properties of food products and their mechanisms: an updated review. *Journal of Agriculture and Food Research*, *15*, 101076. https://doi.org/10.1016/j.jafr.2024.101076

Alirezalu, K., Munekata, P. E. S., Parniakov, O., Barba, F. J., Witt, J., Toepfl, S., Wiktor, A., & Lorenzo, J. M. (2020). Pulsed electric field and mild heating for milk processing: a review on recent advances. *Journal of the Science of Food and Agriculture, 100*(1), 16–24. https://doi.org/10.1002/jsfa.9942

Alzahrani, M., Silva, F. V. M., & Alkhafaji, S. (2022). Non-thermal processing of a protein functional beverage using pulsed electric fields: *Escherichia coli* inactivation and effect on proteins. *Beverages*, *8*(4), 68. https://doi.org/10.3390/beverages8040068

Arnal, Á. J., Royo, P., Pataro, G., Ferrari, G., Ferreira, V. J., López-Sabirón, A. M., & Ferreira, G. A. (2018). Implementation of PEF treatment at real-scale tomatoes processing considering LCA methodology as an innovation strategy in the agri-food sector. *Sustainability*, *10*(4), 979. https://doi.org/10.3390/su10040979

Aronsson, K., Borch, E., Stenlöf, B., & Rönner, U. (2004). Growth of pulsed electric field exposed *Escherichia coli* in relation to inactivation and environmental factors.

International Journal of Food Microbiology, *93*(1), 1–10. https://doi.org/10.1016/S0168-1605(03)00071-0

Arshad, R. N., Abdul-Malek, Z., Roobab, U., Munir, M. A., Naderipour, A., Qureshi, M. I., El-Din Bekhit, A., Liu, Z. W., & Aadil, R. M. (2021). Pulsed electric field: a potential alternative towards a sustainable food processing. *Trends in Food Science and Technology*, *111*, 43–54. https://doi.org/10.1016/j.tifs.2021.02.041

Avelar, Z., Saraiva, J. A., Vicente, A. A., & Rodrigues, R. M. (2024). Unravelling the impact of ohmic heating on commercial pea protein structure. *Food Hydrocolloids*, *150,* 109748. https://doi.org/10.1016/j.foodhyd.2024.109748

Axelrod, R., Beyrer, M., & Mathys, A. (2022). Impact of the electric field intensity and treatment time on whey protein aggregate formation. *Journal of Dairy Science, 105*(*8*), 6589–6600. https://doi.org/10.3168/jds.2021-21395

Barka, A., & Blecker, C. (2016). Microalgae as a potential source of single-cell proteins. A review. *Biotechnology, Agronomy, Society and Environment, 20*(3), 427–436, https://doi.org/10.25518/1780-4507.13132

Batista, A. P., Nunes, M. C., Raymundo, A., Gouveia, L., Sousa, I., Cordobés, F., Guerrero, A., & Franco, J. M. (2011). Microalgae biomass interaction in biopolymer gelled systems. *Food Hydrocolloids, 25*(4), 817–825. https://doi.org/10.1016/j.foodhyd.2010.09.018

Becker, E. W. (2007). Micro-algae as a source of protein. *Biotechnology Advances, 25*(2), 207–210). https://doi.org/10.1016/j.biotechadv.2006.11.002

Berardy, A., Costello, C., & Seager, T. (2015). Life cycle assessment of soy protein isolate. *International Symposium on Sustainable Systems and Technologies (ISSST)*, *3*, 13. http://dx.doi.org/10.6084/m9.figshare.1517821

Bernaerts, T. M. M., Panozzo, A., Doumen, V., Foubert, I., Gheysen, L., Goiris, K., Moldenaers, P., Hendrickx, M. E., & Van Loey, A. M. (2017). Microalgal biomass as a (multi)functional ingredient in food products: rheological properties of microalgal suspensions as affected by mechanical and thermal processing. *Algal Research*, *25*, 452–463. https://doi.org/10.1016/j.algal.2017.05.014

Bernaerts, T. M. M., Panozzo, A., Verhaegen, K. A. F., Gheysen, L., Foubert, I., Moldenaers, P., Hendrickx, M. E., & Van Loey, A. M. (2018). Impact of different sequences of mechanical and thermal processing on the rheological properties of *Porphyridium cruentum* and *Chlorella vulgaris* as functional food ingredients. *Food and Function, 9*(4), 2433–2446. https://doi.org/10.1039/c8fo00261d

Bermúdez-Aguirre, D. (2018). Technological hurdles and research pathways on emerging technologies for food preservation. In Barba, F. J., Sant'Ana, A. S., Orlien, V., & Koubaa, M. *Innovative technologies for food preservation* (pp. 277–303). *Academic, London.* https://doi.org/10.1016/B978-0-12-811031-7.00009-1

Beyrer, M., Cachelin, C., & Rapillard L. (2020). Nozzle for extruding a material rich in protein and water, as well as an extrusion machine comprising such a nozzle. Patent n°WO2022018084A1.

Bito, T., Okumura, E., Fujishima, M., & Watanabe, F. (2020). Potential of *Chlorella* as a dietary supplement to promote human health. *Nutrients, 12*(9), 1–21. https://doi.org/10.3390/nu12092524

Cai, Y., Liu, Y., Liu, T., Gao, K., Zhang, Q., Cao, L., Wang, Y., Wu, X., Zheng, H., Peng, H., & Ruan, R. (2021). Heterotrophic cultivation of *Chlorella vulgaris* using broken rice hydrolysate as carbon source for biomass and pigment production. *Bioresource Technology*, *323*, 124607. https://doi.org/10.1016/j.biortech.2020.124607

Cal-Sabater, P., Caro, I., Castro, M. J., Cao, M. J., Mateo, J., & Quinto, E. J. (2019). Flow cytometry to assess the counts and physiological state of *Cronobacter sakazakii* cells after heat exposure. *Foods*, *8*(12), 688. https://doi.org/10.3390/foods8120688

Campos-Vega, R., Loarca-Piña, G., & Oomah, B. D. (2010). Minor components of pulses and their potential impact on human health. *Food Research International*, *43*(2), 461–482. https://doi.org/10.1016/j.foodres.2009.09.004

Canelli, G., Neutsch, L., Carpine, R., Tevere, S., Giuffrida, F., Rohfritsch, Z., Dionisi, F., Bolten, C. J., Mathys, A. (2020a). *Chlorella vulgaris* in a heterotrophic bioprocess: study of the lipid bioaccessibility and oxidative stability. *Algal Research, 45,* 101754. https://doi.org/10.1016/j.algal.2019.101754

Canelli, G., Tarnutzer, C., Carpine, R., Neutsch, L., Bolten, C. J., Dionisi, F., Mathys, A. (2020b). Biochemical and nutritional evaluation of *Chlorella* and *Auxenochlorella*

biomasses relevant for food application. *Frontiers in Nutrition, 7*, 1–9. https://doi.org/10.3389/fnut.2020.565996

Caporgno, M. P., & Mathys, A. (2018). Trends in microalgae incorporation into innovative food products with potential health benefits. *Frontiers in Nutrition, 5*(58). https://doi.org/10.3389/fnut.2018.00058

Caporgno, M. P., Haberkorn, I., Böcker, L., & Mathys, A. (2019). Cultivation of *Chlorella protothecoides* under different growth modes and its utilization in oil/water emulsions. *Bioresource Technology*, *288*, 121476. https://doi.org/10.1016/j.biortech.2019.121476

Carullo, D., Abera, B. D., Casazza, A. A., Donsì, F., Perego, P., Ferrari, G., & Pataro, G. (2018). Effect of pulsed electric fields and high-pressure homogenization on the aqueous extraction of intracellular compounds from the microalgae *Chlorella vulgaris*. *Algal Research, 31*, 60–69. https://doi.org/10.1016/j.algal.2018.01.017

Cavalcanti, R. N., Balthazar, C. F., Margalho, L. P., Freitas, M. Q., Sant'Ana, A. S., & Cruz, A. G. (2023). Pulsed electric field-based technology for microbial inactivation in milk and dairy products. *Current Opinion in Food Science*, *54*, 101087. https://doi.org/10.1016/j.cofs.2023.101087

Cebrián, G., Raso, J., Condón, S., & Mañas, P. (2012). Acquisition of pulsed electric fields resistance in *Staphylococcus aureus* after exposure to heat and alkaline shocks. *Food Control,* 25(1), 407–414. https://doi.org/10.1016/j.foodcont.2011.10.048

Cebrián, G., Mañas, P., & Condón, S. (2016). Comparative resistance of bacterial foodborne pathogens to non-thermal technologies for food preservation. *Frontiers in Microbiology, 7*, 734. https://doi.org/10.3389/fmicb.2016.00734

Chartrel, V., Dugat-Bony, E., Sarthou, A. S., Huchette, S., Bonnarme, P., & Irlinger, F. (2021). The microbial community associated with pea seeds (*Pisum sativum*) of different geographical origins. *Plant and Soil*, *462*(1–2), 405–427. https://doi.org/10.1007/s11104-021-04856-6

Chegukrishnamurthi, M., Shahabazuddin, M., Sreevathsan, S., Sarada, R., & Mudliar, S. N. (2020). Ozonation as non-thermal option for bacterial load reduction of *Chlorella* biomass cultivated in airlift photobioreactor. *Journal of Cleaner Production*, *276*, 123029. https://doi.org/10.1016/j.jclepro.2020.123029

Chen, C., Chaudhary, A., & Mathys, A. (2019). Dietary change scenarios and implications for environmental, nutrition, human health and economic dimensions of food sustainability. *Nutrients, 11*(4), 1–21. https://doi.org/10.3390/nu11040856

Chen, C., Chaudhary, A., & Mathys, A. (2022a). Dietary change and global sustainable development goals. *Frontiers in Sustainable Food Systems*, *6*, 1–22. https://doi.org/10.3389/fsufs.2022.771041

Chen, Y., Wang, T., Zhang, Y., Yang, X., Du, J., Yu, D., & Xie, F. (2022b). Effect of moderate electric fields on the structural and gelation properties of pea protein isolate. *Innovative Food Science and Emerging Technologies*, *77,* 102959. https://doi.org/10.1016/j.ifset.2022.102959

Cornet, S. H. V., Snel, S. J. E., Schreuders, F. K. G., Van der Sman, R. G. M., Beyrer, M., & Van der Goot, A. J. (2021). Thermo-mechanical processing of plant proteins using shear cell and high-moisture extrusion cooking. *Critical Reviews in Food Science and Nutrition*, *62*(12), 3264–3280. https://doi.org/10.1080/10408398.2020.1864618

Coster H. G. L. & Zimmermann U. (1975). The mechanism of electrical breakdown in the membranes of *Valonia utricularis*. *The Journal of Membrane Biology, 22*(1), 73–90. https://doi.org/10.1007/BF01868164

D'Alessio, G., Flamminii, F., Faieta, M., Prete, R., Di Michele, A., Pittia, P., & Di Mattia, C. D. (2023). High pressure homogenization to boost the technological functionality of native pea proteins. *Current Research in Food Science*, *6,* 100499. https://doi.org/10.1016/j.crfs.2023.100499

De Gol, C., Snel, S., Rodriguez, Y., & Beyrer, M. (2023). Gelling capacity of cell-disrupted *Chlorella vulgaris* and its texture effect in extruded meat substitutes. *Food Structure*, *37,* 100332. https://doi.org/10.1016/j.foostr.2023.100332

De Gol, C., Moodycliffe, A., Den Besten, H. M. W., Zwietering, M. H., & Beyrer, M. (2024a). Pulsed electric field treatment for preservation of *Chlorella* suspensions and retention of gelling capacity. *Food Research International*, *182,* 114154. https://doi.org/10.1016/j.foodres.2024.114154

De Gol, C., Etschmann, N., Zwietering, M. H., Den Besten, H. M. W., & Beyrer, M. (2024b). Pulsed electric field combined with preheating to preserve mildly extracted pea protein.

LWT – Food Science and Technology, *214,* 117100. https://doi.org/10.1016/j.lwt.2024.117100

Dekkers, B. L., Boom, R. M., & Van der Goot, A. J. (2018). Structuring processes for meat analogues. *Trends in Food Science and Technology, 81,* 25–36. https://doi.org/10.1016/j.tifs.2018.08.011

Delso, C., Martinez, J. M., Cebrián, G., Condón, S., Raso, J., & Alvarez, I. (2022). Microbial inactivation by pulsed electric fields. In Raso, J., Heinz, V., Alvarez, I., & Toepfl, S. (2nd ed.). *Pulsed Electric Fields Technology for the Food Industry* (pp. 169–207). *Food Engineering Series*. https://doi.org/10.1007/978-3-030-70586-2_5

Demarco, M., Oliveira de Moraes, J., Matos, Â. P., Derner, R. B., de Farias Neves, F., & Tribuzi, G. (2022). Digestibility, bioaccessibility and bioactivity of compounds from algae. *Trends in Food Science and Technology, 121,* 114–128. https://doi.org/10.1016/j.tifs.2022.02.004

Durmaz, U., Ozdemir, M., & Pehlivan, H. (2018). An experimental investigation into heat transfer in milk cooling vessels. *Scientia Iranica*, *25*(3), 1258–1265. https://doi.org/10.24200/sci.2017.4336

Dziadek, K., Kopeć, A., Dróżdż, T., Kiełbasa, P., Ostafin, M., Bulski, K., & Oziembłowski, M. (2019). Effect of pulsed electric field treatment on shelf life and nutritional value of apple juice. *Journal of Food Science and Technology*, *56*(3), 1184–1191. https://doi.org/10.1007/s13197-019-03581-4

Dziuba, J., Szerszunowicz, I., Nałęcz, D., & Dziuba, M. (2014). Proteomic analysis of albumin and globulin fractions of pea (*Pisum sativum L.*) seeds. *Acta Scientiarum Polonorum, 13*(2), 181–190. https://doi.org/10.17306/J.AFS.2014.2.7

Elez-Martínez, P., Odriozola-Serrano, I., Oms-Oliu, G., Soliva-Fortuny, R., & Martín-Belloso, O. (2017). Effects of pulsed electric fields processing strategies on health-related compounds of plant-based foods. *Food Engineering Reviews*, *9*(3), 213-225. https://doi.org/10.1007/s12393-017-9162-x

Emanuel, E., Dubrovin, I., Pogreb, R., Pinhasi, G. A., & Cahan, R. (2021). Resuscitation of pulsed electric field-treated *Staphylococcus aureus* and *Pseudomonas putida* in a rich nutrient medium. *Foods*, *10*(3), 660. https://doi.org/10.3390/foods10030660

European commission (EC), Directorate-General for Agriculture and Rural Development, Agrosynergie, COGEA, & Oréade-Brèche (2019). Market developments and policy evaluation aspects of the plant protein sector in the EU. https://data.europa.eu/doi/10.2762/022741

European Commission (EC), Joint Research Centre, Crippa, M., Guizzardi, D., Pagani, F., Banja, M., Muntean, M., Schaaf, E., Monforti-Ferrario, F., Becker, W.E., Quadrelli, R., Risquez Martin, A., Taghavi-Moharamli, P., Köykkä, J., Grassi, G., Rossi, S., Melo, J., Oom, D., Branco, A., San-Miguel, J., Manca, G., Pisoni, E., Vignati, E. and Pekar, F. (2024). GHG emissions of all world countries. https://data.europa.eu/doi/10.2760/4002897, JRC138862.

Fernández, A., Cebrián, G., Álvarez-Ordóñez, A., Prieto, M., Bernardo, A., & López, M. (2018). Influence of acid and low-temperature adaptation on pulsed electric fields resistance of *Enterococcus faecium* in media of different pH. *Innovative Food Science & Emerging Technologies, 45*, 382–389. https://doi.org/10.1016/j.ifset.2017.12.001

Flisar, K., Meglic, S. H., Morelj, J., Golob, J., & Miklavcic, D. (2014). Testing a prototype pulse generator for a continuous flow system and its use for *E. coli* inactivation and microalgae lipid extraction. *Bioelectrochemistry*, *100*, 44–51. https://doi.org/10.1016/j.bioelechem.2014.03.008

Food and Agriculture Organization of the United Nations (FAO). (2024a). Per capita meat consumption by type, 2022 [dataset]. *Our World in Data*. https://ourworldindata.org/grapher/per-capita-meat-consumption-by-type-kilograms-per-year?tab=table2022

Food and Agriculture Organization of the United Nations (FAO). (2024b). Daily protein supply from animal and plant-based foods, 2022 [dataset]. *Our World in Data*. https://ourworldindata.org/grapher/daily-protein-supply-from-animal-and-plant-based-foods

Frey, J. (2013). *Classification of Organisms. Bacteria, viruses, parasites, fungi*. Federal Office for the Environment FOEN/FOPH. Bern

Fu, Y., Chen, T., Chen, S. H. Y., Liu, B., Sun, P., Sun, H., & Chen, F. (2021). The potentials and challenges of using microalgae as an ingredient to produce meat analogues.

Trends in Food Science and Technology, *112*, 188–200. https://doi.org/10.1016/j.tifs.2021.03.050

Funami, T., & Nakauma, M. (2022). Instrumental food texture evaluation in relation to human perception. *Food Hydrocolloids*, *124*, 107253. https://doi.org/10.1016/j.foodhyd.2021.107253

García, D., Gómez, N., Raso, J., & Pagán, R. (2005). Bacterial resistance after pulsed electric fields depending on the treatment medium pH. *Innovative Food Science and Emerging Technologies*, *6*(4), 388–395. https://doi.org/10.1016/j.ifset.2005.04.003

García, D., Mañas, P., Gómez, N., Raso, J., & Pagán, R. (2006). Biosynthetic requirements for the repair of sublethal membrane damage in *Escherichia coli* cells after pulsed electric fields. *Journal of Applied Microbiology*, *100*(3), 428–435. https://doi.org/10.1111/j.1365-2672.2005.02795.x

García, D., Gómez, N., Mañas, P., Raso, J., & Pagán, R. (2007). Pulsed electric fields cause bacterial envelopes permeabilization depending on the treatment intensity, the treatment medium pH and the microorganism investigated. *International Journal of Food Microbiology, 113*(2), 219–227. https://doi.org/10.1016/j.ijfoodmicro.2006.07.007

Garner, A. L. (2019). Pulsed electric field inactivation of microorganisms: from fundamental biophysics to synergistic treatments. *Applied Microbiology and Biotechnology*, *103*(19), 7917–7929. https://doi.org/10.1007/s00253-019-10067-y

Garre, A., Koomen, J., Den Besten, H. M. W., & Zwietering, M. H. (2023). Modelling population growth in R with the biogrowth package. *Journal of Statistical Software*, *107*(1), 1–51. https://doi.org/10.18637/jss.v107.i01

Geerts, M. E. J., Nikiforidis, C. V., Van der Goot, A. J., & Van der Padt, A. (2017). Protein nativity explains emulsifying properties of aqueous extracted protein components from yellow pea. *Food Structure*, *14*, 104–111. https://doi.org/10.1016/j.foostr.2017.09.001

Georget, E., Sauvageat, J. L., Burbidge, A., & Mathys, A. (2013). Residence time distributions in a modular micro reaction system. *Journal of Food Engineering*, *116*(4), 910–919. https://doi.org/10.1016/j.jfoodeng.2013.01.041

Giteru, S. G., Oey, I., & Ali, M. A. (2018). Feasibility of using pulsed electric fields to modify biomacromolecules: a review. *Trends in Food Science and Technology*, *72*, 91–113. https://doi.org/10.1016/j.tifs.2017.12.009

Godebo, A. T., Germida, J. J., & Walley, F. L. (2020). Isolation, identification, and assessment of soil bacteria as biocontrol agents of pea root rot caused by *Aphanomyces euteiches*. *Canadian Journal of Soil Science*, *100*(3), 206–216. https://doi.org/10.1139/cjss-2019-0133

Gräfenhahn, M., & Beyrer, M. (2024). Plant-based meat analogues in the human diet: what are the hazards? *Foods*, *13*(10), 1541. https://doi.org/10.3390/foods13101541

Grahl, S., Palanisamy, M., Strack, M., Meier-Dinkel, L., Toepfl, S., & Mörlein, D. (2018). Towards more sustainable meat alternatives: how technical parameters affect the sensory properties of extrusion products derived from soy and algae. *Journal of Cleaner Production, 198*, 962–971. https://doi.org/10.1016/j.jclepro.2018.07.041

Grossmann, L., Hinrichs, J., & Weiss, J. (2020). Cultivation and downstream processing of microalgae and cyanobacteria to generate protein-based technofunctional food ingredients. *Critical Reviews in Food Science and Nutrition, 60*(17), 2961–2989. https://doi.org/10.1080/10408398.2019.1672137

Guan, T., Sägesser, C., Villiger, R., Zychowski, L., Kohlbrecher, J., Dumpler, J., Mathys, A., Rühs, P., Fischer, P., & Matsarskaia, O. (2024). In situ studies of plant-based meat analog texturization. *Food Hydrocolloids*, *155,* 110215. https://doi.org/10.1016/j.foodhyd.2024.110215

Guo, L., Nie, X. M., Yang, Y. H., Ren, Y., Ding, X., & Qian, J. Y. (2023). Using electric field to modify wet gluten as meat analogue material: a comparative study between pulsed and direct current electric fields. *Innovative Food Science and Emerging Technologies*, *84,* 103300. https://doi.org/10.1016/j.ifset.2023.103300

Guo, L., Wang, X., Ren, Y., Zhang, X., Li, Q., Zhang, C., & Qian, J. Y. (2024). Outcomes of structure, function and flavor of pea protein isolate treated by AC, DC and pulsed electric fields. *Food Research International*, *176,* 113817. https://doi.org/10.1016/j.foodres.2023.113817

Hall, C., Hillen, C., & Robinson, J. G. (2017). Composition, nutritional value, and health benefits of pulses. *Cereal Chemistry, 94*(1), 11–31. https://doi.org/10.1094/CCHEM-03-16-0069-FI

Han, Z., Cai, M. J., Cheng, J. H., & Sun, D. W. (2018). Effects of electric fields and electromagnetic wave on food protein structure and functionality: a review. *Trends in Food Science and Technology*, *75*, 1–9. https://doi.org/10.1016/j.tifs.2018.02.017

He, J., Evans, N. M., Liu, H., & Shao, S. (2020). A review of research on plant-based meat alternatives: driving forces, history, manufacturing, and consumer attitudes. *Comprehensive Reviews in Food Science and Food Safety*, *19*(5), 2639–2656. https://doi.org/10.1111/1541-4337.12610

Higgins, T. J. V, Chandler, P. M., Randall, P. J., Spencer, D., Beach, L. R., Blagroves, R. J., Kortt, A. A., & Inglis, A. S. (1986). Gene structure, protein structure, and regulation of the synthesis of a sulfur-rich protein in pea seeds. *The Journal of Biological Chemistry, 261*(24), 11124–11130. https://doi.org/10.1016/S0021-9258(18)67357-0

Horlacher, N., Oey, I., & Leong, S. Y. (2024). Effect of pulsed electric field processing on microbial and enzyme inactivation in blended plant-based milk alternatives: a case study on a microbial challenge test for a non-presterilized oat-based beverage enriched with pea protein. *Innovative Food Science and Emerging Technologies*, *94,* 103699. https://doi.org/10.1016/j.ifset.2024.103699

Hou, F., Ding, W., Qu, W., Oladejo, A. O., Xiong, F., Zhang, W., He, R., & Ma, H. (2017). Alkali solution extraction of rice residue protein isolates: influence of alkali concentration on protein functional, structural properties and lysinoalanine formation. *Food Chemistry*, *218*, 207–215. https://doi.org/10.1016/j.foodchem.2016.09.064

Hülsheger H, Potel J, Niemann E. G. (1981). Killing of bacteria with electric pulses of high field strength. *Radiation and Environmental Biophysics*, *20*(1), 53–65. https://doi.org/10.1007/BF01323926

Imai, K., Nemoto, R., Kodana, M., Tarumoto, N., Sakai, J., Kawamura, T., Ikebuchi, K., Mitsutake, K., Murakami, T., Maesaki, S., Fujiwara, T., Hayakawa, S., Hoshino, T., Seki, M., & Maeda, T. (2020). Rapid and accurate species identification of mitis group streptococci using the MinION nanopore sequencer. *Frontiers in Cellular and Infection Microbiology*, *10,* 11. https://doi.org/10.3389/fcimb.2020.00011

Imamoglu, E. (2015). Simulation design for microalgal protein optimization. *Bioengineered, 6*(6), 342–346. https://doi.org/10.1080/21655979.2015.1098792

Intergovernmental Panel on Climate Change (IPCC), (2023). Summary for Policymakers. In Lee, H., & Romero, J. *Climate Change 2023: Synthesis Report. Contribution of Working Groups I, II and III to the Sixth Assessment Report of the Intergovernmental Panel on Climate Change* (pp. 1-34). https://doi.org/10.59327/IPCC/AR6-9789291691647.001

Jadhav, H. B., Annapure, U. S., & Deshmukh, R. R. (2021). Non-thermal technologies for food processing. *Frontiers in Nutrition, 8*, 657090. https://doi.org/10.3389/fnut.2021.657090

Jay, J. M. (1992). *Modern Food Microbiology* (4th ed.). Chapman & Hall (pp. 455–478). Van Nostrand Reinhold

Jaeger, H., Meneses, N., & Knorr, D. (2009a). Impact of PEF treatment inhomogeneity such as electric field distribution, flow characteristics and temperature effects on the inactivation of *E. coli* and milk alkaline phosphatase. *Innovative Food Science and Emerging Technologies*, *10*(4), 470–480. https://doi.org/10.1016/j.ifset.2009.03.001

Jaeger, H., Schulz, A., Karapetkov, N., & Knorr, D. (2009b). Protective effect of milk constituents and sublethal injuries limiting process effectiveness during PEF inactivation of *Lb. rhamnosus*. *International Journal of Food Microbiology*, *134*(1–2), 154–161. https://doi.org/10.1016/j.ijfoodmicro.2009.06.007

Jaeger, H., Fauster, T., & Schottroff, F. (2022). Pulsed electric field process performance analysis. In Raso, J., Heinz, V., Alvarez, I., & Toepfl, S. (2nd ed.). *Pulsed Electric Fields Technology for the Food Industry* (pp. 469–488). *Food Engineering Series.* https://doi.org/10.1007/978-3-030-70586-2_16

Kandušer, M., Šentjurc, M., & Miklavčič, D. (2008). The temperature effect during pulse application on cell membrane fluidity and permeabilization. *Bioelectrochemistry*, *74*(1), 52–57. https://doi.org/10.1016/j.bioelechem.2008.04.012

Kessler, H. G. (2002). *Food and bioprocess engineering*. Dairy technology, (pp. 645–646). Verlag A

Khan, A. U. M., Torelli, A., Wolf, I., & Gretz, N. (2018). AutoCellSeg: robust automatic colony forming unit (CFU)/cell analysis using adaptive image segmentation and easy-to-use post-editing techniques. *Scientific Reports*, *8*(1), 7302. https://doi.org/10.1038/s41598-018-24916-9

Kogar, N. M., Scott, P. P., & Bess, A. (2024). Key findings and opportunities: comparative life cycle assessment of plant- and animal-based meats. *The Good Food Institute* https://doi.org/10.62468/yieg1161

Kornet, C., Venema, P., Nijsse, J., Van der Linden, E., Van der Goot, A. J., & Meinders, M. (2020). Yellow pea aqueous fractionation increases the specific volume fraction and viscosity of its dispersions. *Food Hydrocolloids*, *99,* 105332. https://doi.org/10.1016/j.foodhyd.2019.105332

Kornet, R., Veenemans, J., Venema, P., Van der Goot, A. J., Meinders, M., Sagis, L., & Van der Linden, E. (2021a). Less is more: limited fractionation yields stronger gels for pea proteins. *Food Hydrocolloids*, *112,* 106285. https://doi.org/10.1016/j.foodhyd.2020.106285

Kornet, R., Penris, S., Venema, P., Van der Goot, A. J., Meinders, M. B. J., & Van der Linden, E. (2021b). How pea fractions with different protein composition and purity can substitute WPI in heat-set gels. *Food Hydrocolloids*, *120,* 106891. https://doi.org/10.1016/j.foodhyd.2021.106891

Kornet, R., Yang, J., Venema, P., Van der Linden, E., & Sagis, L. M. C. (2022). Optimizing pea protein fractionation to yield protein fractions with a high foaming and emulsifying capacity. *Food Hydrocolloids*, *126,* 107456. https://doi.org/10.1016/j.foodhyd.2021.107456

Kuang, J., Hamon, P., Lechevalier, V., & Saurel, R. (2023). Thermal behavior of pea and egg white protein mixtures. *Foods*, *12*(13), 2528. https://doi.org/10.3390/foods12132528

Kusmayadi, A., Leong, Y. K., Yen, H. W., Huang, C. Y., Chang, J. S. (2021). Microalgae as sustainable food and feed sources for animals and humans – biotechnological and environmental aspects. *Chemosphere, 271*. 129800. https://doi.org/10.1016/j.chemosphere.2021.129800

Kyrylenko, A., Eijlander, R. T., Alliney, G., Van de Bos, E. L., & Wells-Bennik, M. H. J. (2023). Levels and types of microbial contaminants in different plant-based ingredients used

in dairy alternatives. *International Journal of Food Microbiology*, *407*, 110392. https://doi.org/10.1016/j.ijfoodmicro.2023.110392

Lafarga, T. (2019). Effect of microalgal biomass incorporation into foods: nutritional and sensorial attributes of the end products. *Algal Research, 41*, 101566. https://doi.org/10.1016/j.algal.2019.101566

Li, C., & Ganjyal, G. M. (2017). Chemical composition, pasting, and thermal properties of 22 different varieties of peas and lentils. *Cereal Chemistry*, *94*(3), 392–399. https://doi.org/10.1094/CCHEM-04-16-0080-R

Li, R., Kirkensgaard, J. J. K., & Corredig, M. (2024). Structural evolution of pea-derived albumins during pH and heat treatment studied with light and X-ray scattering. *Food Research International*, *186,* 114380. https://doi.org/10.1016/j.foodres.2024.114380

Li, Y.-Q. (2012). Structure changes of soybean protein isolates by pulsed electric fields. *Physics Procedia*, *33*, 132–137. https://doi.org/10.1016/j.phpro.2012.05.040

Li, Z., Yang, Q., Du, H., & Wu, W. (2023). Advances of pulsed electric field for foodborne pathogen sterilization. *Food Reviews International, 39*(7), 3603-3619. https://doi.org/10.1080/87559129.2021.2012798

Lie-Piang, A., Braconi, N., Boom, R. M., & Van der Padt, A. (2021). Less refined ingredients have lower environmental impact – a life cycle assessment of protein-rich ingredients from oil- and starch-bearing crops. *Journal of Cleaner Production*, *292,* 126046. https://doi.org/10.1016/j.jclepro.2021.126046

Liu, Y. Y., Zeng, X. A., Deng, Z., Yu, S. J., & Yamasaki, S. (2011). Effect of pulsed electric field on the secondary structure and thermal properties of soy protein isolate. *European Food Research and Technology*, *233*(5), 841–850. https://doi.org/10.1007/s00217-011-1580-z

Liu, Y. Y., Zhang, Y., Zeng, X. A., El-Mashad, H., Pan, Z. L., & Wang, Q. J. (2013). Effect of pulsed electric field on microstructure of some amino acid group of soy protein isolates. *International Journal of Food Engineering*, *10*(1), 113–120. https://doi.org/10.1515/ijfe-2013-0033

Löffler, M. J. (2022). Generation and application of high intensity pulsed electric fields. In Raso, J., Heinz, V., Alvarez, I., & Toepfl, S. (2nd ed.). *Pulsed Electric Fields Technology*

for the Food Industry (pp. 55–106). *Food Engineering Series*. https://doi.org/10.1007/978-3-030-70586-2_2

Lu, Z. X., He, J. F., Zhang, Y. C., & Bing, D. J. (2020). Composition, physicochemical properties of pea protein and its application in functional foods. *Critical Reviews in Food Science and Nutrition*, *60*(15), 2593–2605. https://doi.org/10.1080/10408398.2019.1651248

Lucić, R., Raposo, M., Chervinska, A., Domingos, T., & Teixeira, R. F. M. (2025). Global greenhouse gas emissions and land use impacts of soybean production: systematic review and analysis. *Sustainability*, *17*(8), 3396. https://doi.org/10.3390/su17083396

Ma, Z., Boye, J. I., & Hu, X. (2017). In vitro digestibility, protein composition and techno-functional properties of Saskatchewan grown yellow field peas (*Pisum sativum L.*) as affected by processing. *Food Research International*, *92*, 64–78. https://doi.org/10.1016/j.foodres.2016.12.012

Magpusao, J., Giteru, S., Oey, I., & Kebede, B. (2021). Effect of high-pressure homogenization on microstructural and rheological properties of *A. platensis, Isochrysis*, *Nannochloropsis* and *Tetraselmis* species. *Algal Research, 56*, 102327. https://doi.org/10.1016/j.algal.2021.102327

Malik, M. A., Sheikh, M. A., & Mir, N. A. (2024). A review on pulsed electric field modification of proteins: effect on the functional and structural properties. *Food Bioscience, 61*(1), 104636. https://doi.org/10.1016/j.fbio.2024.104636

Marcos-Fernández, R., Sánchez, B., Ruiz, L., & Margolles, A. (2022). Convergence of flow cytometry and bacteriology. Current and future applications: a focus on food and clinical microbiology. *Critical Reviews in Microbiology*, *49*(5), 556–577. https://doi.org/10.1080/1040841X.2022.2086035

Martin-Belloso, O., Soliva-Fortuny, R., & Morales-de la Pena, M. (2022). Effect of pulsed electric fields on food quality. In Raso, J., Heinz, V., Alvarez, I., & Toepfl, S. (2nd ed.). *Pulsed Electric Fields Technology for the Food Industry* (pp. 271–298). *Food Engineering Series*, https://doi.org/10.1007/978-3-030-70586-2_7

Masood, H., Trujillo, F. J., Knoerzer, K., & Juliano, P. (2018). Designing, modeling, and optimizing processes to ensure microbial safety and stability through emerging technologies. In Barba, F. J., Sant'Ana, A. S., Orlien, V., & Koubaa, M. Innovative

technologies for food preservation, (pp. 187–229), Academic London. http://dx.doi.org/10.1016/B978-0-12-811031-7.00006-6

Melchior, S., Calligaris, S., Bisson, G., & Manzocco, L. (2020). Understanding the impact of moderate-intensity pulsed electric fields (MIPEF) on structural and functional characteristics of pea, rice and gluten concentrates. *Food and Bioprocess Technology, 13*, 2145–2155. https://doi.org/10.1007/s11947-020-02554-2

Meneses, Y. E., Stratton, J., & Flores, R. A. (2017). Water reconditioning and reuse in the food processing industry: current situation and challenges. *Trends in Food Science and Technology*, *61*, 72–79. https://doi.org/10.1016/j.tifs.2016.12.008

Message, J. L., Sok, N., Assifaoui, A., & Saurel, R. (2013). Thermal denaturation of pea globulins (*Pisum sativum L.*) - molecular interactions leading to heat-induced protein aggregation. *Journal of Agricultural and Food Chemistry*, *61*(6), 1196–1204. https://doi.org/10.1021/jf303739n

Meulleneti, J. (1998). Relationship between sensory and instrumental texture profile attributes. *Journal of Sensory Studies, 13*(1998), 77–93. https://doi.org/10.1111/j.1745-459X.1998.tb00076.x

Mezger, T. G. (2014). The Rheology Handbook (4th ed.). Vincentz Network.

Michel, F., Hartmann, C., & Siegrist, M. (2021). Consumers' associations, perceptions and acceptance of meat and plant-based meat alternatives. *Food Quality and Preference*, *87,* 104063. https://doi.org/10.1016/j.foodqual.2020.104063

Milana, M., Van Asselt, E. D., & Van der Fels-Klerx, H. J. (2024). The chemical and microbiological safety of emerging alternative protein sources and derived analogues: a review. *Comprehensive Reviews in Food Science and Food Safety*, *23*(4), 1–24. https://doi.org/10.1111/1541-4337.13377

Millar, K. A., Gallagher, E., Burke, R., McCarthy, S., & Barry-Ryan, C. (2019). Proximate composition and anti-nutritional factors of fava-bean (*Vicia faba*), green-pea and yellow-pea (*Pisum sativum*) flour. *Journal of Food Composition and Analysis*, *82,* 103233. https://doi.org/10.1016/j.jfca.2019.103233

Miranda, C. G., Rodrigues, R. M., Pereira, R. N., Speranza, P., Kurozawa, L. E., Vicente, A. A., & Sato, A. C. K. (2023). Influence of ohmic heating on lentil protein structure and

protein-pectin interactions. *Innovative Food Science and Emerging Technologies*, *87,* 103413. https://doi.org/10.1016/j.ifset.2023.103413

Möller, A. C., Van der Padt, A., & Van der Goot, A. J. (2022). Influence of the fractionation method on the protein composition and functional properties. *Innovative Food Science and Emerging Technologies*, *81,* 103144. https://doi.org/10.1016/j.ifset.2022.103144

Nowosad, K., Sujka, M., Pankiewicz, U., & Kowalski, R. (2021). The application of PEF technology in food processing and human nutrition. *Journal of Food Science and Technology*, *58*(2), 397–411. https://doi.org/10.1007/s13197-020-04512-4

Nunes, M. C., Graça, C., Vlaisavljević, S., Tenreiro, A., Sousa, I., & Raymundo, A. (2020). Microalgal cell disruption: effect on the bioactivity and rheology of wheat bread. *Algal Research, 45,* 101749. https://doi.org/10.1016/j.algal.2019.101749

O'Kane, F. E., Happe, R. P., Vereijken, J. M., Gruppen, H., & Van Boekel, M. A. J. S. (2004). Heat-induced gelation of pea legumin: comparison with soybean glycinin. *Journal of Agricultural and Food Chemistry*, *52*(16), 5071–5078. https://doi.org/10.1021/jf035215h

Oppen, D., Grossmann, L., & Weiss, J. (2022). Insights into characterizing and producing anisotropic food structures. *Critical Reviews in Food Science and Nutrition, 64*(4), 1158–1176. https://doi.org/10.1080/10408398.2022.2113365

Osen, R., Toelstede, S., Wild, F., Eisner, P., & Schweiggert-Weisz, U. (2014). High moisture extrusion cooking of pea protein isolates: raw material characteristics, extruder responses, and texture properties. *Journal of Food Engineering*, *127*, 67–74. https://doi.org/10.1016/j.jfoodeng.2013.11.023

Osorio-Arias, J. C., Vega-Castro, O., & Martinez-Monteagudo, S. I. (2020). Fundamentals of high-pressure homogenization of foods. In Innovative Food Processing Technologies: A Comprehensive Review (pp. 244–273). Elsevier. https://doi.org/10.1016/b978-0-08-100596-5.23021-7

Palanisamy, M., Töpfl, S., Berger, R. G., & Hertel, C. (2019). Physico-chemical and nutritional properties of meat analogues based on Spirulina/lupin protein mixtures. *European Food Research and Technology, 245*(9), 1889–1898. https://doi.org/10.1007/s00217-019-03298-w

Pelgrom, P. J. M., Boom, R. M., & Schutyser, M. A. I. (2015). Functional analysis of mildly refined fractions from yellow pea. *Food Hydrocolloids*, *44*, 12–22. https://doi.org/10.1016/j.foodhyd.2014.09.001

Pereira, R. N., Rodrigues, R., Avelar, Z., Leite, A. C., Leal, R., Pereira, R. S., & Vicente, A. (2024). Electrical fields in the processing of protein-based foods. *Foods*, *13*(4), 577. https://doi.org/10.3390/foods13040577

Picart-Palmade, L., Cunault, C., Chevalier-Lucia, D., Belleville, M. P., & Marchesseau, S. (2019). Potentialities and limits of some non-thermal technologies to improve sustainability of food processing. *Frontiers in Nutrition*, *5,* 130. https://doi.org/10.3389/fnut.2018.00130

Poore, J., & Nemecek, T. (2018). Reducing food's environmental impacts through producers and consumers. *Science*, *360*(6392), 987–992. https://doi.org/10.1126/science.aaq0216

Puligundla, P., Pyun, Y. R., & Mok, C. (2018). Pulsed electric field (PEF) technology for microbial inactivation in low-alcohol red wine. *Food Science and Biotechnology*, *27*(6), 1691–1696. https://doi.org/10.1007/s10068-018-0422-1

Qiu, S., Abbaspourrad, A., & Padilla-Zakour, O. I. (2021). Changes in the glutinous rice grain and physicochemical properties of its starch upon moderate treatment with pulsed electric field. *Foods*, *10*(2), 1–14. https://doi.org/10.3390/foods10020395

Rajeswari, K., Anand, M. T., & Mahendran, R. (2024). Protein gels influence of moderate electric field on its structure, aggregation, and gelation properties ─ a recent update. *ACS Food Science and Technology,* *4*(9), 1979–1996. https://doi.org/10.1021/acsfoodscitech.4c00135

Ranasinghesagara, J., Hsieh, F., & Yao, G. (2006). A photon migration method for characterizing fiber formation in meat analogs. *Journal of Food Science, 71*(5), 227–231. https://doi.org/10.1111/j.1750-3841.2006.00038.x

Raso, J., & Álvarez, I. (2016). Pulsed electric field processing: cold pasteurization. *Innovative Food Processing Technologies,* *1*(17), 288-296. https://doi.org/10.1016/B978-0-12-815781-7.03103-6

Raso, J., Frey, W., Ferrari, G., Pataro, G., Knorr, D., Teissie, J., & Miklavčič, D. (2016). Recommendations guidelines on the key information to be reported in studies of application of PEF technology in food and biotechnological processes. *Innovative Food Science and Emerging Technologies*, *37*, 312–321. https://doi.org/10.1016/j.ifset.2016.08.003

Raso, J., Heinz, V., Alvarez, I., & Toepfl, S. (2022). Pulsed electric fields technology for the food industry: fundamentals and applications (2nd ed.). In Aguilar-Machado, D., Montañez, J., Raso, J., & Martínet, J.M, Other applications of pulsed electric fields technology for the food industry (pp. 439–468). Springer. https://doi.org/10.1007/978-3-030-70586-2

Rawindran, H., Lim, J. W., Lam, M. K., Supramaniam, U., Tong, W. Y., Ng, H. S., Shahid, M. K., Lin, C., Usman, A., & Samdani, M. S. (2023). Assessing microalgal protein's impact on environment and energy footprint via life cycle analysis*. Molecular Biotechnology*. https://doi.org/10.1007/s12033-023-00955-0

Reimer, L. C., Sardà Carbasse, J., Koblitz, J., Ebeling, C., Podstawka, A., & Overmann, J. (2022). BacDive in 2022: the knowledge base for standardized bacterial and archaeal data. *Nucleic Acids Research, 50*(1), 741–746. https://doi.org/10.1093/nar/gkab961

Reinkensmeier, A., Bußler, S., Schlüter, O., Rohn, S., & Rawel, H. M. (2015). Characterization of individual proteins in pea protein isolates and air classified samples. *Food Research International*, *76*(P1), 160–167. https://doi.org/10.1016/j.foodres.2015.05.009

Rincon-Londono, N., Vega-Rojas, L. J., Contreras-Padilla, M., Acosta-Osorio, A. A., & Rodríguez-García, M. E. (2016). Analysis of the pasting profile in corn starch: structural, morphological, and thermal transformations, Part I. *International journal of biological macromolecules,* *91*, 106-114. https://doi.org/10.1016/j.ijbiomac.2016.05.070

Ritchie, H., Reay, D. S., & Higgins, P. (2018). Potential of meat substitutes for climate change mitigation and improved human health in high-income markets. *Frontiers in Sustainable Food Systems*, *2,* 16. https://doi.org/10.3389/fsufs.2018.00016

Rodrigues, R. M., Avelar, Z., Machado, L., Pereira, R. N., & Vicente, A. A. (2020). Electric field effects on proteins – novel perspectives on food and potential health implications.

Food Research International, *137,* 109709. https://doi.org/10.1016/j.foodres.2020.109709

Rodriguez, Y., & Beyrer, M. (2023). Impact of native pea proteins on the gelation properties of pea protein isolates. *Food Structure, 37*, 100340. https://doi.org/10.1016/j.foostr.2023.100340

Roobab, U., Aadil, R. M., Madni, G. M., & Bekhit, A. E. D. (2018). The impact of non-thermal technologies on the microbiological quality of juices: a review. *Comprehensive Reviews in Food Science and Food Safety*, *17*(2), 437–457. https://doi.org/10.1111/1541-4337.12336

Safi, C., Charton, M., Pignolet, O., Silvestre, F., Vaca-Garcia, C., & Pontalier, P. Y. (2013). Influence of microalgae cell wall characteristics on protein extractability and determination of nitrogen-to-protein conversion factors. *Journal of Applied Phycology, 25*(2), 523–529. https://doi.org/10.1007/s10811-012-9886-1

Safi, C., Zebib, B., Merah, O., Pontalier, P. Y., & Vaca-Garcia, C. (2014). Morphology, composition, production, processing and applications of *Chlorella vulgaris*: a review. *Renewable and Sustainable Energy Reviews, 35*, 265–278. https://doi.org/10.1016/j.rser.2014.04.007

Safi, C., Olivieri, G., Campos, R. P., Engelen-Smit, N., Mulder, W. J., Van den Broek, L. A. M., & Sijtsma, L. (2017). Biorefinery of microalgal soluble proteins by sequential processing and membrane filtration. *Bioresource Technology, 225*, 151–158. https://doi.org/10.1016/j.biortech.2016.11.068

Saget, S., Costa, M., Santos, C. S., Vasconcelos, M. W., Gibbons, J., Styles, D., & Williams, M. (2021). Substitution of beef with pea protein reduces the environmental footprint of meat balls whilst supporting health and climate stabilisation goals. *Journal of Cleaner Production*, *297,* 126447. https://doi.org/10.1016/j.jclepro.2021.126447

Šalaševičius, A., Uždavinytė, D., Visockis, M., Ruzgys, P., & Šatkauskas, S. (2021). Effect of pulsed electric field (PEF) on bacterial viability and whey protein in the processing of raw milk. *Applied Sciences*, *11*(23), 11281. https://doi.org/10.3390/app112311281

Saldaña, G., Puértolas, E., López, N., García, D., Álvarez, I., & Raso, J. (2009). Comparing the PEF resistance and occurrence of sublethal injury on different strains of *Escherichia coli, Salmonella* Typhimurium*, Listeria monocytogenes* and

Staphylococcus aureus in media of pH 4 and 7. *Innovative Food Science and Emerging Technologies*, *10*(2), 160–165. https://doi.org/10.1016/j.ifset.2008.11.003

Sampedro, F., McAloon, A., Yee, W., Fan, X., & Geveke, D. J. (2014). Cost analysis and environmental impact of pulsed electric fields and high-pressure processing in comparison with thermal pasteurization. *Food and Bioprocess Technology*, *7*, 1928–1937. https://doi.org/10.1007/s11947-014-1298-6

Sayar, S., Koksel, H., Turhan, M. (2005). The effects of protein-rich fraction and defatting on pasting behavior of chickpea starch. *Starch/Stärke, 57*(12), 599–604. https://doi.org/10.1002/star.200500397

Schilling, S., Toepfl, S., Ludwig, M., Dietrich, H., Knorr, D., Neidhart, S., Schieber, A., & Carle, R. (2008). Comparative study of juice production by pulsed electric field treatment and enzymatic maceration of apple mash. *European Food Research and Technology*, *226*(6), 1389–1398. https://doi.org/10.1007/s00217-007-0669-x

Schlangen, M., Taghian Dinani, S., Schutyser, M. A. I., & Van der Goot, A. J. (2022). Dry fractionation to produce functional fractions from mung bean, yellow pea and cowpea flour. *Innovative Food Science and Emerging Technologies, 78*, 103018. https://doi.org/10.1016/j.ifset.2022.103018

Schottroff, F., Krottenthaler, A., Jaeger, H., (2017). Stress induction and response, inactivation, and recovery of vegetative microorganisms by pulsed electric fields. *Handbook of Electroporation,* (pp.1–19). Springer. https://doi.org/10.1007/978-3-319-26779-1_183-1

Schottroff, F., Gratz, M., Krottenthaler, A., Johnson, N. B., Bédard, M. F., & Jaeger, H. (2019). Pulsed electric field preservation of liquid whey protein formulations – influence of process parameters, pH, and protein content on the inactivation of *Listeria innocua* and the retention of bioactive ingredients. *Journal of Food Engineering*, *243*, 142–152. https://doi.org/10.1016/j.jfoodeng.2018.09.003

Schottroff, F., & Jaeger, H. (2020). Differentiation of electric field and thermal effects during pulsed electric field and ohmic heating treatments. *Innovative Food Processing Technologies: A Comprehensive Review*, (pp. 199–210). Elsevier https://doi.org/10.1016/b978-0-08-100596-5.22960-0

Schottroff, F., Johnson, K., Johnson, N. B., Bédard, M. F., & Jaeger, H. (2020). Challenges and limitations for the decontamination of high solids protein solutions at neutral pH using pulsed electric fields. *Journal of Food Engineering*, *268,* 109737. https://doi.org/10.1016/j.jfoodeng.2019.109737

Schutyser, M. A. I., & Van der Goot, A. J. (2011). The potential of dry fractionation processes for sustainable plant protein production. *Trends in Food Science and Technology, 22*(4), 154–164. https://doi.org/10.1016/j.tifs.2010.11.006

Schutyser, M. A. I., Pelgrom, P. J. M., Van der Goot, A. J., & Boom, R. M. (2015). Dry fractionation for sustainable production of functional legume protein concentrates. *Trends in Food Science and Technology*, *45*(2), 327–335. https://doi.org/10.1016/j.tifs.2015.04.013

Selma, M. V., Salmerón, M. C., Valero, M., & Fernández, P. S. (2004). Control of *Lactobacillus plantarum* and *Escherichia coli* by pulsed electric fields in MRS broth, nutrient broth and orange-carrot juice. *Food Microbiology*, *21*(5), 519–525. https://doi.org/10.1016/j.fm.2003.12.004

Seyfabadi, J., Ramezanpour, Z., & Khoeyi, Z. A. (2011). Protein, fatty acid, and pigment content of *Chlorella vulgaris* under different light regimes. *Journal of Applied Phycology, 23*(4), 721–726. https://doi.org/10.1007/s10811-010-9569-8

Shanthakumar, P., Klepacka, J., Bains, A., Chawla, P., Dhull, S. B., & Najda, A. (2022). The current situation of pea protein and its application in the food industry. *Molecules*, *27*(16), 5354. https://doi.org/10.3390/molecules27165354

Sharma, P., Bremer, P., Oey, I., & Everett, D. W. (2014). Bacterial inactivation in whole milk using pulsed electric field processing. *International Dairy Journal*, *35*(1), 49–56. https://doi.org/10.1016/j.idairyj.2013.10.005

Show, K. Y., Lee, D. J., Tay, J. H., Lee, T. M., Chang, J. S. (2015). Microalgal drying and cell disruption - recent advances. *Bioresource Technology, 184*, 258–266. https://doi.org/10.1016/j.biortech.2014.10.139

Shrestha, S., Van ’t Hag, L., Haritos, V., & Dhital, S. (2023). Comparative study on molecular and higher-order structures of legume seed protein isolates: lentil, mungbean and yellow pea. *Food Chemistry*, *411,* 135464. https://doi.org/10.1016/j.foodchem.2023.135464

Siderakou, D., Zilelidou, E., Poimenidou, S., Tsipra, I., Ouranou, E., Papadimitriou, K., & Skandamis, P. (2021). Assessing the survival and sublethal injury kinetics of *Listeria monocytogenes* under different food processing-related stresses. *International Journal of Food Microbiology, 346*, 109159. https://doi.org/10.1016/j.ijfoodmicro.2021.109159

Siegrist, A., Green, A., Michel, F., & Mathys, A. (2024). Comparing the nutritional value and prices of meat and milk substitutes with their animal-based benchmarks across six European countries. *Food Research International*, *197*, 115213. https://doi.org/10.1016/j.foodres.2024.115213

Smetana, S., Mathys, A., Knoch, A., & Heinz, V. (2015). Meat alternatives: life cycle assessment of most known meat substitutes. *International Journal of Life Cycle Assessment*, *20*(9), 1254–1267. https://doi.org/10.1007/s11367-015-0931-6

Smetana, S., Sandmann, M., Rohn, S., Pleissner, D., & Heinz, V. (2017). Autotrophic and heterotrophic microalgae and cyanobacteria cultivation for food and feed: life cycle assessment. *Bioresource Technology, 245*, 162–170. https://doi.org/10.1016/j.biortech.2017.08.113

Smetana, S., Ristic, D., Pleissner, D., Tuomisto, H. L., Parniakov, O., & Heinz, V. (2023). Meat substitutes: resource demands and environmental footprints. *Resources, Conservation and Recycling, 190*, 106831. https://doi.org/10.1016/j.resconrec.2022.106831

Snel, S. J. E., Bellwald, Y., Van der Goot, A. J., & Beyrer, M. (2022). Novel rotating die coupled to a twin-screw extruder as a new route to produce meat analogues with soy, pea and gluten. *Innovative Food Science & Emerging Technologies, 81*, 103152. https://doi.org/10.1016/j.ifset.2022.103152

Song, J., Joshi, R. P., & Schoenbach, K. H. (2011). Synergistic effects of local temperature enhancements on cellular responses in the context of high-intensity, ultrashort electric pulses. *Medical & Biological Engineering & Computing*, *49*(6), 713–718 https://doi.org/10.1007/s11517-011-0745-z

Soni, A., Oey, I., Silcock, P., & Bremer, P. J. (2018). Impact of temperature, nutrients, pH and cold storage on the germination, growth and resistance of *Bacillus cereus* spores in egg white. *Food Research International*, *106*, 394–403. https://doi.org/10.1016/j.foodres.2018.01.006

Soto-Sierra, L., Stoykova, P., & Nikolov, Z. L. (2018). Extraction and fractionation of microalgae-based protein products. *Algal Research, 36,* 175–192. https://doi.org/10.1016/j.algal.2018.10.023

Spiden, E. M., Yap, B. H. J., Hill, D. R. A., Kentish, S. E., Scales, P. J., & Martin, G. J. O. (2013). Quantitative evaluation of the ease of rupture of industrially promising microalgae by high pressure homogenization. *Bioresource Technology, 140*, 165–171. https://doi.org/10.1016/j.biortech.2013.04.074

Springmann, M., Wiebe, K., Mason-D'Croz, D., Sulser, T. B., Rayner, M., & Scarborough, P. (2018). Health and nutritional aspects of sustainable diet strategies and their association with environmental impacts: a global modelling analysis with country-level detail. *The Lancet Planetary Health*, *2*(10), 451–461. https://doi.org/10.1016/S2542-5196(18)30206-7

Sun, X. D., & Arntfield, S. D. (2011). Dynamic oscillatory rheological measurement and thermal properties of pea protein extracted by salt method: effect of pH and NaCl. *Journal of Food Engineering, 105*(3), 577-582. https://doi.org/10.1016/j.jfoodeng.2011.03.008

Taha, A., Casanova, F., Šimonis, P., Stankevič, V., Gomaa, M. A. E., & Stirkė, A. (2022). Pulsed electric field: fundamentals and effects on the structural and techno-functional properties of dairy and plant proteins. *Foods, 11*(11), 1556. https://doi.org/10.3390/foods11111556

Tang, M., Miri, T., Soltani, F., Onyeaka, H., & Al-Sharify, Z. T. (2024). Life cycle assessment of plant-based vs. beef burgers: a case study in the UK. *Sustainability*, *16*(11), 4417. https://doi.org/10.3390/su16114417

Tanger, C., Engel, J., & Kulozik, U. (2020). Influence of extraction conditions on the conformational alteration of pea protein extracted from pea flour. *Food Hydrocolloids, 107*, 105949. https://doi.org/10.1016/j.foodhyd.2020.105949

Thamsuaidee, A., Schaefer, E., Schneider, D., Siemer, C., & Valdramidis, V. P. (2024). Disentangling the effects of electroporation and heat during pulsed electric field (PEF) processing of oat-based milk alternative: a case study on *Lactiplantibacillus plantarum* inactivation. *Innovative Food Science and Emerging Technologies*, *94,* 103691. https://doi.org/10.1016/j.ifset.2024.103691

Timmermans, R. A. H., Nederhoff, A. L., Nierop Groot, M. N., Van Boekel, M. A. J. S., & Mastwijk, H. C. (2016). Effect of electrical field strength applied by PEF processing and storage temperature on the outgrowth of yeasts and moulds naturally present in a fresh fruit smoothie. *International Journal of Food Microbiology*, *230*, 21–30. https://doi.org/10.1016/j.ijfoodmicro.2016.04.014

Timmermans, R. A. H., Roland, W. S. U., Van Kekem, K., Matser, A. M., & Van Boekel, M. A. J. S. (2022). Effect of pasteurization by moderate intensity pulsed electric fields (PEF) treatment compared to thermal treatment on quality attributes of fresh orange juice. *Foods*, *11*(21), 3360. https://doi.org/10.3390/foods11213360

Toepfl, S., Mathys, A., Heinz, V., & Knorr, D. (2006). Review: potential of high hydrostatic pressure and pulsed electric fields for energy efficient and environmentally friendly food processing. *Food Reviews International*, *22*(4), 405–423. https://doi.org/10.1080/87559120600865164

Toepfl, S., & Heinz, V. (2011). Pulsed electric field assisted extraction - a case study. In Zhang, H. Q., Barbosa-Canovas G. V., Balasubramaniam V. M., Dunne, C. P., Farkas, D. F., & Yuan, J. T. C. *Non-thermal processing technologies for food*. *Section II: electromagnetic processes* (pp. 190–200). *Blackwell and Institute of Food Technologist.* https://doi.org/10.1002/9780470958360.ch13

Tolkach, A., & Kulozik, U. (2007). Reaction kinetic pathway of reversible and irreversible thermal denaturation of β-lactoglobulin. *Dairy Science and Technology, 87*(4–5), 301–315. https://doi.org/10.1051/lait:2007012

Trout, G. R. (1988). Techniques for measuring water-binding capacity in muscle foods: a review of methodology. *Meat Science, 23*(4), 235–252. https://doi.org/10.1016/0309-1740(88)90009-5

Tubiello, F. N., Karl, K., Flammini, A., Gütschow, J., Obli-Laryea, G., Conchedda, G., Pan, X., Qi, S. Y., Halldórudóttir Heiðarsdóttir, H., Wanner, N., Quadrelli, R., Rocha Souza, L., Benoit, P., Hayek, M., Sandalow, D., Mencos Contreras, E., Rosenzweig, C., Rosero Moncayo, J., Conforti, P., & Torero, M. (2022). Pre- and post-production processes increasingly dominate greenhouse gas emissions from agri-food systems. *Earth System Science Data*, *14*(4), 1795–1809. https://doi.org/10.5194/essd-14-1795-2022

Tzitzikas, E. N., Vincken, J., de Groot, J., Gruppen, H., & Visser, R. G. F. (2006). Genetic variation in pea seed globulin composition. *Journal of Agricultural and Food Chemistry*, *54*(2), 425-33. https://doi.org/10.1021/jf0519008.

Uran, M., Caporgno, M., Zinn, M., Tremblay, P., & Pott, J. (2021) Methods of growing microalgae & products thereof. Patent n°EP4122330A1. https://www.epo.org/

Ursu, A. V., Marcati, A., Sayd, T., Sante-Lhoutellier, V., Djelveh, G., & Michaud, P. (2014). Extraction, fractionation and functional properties of proteins from the microalgae *Chlorella vulgaris*. *Bioresource Technology, 157*, 134–139. https://doi.org/10.1016/j.biortech.2014.01.071

Vaessen, E. M. J., Timmermans, R. A. H., Tempelaars, M. H., Schutyser, M. A. I., & Den Besten, H. M. W. (2019). Reversibility of membrane permeabilization upon pulsed electric field treatment in *Lactobacillus plantarum* WCFS1. *Scientific Reports*, *9*(1), 1–11. https://doi.org/10.1038/s41598-019-56299-w

Van der Goot, A. J., Pelgrom, P. J. M., Berghout, J. A. M., Geerts, M. E. J., Jankowiak, L., Hardt, N. A., Keijer, J., Schutyser, M. A. I., Nikiforidis, C. V., & Boom, R. M. (2016). Concepts for further sustainable production of foods. *Journal of Food Engineering, 168*, 42–51. https://doi.org/10.1016/j.jfoodeng.2015.07.010

Van der Sman, R. G. M., & Van der Goot, A. J. (2023). Hypotheses concerning structuring of extruded meat analogs. *Current Research in Food Science, 6*. https://doi.org/10.1016/j.crfs.2023.100510

Vanga, S. K., Wang, J., Jayaram, S., & Raghavan, V. (2021). Effects of pulsed electric fields and ultrasound processing on proteins and enzymes: a review. *Processes*, *9*(4), 722. https://doi.org/10.3390/pr9040722

Vidal-Valverde, C., Frias, J., Hernández, A., Martín-Alvarez, P. J., Sierra, I., Rodríguez, C., Blazquez, I., & Vicente, G. (2003). Assessment of nutritional compounds and antinutritional factors in pea (*Pisum sativum*) seeds. *Journal of the Science of Food and Agriculture*, *83*(4), 298–306. https://doi.org/10.1002/jsfa.1309

Wang, M. S., Wang, L. H., Bekhit, A. E. D. A., Yang, J., Hou, Z. P., Wang, Y. Z., Dai, Q. Z., & Zeng, X. A. (2018). A review of sublethal effects of pulsed electric field on cells in food processing. *Journal of Food Engineering*, *223*, 32–41. https://doi.org/10.1016/j.jfoodeng.2017.11.035

Wang, R. Y., Yun, O., Zeng, X. A., & Guo, C. J. (2019). Membrane fatty acids composition and fluidity modification in *Salmonella* Typhimurium by culture temperature and resistance under pulsed electric fields. *International Journal of Food Science and Technology, 54*(6), 2236–2245. https://doi.org/10.1111/ijfs.14137

Wang, R., Wang, L. H., Wen, Q. H., He, F., Xu, F. Y., Chen, B. R., & Zeng, X. A. (2023). Combination of pulsed electric field and pH shifting improves the solubility, emulsifying, foaming of commercial soy protein isolate. *Food Hydrocolloids*, *134,* 108049. https://doi.org/10.1016/j.foodhyd.2022.108049

Wang, Y., Tibbetts, S. M., Berrue, F., McGinn, P. J., MacQuarrie, S. P., Puttaswamy, A., Patelakis, S., Schmidt, D., Melanson, R., & MacKenzie, S. E. (2020). A rat study to evaluate the protein quality of three green microalgal species and the impact of mechanical cell wall disruption. *Foods, 9*(11), 1531. https://doi.org/10.3390/foods9111531

Wijayanti, H. B., Bansal, N., & Deeth, H. C. (2014). Stability of whey proteins during thermal processing: a review. *Comprehensive Reviews in Food Science and Food Safety*, *13*(6), 1235–1251. https://doi.org/10.1111/1541-4337.12105

Wild, F., Czerny, M., Janssen, A. M., Kole, A. P. W., Zunabovic, M., Domig, K. J. (2014). The evolution of a plant-based alternative to meat: from niche markets to widely accepted meat alternatives. *Agro Food Industry Hi Tech, 25*(1), 45–49.

Willett, W., Rockström, J., Loken, B., Springmann, M., Lang, T., Vermeulen, S., Garnett, T., Tilman, D., DeClerck, F., Wood, A., Jonell, M., Clark, M., Gordon, L. J., Fanzo, J., Hawkes, C., Zurayk, R., Rivera, J. A., De Vries, W., Majele Sibanda, L. M., Afshin, A., Chaudhary, A., Herrero, M., Agustina, R., Branca, F., Lartey, A., Fan, S., Crona, B., Fox, E., Bignet, V., Troell, M., Lindahl, T., Singh, S., Cornell, S. E., Reddy, K. S., Narain, S., Nishtar, S., & Murray, C. J. L. (2019). Food in the Anthropocene: the EAT–Lancet Commission on healthy diets from sustainable food systems. *The Lancet, 393*(10170), 447–492. https://doi.org/10.1016/S0140-6736(18)31788-4

Witt, J., Siemer, C., Bostelmann, A., & Toepfl, S. (2020). Juice preservation by pulsed electric fields. *Innovative Food Processing Technologies: A Comprehensive Review*, (pp. 305–317). Elsevier. https://doi.org/10.1016/b978-0-12-815781-7.00026-3

Wu, W. J., & Chang, J. (2022). Inactivation of vegetative cells, germinated spores, and dormant spores of *Bacillus atrophaeus* by pulsed electric field with fixed energy input. *Journal of Food Process Engineering*, *45*(2), 1–7. https://doi.org/10.1111/jfpe.13959

Xiang, B. Y., Ngadi, M. O., Simpson, B. K., & Simpson, M. V. (2011). Pulsed electric field induced structural modification of soy protein isolate as studied by fluorescence spectroscopy. *Journal of Food Processing and Preservation*, *35*(5), 563–570. https://doi.org/10.1111/j.1745-4549.2010.00501.x

Yarmush, M. L., Golberg, A., Serša, G., Kotnik, T., & Miklavčič, D. (2014). Electroporation-based technologies for medicine: principles, applications, and challenges. *Annual Review of Biomedical Engineering, 16*, 295–320. https://doi.org/10.1146/annurev-bioeng-071813-104622

Yan, Z., Yin, L., Hao, C., Liu, K., & Qiu, J. (2021). Synergistic effect of pulsed electric fields and temperature on the inactivation of microorganisms. *AMB Express*, *11*(1), 47. https://doi.org/10.1186/s13568-021-01206-8

Yao, G., Liu, K. S., & Hsieh, F. (2004). A new method for characterizing fiber formation in meat analogs during high-moisture extrusion. *Journal of Food Science, 69*(7), 303–307. https://doi.org/10.1111/j.1365-2621.2004.tb13634.x

Zand, E., Froehling, A., Schoenher, C., Zunabovic-Pichler, M., Schlueter, O., & Jaeger, H. (2021). Potential of flow cytometric approaches for rapid microbial detection and characterization in the food Industry – a review. *Foods*, *10*(12), 3112. https://doi.org/10.3390/foods10123112

Zare, F., Ghasemi, N., Bansal, N., & Hosano, H. (2023). Advances in pulsed electric stimuli as a physical method for treating liquid foods. *Physics of Life Reviews*, *44*, 207–266. https://doi.org/10.1016/j.plrev.2023.01.007

Zhang, C., Yang, Y. H., Zhao, X. D., Zhang, L., Li, Q., Wu, C., Ding, X., & Qian, J. Y. (2021). Assessment of impact of pulsed electric field on functional, rheological and structural properties of vital wheat gluten. *LWT – Food Science and Technology*, *147,* 11536. https://doi.org/10.1016/j.lwt.2021.111536

Zhang, L., Wang, L. J., Jiang, W., & Qian, J. Y. (2017). Effect of pulsed electric field on functional and structural properties of canola protein by pretreating seeds to elevate oil

yield. *LWT – Food Science and Technology*, *84*, 73–81. https://doi.org/10.1016/j.lwt.2017.05.048

Zhao, W., & Yang, R. (2008). Comparative study of inactivation and conformational change of lysozyme induced by pulsed electric fields and heat. *European Food Research and Technology*, *228*(1), 47–54. https://doi.org/10.1007/s00217-008-0905-z

Zhao, W., Yang, R., & Wang, M. (2009). Cold storage temperature following pulsed electric fields treatment to inactivate sublethally injured microorganisms and extend the shelf life of green tea infusions. *International Journal of Food Microbiology*, *129*(2), 204–208. https://doi.org/10.1016/j.ijfoodmicro.2008.12.006

Zhao, W., & Yang, R. (2010). Experimental study on conformational changes of lysozyme in solution induced by pulsed electric field and thermal stresses. *Journal of Physical Chemistry B*, *114*(1), 503–510. https://doi.org/10.1021/jp9081189

Zhao, W., Yang, R., & Zhang, H. Q. (2012). Recent advances in the action of pulsed electric fields on enzymes and food component proteins. *Trends in Food Science and Technology, 27*(2), 83–96. https://doi.org/10.1016/j.tifs.2012.05.007

Zhao, W., Tang, Y., Lu, L., Chen, X., & Li, C. (2014). Review: pulsed electric fields processing of protein-based foods. *Food and Bioprocess Technology, 7*(1), 114–125. https://doi.org/10.1007/s11947-012-1040-1

Zheng, Z., Jin, Y., Zhang, L., Xu, X., & Yang, N. (2024). Inactivation of microorganisms in foods by electric field processing: a review. *Journal of Agriculture and Food Research*, *16,* 101109. https://doi.org/10.1016/j.jafr.2024.101109

Zhi, Z., Yan, L., Li, H., Dewettinck, K., Van der Meeren, P., Liu, R., & Van Bockstaele, F. (2022). A combined approach for modifying pea protein isolate to greatly improve its solubility and emulsifying stability. *Food Chemistry*, *380,* 131832. https://doi.org/10.1016/j.foodchem.2021.131832

Zhu, H. G., Tang, H. Q., Cheng, Y. Q., Li, Z. G., & Tong, L. T. (2021). Potential of preparing meat analogue by functional dry and wet pea (*Pisum sativum*) protein isolate. *LWT – Food Science and Technology*, *148,* 100744. https://doi.org/10.1016/j.crfs.2024.100744

Zink, J. I., Zehnder-Wyss, O., Dällenbach, D., Nyström, L., & Windhab, E. J. (2024). Enzymatic degradation of pea fibers changes pea protein concentrate functionality. *Current Research in Food Science*, *8,* 100744. https://doi.org/10.1016/j.crfs.2024.100744

Zwietering, M. H., Jongenburger, I., Rombouts, F. M., & Van 't Riet, K. (1990). Modeling of the bacterial growth curve. *Applied and Environmental Microbiology, 56*(6), 1875–1881. https://doi.org/10.1128/aem.56.6.1875-1881.1990

Summary

Plant-based food products are rapidly gaining market share as consumers shift toward more sustainable and healthy diets. Compared to animal-based products, their production requires less land and water and generates a substantially lower carbon footprint. Among them, meat substitutes have become particularly popular for their ease of use. They are typically produced by extrusion, where plant-based protein isolate powders are hydrated and texturized into meat-like products. The functionality of the protein, primarily its gelling properties, is therefore crucial for the process. Conventional protein extraction from the raw material and drying steps involve high temperatures and chemical use, which not only consume large amounts of energy but also impair the gelling properties of the proteins. Additionally, most commercial meat substitutes are soy-based, raising concerns about deforestation, large-scale monoculture and global transport dependence.

This thesis aims to advance the development of plant-based food products by rethinking meat substitute manufacturing. It proposes **replacing imported soy protein isolates by locally sourced protein ingredients and eliminating conventional energy-intensive protein extraction and drying steps**. Instead, **minimal processing of proteins** was developed. Two protein ingredients, *Chlorella vulgaris* (*Cv)* suspension and yellow pea protein extract (PPE) were considered. PPE was obtained from air classified pea protein concentrate under mild, aqueous and room temperature conditions. A life cycle assessment (**Chapter 6**) revealed that substituting soy with pea reduces the protein's carbon footprint by a factor of 5.5, and using PPE instead of pea protein isolate (PPI) powder lowers it by an additional factor of 1.8. Moreover, **Chapter 2** demonstrated the **feasibility of incorporating protein-rich plant-based liquids into extrusion** without compromising the properties of the final product.

A major challenge with handling liquids is their **microbial instability**. While extrusion (high temperature, pressure and residence time) ensures the microbial safety of the final product, quality deterioration of the liquid during refrigerated storage and prior to extrusion limits processing flexibility. Key spoilage bacteria were identified in *Cv* (*Pseudomonas guariconensis*, *Enterobacter soli* and *Lactococcus lactis*) and PPE *(Pseudomonas trivalis* and *Erwinia gerundensis)* (**Chapters 3 and 4**). **Pulsed electric field (PEF) treatment combined with cold storage** was investigated as a mild preservation strategy. PEF treatment is based on the application of high-voltage short pulses to liquids, inactivating

bacteria with minimal temperature increase and reduced damage to heat-sensitive compounds, predominantly present in liquid foods.

In **Chapter 3**, challenge tests using pilot-scale PEF treatment in continuous mode were performed on *Cv*. The optimized conditions (E_{el} = 28 kV/cm, f = 120 Hz, τ = 20 µs, t = 225 µs, T_{in} = 30 °C, T_{out} < 55 °C) allowed **microbial reductions of ~ 4 logs** for *P. guariconensis, E. soli* and *L. lactis*. These reductions enabled **shelf-life extension of up to five days** at 10 °C, which could be further increased through **repetitive PEF cycles**. Similarly, **Chapter 4** demonstrated PEF-induced microbial reductions of ~ 4 logs for *P. trivalis* and *E. gerundensis* inoculated into PPE (E_{el} = 24 kV/cm, f = 50 Hz, τ = 20 µs, t = 126 µs, T_{in} = 40 °C, T_{out} < 60 °C). Shelf-life was extended by three days at 10 °C storage and six days at 5 °C. When applied to the PPE **native microbiota, PEF caused a four-day lag phase extension** at 5 °C storage, accompanied by a shelf-life extension of six days and a pH stability of ten days. Overall, PEF effectively preserved the quality of *Cv* and PPE with significant inactivation effects on both targeted spoilage bacteria and native microbiota.

The implementation of PEF in the supply chain of plant-based foods was evaluated in **Chapter 6**. **The growth rate of PEF-treated *E. soli* was significantly reduced, and the lag phase duration was extended** when introducing one day storage (10 °C) prior to PEF.

Chapter 6 further investigates the PEF-induced electroporation of the bacterial membrane, aiming for consistent lag phase extension to further enhance storage stability. In addition to lethal effects, PEF at high intensity (E_{el} = 28 kV/cm) caused the **formation of sublethal injury** in *E. soli*. Despite exhibiting delayed colony formation, detected as smaller colony size upon plating, this injury was not associated with a prolonged lag phase duration during shelf-life.

The viability of PEF as a preservation method depends on its ability to maintain protein functionality. **Chapter 5** examined the impact of PEF on pea proteins (albumins and globulins) structure and functionality and compared it with conventional heat pasteurization. Spectroscopic measurements revealed **partial protein unfolding following PEF, promoting intermolecular interaction and enhanced (> 50%) gelling properties**. In contrast, heat pasteurization caused protein aggregation and 60% reduction in gelling properties for equivalent microbial inactivation levels. Moreover, lab-scale extrusion trials (**Chapter 6**) confirmed that the incorporating (30%) of PEF-treated PPE in PPI did not affect

the meat substitute texture, whereas the textural parameters were reduced with thermally treated PPE.

To conclude, the proposed approach – combining local sourcing, minimal processing, and mild preservation – significantly reduces carbon footprint and enhances protein functionality for meat substitute production. However, to validate its technological feasibility, further work is required to optimize processing for higher conductivity liquids (**Chapter 6**), to understand batch-to-batch variability (**Chapter 2**), and to assess potential adverse effects of increased protein concentration on inactivation level (**Chapter 6**). Overall, this thesis advanced the development of plant-based protein ingredients, bridging sustainability and functionality through innovative use of PEF technology.

List of symbols

A	Surface area (m^2) or difference $\log_{10}N_{max}$ and $\log_{10}N_0$ ($\log_{10}$ CFU/mL)
$[AA]_{protein}$	Mass concentration of amino acids in protein ($g_{AA}/g_{protein}$)
b_R	Temperature coefficient (K^{-1})
c_p	Specific heat capacity (kJ/(kg·K))
d	Distance (m)
d_i	Thickness of the insulation layer (m)
d_s	Thickness of the stainless-steel wall (m)
D	Pipe hydraulic diameter (m)
E_{crit}	Critical electric field strength (kV/cm)
E_{el}	Electric field strength (kV/cm)
E_{PEF}	Specific energy at PEF treatment (kJ/kg)
E_{TT}	Specific energy at thermal treatment (kJ/kg)
f	Pulse repetition rate (Hz)
F	Flow rate (m^3/s)
G'	Storage modulus (Pa)
G''	Loss modulus (Pa)
ΔH	Reaction enthalpy (J/g)
I	Current (A)
m	Mass (kg)
M_W	Molecular weight (g/mol)
n	Number of pulse (-)
n_N	Number of nitrogen atoms (-)
N	Microbial load or concentration (CFU/mL)
N_{max}	Maximal microbial concentration (CFU/mL)
N_0	Initial microbial load or concentration (CFU/mL)
$[N]_{protein}$	Mass concentration of nitrogen in proteins ($g_N/g_{protein}$)
$[N]_{AA}$	Mass concentration of nitrogen in amino acids (g_N/g_{AA})
p_d	Pulse power (kJ/(s·cm^3))
Δp	Pressure (Pa)
$\dot{Q}$	Heat (W)
R	Electrical resistance (S^{-1})
t	Treatment time (s)

t_r	Residence time (s)
T	Temperature (K)
T_{crit}	Critical temperature (K)
T_{in}	Initial or inlet temperature (K)
T_{onset}	Onset temperature (K)
T_{out}	Outlet temperature (K)
T_{outlet}	Outlet temperature (K)
T_p	Process temperature (K)
T_{peak}	Peak maximum temperature (K)
T_{PH}	Temperature after pre-heating (K)
ΔT	Temperature increase (K)
U	Voltage (kV) or heat transfer coefficient (W/(m^2·K))
v	Fluid velocity (m/s)
V	Volume (cm^3)
$V_{chamber}$	Volume of the PEF chamber (m^3)
W_d	Pulse energy input (kJ/cm^3)
W_s	Total specific energy input (kJ/kg)
X_i	Relative mass fraction of the component i (-)
τ	Pulse duration (s) or shear stress (Pa)
δ	Temperature change due to the heat of compression (K)
ζ	Zeta potential (mV)
λ	Lag phase (d)
λ_i	Thermal conductivity of the component i or insulation layer (W/(m·K))
λ_s	Thermal conductivity of stainless-steel wall (W/(m·K))
μ	Dynamic viscosity (Pa·s) or growth rate ($\log_{10}$d^{-1})
$\mu_{app,\ initial}$	Apparent initial viscosity (mPa·s)
$\mu_{app,\ final}$	Apparent final viscosity (mPa·s)
$\mu_{app,\ peak}$	Apparent peak viscosity (mPa·s)
ξ	Temperature change due to homogenization (K)
ρ	Density (kg/cm^3)
σ	Conductivity (S/cm)
σ_R	Referential conductivity (S/cm)

List of abbreviations

AA	Amino acid
AI	Anisotropic index
BB	Beef burger
bw	body weight
CD	Circular dichroism
CFU	Colony forming unit
CLSM	Confocal laser scanning microscopy
CTRW	Continuous time random walk
Cv	*Chlorella vulgaris*
DNA	Deoxyribonucleic acid
DM	Dry matter
DSC	Differential scanning calorimetry
DSP	Downstream processing
EAA	Essential amino acid
E. gerundensis	*Erwinia gerundensis*
E. soli	*Enterobacter soli*
EU	European Union
FD	Freeze drying
FFC	Fluorescence flow cytometry
GHG	Greenhouse gas
GHGE	Greenhouse gas emission
HMEC	High moisture extrusion cooking
HPH	High-pressure homogenization
HPLC	High performance liquid chromatography
HT	Heat treatment
id	Identification
IEX	Ion exchange chromatography
IPCC	Intergovernmental panel on climate change
ITF	Intrinsic tryptophane fluorescence
LCA	Life cycle assessment
L. lactis	*Lactococcus lactis*
LVER	Linear viscoelastic region

MA	Microalgae
MALDI-TOF	Matrix-assisted laser desorption/ionization - time of flight
MCR	Modular compact rheometer
MMRS	Modular microfluidic reactor system
MRD	Maximum recovery diluent
MS	Mass spectrometry or meat substitute
n.a.	not analyzed
n.d.	not detected
n.i.	not identified
NPCF	Nitrogen-to-protein conversion factor
OSAV	Office of food safety and veterinary affairs
P. guariconensis	*Pseudomonas guariconensis*
P. trivalis	*Pseudomonas trivalis*
PAPMID	Putative assigned protein masses for the identification database
PCA	Plate count agar
PEF	Pulsed electric field
pH	Potential of hydrogen
pI	Isoelectric point
PI	Propidium Iodide
PPC	Pea protein concentrate
PPE	Pea protein extract
PPI	Pea protein isolate
Re	Reynolds number
REF	Reference
RID	Refractive index detector
SD	Standard deviation
SDGs	Sustainable development goals
SEC	Size exclusion chromatography
Sp.	Species
SPC	Soy protein concentrate
SPE	Soy protein extract
SPI	Soy protein isolate
SQST	Swiss quality testing services
SSp	SuperSpectra

TN	Total nitrogen
TOC	Total organic carbon
TPA	Texture profile analysis
TPC	Total plate count
Trp	Tryptophan
TSB	Tryptic-casein soy broth
T-sweep	Temperature sweep
TT	Thermal treatment
TVP	Texturized vegetable protein
USA	United States
WGS	Whole-genome sequencing

Acknowledgements

As I reach the end of my PhD journey, I realize how much this achievement depends on the support and collaboration of so many people.

First, I would like to express my gratitude to my supervisors **Michael Beyrer**, **Heidy den Besten** and **Marcel Zwietering** who guided me toward the success of my PhD. **Michael**, from the moment I first visited the School of Engineering (HES-SO), I knew I was in a supportive and respectful working environment. You gave me a lot of freedom to work independently, but you were always present when I needed help. **Heidy** and **Marcel**, I am so grateful for the opportunity to do this PhD journey with Wageningen University. Even as an external PhD candidate, I always felt very welcome during my visits on the campus. Your time, expertise and kindness played a huge role in the success of my PhD.

Thanks are also addressed to **Gaetan Cherix**, the Director of the School of Engineering in Sion, and **Sergio Schmid**, the Director of the Institute of Life Sciences, for the possibility to join the HES-SO team. A big thank you to my colleagues in the Sustainable Food System research group, **Ysamar Rodriguez**, **Silvia Snel**, **Maria Gräfenhahn** and **Ailsa Moodycliffe** for all the fruitful discussions, feedback, and shared hours in the lab. **Ysamar** and **Silvia**, you made my start in the team so much easier, and I was fortunate to have you by my side during the process of my 1st publication. **Maria**, since you joined the group, you have been a mentor to me, and I greatly appreciate the time you took to comment on my presentations and publications. **Ailsa**, as my first student, you were a perfect fit, and I learned so much from our collaboration. Thank you for the numerous proofreading efforts and your contribution to my 2nd publication. **Animesh Singh Sengar**, I valued our collaboration during your internship at HES-SO. Thank you for your help with the analyses during my pregnancy. A particular and immense thank you to **Frédéric Maruel**, whose support was more than appreciated. Your energy, humor and assistance made my life in the pilot plant easier. I would like to acknowledge the many colleagues at HES-SO who contributed to my research: **Dimitri Bocquel**, **Laurence Nicolay** and **Sandra Galle** for organizing the pilot plant; **Bruno Lehner**, **Martine Baudin**, **Martine Emery Mabillard** and **Fabienne Giromini** for your invaluable help in the microbiology lab and for supporting my students; **Véronique Amstutz**, **Julien Pott**, **Florian Miserez** and **Priscilla Tremblay** for introducing me to new equipment (FCM, TOC-TN) and assisting during the Master F1 module lecture; **Nancy Nicolet** for your help with Kjeldahl and HPLC analyses and for the shared coffee breaks; **Rémy Dufresne** for your assistance with various equipment (SEC,

AEX, HPH, microscopy) and for the enjoyable discussions about our respective house building projects; **Pascal Jacquemettaz**, **Stefan Willen**, **Sarah Wegmüller**, **Alexandre Kuhn** and **Vanessa Gaillard** for helping with analytical measurements (FTIR, DC, WGS); **David Martinet** for your support with the PEF and oscilloscope installation; **David Berthouzoz** for the mechanical work and construction of the PEF batch cell; **Mathieu Schopfer** for installing the MMRS system; **Robert Axelrod** for your advice on PEF; **Laëtitia Nicolas** for the nice discussions and sensory testing; **Thierry Delaloye** for managing logistics and materials; **Alexia Crettenand** for your administrative support; **Isabelle Fournier**, from the MOVE association, for assisting with the tasks required to welcome my three Master students; and **Isabelle Skakni** for helping me strengthen my application for the mobility funding.

I would like to extend my thanks to the people at Wageningen University: **Jarno Gieteling** and **Norbert de Ruijter** for the CLSM imaging; **Georgios Pampoukis** and **Domiziana Battaggia** for the scientific discussions over coffee; **Aaditya Venkatachalam** it was a pleasure meeting you at the PhD week, and I always look forward to our coffees or walks during my visits to WUR; **Gerda van Laar-Engelen** for your administrative work; **Yvonne Smolders** for your assistance with the PhD school and TSP.

Conducting applied research at HES-SO provided the unique advantage of direct contact with industrial partners. Thank you to **Adrian Caramaschi** from Hochdorf Swiss Nutrition AG, **Mine Uran** and **Aslin Sarikaya** from Alver AG, **Anik Thaler** and **Katharina Pälchen** from Fabas Foods and **Valérie Vincent** from GMSA, for the valuable research discussions and assistance in the development of patents, publications and research reports. Thank you, **Valérie**, for the on-site visit, and **Aslin**, **Valérie** and **Katharina** for serving as experts for the different bachelor thesis defenses. **Katharina**, it was a pleasure to work with you in the lab in Sion and to share lunches and after-work drinks.

My research would not have been the same without the precious help from my students. To my three Bachelor students, **Ailsa Moodycliffe**, **Amina Bouguenna** and **Alix Rouge**, your dedication and countless hours of work were deeply appreciated. Thank you as well to my three Master students from WUR, ETHZ and Namur University, **Alexandra Batsila**, **Nicolas Etschmann** and **Valentin De Ridder**. **Alexandra**, your support during a challenging phase of the project was invaluable, and beyond your research skills, you are an awesome person. **Nicolas**, thank you for your contribution to my 3rd publication. **Valentin**, the Belgium

kindness made the months of collaboration with you good memories from my PhD that I will keep preciously. Your expertise in protein characterization was essential in achieving the final objective of the project and the 4th publication. Supervising students with diverse skills, personalities and cultures has contributed significantly to my personal and professional growth.

To my dear lunch or running partners, **Ysamar**, **Silvia**, **Ailsa**, **Maria**, **Anika**, **Hugo**, **Aurélien**, **Mattéo**, **Ludo** and **Maxime**, thank you for your company during breaks. **Anika**, best of luck in your next running goal, perhaps 100 km ?; **Hugo**, my PhD buddy, having someone at the same stage of the PhD journey was reassuring, and I am grateful for our mutual support during this nice adventure; **Aurélien** and **Mattéo**, I sincerely hope you will pursue your impressive journey with ProSeed, and perhaps our paths will cross again; **Ludo** it was such a joy to share lunch runs and PhD highs and lows with you; **Maxime** who would have thought, 10 years ago, that we would both be pursuing PhDs? I appreciate our common awareness of environmental concerns and values we share, and I hope we will stay in touch.

Special thanks to my two paranymphs **Silvia** and **Ysamar**. I am truly honored to experience the big day – my thesis defense at WUR – with you by my side.

To my friends, who stood by me throughout this challenging journey. **Corina**, it was a great moment when we both realized we were embarking on our PhDs at the same time. You are a great researcher, and I continue to learn from you. Thank you for our sports trips, whether on bikes or skis. **Estelle** and **Victoria**, the best colleagues ever, thank you for your presence at the beginning of my PhD. You know what it meant to me. To all my friends with whom I shared precious moments over the past four years, thank you for your understanding and patience as I juggled my PhD, house renovation, and the arrival of our first child. **Bérangère**, **Delphine**, **Lisa, Les Paons** and **Les Kitanes**.

A PhD project cannot be completed without the support of family, especially when renovating a house on the side. Thank you to my parents-in-law, **Bernard** and **Ingrid**, for their immeasurable help with the house. To my favorite ones, **Patrice**, **Marylène**, **Killian**, **Solène**, **Julien** and **Camille**, thank you for being there for me, supporting my ambitious projects and providing a stable and loving family environment. You are the foundation of my happy life! A special and immense thank you to my incredible husband **Basile** for being the best chemistry advisor, unwavering supporter and above all the best father for our little sunshine **Ellia**!

About the author



Cora De Gol was born October 22, 1992, in the heart of the Swiss mountains, in Valais. Growing up, she was deeply inspired by her twin brother, who has been committed to protecting our planet's resources, from a young age. This made it clear to her which path to take and how she wanted to invest her time and energy. After her first visit at the School of Engineering (HES-SO) and FoodTech pilot plant, when she was approximately 18 years old, her interest in Food Sciences only rose. She completed a bachelor's degree in Chemistry and Chemical engineering with a specialization in Food Chemistry from the Ecole Polytechnique Fédérale de Lausanne (EPFL) in 2016. Afterwards, she spent 6 months as a research assistant at Nestlé, where she worked on "*the hydrolysis of starch and fiber of oat flour and aggregation reaction of milk and oat proteins*". In 2017, she started a master's program in Chemical and Bioengineering at the Eidgenössische Technische Hochschule Zürich (ETHZ) and joined the research group of Sustainable Food Processing for her master's thesis. Her topic was about "*the isolation and characterization of high pressure superdormant spores*". In 2018, she gained experience working at a start-up from EPFL on "*a catalytic technology for the extraction of bioactive compounds from lignocellulosic biomass or microorganisms*". She decided to pursue a PhD in May 2021 and joined the Sustainable Food System research group at HES-SO in Sion, Switzerland. She was co-supervised by experts from the Food Microbiology group at Wageningen University & Research (WUR), in The Netherlands.

List of publications

Scientific publications

De Gol, C., Snel, S., Rodriguez, Y., & Beyrer, M. (2023). Gelling capacity of cell-disrupted *Chlorella vulgaris* and its texture effect in extruded meat substitutes. *Food Structure, 37*, 100332. https://doi.org/10.1016/j.foostr.2023.100332

De Gol, C., Moodycliffe, A., Den Besten, H. M. W., Zwietering, M. H., & Beyrer, M. (2024). Pulsed electric field treatment for preservation of *Chlorella* suspensions and retention of gelling capacity. *Food Research International, 182*, 114154. https://doi.org/10.1016/j.foodres.2024.114154

De Gol, C., Etschmann, N., Zwietering, M. H., Den Besten, H. M. W., & Beyrer, M. (2024). Pulsed electric field combined with preheating to preserve mildly extracted pea protein. *LWT – Food Science and Technology*, *214,* 117100. https://doi.org/10.1016/j.lwt.2024.117100

De Gol, C., De Ridder, V., Zwietering, M. H., Den Besten, H. M. W., & Beyrer, M. (2025). Effects of pulsed electric field and thermal treatment on the structural and techno-functional properties of mildly extracted pea proteins. *LWT – Food Science and Technology, 238*, 118757. https://doi.org/10.1016/j.lwt.2025.118757

Patents & Articles in professional journals

Uran, M., Sarikaya, A., **De Gol, C.**, & Beyrer, M. (2022). Methods of preparation of a food or a feed product or ingredient from non-refined microalgae & uses thereof. *Patent n°EP22208302.4*.

De Gol, C., & Beyrer, M. (2024). Eliminer les bactéries, préserver les propriétés nutritives. *Foodaktuell.* https://www.foodaktuell.ch/2024/02/01/verbesserte-proteinfunktionalitaet-durch-kalt-pasteurisieren

Rouge A., **De Gol, C.**, & Beyrer, M. (2025). Längere Haltbarkeit von Protein-lösungen durch gepulste Felder. *Lebensmittel-Industrie, 9/10,* 14–15. https://www.lebensmittelindustrie.com/news/news-details/laengere-haltbarkeit-von-proteinloesungen-durch-gepulste-felder

Overview of training activities

Discipline specific activities

Scientific courses at post graduate level

Food extrusion technology (Food stream / HES-SO, Switzerland)	2022
Healthy and sustainable diets (VLAG, Wageningen, The Netherlands)	2023
Food proteins (VLAG, Wageningen, The Netherlands)	2024

Scientific courses at MSc level

Advanced food microbiology: minimal processing, preservation and fermentation (VLAG, Wageningen, The Netherlands)	2023

*Conferences and scientific meetings *Oral presentation, **Poster*

EFFOST (Lausanne, Switzerland)	2022
2nd Microbiological Risk Assessment Seminar 2023 (Berne, Switzerland) *	2023
EFFOST (Valencia, Spain) **	2023
PhD symposium HES-SO (Renens, Switzerland) *	2023
IAFP European Symposium on Food Safety (Geneva, Switzerland) *	2024
IUFoST (Rimini, Italy) *	2024
WC 2024 (Rome, Italy) *	2024

General courses

Science and engineering teaching and learning (EPFL, Switzerland)	2021
VLAG PhD week (Baarlo, The Netherlands)	2022
Intensive writing week (WGS, Wageningen, The Netherlands)	2022
Project and time management (WGS, Wageningen, The Netherlands)	2022
Searching and organizing literature for PhD (WGS, Wageningen, The Netherlands)	2022
Research and data management (WGS, Wageningen, The Netherlands)	2022

Teaching and supervision activities

Practical courses, tutorials, lecturing

Progress in food processing (course + practical MSc) (HES-SO, Switzerland)	2022
Food engineering (practical BSc) (HES-SO, Switzerland)	2022

BSc / MSc thesis supervision

BSc (Ailsa Moodycliffe, Amina Bouguenna, Alix Rouge)	2022-2024
MSc (Nicolas Etschmann, Alexandra Batsila, Valentin De Ridder)	2023-2024

Other activities

Internal scientific meetings

Preparation of research proposal (VLAG, Wageningen, The Netherlands)	2022
Research meeting – FHM (Wageningen, The Netherlands)	2022-2024
Research meeting – SFS (HES-SO, Switzerland)	2021-2024
Research meeting – PhD student (HES-SO, Switzerland)	2023

Societally relevant exposure

Interview by Imaginastudio (HES-SO, Switzerland)	2022
Interview for the magazine Hespresso (HES-SO, Switzerland)	2023

MSc courses

Advanced Food microbiology-Tools in Safety management (VLAG, Wageningen, The Netherlands)	2022

Authorship statement

Chapter 1 *General introduction.* The general thesis research question was proposed by my co-promotor. The research objectives were defined together with my promotors. I prepared the first layout, which I modified slightly after discussion with my co-promotor. I revised the text following comments from my promotors.

Chapter 2 *Gelling capacity of cell-disrupted Chlorella vulgaris and its texture effect in extruded meat substitutes.* The research question was defined by my co-promotor. I contributed to the methodology and experimental design, and I conducted the research with support from a lab technician, and the second and third co-authors. I performed the data analysis with these co-authors. I prepared the graphs and text layout. I wrote the first draft with their assistance, and I revised the text following comments from my co-promotor.

Chapter 3 *Pulsed electric field treatment for preservation of Chlorella suspensions and retention of gelling capacity.* I developed methodology and experimental design after six-months of pre-trials and discussions with my (co-)promotors and scientific collaborators. I carried out experiments and data collection together with a BSc student, whom I supervised. I performed the data analysis and prepared the graphs and text, incorporating suggestions from my (co-)promotors.

Chapter 4 *Pulsed electric field combined with preheating to preserve mildly extracted pea protein.* I proposed the experimental design (based on the work done in **Chapter 3**) and carried out research and data collection with support from a lab technician and an MSc student, whom I supervised. I performed the data analysis and prepared the graphs and first draft and implemented comments from my (co-)promotors.

Chapter 5 *Effects of pulsed electric field and thermal treatment on the structural and techno-functional properties of mildly extracted pea proteins.* I elaborated on the research question after discussions with (co-)promotors and an MSc student, whom I supervised. I contributed to the experimental design and conducted the experiments following pre-trials carried out with the MSc student to determine the methodology. I did the data collection with support from scientific collaborators and another PhD student. I performed the data analysis, and I wrote the draft with input from the co-authors.

Chapter 6 *General discussion.* I carried out additional research with support from two students (BSc and MSc), whom I supervised. I performed the data analysis, incorporating

few data from research partners and another PhD student. I made the graphs and wrote the first draft. I revised the layout and text after discussions with my (co-)promotors.

I used AI writing assistance (Grammarly and ChatGPT) to improve the text formulations. The improvements were critically assessed.

The research described in this thesis was financially supported by the Swiss Innovation Agency “Innosuisse” under application numbers 36440.1 IP-LS and 104.851 IP-LS, and the Canton of Fribourg (Switzerland) in the frame of the flagship program “biomass valorization” 2022.

Travel costs were partially financed by the State Secretariat for Education, Research and Innovation (SERI). The Research and Innovation Department of the HES-SO Rectorate supported financially the end of the thesis and last steps of the writing process.

Financial support from Wageningen University for printing this thesis is gratefully acknowledged.

Cover design and printed by: ProefschriftMaken // www.proefschriftmaken.nl